Molecular characterisation of CRYPα, an axonal receptor protein tyrosine phosphatase

Alexandru Radu Aricescu

A thesis submitted for the degree of Doctor of Philosophy
in the University of London

November 2001

University College London
Institute of Child Health
Neural Development Unit
30 Guilford Street
London, WC1N 1EH

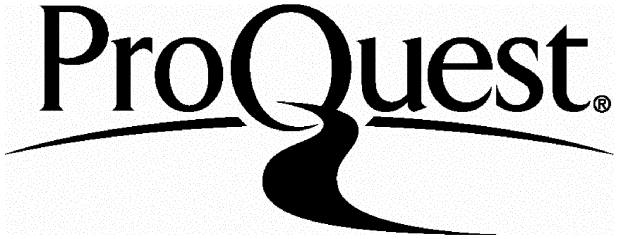

Dedication

This thesis is dedicated

to my mother, for luring me into biological research... the smell of a small lab hidden in the backyard of the National Institute of Geriatrics and Gerontology in Bucharest will be forever imprinted in my soul...

to Ana-Maria, whose love and support is behind everything I achieve...

to Ilinca and Teodor, for beautifully decorating various drafts of this manuscript...

Acknowledgements

I would like to thank first of all Andy Stoker for his continuous support during the past four years of my life. I had the chance to experience in his lab, first in Oxford and then in London, an extremely stimulating scientific environment and a unique atmosphere of friendship, fun and freedom.
Here I met very special friends like Iain McKinnell, John Chilton, Fiza Rashid-Doubell and Fawaz Haj.
In particular Iain (also my official translator) and John (a skilful artist) became hard-core, life-long and well-behaved supporters of the ever-successful Romanian football team, as clearly demonstrated in Figure 0.1:

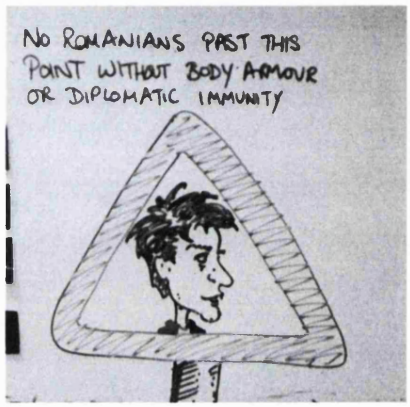

Figure 0.1: Innocent scientist victimised as a result of yet another glorious performance of the Romanian football team (World Cup 1998, France: *Romania* 2 – *England* 1). No copyright obtained, for security reasons.

Moving in London has offered us the opportunity to join another special research group, in the form of a Spanish-speakers-dominated Neural Development Unit. I owe special thanks to Andy Copp for his support. And, also, to every single member of this Unit who patiently tolerated various temperamental bursts I (apparently) had from time to time. Not to forget the Latin Corner, a merry office area enriched with literature samples from London's entertaining phone boxes.

More thanks are earmarked for Caroline Paternotte, aka Agent ABI-377. She kindly helped me with DNA sequencing, but she also loved this thesis. How else can I explain the long nights she - and John - have spent reading it?

Newer members of the Stoker group, like Mike, Gustavo (or Paco?) and Simon also deserve a special mention: they were among the few who knew that the abbreviation "RPTP" is not a coded start signal for the sleeping session during the looong Monday morning-afternoon group meetings.

I am also grateful to Paco (or Gustavo?) for helping me to see a damn minuscule yellow embryo on a yellow background, God knows why it was made this way...

Finally, I thank Willi Halfter (University of Pittsburgh) for agrin, collagen XVIII and antibody samples, Stéphane Swillens (Université Libre de Bruxelles) for advice regarding nonlinear regression analysis of ligand-receptor binding data and Susanne Schmidt (CNRS Montpellier) for the yeast two-hybrid system assays.

Abstract

Receptor protein tyrosine phosphatases (RPTPs) represent a major research focus in developmental biology, oncology and immunology. Specifically, cell adhesion molecule–like RPTPs, including CRYPα, have recently emerged as key regulators of nervous system development, being involved in axonal growth and guidance, and nerve repair. However, very little is known about their signal transduction mechanisms since the identity of various interacting molecules is far from being completely elucidated. In this thesis I demonstrate that CRYPα has a novel, heparin-binding activity and that its interaction with the retinal basal lamina is mediated by the heparan sulphate chains of extracellular matrix proteoglycans. Using molecular modelling and site-directed mutagenesis, I have mapped the heparin/heparan sulphate binding site in the first immunoglobulin-like domain of CRYPα. I also describe the first identification of heterotypic ligands for a type II neural RPTP, namely the secreted isoforms of agrin and collagen XVIII. Given the broad functional spectrum of these molecules, a novel perspective towards understanding CRYPα's functions and regulation has been opened. In addition, it became apparent that this RPTP itself can be phosphorylated *in vivo* and preliminary experiments suggest the existence of a ~75 kDa putative substrate for its enzymatic activity. Altogether, these data contribute to the molecular characterisation of CRYPα and suggest potential ways to modulate its signalling function in pathological conditions.

Abbreviations

AP	Alkaline phosphatase
ATP	Adenosine-5'-triphosphate
BCA	Bicinchoninic acid
BCIP	5-Bromo-4-chloro-3-indolyl-phosphate
BL	Basal lamina
bp	Base pair
BSA	Bovine serum albumin
CAM	Cell adhesion molecule
cAMP	adenosine 3',5'-monophosphate
CC	Comb cell
Cdk2	Cyclin-dependent kinase 2
cDNA	Complementary DNA
CEF	Chick embryo fibroblast
CMF	Ca^{2+}/Mg^{2+} free Hanks' balanced salt solution
CNS	Central nervous system
CS	Chondroitin sulphate
CSPG	Chondroitin sulphate proteoglycan
D1	Membrane proximal phosphatase domain
D2	Membrane distal phosphatase domain
DAB	3,3'-Diaminobenzidine
DAG	Diacylglycerol
DCC	Deleted in colorectal cancer
DCCD	N,N'-dicyclohexylcarbodiimide
DEPC	Diethylpyrocarbonate
DMEM	Dulbecco's Modified Eagle's Medium
DMSO	Dimethyl sulfoxide
DNA	Deoxyribonucleic acid
DNase	Deoxyribonuclease
dNTP	Deoxynucleoside triphosphate
DRG	Dorsal root ganglion (ganglia)
DSP	Dual specificity phosphatase
DTNB	Dithionitrobenzene

DTT	1,4-Dithiothreitol
E	Embryonic day
ECL	Enhanced chemiluminescence
ECM	extracellular matrix
EDTA	Ethylenediamine tetraacetic acid
EGFR	Epidermal growth factor receptor
FCS	Foetal calf serum
FGF	Fibroblast growth factor
FGFR	FGF receptor
FITC	Fluorescein isothiocyanate
FNIII	Fibronectin type III
GAG	glycosaminoglycan
GFAP	Glial fibrillary acidic protein
GPI	glycosylphosphatidylinositol
GTPase	Guanosine-5'-triphosphatase
HB-GAM	Heparin-binding growth-associated molecule
HBSS	Hank's balanced salt solution
HEPES	4-[2-Hydroxyethyl]-1-piperazineethanesulfonic acid
HfV	HSPG-enriched fraction from the vitreous body
HRP	Horseradish peroxidase
HS	Heparan sulphate
HSPG	Heparan sulphate proteoglycan
Ig	Immunoglobulin
IMS	Industrial methylated spirits
IPTG	Isopropyl-β-thiogalactopyranoside
IRS	Insulin receptor substrate
ISN	Intersegmental nerve
ITAM	Immunoreceptor tyrosine-based activation motif
kb	Kilobase
kDa	Kilodalton
LB	Luria-Bertani
LMW-PTP	Low-molecular weight protein tyrosine phosphatase
MAM	Meprin/A5/RPTPμ
MAPK	Mitogen-activated protein kinase
MKP	MAPK phosphatase

MOPS	4-Morpholinepropanesulfonic acid
mRNA	Messenger RNA
NAI	1-acetylimidazole
NBT	4-Nitro blue tetrazolium chloride
NCAM	Neuronal cell adhesion molecule
NgCAM	Neural-glial cell adhesion molecule
NgR	Nogo receptor
NrCAM	NgCAM-related cell adhesion molecule
OD	Optical density
PBS	Phosphate-buffered saline
PCR	Polymerase chain reaction
PDGFR	Platelet-derived growth factor receptor
PDZ	PSD-95/Discs-large/ZO-1
PGO	Phenylglyoxal
PI3K	Phosphatidyl-inositol-3-kinase
PKA	Protein kinase A
PLL	Poly-L-lysine
pNPP	4-nitrophenyl disodium orthophosphate
PSA	Polysialic acid
PTK	Protein tyrosine kinase
PTP	Protein tyrosine phosphatase
PVDF	Polyvinylidene difluoride
RAP	Receptor affinity probe
RCAS	**R**eplication-**c**ompetent, **a**vian leukaemia virus, long terminal repeats, **s**plice acceptor
RGC	Retinal ganglion cell
RIPA	Radioimmunoprecipitation
RNA	Ribonucleic acid
RNase	Ribonuclease
rpm	Revolutions per minute
RPTK	Receptor tyrosine kinase
RPTP	Receptor protein tyrosine phosphatase
SDS	Sodium dodecyl sulphate
SEAP	Secreted alkaline phosphatase
TAE	Tris-acetate-EDTA

TBS	Tris-buffered saline
TE	Tris-EDTA
TEMED	N,N,N',N'-tetramethylethylenediamine
Tris	Tris[hydroxymethyl]-amino-methane
tRNA	Transfer RNA
U	Units
VLM	Ventrolateral muscles
VSV	Vesicular stomatosis virus
v/v	Volume/volume
w/v	Weight/volume

Table of Contents

Acknowledgements 3

Abstract 4

Abbreviations 5

Table of Contents 9

List of Figures 13

Chapter 1. **INTRODUCTION** **15**

1.1. General introduction 15

1.2. Receptor protein tyrosine phosphatases: form and function 16

1.2.1 The protein tyrosine phosphatase superfamily 16

1.2.2 The extracellular region of RPTPs 20

1.2.3 The intracellular region of RPTPs 24

1.2.4 *In vivo* functions of RPTPs 29

1.3. Axon growth and guidance mechanisms. The role of RPTPs 35

1.3.1 Introduction 35

1.3.2 Receptor protein tyrosine phosphatases in axon growth and guidance 48

1.4. The receptor protein tyrosine phosphatase CRYPα 58

1.5. The aim of this thesis 64

Chapter 2. **GENERAL METHODS** **66**

2.1. DNA methods 66

2.1.1 Plasmid DNA preparation – microprep 66

2.1.2 Plasmid DNA preparation – miniprep 67

2.1.3 Plasmid DNA preparation – maxiprep 68

2.1.4 Plasmid DNA extraction from fixed mammalian cells 71

2.1.5 Restriction enzyme cleavage of DNA 72

2.1.6 Klenow filling of DNA recessed 3' termini 73

2.1.7 Alkaline phosphatase treatment of DNA fragments 74

2.1.8 Agarose gel electrophoresis 75

2.1.9 Purification of DNA fragments from agarose gels 76

2.1.10 Ligation of DNA fragments 77

2.1.11 Preparation of electrocompetent *E. coli* 78

2.1.12 Transformation of bacteria by electroporation 80
2.1.13 Polymerase Chain Reaction (PCR) 81
2.1.14 Site-directed mutagenesis 82
2.1.15 DNA sequencing 83
2.1.16 Preparation of DNA linkers 84
2.2 RNA methods 85
2.2.1 Total RNA isolation from tissue samples 85
2.2.2 Poly(A)$^+$ mRNA purification 86
2.2.3 RNA electrophoresis in agarose gels 88
2.3 Protein methods 89
2.3.1 Protein quantitation using bicinchoninic acid 89
2.3.2 Filter paper dye-binding assay for protein quantitation 90
2.3.3 Sodium Dodecyl Sulphate – Polyacrylamide Gel Electrophoresis (SDS-PAGE) 91
2.3.4 Staining SDS-PAGE gels with Coomassie Brilliant Blue 94
2.3.5 Staining SDS-PAGE gels with silver nitrate 95
2.3.6 Western immunoblotting 96
2.3.7 Blot-overlay assay 98
2.3.8 Immunoprecipitation of target proteins 98
2.4 Cell culture methods 99
2.4.1 Basic cell culture procedures 99
2.4.2 Line 0 chick embryo fibroblasts (CEF) primary cultures 101
2.4.3 Retinal glial cell primary cultures 102
2.4.4 Retinal explant cultures 103
2.4.5 Transient transfection of adherent cells 105
2.5 Histology/cytology methods 107
2.5.1 Preparation of tissue cryosections 107
2.5.2 Immunohistochemistry and immunocytochemistry 108
2.5.3 Receptor Affinity Probe (RAP) *in situ* 110
2.6 Chick embryo manipulation methods 111
2.6.1 *In ovo* electroporation 111

Chapter 3. **EXPRESSION CLONING ATTEMPTS TO IDENTIFY CRYPα LIGANDS** **114**

3.1 Introduction 114

3.2 Experimental procedures 116

3.3 Results 119

3.3.1 Construction of an E7 chicken optic tectum expression cDNA library 119

3.3.2 Retroviral expression of the CRYPα1-AP fusion protein 120

3.3.3 Expresison cloning attempts 122

3.4 Discussion 126

Chapter 4. **CRYPα IS A HEPARIN-BINDING PROTEIN** **130**

4.1 Introduction 130

4.2 Experimental procedures 132

4.3. Results 135

4.3.1. The molecular nature of the retinal basal lamina ligand(s) 135

4.3.2. CRYPα is a heparin-binding protein 138

4.3.3. The first Ig-like domain of CRYPα contains a putative heparin-binding site 138

4.3.4. The heparin-binding site of CRYPα is essential for binding to the retinal basal lamina 143

4.3.5. Radial glial cells (appear to) express two classes of CRYPα ligands 146

4.4 Discussion 149

Chapter 5. **HEPARAN SULPHATE PROTEOGLYCANS ARE LIGANDS FOR CRYPα** **154**

5.1 Introduction 154

5.2 Experimental procedures 161

5.3 Results 166

5.3.1 CRYPα binds to retinal HSPGs 166

5.3.2 CRYPα binds to the extracellular matrix HSPGs agrin and collagen XVIII 170

5.3.3 Overlapping expression patterns of CRYPα, agrin and collagen XVIII in the developing chick retina 174
5.3.4 A non-HSPG class of ligands appears to be expressed on Müller glia endfeet 176
5.4 Discussion 176

Chapter 6. **PUTATIVE INTERACTION PARTNERS FOR THE INTRACELLULAR REGION OF CRYPα** **184**
6.1 Introduction 184
6.2 Experimental procedures 189
6.3 Results 193
6.3.1. Efficient expression of CRYPα intracellular region constructs in 293T cells 193
6.3.2. CRYPα can be tyrosine phosphorylated *in vivo* 195
6.3.3. A putative substrate for CRYPα 198
6.3.4. CRYPα interacts with the multifunctional protein Trio in yeast two-hybrid assays 199
6.4 Technical appendix: Efficient gene transfer in the developing chick retina by *in ovo* electroporation 201
6.5 Discussion 206

Chapter 7. **CONCLUDING REMARKS** **214**

References **218**

List of Figures

Figure 1.1. Schematic representation of the receptor protein tyrosine phosphatase family. 21

Figure 1.2. The human receptor protein tyrosine phosphatases. 34

Figure 1.3. CRYPα schematic structure and putative post-translational modifications. 59

Figure 3.1. Expression of alkaline phosphatase and CRYPα1-AP fusion protein in the quail fibroblast cell line QT6. 121

Figure 3.2. RAP *in situ* staining of non-transfected COS-7 cells in culture. 123

Figure 3.3. CRYPα1-AP screening of the LTc1R expression library transfected in COS-7 cells. 125

Figure 4.1. The effect of protein modification reagents, sodium chloride and heparin on CRYPα binding to its basal lamina ligand(s). 137

Figure 4.2. Solid-phase binding of CRYPα to heparin. 139

Figure 4.3. Structural model of the Ig-1 domain of CRYPα and sequence alignment with the Ig domains of telokin, NCAM (Ig-2) and FGFR1 (Ig-2). 140

Figure 4.4. Identification of the CRYPα heparin-binding site by site-directed mutagenesis. 144

Figure 4.5. The heparin/heparan sulphate binding site in domain Ig-1 is essential for retinal basal lamina binding. 145

Figure 4.6. Sodium chloride and heparin abolish CRYPα binding to cultured retinal cells. 147

Figure 4.7. CRYPα binding to its glial endfeet ligand(s) cannot be completely abolished by heparin or mutations in the heparin-binding site. 148

Figure 5.1. Schematic representation of agrin and collagen XVIII HSPGs. 160

Figure 5.2. CRYPα binding to the E6 chick retinal basal lamina is mediated by heparan sulphate chains. 167

Figure 5.3. Various anti-HSPG monoclonal antibodies affect CRYPα binding to the retinal BL in a differential manner. 168-9

Figure 5.4. Solid-phase binding of CRYPα to agrin and collagen XVIII. 171

Figure 5.5. CRYPα binds the extracellular matrix proteoglycans agrin and collagen XVIII via their heparan sulphate chains. 173

Figure 5.6. Expression patterns of CRYPα, agrin and collagen XVIII in the developing chick retina. 175
Figure 5.7. Retinal cells in culture express an HSPG ligand for CRYPα. 177
Figure 5.8. Müller glia endfeet appear to express two classes of CRYPα ligands. 178
Figure 6.1. Sequence alignment results (percentage identity) for various regions of the typeII RPTP family members. 185
Figure 6.2. Expression of recombinant CRYPα intracellular region constructs. 194
Figure 6.3. Kinetic assay of the CRYPα intracellular constructs. 196
Figure 6.4. CRYPα is tyrosine phosphorylated *in vivo* and it dephosphorylates a putative 75 kDa substrate. 197
Figure 6.5. CRYPα can interact with the multidomain protein Trio in yeast two-hybrid assays. 200
Figure 6.6. *In ovo* electroporation of stage 10 chick embryos optic primordium and reporter gene expression analysis. 203
Figure 6.7. Enhanced green fluorescent protein (EGFP) expression into E4.5 chick embryo eyes. 204
Figure 6.8. 3D model of the intracellular region of CRYPα. 209

Chapter 1. **Introduction**

1.1 General introduction

Life makes no sense in a closed system. Therefore, any living entity will exchange matter and information with its environment. A rapid adaptation to an external challenge (stimulus) is the key for survival. Biochemically, a cell is just a molecular network. Extremely complex, as we judge it today, and also extremely efficient and robust. Any bit of information travelling through this network does so along signal transduction pathways. They consist of molecules able to "receive" (receptors), "integrate" (protein complexes), "translate" (enzymes) and "transmit" (activated molecules) a signal, ultimately to the genetic material, which (hopefully) contains the necessary answer. This answer is the expression of a gene (group of genes) which triggers a molecular response (ultimately seen as "behaviour") transmitted via a similar pathway.

A dynamic equilibrium between two simple biochemical reactions represents the major mechanism for reversible regulation of protein activity and function, during both signal transduction and cellular response. The transfer of a phosphate group from a donor ATP molecule to an amino acid side chain (serine, threonine, tyrosine or histidine, as known so far), catalysed by protein kinases, is thought to be the most common type of protein modification. The equilibrium is maintained by the opposite reaction, removal of phosphate groups from protein residues, catalysed by protein phosphatases.

Only about 0.05% of the total protein-bound phosphate in normal vertebrate cells is attached to tyrosine residues (for comparison phosphoserine accounts for circa 90% and phosphothreonine for circa 10%; Hunter and Sefton, 1980). However, the number and diversity of cellular events thus controlled highlights its importance: cell

growth (and oncogenesis), cell shape and attachment, cell differentiation and development, cell cycle control, programmed cell death (apoptosis), intracellular signalling, gene transcription, glucose uptake, platelet activation in blood clotting, angiogenesis, regulation of ion channel activity in neural transmission, regulation of the immune response etc. (reviewed in Hunter, 1998; Fischer, 1999).

This thesis is built around a molecule named Chick Receptor protein tYrosine Phosphatase α (CRYPα), the first vertebrate receptor protein tyrosine phosphatase (RPTP) found localised in the plasma membrane of migrating axonal growth cones (Stoker *et al.*, 1995). Further studies confirmed its involvement in nervous system development, in particular in axon growth and (possibly) guidance. My main target was the identification of extracellular molecules signalling or modulating the signals transduced via CRYPα, in order to contribute to its functional characterisation in particular and to a better understanding of RPTPs in general.

1.2 Receptor protein tyrosine phosphatases: form and function

1.2.1 The protein tyrosine phosphatase superfamily

The possibility of finding phosphate groups covalently attached to proteins was suggested almost one hundred years ago and indeed in 1933 the existence of serine and threonine phosphate esters was reported. Tyrosine phosphorylation however was only discovered in 1979 and the identification of the first protein tyrosine kinases was reported in 1980 (reviewed in Hunter, 1998). A huge research effort in this field was triggered by the observation that protein tyrosine kinases, when freed from the strict cellular control mechanisms, are very powerful oncogenes (reviewed in Fischer, 1999). Hence, the search for the counter-balancing enzymes was soon open and in 1988 the first protein tyrosine phosphatase (PTP) was identified (Tonks *et al.*, 1988). A frantic cloning period followed and the findings were unexpected: the PTPs (EC 3.1.3.48),

once thought to be simply some sort of scavenger enzymes, represent a large family of enzymes and display a great structural variability. More than 75 members have been identified and partially characterised in the last ten years in eukaryotes and some bacterial species. Initial sequence analysis of the nearly completed human genome revealed 112 human PTPs (International Human Genome Sequencing Consortium, 2001).

Structural studies suggest the existence of three distinct evolutionary branches in the PTP superfamily, with different three-dimensional topologies (Denu and Dixon, 1998). The first group contains the classical phosphatases and the dual specificity phosphatases. The classical phosphatases are distinguished by the presence of one or two highly conserved PTP domains of 200-300 amino acids, sharing more than 30% identity and containing the (I/V)HCxAGxxR(S/T)G active site motif, which includes the cysteine (Cys) residue essential for catalytic activity. Extensive kinetic studies led to a good understanding of the catalytic mechanism, formally described in two steps. In the first step the thiolate anion from the active site Cys attacks nucleophilically the phosphorus atom of the substrate (phosphotyrosine). Cleavage of the scissile P-O bond is then facilitated by protonation of the phenolic oxygen by a general acid aspartate (Asp) residue from a neighbouring loop ("WPD"), leading to the formation of a phospho-cysteine intermediate. In the second step the intermediate is hydrolysed by a water molecule activated by the same Asp residue, which now functions as a general base (Li and Dixon, 2000; Barford *et al.*, 1998). Classical PTPs can only dephosphorylate phosphotyrosine residues (and not phosphoserine or phosphothreonine) mainly due to the depth of their active-site cleft (~9 Å for PTP1B, Barford *et al.*, 1994). Based on their cellular localisation they can be sub-divided into intracellular and receptor-like (RPTPs).

Intracellular PTPs contain a single phosphatase domain, linked to a variety of localisation motifs (e.g. nuclear, endoplasmic reticulum, cytoplasmic) and other domains [e.g. SH2 (Src-homology 2), PDZ (PSD-95/Discs-large/ZO-1)] responsible for distributing the enzyme to different cellular compartments, modulating its catalytic activity and interaction with substrates and other binding partners, and adding integrative functions in the signalling networks. As a consequence of this structural diversity, intracellular PTPs have numerous biological functions; just a few examples are given here. PTP1B can directly dephosphorylate growth factor receptors such as EGFR (epidermal growth factor receptor) and PDGFR (platelet-derived growth factor receptors), but also the insulin receptor. PTP1B-/- mice have increased insulin-sensitivity, in a tissue-specific fashion, and are also resistant to high-fat diet induced obesity (reviewed in Tonks and Neel, 2001). Therefore PTP1B is thought to be a putative drug target for insulin-resistant states such as obesity and type II diabetes mellitus. The PTPs containing SH2 domains (SHPs) have also been studied in great detail. Homozygotic mutations in SHP-1 give rise to the *motheaten* (*me/me*) mice, which display a multitude of hematopoietic abnormalities leading to early death (Neel, 1993). SHP-2, homologue to the *corkscrew* (*Csw*) gene in *Drosophila*, plays a critical role in vertebrate development. Experiments in *Xenopus* have shown that dominant negative mutants of SHP-2 disrupt gastrulation, cause severe tail truncations and block fibroblast growth factor (FGF)-induced mesoderm induction and elongation in ectodermal explants, consistent with a role in FGF signalling modulation *in vivo* (Tang *et al.*, 1995). PTP-PEST, another intracellular PTP, was shown to regulate fibroblast motility (focal adhesion disassembly, migration and cytokinesis), at least in part by dephosphorylating the docking protein p130cas (Angers-Loustau *et al.*, 1999).

All RPTPs known to date are type I transmembrane proteins containing a highly variable extracellular domain followed by a single transmembrane region and one or

(usually) two intracellular PTP domains. Where two PTP domains are present, the membrane-proximal one retains most if not all the phosphatase activity. Based on the structure of their extracellular domains, the RPTPs are currently classified in seven subfamilies. A detailed description of their structure, mechanisms of regulation and functions will be presented in the following sub-chapters.

The dual specificity phosphatases (DSPs) can dephosphorylate both phosphoserine/threonine and phosphotyrosine residues. They share the overall structure and catalytic mechanism of classical PTPs, and their additional ability to hydrolyse phosphoserine/threonine has been attributed to a slight change in their active-site pocket leading to a smaller depth (only 6 Å) which allows the phosphate groups attached to the (shorter) side-chains of serine and threonine to reach the catalytic Cys residue. Despite this, some DSPs show a remarkable degree of specificity *in vivo*, primarily dephosphorylating only one type of phosphoamino acid. The DSP KAP for example dephosphorylates only Thr160 from the activation loop of cyclin-dependent kinase 2 (Cdk2; Poon and Hunter, 1995). Other important examples of DSPs include the MAP kinase phosphatases (MKPs) and the vaccinia virus protein VH1 (Tonks and Neel, 2001). Unexpectedly, the physiological substrates for some of the DSPs are not phosphorylated proteins, but phospholipids. PTEN for example, the only PTP clearly demonstrated to be encoded by a tumour supressor gene, is absolutely specific for the phosphate in position 3 on the sugar ring of phosphatidylinositol (3,4,5)P_3 (Maehama and Dixon, 1998).

Another subgroup of the PTP superfamily is represented by the low molecular weight phosphatases (LMW-PTP). These share only little sequence and structural conservation with other PTPs but have a similar catalytic motif, $HC(X)_5R$, and an Asp residues functions as general acid. Very little is known about their cellular functions, although they are highly conserved from yeast to human. LMW-PTPs can be found in

two distinct intracellular locations, being distributed between a "cytosolic" and a "cytoskeleton-associated" pools. Recent studies *in vitro* have shown that cytosolic LMW-PTPs can bind and dephosphorylate activated PDGF and insulin receptors, modulating the onset of mitogenic processes, while the cytoskeleton-associated LMW-PTPs, specifically phosphorylated on two tyrosine residues by c-Src in response to PDGF stimulation, are involved in cytoskeletal rearrangement acting on p190Rho-GAP (Taddei *et al.*, 2000; Chiarugi *et al.*, 2000).

Finally, the X-ray structure of Cdc25 (Fauman *et al.*, 1998), the cell cycle phosphatase that dephosphorylates the cyclin-dependent kinase $p34^{cdc2}$, shows a distinct three-dimensional topology, suggesting that it represents a third evolutionary branch of the PTP superfamily.

1.2.2 The extracellular region of RPTPs

The RPTPs contain a diversity of domains in the extracellular region on which their sub-classification is based (Figure 1.1). These include domains reminiscent of classical cell adhesion molecules [immunoglobulin (Ig)-like, fibronectin type III (FNIII)-like and meprin/A5/μ (MAM)], domains with high homology to carbonic anhydrases and Cys-rich domains. Some representatives contain long chains of FNIII and Ig modules (e.g. type II and type III RPTPs) others present very short and highly glycosylated domains (e.g. RPTPε, just 27 residues).

In several cases the ectodomains are cleaved by specific proteases and they can be shed from the cell surface, thereby either masking binding sites on putative interaction partners or regulating cell responsiveness to extracellular stimuli. This may also represent an important mechanism for cell adhesion regulation. The ectodomain cleavage seems to occur during the normal processing of the RPTP, which can be detected in two subunits: E (contains the ectodomain) and P (contains a short fragment

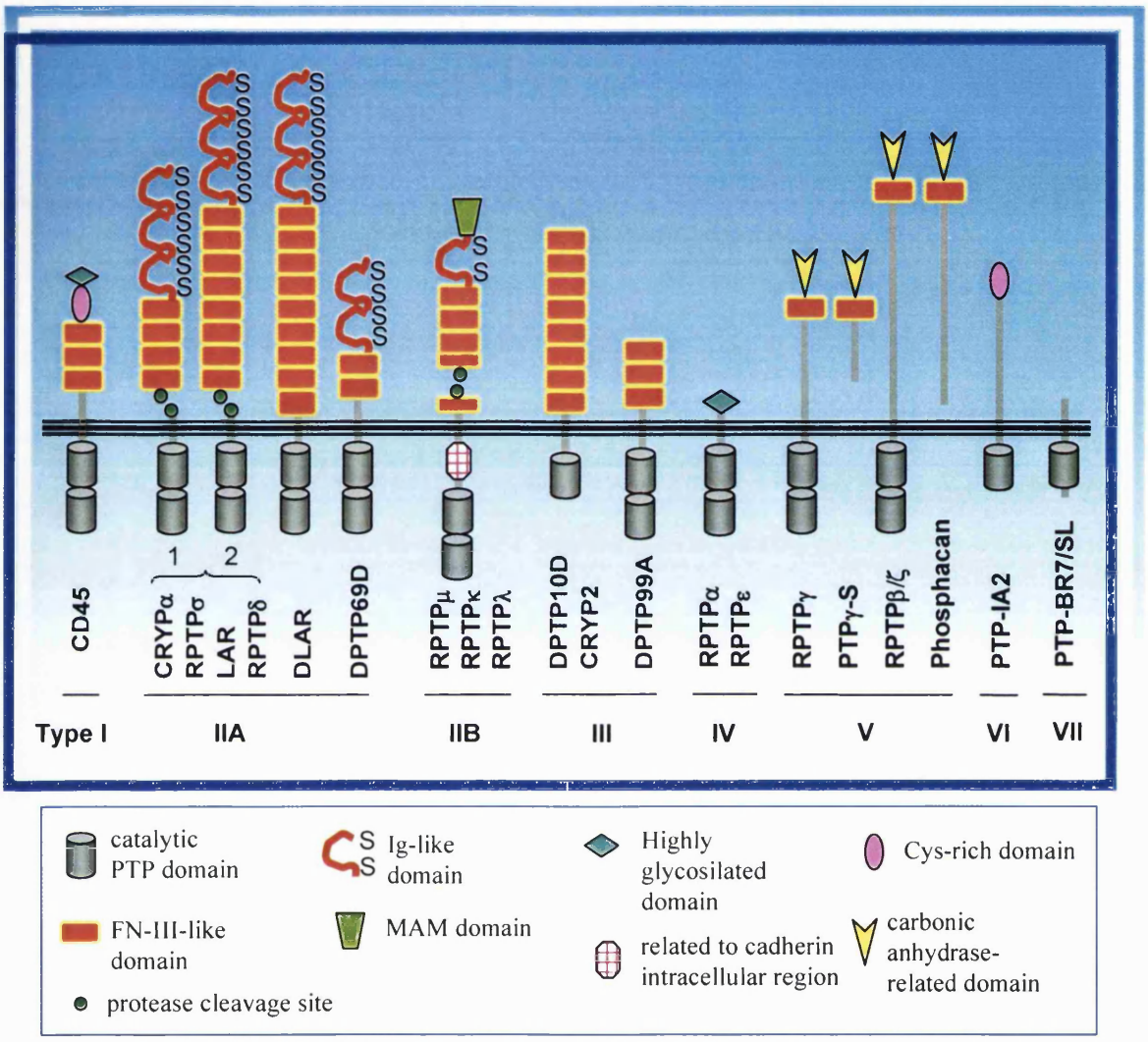

Figure 1.1. Schematic representation of the receptor protein tyrosine phosphatase family. The subgroup classification is based on the structure of the extracellular region. The subfamily of LAR-like type IIA enzymes are expressed in vertebrates as two major isoforms, numbered 1 and 2. Isoform 1 is considered to be neural specific. In several cases the extracellular region is proteolytically cleaved and shed from the cell surface, as one of the regulatory mechanisms for these receptors. Secreted isoforms also exist in the case of type V receptor protein tyrosine phosphatases.

of the ectodomain, the transmembrane region and the intact intracellular region). The two subunits remain attached to each other via non-covalent interactions, but, at high cell density, shedding of the E-subunit has been demonstrated for LAR (Streuli *et al.*, 1992; Aicher *et al.*, 1997), RPTPμ (Gebbink *et al.*, 1995), RPTPδ (Pulido *et al.*, 1995a), RPTPσ (Aicher *et al.*, 1997) and CRYPα (Stoker *et al.*, 1995).

The type I transmembrane organisation of RPTPs, the structural variety of their extracellular region and the enzymatic activity of the intracellular region had guaranteed the label "receptor" (or "receptor-like") for RPTPs long before any ligand had been identified. A major research effort has been focused in this direction in the last couple of years, although with only limited success. RPTP ligands still remain largely elusive and, with the exception of RPTPβ/ζ (Meng *et al.*, 2000), no evidence of any effect of ligand binding on phosphatase activity or phosphorylation state of a known substrate has been provided. This is mainly due to technical difficulties usually encountered when attempting to obtain such proteins in quantities large enough for biochemical studies. The very few successful cases will be detailed below.

CD45, the first RPTP characterised, was shown to be involved in multiple signalling events in B cells and T cells (for review see Li and Dixon, 2000). The B cell differentiation marker CD22 has been proposed as a ligand, however the functional significance seems to be unclear (Stamenkovic *et al.*, 1991). More recently, galectin-1 was proposed as a physiological ligand for CD45 and their interaction was related to the induction of apoptosis in Jurkat T cells (Walzel *et al.*, 1999).

A particular (non-neural) isoform of LAR interacts with the laminin/nidogen complex (O'Grady *et al.*, 1998), possibly modulating the cellular actin cytoskeletal structure. The laminin/nidogen-LAR interaction was completely disrupted by the insertion of a small exon in the fifth fibronectin III -like domain. The splicing of this

exon was found to be regulated in a tissue-specific and temporal fashion during development (O'Grady *et al.*, 1994; Pulido *et al.*, 1995b).

The extracellular regions of both RPTPμ and RPTPκ have been shown to interact in a homophilic manner in *trans*, therefore these RPTPs may provide a link between cell-cell contact and cellular signalling events involving tyrosine phosphorylation (Gebbink *et al.*, 1995; Sap *et al.*, 1994). These interactions were found responsible for the neurite outgrowth promoting properties of both RPTPμ and RPTPκ (Burden-Gulley and Brady-Kalnay, 1999; Drosopoulos *et al.*, 1999). It is worth mentioning that further studies have demonstrated that RPTPμ dynamically interacts in *cis* with N-cadherin, E-cadherin, and cadherin-4 (also called R-cadherin), adding to the growing body of evidence which implicates reversible tyrosine phosphorylation as an important mechanism in the control of the adhesive function of cadherins (Brady-Kalnay *et al.*, 1998; Burden-Gulley and Brady-Kalnay, 1999). Homophilic interaction has been recently shown for the extracellular region of RPTPδ, which also supports adhesion of chick neurons and promotes neurite outgrowth from forebrain neurons (Wang and Bixby, 1999).

The ligand binding properties of RPTPβ/ζ are known in by far the greatest detail. A truncated isoform containing only the extracellular domain (termed phosphacan or 3F8) has been described by Rauch *et al.* (1991) and represents one of the major chondroitin-sulphate proteoglycans in the brain. As a consequence, a large number of ligands have been described, including cell adhesion molecules such as NgCAM, NCAM and NrCAM (Milev *et al.*, 1994; Sakurai *et al.*, 1997), GPI anchored proteins such as contactin (Peles *et al.*, 1995) and TAG-1 (Milev *et al.*, 1996), and small cytokines such as pleiotrophin (Maeda *et al.*, 1996) and midkine (Maeda *et al.*, 1999). The overlapping expression patterns of RPTPβ/ζ, or its secreted isoform, phosphacan, with all the above mentioned molecules, together with the multitude of functional data

associated with them, suggest many potential roles *in vivo* for the interactions observed: control of cell proliferation, migration, adhesion, neurite outgrowth and pathfinding in the developing brain. However, a direct downstream effect following ligand binding, has been shown only for the interaction with pleiotrophin: the phosphatase activity of RPTPβ/ζ was inhibited and this lead to increased tyrosine phosphorylation of β-catenin (Meng *et al.*, 2000).

The identity of extracellular ligands for most RPTPs remains a largely unmapped area. However, since more and more functional studies establish the RPTPs as key players in many cellular events, with potential clinical relevance, a lot of effort is currently being channelled in this direction.

1.2.3 The intracellular region of RPTPs

Unlike the large variability in ectodomains, the intracellular region of RPTPs usually contains a tandem of catalytic domains, from which the membrane-proximal one (D1) accounts for the majority of catalytic activity, at least *in vitro* and using artificial substrates. Occasionally, the second phosphatase domain (D2) may display weak enzyme activity, as in the case of RPTPα (Wang and Pallen, 1991; Wu *et al.*, 1997), CD45 (Tan *et al.*, 1993) or LAR (Pot *et al.*, 1991). However, D2 is generally believed to regulate either enzyme activity or substrate specificity of D1. Indeed, recent studies have demonstrated regulatory interactions between D1 and D2 in CD45 (Felberg and Johnson, 2000) and RPTPμ (Feiken *et al.*, 2000; Aricescu *et al.*, 2001). In addition, D2 seems to represent a docking port for other intracellular interaction partners, such as liprins (for LAR, RPTPσ and RPTPδ; Serra-Pages *et al.*, 1998; Pulido *et al.*, 1995) and possibly Trio (for LAR; Debant *et al.*, 1996). Interestingly, the D2 domain of RPTPδ was found to be able to interact and inhibit the phosphatase activity of RPTPσ D1 (Wallace *et al.*, 1998), an observation extended later to RPTPσ-D2, RPTPα-D2, LAR-

D2, RPTPδ-D2 and RPTPμ-D2, all shown to bind RPTPα-D1 (Blanchetot and den Hertog, 2000). All these interaction networks between various phosphatase domains suggest the existence of very complex regulatory mechanisms inside the RPTP subfamily, however its relevance *in vivo* is not fully understood yet, since it is not clear how many of them are co-expressed in a temporal and spatial fashion. On the other hand, in many cases the key catalytic residues are well conserved in D2. X-ray crystallography studies revealed highly similar structures for the two phosphatase domains of LAR (Nam *et al.*, 1999) and site-directed mutagenesis experiments on LAR-D2 and RPTPα-D2 have shown that just two amino acid substitutions, outside the phosphatase signature motif (the Tyr in the KNRY motif and the Asp in the WPD loop), are enough to generate a very active construct towards artificial substrates (Nam *et al.*, 1999; Buist *et al.*, 1999). Therefore, it may well be possible that *in vivo* D2 itself is an active enzyme, at least for some RPTPs, with different substrate specificity compared to D1.

Several RPTPs have been found containing only a single phosphatase domain. Interestingly, some of these (e.g. IA-2; Lu *et al.*, 1994) do not display detectable PTP activity, suggesting that either the substrates tested were not appropriate or that these RPTPs do not function by dephosphorylation of cytoplasmic substrates but, instead, by binding to phosphotyrosine-containing proteins. In fact, a novel protein interaction domain, termed STYX (phospho-Serine or Threonine or tYrosine interaction protein) has been recently described (Wishart and Dixon, 1998). This is very similar to a PTP domain and is able to bind phosphorylated (protein) substrates, but lacks the enzymatic activity. The inactive phosphatase domains currently classified as STYX are considered to have appeared in evolution by PTP gene duplication and variation.

The catalytic mechanism of PTPs has been extensively studied in the last couple of years, and several crystal structures of phosphatase domains, alone or bound with

various artificial substrates have been reported (reviewed in Barford *et al.*, 1998, see 1.2.1 for more details). However, their structural studies have unexpectedly raised an issue regarding the putative regulation of enzyme activity by dimerization, currently still subject to controversy. It seems that at least some representatives, including RPTPα and CD45 contain a so called "inhibitory wedge" made of two alpha-helices at the N-terminus of D1, able to sterically block the enzyme activity of the neighbouring D1 in a symmetrical dimer pair (dimerization induced either by the crystallisation conditions or by artificial ligand binding, Bilwes *et al.*, 1996; Jiang *et al.*, 1999; Blanchetot and den Hertog, 2000). On the other hand, the crystal structures obtained for RPTPμ (Hoffmann *et al.*, 1997), LAR (Nam *et al.*, 1999) and PTP-SL/BR7 (Szedlacsek *et al.*, 2001) suggest lack of reciprocal inhibition between subunits despite containing an equivalent wedge region. Generally, modulation of signal transduction via receptor dimerization is a well established mechanism in the case of receptor protein tyrosine kinases, whereby ligand binding induces dimerization and transactivation (reviewed in Weiss and Schlessinger, 1998). It is very tempting to speculate about an opposite behaviour in the case of at least some RPTPs. Further experiments are still needed to clarify this issue, ideally using the emerging physiological ligands as putative modulators of receptor dimerization. On the other hand, the correct evaluation of the activation state *in vivo* should assess the tyrosine phosphorylation of the known physiological substrates for RPTPs. A sustained research effort led to the identification of many substrates and just a few examples are given below for CD45 (the Src-family members Lck and Fyn: Mustelin *et al.*, 1989; Ostergaard *et al.*, 1989; Shiroo *et al.*, 1992), RPTPα (p130-Cas, Src, Fyn: Buist *et al.*, 2000; Zheng *et al.*, 1992; den Hertog *et al.*, 1993), RPTPμ (the catenin $p120^{ctn}$: Zondag *et al.*, 2000), LAR (p130-Cas, IRS-1: Weng *et al.*, 1999; Goldstein *et al.*, 2000) and DLAR (Abl and Ena: Wills *et al.*, 1999). Nevertheless, there are still many RPTPs for which the physiological substrate(s) still have to be identified,

a key question for understanding their role in signalling pathways and their functions *in vivo*.

In addition to the regulatory mechanisms mentioned above (ectodomain shedding, inactivation by protein dimerization - still unclear whether ligand-mediated), reversible oxidation of the catalytic centre (the essential Cys residue) as well as serine/threonine and tyrosine phosphorylation have been shown to modulate the activity of several RPTPs. A very interesting observation, extensively supported by experiments in the last couple of years, is that agents like oxidants and radiation (in particular UV) can induce ligand-independent activation of growth-factor receptors and the downstream signalling cascades (Gross *et al.*, 1999 and references therein). Oxidants and thiol-directed reagents cause a rapid and significant increase in the level of tyrosine phosphorylation in treated cells (Knebel *et al.*, 1996). This can either happen by increasing the protein tyrosine kinase activity [stabilising receptor protein tyrosine kinase (RPTK) dimers for example] or, as it has been proven to be, by inhibiting the activity of the PTPs. Three RPTPs (RPTPα, RPTPσ and DEP-1; Gross *et al.*, 1999) have been found to be partially inactivated upon UV irradiation, most probably via an unidentified reactive intermediate that oxidises the catalytic Cys. In addition, hydrogen peroxide can inactivate PTPs (including LAR; Denu and Tanner, 1998) by oxidising the catalytic Cys to its sulfenic acid. The inactivation is specific in that it does not affect serine/threonine phosphatases, and is reversible, as one would expect for a physiologically relevant mechanism. This is particularly interesting considering the recent findings that growth factor stimulation of cultured cells leads to a transient increase in the cellular level of hydrogen peroxide which is required for the growth factor-induced tyrosine phosphorylation. An intracellular PTP (PTP1B) has been found to be reversibly inactivated by the hydrogen peroxide produced in response to EGF

stimulation in A431 carcinoma cells (Lee *et al.*, 1998), and the same can happen for RPTPs as well.

Reversible protein phosphorylation seems to play an important role in the regulation of RPTP activity, as suggested by studies on CD45 and RPTPα. In particular, serine (Ser) phosphorylation of CD45 was reduced following treatment of T cell lines with ionomycin, which increased the intracellular calcium concentration. As a possibly direct consequence, the PTPase activity of CD45 was reduced (Ostergaard and Trowbridge, 1991). A similar effect of Ser phosphorylation on RPTPα activity has been described by den Hertog *et al.* (1995). Treatment of transfected cells expressing RPTPα with the phorbol ester 12-O-tetradecanoyl-phorbol-13-acetate, an activator of protein kinase C, induced a transient increase of RPTPα Ser phosphorylation, concomitant to an increase in its PTPase activity. The Ser phosphorylation sites have been identified as Ser180 and Ser204, in the juxtamembrane domain, and they represent a direct substrate of protein kinase C (Tracy *et al.*, 1995). On the other hand, both CD45 and RPTPα are known to be regulated by tyrosine (Tyr) phosphorylation. It is difficult to study the effect of PTP Tyr phosphorylation on their enzymatic activity due to their efficient autodephosphorylation ability. Nevertheless, work on CD45 demonstrated that its phosphorylation on two Tyr residues, by the p50csk kinase, creates a binding site for another kinase, p56lck, and also causes an increase in the PTPase activity (Autero *et al.*, 1994). As for RPTPα, it is Tyr phosphorylated at least on a C terminal residue (Y789), which creates a binding site for the adapter protein Grb2, without concomitant Sos recruitment (den Hertog and Hunter, 1996; den Hertog *et al.*, 1994; Su *et al.*, 1994). Grb2 attachment may modulate the accessibility of various substrates to RPTPα. In addition, Tyr789 phosphorylation enhances the activity and specificity of RPTPα towards Src pTyr527, as compared to pTyr416 (Zheng *et al.*, 2000).

1.2.4 *In vivo* functions of RPTPs

Novel reports concerning putative functions for RPTPs are currently being published almost weekly, mostly from tissue culture and biochemical experiments. However, the results reported are often contradictory, highly dependent on the experimental design, and rarely tested and confirmed by *in vivo* experiments. A typical example is that of the RPTPβ/ζ, a type V RPTP. As mentioned above, this is by far the best characterised RPTP in terms of ligand binding properties, being shown to interact with a multitude of proteins, either cell surface attached or from the extracellular matrix or circulating cytokines. In addition, a splicing isoform containing only the extracellular region, termed phosphacan, represents one of the most abundant chondroitin sulphate proteoglycans in the brain. Just recently, however, the phenotype of mice deficient in this RPTP has been reported and absolutely none of the predicted abnormalities has been found (Harroch *et al.*, 2000). This may be due either to a redundancy of RPTPs within the central nervous system, or to other compensation mechanisms at downstream levels, reflecting the robustness of the cellular signal transduction pathways. Alternatively, this could be taken as a warning for potential lack of applicability of *in vitro* observations to the *in vivo* situation. Similar comments are valid for members of other RPTP subfamilies, such as RPTPα, RPTPμ or RPTPκ.

In particular, the case of RPTPμ is worth detailing. Initial expression studies have suggested a crucial role for this RPTP in angiogenesis, since it is expressed at high levels in a developmentally regulated fashion, in the forming capillaries of early mouse embryos (Sommer *et al.*, 1997; Fuchs *et al.*, 1998). This triggered a high interest in the light of the new anti-cancer therapies based on angiogenesis inhibitors (reviewed in Kerbel, 2000). RPTPμ was also found to be localised on axonal growth cones and *in vitro* experiments have confirmed its role in modulating the N-cadherin-stimulated outgrowth of the retinal ganglion cells neurites (Burden-Gulley and Brady-Kalnay,

1999). Surprisingly, mice deficient in RPTPμ have no apparent vascular or neural phenotype. Recently, however, a multitude of highly similar receptors has been described, including RPTPλ, RPTPψ, RPTPo and RPTPρ. This suggests that a high level of functional redundancy may indeed protect the stability of key signalling pathways and prevent generation of clear phenotypes in single knockout experiments. At the moment, the detailed molecular mechanisms underlying signal transduction via RPTPμ and its homologues are not known, since no structural data are available for the extracellular region domains. Such experiments may reveal key residues involved in the receptor-ligand interactions, presumably highly conserved in the whole subfamily, and may allow the design of an inhibitory domain able to disrupt such interactions efficiently.

For some RPTPs however, consistent *in vitro* and *in vivo* results have been reported. In particular, the involvement of type II RPTPs in neural development (mainly in axon growth and guidance) has very strong experimental support (reviewed in Stoker, 2001). This subject will be discussed in detail in the sub-chapter 1.3.2.

Two groups have recently generated RPTPσ deficient mice by gene targeting (Elchebly *et al.*, 1999; Wallace *et al.*, 1999). Multiple defects in the central and peripheral nervous system have been observed, including: reduction and hypocellularity of the anterior and posterior pituitary, a severe depletion of luteinizing hormone-releasing hormone (LHRH)-reactive cells in the hypothalamus, a 50-75% reduction of the choline acetyl-transferase-positive cells in the forebrain, slower conduction velocity in the peripheral nerves and hypomyelination. It would also be of interest to find out the visual system phenotype (intraretinal and the retinal-superior colliculus projection), once the detailed analysis has been completed, in order to compare these results with the chick data *in vivo* (F. Rashid-Doubell, I. McKinnell, A. Aricescu and A. Stoker, manuscript submitted).

A recent study has shown that transcriptional levels of several RPTP genes, including LAR and RPTPσ, are significantly altered following experimental sciatic nerve crush in rats (Haworth *et al.*, 1998). Specifically, the RPTPσ mRNA was increased by 50% after 3 days, while LAR expression dropped by 50%. This suggests that, in addition to the growth and guidance roles during embryo development, type II RPTPs might be involved in nerve repair. Accordingly, recent experiments by two groups on different LAR-deficient mouse strains have shown that axons of sciatic nerves regenerate more slowly after crush injuries (Van der Zee *et al.*, 2000; Xie *et al.*, 2001) compared to control animals, indicating a requirement for LAR in the repair process. On the other hand, preliminary results obtained on RPTPσ-deficient mice suggest that their peripheral motor nerve axons regenerate significantly faster than in control animals (M. Tremblay, personal communication).

RPTPδ, another member of the type IIa subfamily, has recently been implicated in the regulation of hippocampal synaptic plasticity and in processes related to learning and memory, following analysis of deficient mice (Uetani *et al.*, 2000). It may be speculated that RPTPδ, whose extracellular region is known to bind in a homophilic manner (Wang and Bixby, 1999), might be involved in cell-cell interactions and synaptogenesis. On the other hand RPTPδ may regulate, via direct dephosphorylation, ion channel activity at the synapse level. Such an interaction has recently been demonstrated for RPTPε, where a substrate-trapping mutant associates with the voltage-gated potassium channel Kv2.1 (Peretz *et al.*, 2000). RPTPε deficient mice exhibit hypomyelination of sciatic nerve axons together with increased activity and hyperphosphorylation of Kv2.1 and Kv1.5 channel α-subunits in sciatic nerve tissue and in primary Schwann cells. Therefore it seems that *in vivo* RPTPε antagonises activation of Kv channels by tyrosine kinases and is involved in Schwann cell function.

The hematopoietic system represents another well-documented field in which RPTPs are involved. Specifically, the type I subfamily member CD45, with many splice isoforms, is expressed abundantly on all nucleated hematopoietic cells (Alexander, 2000). The extracellular region of CD45 does not resemble cell adhesion molecules, although a single FNIII domain has been identified (Figure 1.1). Gene targeting of exon 6, in mice, abolished expression of all CD45 isoforms in B cells and most T cells (Kishihara *et al.*, 1993). As a consequence, in $CD45^{exon6-/-}$ mice, B cells developed normally while T cell development was severely impaired. CD45 is also involved in modulating signalling events downstream of the T cell receptor (TCR) (reviewed in Frearson and Alexander, 1997; den Hertog *et al.*, 1999). CD45 can dephosphorylate the inhibitory C-terminal pTyr residues in Lck and Fyn, triggering the activation of these Src-family protein tyrosine kinases and therefore phosphorylation of the TCR complex, including CD3ε and TCRζ on so-called Immunoreceptor Tyrosine-based Activation Motifs (ITAMs). This generates binding sites for SH2-containing signalling molecules including the protein tyrosine kinase ZAP-70, thereby initiating subsequent intracellular signalling (Qian and Weiss, 1997). CD45 seems to be essential for TCR signalling since Lck and Fyn are inactive in $CD45^{-/-}$ thymocytes, the TCR complex is not phosphorylated and downstream signalling is abolished.

Most recently, a new research area regarding the involvement of RPTPs in human diseases has been opened. Studies of obese humans and rodents demonstrate that the expression and/or activity of specific PTPs, including the type II RPTP LAR, are significantly increased in muscle, liver and adipose tissue (Zabolotny *et al.*, 2001 and references therein). In cell cultures LAR overexpression inhibits tyrosine phosphorylation of the insulin receptor and insulin receptor substrate 1 (IRS1) thereby modulating insulin signalling (Zhang *et al.*, 1996; Li *et al.*, 1996). LAR transgenic mice that overexpress human LAR specifically in muscle, to levels comparable to those

reported in obese (insulin-resistant) humans, manifest whole-body insulin resistance (Zabolotny *et al.*, 2001). This seems to be caused by LAR-induced dephosphorylation of specific pTyr residues on the IRS proteins, mainly IRS2, which reduced their association to other downstream molecules in the insulin signalling pathway such as p85α and PI3K. Therefore, it appears that overexpression of LAR and (possibly) other PTPs with similar substrate specificities has an important pathogenic role in the development of insulin resistance, thus representing potential targets in antidiabetic therapies.

Conclusions

Receptor protein tyrosine phosphatases are a diverse family of receptor enzymes, both at structural and functional levels. Twenty RPTPs have been identified in the human genome so far (Figure 1.2). Many questions are still to be answered regarding the identity of the ligands for the extracellular domains of most representatives and the molecular mechanisms by which these receptor-ligand interactions modulate the enzyme activity and trigger intracellular signalling reactions. More important is to fully characterise the functions of these receptors *in vivo*, since in most cases these could have clinical significance. In particular, modulating the functions of cell adhesion molecule-like RPTPs, many of them involved in nervous system development and nerve repair, may be useful in certain pathological conditions.

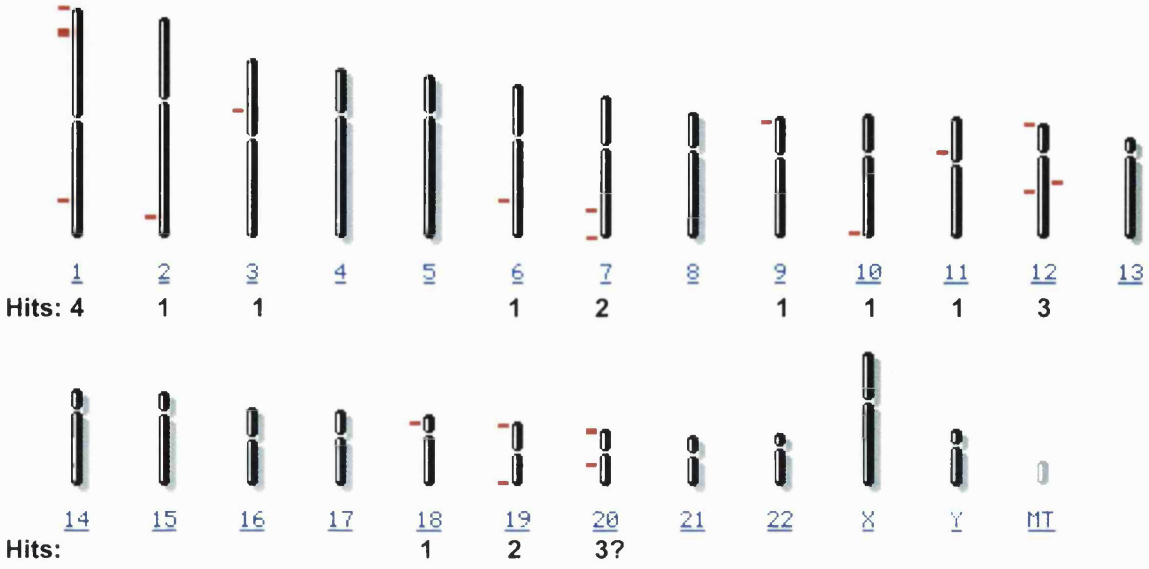

Chromosome	Cytogenetic map	Gene	Name	RPTP Type
1	1p36.3	*Ptprz2*	HPTPζ2	V
1	1p35.3-p35.1	*Ptpru*	PCP2, RPTPψ RPTPπ, HPTP-J	II b
1	1p34	*Ptprf*	LAR	II a
1	1q31-1q32	*Ptprc*	CD45, LCA	I
2	2q35-q36.1	*Ptprn*	IA2	VI
3	3p21-p14	*Ptprg*	RPTPγ	V
6	6q22.2-q23.1	*Ptprk*	RPTPκ	II b
7	7q31.3	*Ptprz1*	RPTPζ/β1	V
7	7q36	*Ptprn2*	IA2β	VI
9	9p23-p24.3	*Ptprd*	RPTPδ	II a
10	10q26	*Ptpre*	RPTPε	IV
11	11p11.2	*Ptprj*	DEP1, HPTPη	III
12	12	*Ptprr*	PTPBR7, PTP-SL	VII
12	12p13.3-p13.2	*Ptpro*	GLEPP1, PTP-U2	III
12	12q15-q21	*Ptprb*	RPTPβ	III
18	18p11.2	*Ptprm*	RPTPμ	II b
19	19p13.3	*Ptprs*	RPTPσ	II a
19	19q13.4	*Ptprh*	SAP-1, PTPRH	III
20	?	LOC82334	"RPTPα-like"	IV
20	20p13	*Ptpra*	RPTPα	IV
20	20q12-q13	*Ptprt*	RPTPρ	II b

Figure 1.2. The human receptor protein tyrosine phosphatases.

1.3 Axon growth and guidance mechanisms. The role of RPTPs

1.3.1 Introduction

The nervous system is an extremely efficient information-processing unit, built as a very complex and precise network of excitable cells (the neurons) intimately associated with essential support cells (the glia). Over a trillion neurons are present in an adult human brain and each one makes (on average) about one thousand connections with target cells (Tessier-Lavigne and Goodman, 1996). The accuracy of this connectivity pattern, established mainly during embryogenesis, is vital for the proper functioning of the nervous system. Of course, the physical establishment of the neural networks represents only the initial step in their development (so-called "activity-independent"). They will be subsequently refined and strengthened under the influence of the precise patterns of electrical activity in neurons (Tessier-Lavigne and Goodman, 1996).

Many neurons must send long cellular extensions (axons) in order to reach targets located as far away as over a thousand times the diameter of their cell body. Axon growth is in fact a very special form of cellular movement in which only a very small part of the cell, the growth cone, is motile. This motility is a direct expression of the continuous remodelling of the growth cone cytoskeleton, which mainly consists of a very dense network of actin filaments. The complex environment surrounding the growth cone, which provides numerous signals, largely determines the rate and direction of axon growth. All these signals are continuously being "recorded" by the growth cone's highly specialised plasma membrane, via its large collection of receptors, then integrated down the signalling pathways and finally transferred to the dynamic actin cytoskeleton thus modulating its polymerization rate and direction.

According to Tessier-Lavigne and Goodman (1996), four types of mechanisms contribute to guiding growth cones through their environment: contact attraction,

chemoattraction, contact repulsion and chemorepulsion. However, the molecular basis of these mechanisms seems to be rather complicated. One cannot find discrete classes of diffusible (long-range) and non-diffusible (short-range) factors, some attractive and others repulsive. A diffusible chemotropic factor can act locally and function in a contact-dependent fashion by binding to extracellular matrix components or to cell surfaces. On the other hand, nondiffusible molecules are sometimes expressed in linear gradients over a certain area, hence behaving as chemotropic cues, like the *bona fide* diffusible factors (Mueller, 1999). In addition, the way the axon reacts to extracellular signals is highly dependent on its own physiological state. For example, a single growth cone can respond to the same diffusible cue (such as neurotrophins and netrins) in a manner dependant on the cytosolic level of cAMP, resulting in either attraction or repulsion (see netrins paragraph below).

Many of the ligand-receptor pairs that control axon growth and guidance have been described in the last ten years (extensively reviewed in Tessier-Lavigne and Goodman, 1996; Mueller 1999; Chisholm and Tessier-Lavigne, 1999; Van Vactor and Lorenz, 1999; Stoker, 2001). Recent advances concerning the most important ones, as currently understood, will be briefly discussed below, followed by a review of the role played by RPTPs in these processes.

Cell adhesion molecules (CAMs). A common observation regarding nervous system development is that growing axons usually travel in large fascicles (tracts) which follow pre-defined pathways, established by so-called "pioneer" axons. Therefore, the cell-cell adhesion between axons comprising a fascicle is an essential phenomenon, and is one in which CAMs are actively involved. Two major types of protein-protein interactions support the CAM functions and represent criteria for their classification: calcium-mediated protein binding involving cadherins such as N- and R-cadherin (both

shown to be able to promote neurite outgrowth) and direct protein binding, usually mediated by immunoglobulin-like domains (the Ig-CAM superfamily) (reviewed in Van Vactor, 1998; Doherty *et al.*, 2000).

The Ig-CAMs, all of them type I transmembrane proteins, usually contain a large ectodomain but only very short intracellular regions, lacking obvious motifs that would promote interaction with other signalling molecules. Therefore they were thought to promote axonal growth by directly modulating the adhesion of the growth cone to cellular substrates, predominantly in a homophilic fashion. Recent results however have challenged this view. NCAM and L1 (reviewed in Walsh and Doherty, 1997) and also N-cadherin (Peluso, 2000), following homophilic binding, can interact most probably in *cis* with FGF receptors within the growth cone. This interaction activates a receptor tyrosine kinase signalling cascade involving activation of PLCγ to generate diacylglycerol (DAG), hydrolysis of DAG to arachidonic acid by DAG lipase, an arachidonic acid-induced increase in calcium channel permeability and activation of Ca^{2+}/calmodulin-activated kinase (Williams *et al.*, 1995).

As mentioned above, CAMs are seen as key promoters of axonal fasciculation. However, as axons approach their distinct targets, they need to defasciculate. A very interesting mechanism regulating the affininy of homophilic binding has been recently described for NCAM, by controlled addition/removal of the negatively charged carbohydrate polysialic acid (PSA; Rutishauser and Landmesser, 1996). The addition of PSA to the NCAM extracellular region reduces the NCAM-mediated adhesion, a phenomenon described for motor neurons as axons defasciculate in the plexus region of the chick embryo limb before reaching the appropriate muscular targets. PSA removal by endoneuraminidase N leads to accumulation of significant projection errors (Van Vactor, 1998).

Extracellular matrix (ECM) molecules and their receptors. A large number of ECM molecules including laminins, various collagen types, tenascins, thrombospondin, fibronectin, heparan sulphate and chondroitin sulphate proteoglycans can act either as promoters or inhibitors of neurite outgrowth *in vitro* (Tessier-Lavigne and Goodman, 1996). Most of them are also expressed along axon growth pathways *in vivo*, at key developmental stages. Several classes of axonal receptors for ECM molecules are known, including integrins, Ig superfamily proteins and proteoglycans.

Amongst these receptors, integrins are probably understood in the greatest detail. They are known to form heterodimers between one α (out of eighteen identified to date) and one β (out of eight described) subunit, resulting in more than twenty receptor combinations (Humphries, 2000). Integrins can bind a wide panel of ECM constituents, such as laminin, fibronectin, vitronectin and collagens. Cell culture experiments have definitively established integrins as key regulators of focal adhesion complexes, therefore linking cell-matrix contact events with the actin cytoskeleton reorganisation. Despite this, targeted disruptions of integrin function in vertebrates have generated no significant axonal phenotypes (Van Vactor, 1998). This may be due to such a high variability and possibly redundancy in the integrin family. In *Caenorhabditis elegans* however, mutations in the α-integrin gene *ina-1* resulted in disruption of the axon fasciculation in several pathways (Baum and Garriga, 1997).

The role played by heparan sulphate proteoglycans (HSPGs) in axon growth has also attracted a significant interest in the last couple of years. Since most of this thesis will analyse their relationship with the type II RPTP CRYPα, they will be discussed in more detail in the following chapters. It is worth mentioning here that, as soon as specific antibodies became available, the ECM HSPGs were found to be localised in the basement membranes and all along axon tracts during the time of active axon outgrowth in embryogenesis (Halfter, 1993). Experiments in *Xenopus* reported by Walz *et al.*

(1997) have demonstrated that both heparitinase treatment and addition of soluble heparan sulphate significantly affect retinotectal pathfinding. On the other hand, heparitinase but not chondroitinase ABC pre-treatment of basal laminae inhibits the growth rate of retinal axons (Chai and Morris, 1999). The current view is that HSPGs act as promoters of neurite outgrowth, as opposed to the effect exerted by chondroitin sulphate proteoglycans, most probably by binding, clustering and presenting small circulating heparin-binding molecules (such as growth factors) to their growth cone receptors. Indeed this seems to be the case at least for the fibroblast growth factors, where a HSPG plays a key role in the receptor complex, stabilising the interaction between FGFs and their protein tyrosine kinase receptors. Results reported in this thesis demonstrate, for the first time, that ECM HSPGs can also function as ligands for an axon growth promoting RPTP.

Unexpected but very interesting results concerning an ECM protein abundant in the developing brain, laminin-1, have been recently reported (Hopker *et al.*, 1999). Laminin-1 has the ability to convert netrin-1-induced growth cone attraction into repulsion. The molecular mechanism involved is not fully understood yet but seems to rely on the reduction of cytosolic cAMP levels via the $\alpha 6\beta 1$ integrin receptor. Cytosolic cAMP concentration is known to modulate netrin response (see netrins paragraph below). On the other hand, in the developing retina, laminin-1 is concentrated in the basal laminae and is an excellent growth substrate for pioneer axons. However, the axons must leave the eye at the optic nerve head, a region expressing high levels of the chemoattractant netrin-1. It seems that laminin-1 modulation of netrin signalling can help the axons leave the vitreal side of the retina and dive into the optic nerve.

Receptor protein tyrosine kinases (RPTK). Protein tyrosine phosphorylation, as discussed above, is a key signalling mechanism. Therefore it is not surprising that a

variety of RPTKs have been shown to modulate axon growth and target innervation. These include FGF receptors (McFarlane *et al.*, 1995 and 1996), neurotrophin receptors of the Trk family (Barbacid, 1995) and the *Drosophila* Derailed (Callahan *et al.*, 1995). The Eph receptors, the largest RPTK subfamily, with 14 representatives described to date, are also major modulators of axon growth and guidance. The interaction between Eph receptors and their ephrin ligands is involved in many key processes in vertebrate neural development including the organisation of the retinotectal system, the establishment of topographic maps, forebrain and hindbrain patterning and the formation of certain commissures (reviewed in Flanagan and Vanderhaeghen, 1998; Wilkinson, 2001). The ephrin ligands act as contact-dependent repulsive factors for retinal, motor and cortical axons, and for neural crest cells (Drescher, 1997). In addition, ephrin A5 seems to play a role in axon fasciculation and in formation of axon branches (Caras, 1997).

Probably the most exciting feature of the Eph-ephrin signalling system seems to be their ability to initiate "bi-directional signalling", which means that the ligand and the receptor can switch roles and initiate signalling events in their respective cells following ligation (Wilkinson, 2001). The activation of Eph receptors following ephrin binding leads to phosphorylation of at least ten tyrosine residues in their cytoplasmic region (Kalo and Pasquale, 1999); some of these are required for upregulation of the tyrosine kinase activity, others represent docking sites for SH2 domain-containing adapter proteins (Mellitzer *et al.*, 2000). The regulation of growth cone dynamics via Eph receptors involves modulation of the actin cytoskeleton; however, the exact molecular mechanisms behind this process are still unclear. A recent report shows that a novel guanine nucleotide exchange factor for Rho GTPases, termed ephexin, binds to the EphA receptors and mediates ephrin-A-induced growth cone collapse (Shamah *et al.*, 2001). On the other hand, in the opposing cell, clustering of ephrin-A ligands (GPI

anchored) leads to increased β1-integrin-mediated adhesion and formation of filopodia, which involves the Fyn tyrosine kinase activity (Davy *et al.*, 1999).

Another interesting observation supports the idea that, in certain circumstances, Eph receptor activation can promote cell adhesion rather than repulsion. Ephrin-A5 and EphA7 are co-expressed in the lateral edges of the neural plate and promote adhesion during neural tube closure (Holmberg *et al.*, 2000).

Netrins and their receptors. Netrins are a small family of secreted guidance molecules, highly conserved in evolution, which can exert both attractive and repulsive effects on growing axons, depending on the corresponding receptor expressed at a certain time and location. Initially netrins were identified as chemoattractant molecules expressed at the midline of the nervous system - CNS of insects and vertebrates and nerve cord of nematodes - (reviewed in Tessier-Lavigne and Goodman, 1996). Subsequently it was demonstrated that netrins are not the only midline chemoattractants since loss of netrin function results only in partially penetrant defects in the midline projections and midline cells from netrin knockout mice still retain a weak chemoattractant activity (Serafini *et al.*, 1996). Netrins are also involved in axon guidance during visual system development, attracting retinal ganglion cells' axons into the optic nerve (Deiner *et al.*, 1997). The attractive effect of netrins is mediated by neuronal receptors of the DCC ("Deleted in Colorectal Cancer") family: UNC-40 in *C. elegans*, Frazzled in *Drosophila*, neogenin and DCC in vertebrates (reviewed in Mueller, 1999).

Netrins can also have a repulsive activity for some axons that project away from the midline in *C. elegans* (Tessier-Lavigne and Goodman, 1996), but also in vertebrates netrin-1 can repel trochlear motor axons (Colamarino and Tessier-Lavigne, 1995). The receptors involved in this repulsive function belong to the UNC-5 family which, like

DCC, are type I transmembrane proteins of the Ig superfamily. Although it seems that an UNC-5 receptor is usually sufficient to mediate repulsion, further complications arise from the studies suggesting that UNC-5 may have to associate with DCC to form a receptor complex which converts attraction to repulsion (reviewed in Chisholm and Tessier-Lavigne, 1999).

Recent reports have added an unexpected new dimension to our understanding of axon guidance signalling: the same extracellular cue (netrin-1) is able to elicit completely opposite responses from the growth cone (i.e. attractive or repulsive) depending on the intrinsic metabolic state of the growth cone (Ming *et al.*, 1997; Song *et al.*, 1997; reviewed in Mueller, 1999). Dissociated *Xenopus* spinal neurons, exposed to gradients of soluble netrin-1 released from a micropipette, changed their growth direction being attracted towards the pipette tip. However, when a nonhydrolysable analogue of cAMP (Rp-cAMPS) or a specific inhibitor of protein kinase A (KT5720) were added to the culture medium, netrin-1 induced repulsive turning of the same growth cone. Importantly, addition of a blocking antibody against DCC abolished both the attractive and repulsive responses induced by netrin-1. The downstream signalling pathway responsible for this behaviour is still far from being clear, nevertheless cAMP and PKA are known to have negative effects on the small GTPase RhoA, an important regulator of the actin cytoskeleton. In neuron-like PC12 cells and in primary neuron cultures RhoA activation leads to rapid growth cone collapse and neurite retraction (or neurite growth inhibition), and these effects are prevented by a specific RhoA inhibitor (Tigyi *et al.*, 1996; Kozma *et al.*, 1997).

Slit proteins and their Robo receptors. The recent research efforts aimed at fully characterising the molecular axon guidance mechanisms at the midline in *Drosophila* have unveiled a new molecular system involved in repulsive signalling: the interaction

between the type I receptor proteins Robo (*roundabout*), their soluble ligands (Slit family) and a type II transmembrane protein Comm (*commissureless*), a modulator of Robo expression.

The Robo protein family, with a CAM-like extracellular region have been considered for a long time as receptors for a putative midline repellent molecule (reviewed in Mueller, 1999; Brose and Tessier-Lavigne, 2000). The expression of Robo on the growth cone surface correlates with the axons' inability to cross the midline. Longitudinally projecting neurons, whose axons never cross the midline, express constantly high levels of Robo; commissural neurons however, whose axons cross the midline only once and then grow alongside it, downregulate Robo expression while they cross the midline. When Robo function is lost these axons will cross and recross the midline freely, hence the "roundabout" phenotype. The Comm protein, expressed by the midline glial cells, was found responsible for downregulating the Robo expression level during midline crossing. How it works exactly is unclear, it seems to be transferred via an unknown mechanism into the axon growth cone's plasma membrane (Tear *et al.*, 1996).

Recently, the midline repellent ligands for Robo receptors have been identified as members of the Slit protein family. These are large (~200 kDa) secreted proteins, well conserved across species, and can function in repelling migrating cells and axons but also, unexpectedly, in stimulating elongation and branching of spinal sensory axons (reviewed in Brose and Tessier-Lavigne, 2000). Subsequent studies have established the importance of the Slit-Robo signalling system in the retinal axon growth and pathfinding (Erskine *et al.*, 2000; Ringstedt *et al.*, 2000). Robo1 and Robo2 are expressed in the retinal ganglion cell (RGC) layer, while Slit2 is strongly expressed in the retina, along the optic stalk and in the ventral diencephalon but it is absent from the

ventral midline where the optic chiasm forms. Slit2 can also inhibit RGC axon outgrowth *in vitro*.

Finally, a recent report has revealed a very interesting functional link between the netrin-1/DCC and Slit/Robo signalling mechanisms (Stein and Tessier-Lavigne, 2001). As discussed above, axonal growth cones that cross the nervous system midline are attracted towards it by netrins, signalling via their DCC receptors. In order to cross the growth cones must lose responsiveness to the netrin attractant, despite maintaining the expression of DCC at constant levels, and must also upregulate Robo in order to become repelled by Slit. The authors have shown that upregulation of Robo silences the attractive effect of netrin-1, but not its growth-stimulatory effect, through direct binding between the cytoplasmic domain of Robo to that of DCC. This receptor silencing mechanism requires activation of Robo via ligand binding (either Slit or a growth factor in case of chimaeric Robo constructs containing growth factor receptor-derived extracellular regions). This Robo-DCC binding relation is asymmetric: "activation" of Robo causes binding to DCC but "activation" of DCC does not cause binding to Robo. The functional consequence of such a "hierarchical" organization of guidance receptors is thought to be a better synchronisation of repulsion and loss of attraction, thus ensuring that the growth cone will not stall at the midline.

Semaphorins, neuropilins and plexins. Semaphorins are one of the largest families of guidance molecules consisting of more than thirty members (Mueller, 1999; Chisholm and Tessier-Lavigne, 1999). All members are characterised by the presence of a ~500 amino-acid "sema" domain but outside of this there is little conservation. Some representatives are secreted, others are transmembrane type I proteins or membrane attached via a GPI linkage.

Semaphorins are best known as repulsive guidance cues. The secreted Sema 3A is an extremely potent inducer of growth cone collapse. However, when attached to beads it can repel sensory neuron axons without inducing full growth cone collapse (Fan and Raper, 1995). This situation might have relevance *in vivo* since Sema 3A contains a highly basic region at the C terminus that might represent a proteoglycan attachment site. Sema 3A can also promote axon fasciculation *in vivo*, by repelling responsive axons and thus forcing them together when present in their surrounding environment. However, the *Drosophila* transmembrane Sema-1a seems to be required for defasciculation of motor axons. Therefore, it appears that the membrane attachment state is a key modulator of semaphorin function (Chisholm and Tessier-Lavigne, 1999).

Neuropilins were the first semaphorin receptors identified (He and Tessier-Lavigne, 1997; Kolodkin *et al.*, 1997). They contain a long extracellular region with several domains known to be involved in protein-protein interactions, but their 40 amino acid long intracellular region, highly conserved in vertebrates, contains no obvious motif. In fact the intracellular region of neuropilin-1 is not even required for its biological activity (Nakamura *et al.*, 1998). The observation that although neuropilin-1 is required for Sema 3A action (binding it with high affinity) yet appears to be incapable of transmitting a signal inside the growth cone, has prompted the search for a co-receptor. Recent reports (Tamagnone *et al.*, 1999; Takahashi *et al.*, 1999) have identified this co-receptor as a member of the plexin family. Certain semaphorins, other than Sema 3A, can bind directly to plexins. For example, in *Drosophila* plexin-A is a functional receptor for semaphorin-1a, human plexin-B1 is a receptor for the transmembrane semaphorin Sema 4D and plexin-C1 is a receptor for the GPI-anchored semaphorin Sema 7A. Interestingly, plexins themselves contain a sema domain in their extracellular region. In the case of plexin-A1 this sema domain prevents its activation in the basal state, via an autoinhibitory mechanism; binding to the Sema 3A-neuropilin-1

complex releases this inhibition (Takahashi and Strittmatter, 2001). The intracellular domain of plexins is responsible for triggering the growth cone's response to semaphorins, such as collapse, repulsion, or turning. Details of the downstream signalling pathways are only now emerging; it seems that monomeric G proteins, the Rac1 GTPase and a family of neuronal proteins called CRMPs are all involved but it is not yet clear exactly how (Nakamura *et al.*, 2000). Very recently Driessens *et al.* (2001) found that plexin-B1 receptor interacts directly with active Rac and regulates the actin cytoskeleton by activating Rho, thus establishing the Rho family GTPases as key intermediates in semaphorin signalling.

Finally it is worth mentioning that, as discussed for netrins, the interpretation of semaphorin signals is also highly dependent on the physiological state of the growth cone (as a result of many other signals). For example, elevated levels of cGMP can convert the Sema 3A response of *Xenopus* spinal growth cones from repulsion to attraction (Song *et al.*, 1998).

Nogo and the Nogo receptor. Axons in the embryonic CNS and also in the adult peripheral nervous system can grow and regenerate efficiently after injury. Unfortunately, this is not the case in the adult CNS. Significant research efforts have been directed towards understanding this phenomenon and the first encouraging results demonstrate that axons themselves do not lose the ability to regrow in a permissive environment. Therefore, there must be external inhibitory factors responsible for their growth arrest *in vivo*. Such factors seem to be present in the glial scar which forms at the site of injury, where chondroitin sulphate proteoglycans and possibly other associated molecules appear to be involved, but also in the myelin that ensheats axons in the white matter tracts of the adult CNS (reviewed in Brittis and Flanagan, 2001). Very exciting results have been obtained using a monoclonal antibody (IN-1) raised

against a 250 kDa neurite inhibitory protein of the CNS myelin: IN-1 treatment of rats with a spinal cord injury caused a marked improvement of corticospinal axon regeneration and locomotor function recovery (Bregman *et al.*, 1995; Merkler *et al.*, 2001).

The myelin-associated neurite growth inhibitor recognised by the IN-1 antibody has been recently cloned and named Nogo (Chen *et al.*, 2000; GrandPré *et al.*, 2000; Prinjha *et al.*, 2000). Three Nogo isoforms have been described, the 250 kDa one being Nogo-A. All are transmembrane proteins although the exact topology is still controversial, and they are expressed on the surface of oligodendrocytes. The potent inhibitory function seems to be located in a 66 amino acid region (termed Nogo-66) exposed on the extracellular surface, although a cytoplasmic N-terminus region (termed amino-Nogo) may contribute to the inhibition of axon regeneration at sites of oligodendrocyte lysis. An 85 kDa GPI-anchored protein expressed by spinal cord axons, termed NgR, was recently cloned and shown to be a functional receptor for Nogo-66 (Fournier *et al.*, 2001). Some neuronal populations, such as retinal ganglion cells, do not respond to Nogo-66 and do not express NgR either. However, ectopic expression of NgR in such cells converts their growth cones to a Nogo-66 sensitive state (it induces growth cone collapse). Therefore, NgR seems to be sufficient to bind Nogo-66 and, most probably, it will mediate signal transduction into the growth cone cytoplasm as a part of a receptor complex with a transmembrane protein. Such a protein is still to be identified. Nevertheless, molecules able to block the Nogo-66/NgR interaction may have great pharmaceutical potential as promoters of axonal regeneration for certain neuronal types.

1.3.2 Receptor protein tyrosine phosphatases in axon growth and guidance

A large body of evidence has established that regulated tyrosine phosphorylation is an essential mechanism for controlling various axon growth and guidance events. Studies in the early 1990s have shown that protein tyrosine kinase (PTK) inhibitors can potentiate substrate-induced neurite outgrowth (Bixby and Jhabvala, 1992) and modulate growth cone morphology (Wu and Goldberg, 1993). Specific RPTKs such as the FGF receptors and the Eph receptors (see above), but also non-receptor PTKs like Src, Fyn, Yes, Lyn and Abl (reviewed in Desai *et al.*, 1997; Korey and Van Vactor, 2000) are known to play important roles in controlling growth cone behaviour. Since tyrosine phosphorylation is a reversible event (with a high turnover rate), the PTPs must play equally important roles. Moreover, the RPTPs containing CAM-like ectodomains are particularly well equipped to play a significant role by combining their catalytic function with cell adhesion, a key process for the growth cone. In addition, RPTPs may trigger signalling events following binding to soluble ligands. Early studies have confirmed that RPTPs are present in the right place at the right time, i.e. on the membrane of growing axons (Tian *et al.*, 1991; Yang *et al.*, 1991; Stoker *et al.*, 1995). Since then, an impressive research effort has provided proof that RPTPs also do the predicted job: they modulate axon growth not only *in vitro* but also *in vivo,* in a variety of animal models such as *Drosophila*, leech, *Xenopus*, chicken and mouse (reviewed in Stoker and Dutta, 1998; Van Vactor, 1998; den Hertog *et al.*, 1999; Stoker, 2001). The main findings will be summarised below.

Drosophila *axon guidance in the neuromuscular system.* *Drosophila* genome analysis suggests that there might be up to eight RPTP genes (Morrison *et al.*, 2000). Five of them are characterised thus far and, remarkably, four of these are selectively expressed in CNS axons (Sun *et al.*, 2001 and references therein). These four enzymes

(DPTP10D, DLAR, DPTP69D and DPTP99A, all being type II or type III RPTPs) regulate axon guidance decisions (Desai *et al.*, 1996, 1997; Krueger *et al.*, 1996; Sun *et al.*, 2000, 2001). Mutants lacking DLAR or DPTP69D alone display altered guidance of the intersegmental nerve b (ISNb) axons in the neuromuscular system (Desai *et al.*, 1996; Krueger *et al.*, 1996). When two or more RPTPs are eliminated the observed phenotypes becomes more drastic. For example, when DLAR and DPTP69D are both missing, the ISN stalls at its second intermediate target (Desai *et al.*, 1997). Removal of DLAR, DPTP69D and DPTP99A prevents the ISN root from extending even beyond its first intermediate target. Single mutants lacking DPTP10D or DPTP99A did not show clear phenotypes in the neuromuscular system. Recently though, Sun *et al.* (2001) have reported a very detailed study of these RPTPs, by analysing double-, triple- and quadruple-mutant embryos lacking all possible RPTP combinations. A very complex interaction pattern has emerged: at various choice points (groups of) RPTPs can either be functionally redundant, compete or collaborate.

DPTP10D for example regulates, together with the other three RPTPs, the outgrowth and bifurcation of the SNa (segmental nerve a) motor nerve but loss of DPTP10D partially suppresses the ISN truncation phenotype observed in the DLAR, DPTP69D and DPTP99A triple mutant. Again, DPTP10D acts together with the other three RPTPs to facilitate ISNb defasciculation at the exit junction in order to innervate the ventrolateral muscles (VLM). ISN axon guidance at several decision points is severely disrupted in the quadruple mutants, however other guidance decisions are only moderately affected (Sun *et al.*, 2001). This may be due to competitive interactions between these RPTPs or may suggest that additional RPTPs could be involved or simply that tyrosine phosphorylation is not a significant signalling mechanism for every guidance decision.

The signalling pathways downstream of *Drosophila* RPTPs have recently begun to be unveiled. The protein tyrosine kinase Abl functions as an antagonist of DLAR in regulating the entry of ISNb into the VLM field (Wills *et al.*, 1999). This requires the Abl kinase function but also the presence of Ena, an Abl substrate *in vivo*. Both Abl and Ena can associate with the DLAR membrane-distal phosphatase domain and both can serve as substrates for DLAR *in vitro*. On the other hand Abl can phosphorylate DLAR *in vitro*, suggesting a very interesting cross-regulatory mechanism between these enzymes.

At least three signalling pathways might be modulated by the DLAR/Abl couple (reviewed in Lanier and Gertler, 2000):

- regulation of cadherin/catenin-dependent cell adhesion: LAR associates with the cadherin/catenin complex and loss of Abl expression significantly exacerbates axonogenesis defects observed after Armadillo (β-catenin) disruption.
- regulation of the actin cytoskeleton via Ena: Ena can modulate actin polymerization possibly by interacting with the actin monomer-binding protein profilin.
- regulation of the actin cytoskeleton via the guanine nucleotide exchange factor Trio: the small GTPase Rac1 seems to play a role in the DLAR signalling pathway and human LAR can bind the Rac-activating protein Trio; however, DTrio lacks the Ser/Thr kinase domain necessary for human TRIO in order to bind LAR.

The most probable outcome of the relevant interactions will be a modulatory effect on the growth cone motility, allowing it to slow down, pause, turn, explore choice points, reactivate growth and finally innervate the appropriate target.

Drosophila *axon guidance at the midline.* As already mentioned above, the CNS midline produces both attractive and repulsive signals, thus influencing growth cones' behaviour. Sun *et al.* (2000) have recently shown that RPTPs are involved in

modulating the response to repulsive signals. Specifically, *Drosophila* mutants that lack both DPTP10D and DPTP69D produce a phenotype in which a subset of longitudinal axons are re-routed across the midline. Elimination of all four neural RPTPs leads to conversion of most longitudinal pathways into commissures. DPTP10D and DPTP69D genetically interact with Robo, Slit and Comm. The *comm/Ptp10D/Ptp69D* triple mutant axons are able to cross the midline, which suggests that Robo-mediated repulsion from the midline is reduced in the absence of RPTPs. *Robo/PTP10D/Ptp69D* triple mutants have a severe phenotype in which most of the axons converge on the midline into a thick bundle (similarly to the *slit* phenotype). The removal of just one copy of *slit* from the *Ptp10D/Ptp69D* double mutant significantly enhances its phenotype, whereby more axons cross the midline and the longitudinal tracts move closer together. However, the RPTP genes did not interact with *netrin-1* or *2*, showing specificity in affecting the repulsive system rather than a generalised suppression of any phenotype that reduces midline crossing (Sun *et al.*, 2000). Taken together, all the above observations suggest that RPTPs are positive regulators of the Robo signalling pathways. It is still unclear whether RPTPs modulate Robo by direct dephosphorylation or they are placed in separate pathways that only interact further downstream. Interestingly, recent results suggest that Abl tyrosine kinase and its substrate Ena play direct and opposing roles in Robo signal transduction (Bashaw *et al.*, 2000). Both proteins can directly bind to Robo's cytoplasmic domain and it appears that Robo itself is a substrate for Abl. As discussed above, at least one *Drosophila* RPTP, DLAR, can interact with and dephosphorylate Abl and Ena, but others such as DPTP10D and DPTP69D might do as well (Wills *et al.*, 1999). A detailed study of all these putative interactions might therefore contribute to understanding the molecular mechanisms of RPTP involvement in midline guidance.

Drosophila *retinal axon guidance.* The analysis of *Drosophila* photoreceptor axon guidance has provided further insights into the *in vivo* functions of RPTPs. Adult *Drosophila* visual system development is a very neat model for axon guidance studies. Axons of the eight photoreceptors in each ommatidium fasciculate together and project as a single bundle towards the optic lobes of the brain. Once there, the axons defasciculate and connect to distinct optic lobe layers. R1-R6 axons project to the lamina, while R7 and R8 project to separate layers of the medulla. Garrity *et al.* (1999) found that DPTP69D is required for lamina target specificity. In *DPTP69D* mutants R1-R6 project through the lamina and terminate in the medulla. Immunohistochemical analysis confirmed that DPTP69D is localised in the R1-R6 growth cones and various deletion constructs used for phenotypic rescue demonstrate that both the DPTP69D phosphatase activity and the integrity of the FNIII-like domains in the extracellular region are required for correct targeting.

A recent report shows that DPTP69D is also required for the correct targeting of R7 (Newsome *et al.*, 2000). Mutant R7 axons fail to reach their target in the medulla, stopping instead at the same level as the R8 axons. The authors conclude that DPTP69D plays a permissive rather than an instructive role (as suggested before) possibly by reducing the adhesion of R1-R6 and R7 growth cones to the pioneer R8 axon, thus allowing them to respond independently to specific targeting cues. However, further investigations are required in order to characterise the DPTP69D signalling pathway(s) and hence to understand the observed phenotypes.

Comb cell processes and mutual avoidance. Comb cells are present in pairs in the peripheral body wall in each of the mid-body segments of embryonic *Hirudo* leeches. Their spindle-shaped cell bodies are aligned along the antero-posterior axis and produce approximately 70 neurite-like parallel processes, each bearing large growth

cones. Half of these processes extend anterolaterally and half posteromedially in a striking, oblique pattern thought to provide a scaffold for the developing oblique muscle layer of the embryo; after these muscles are established the Comb cells (CC) die (Baker and Macagno, 2000). The CC processes rarely branch and never overlap with one another, a phenomenon called "mutual avoidance". They express on the surface (including the growth cones) high levels of a LAR-like RPTP, termed HmLAR2 (Gershon *et al.*, 1998). A series of experiments support the hypothesis that HmLAR2 is able to mediate the mutual avoidance by CC processes. Antibodies against HmLAR2 extracellular region, injected into *Hirudo* embryos, cause a severe disruption of the regular parallel pattern and frequent cross-overs can be observed (Gershon *et al.*, 1998). The same cross-over phenotype was observed following HmLAR2 elimination via RNA interference (Baker and Macagno, 2000); in addition this caused a marked reduction in CC processes' length (or growth rate) and significant growth cone collapse. Interestingly, the extracellular region of HmLAR2 seems to exhibit homophilic binding and it was suggested that this might be responsible for the mutual avoidance of sibling processes by triggering growth cone retraction in case of contact.

In vitro *studies: RPTPs as promoters of neurite outgrowth.* A large number of RPTPs are expressed in the nervous system and in most cases *in vitro* studies suggest their involvement in axon growth modulation.

CRYPα, the chick orthologue of RPTPσ, was the first vertebrate RPTP found expressed on the membrane of migrating growth cones, both on lamellipodia and filopodia (Stoker *et al.*, 1995). The CRYPα extracellular region, unlike HmLAR2 or other CAM-like RPTPs, does not bind in a homophilic manner (Haj *et al.*, 1999). A soluble form of the ectodomain however, is able to cause a significant axon growth reduction when added to retinal ganglion cells plated on retinal basal lamina. This

substrate contains physiological ligands (Ledig *et al.*, 1999a) and presumably the ectodomain competes with the endogenous CRYPα for ligand binding. Therefore, it was inferred that the interaction between the growth cone CRYPα and its ligands plays a key role in promoting retinal axon growth. Similar results were obtained when the above interaction was blocked with anti-CRYPα antibodies. On the other hand, recent results suggest that overexpression of an inactive, putative dominant negative, CRYPα intracellular construct in *Xenopus* retinal ganglion cells enhances neurite outgrowth in a substrate-dependent manner (Johnson *et al.*, 2001). The fact that blocking CRYPα-ligand interaction slows down the axons, while competing with its phosphatase function enhances neurite outgrowth, suggests that binding of CRYPα ligands causes a reduction of its phosphatase activity which in turn leads to growth promotion. A more detailed discussion will be presented in subchapter 1.4.

RPTPδ is a type IIa RPTP whose extracellular domain promotes cell adhesion, possibly via its homophilic binding properties (Wang and Bixby, 1999). A variety of neuronal populations such as forebrain, ciliary ganglion, retinal and cerebellar neurons were found to adhere strongly on substrates coated with a RPTPδ ectodomain-Fc fusion protein. RPTPδ can also promote neurite outgrowth but only from forebrain neurons, which suggests that adhesion and neurite growth promotion are separate functions. A soluble form of RPTPδ ectodomain was also able to induce significant neurite outgrowth when added to forebrain neurons plated on a poly-D-lysine substrate. In addition, Sun *et al.* (2000) have recently shown that RPTPδ can also function as a chemoattractant for neurites of forebrain neurons in culture. An RPTPδ ectodomain concentration gradient released from a micropipette induced increased growth rates but also caused turning of growth cones towards the gradient source, in a manner which resembles the netrin- or neurotrophin-mediated attraction mentioned earlier in this chapter. However, RPTPδ chemoattractant effect triggers different molecular

mechanisms inside the growth cone, since it is not influenced by variations in cyclic nucleotides concentration, while tyrosine phosphatase inhibitors can prevent it. Considering that the ectodomain of most type IIa RPTPs is cleaved post-translationally and can be shed from the cell surface, the case described above defines a novel axon guidance cue which might be functionally relevant *in vivo*.

RPTPμ and RPTPκ are type IIb RPTPs whose ectodomains can also bind in a homophilic fashion (Brady-Kalnay *et al.*, 1993; Gebbink *et al.*, 1993; Zondag *et al.*, 1995). RPTPμ is expressed in a subset of ganglion cells during retinal development and in defined layers of the optic tectum. Retinal ganglion cells in culture express RPTPμ along their axons and on the growth cones. Therefore it has been suggested that, together with CRYPα and CRYP-2, RPTPμ plays a role in axon growth and guidance in the retinotectal system (Ledig *et al.*, 1999). RPTPμ is also known to interact with three different calcium-dependent CAMs: N-, R- and E-cadherin (Brady-Kalnay *et al.*, 1998). Recent experiments *in vitro* have demonstrated that RPTPμ plays a dual role in the regulation of neurite outgrowth during retinal development (Burden-Gulley and Brady-Kalnay, 1999). Firstly, it is able to promote neurite outgrowth and cell migration when used as a culture substrate; this effect is blocked by antibodies against the RPTPμ extracellular region. Secondly, it associates with N-cadherin in the retinal ganglion cells and it was suggested that it can modulate N-cadherin-dependent neurite outgrowth. Indeed, downregulation of RPTPμ expression caused a significant decrease in axon growth on a N-cadherin substrate but not on laminin or L1. Moreover, overexpression of a catalytically inactive RPTPμ mutant has also induced a significant reduction in neurite outgrowth on N-cadherin. It is well established that tyrosine phosphorylation of the cadherin/catenin complex correlates with suppression of cadherin-mediated adhesion. The results mentioned above support therefore the idea that RPTPμ might play a significant role in dephosphorylating a component of the N-cadherin signalling

complex. In this way it may modulate the N-cadherin homophilic adhesion that seems to be responsible for promoting axon growth on an N-cadherin substrate.

A soluble RPTPκ ectodomain-Fc construct can also stimulate neurite outgrowth when added to cerebellar neurons in culture (Drosopoulos *et al.*, 1999). It is still unclear whether the homophilic binding properties of RPTPκ are required for this response. An indication of the putative molecular mechanisms involved was obtained by using a peptide able to prevent the adapter molecule Grb2 from coupling (via its SH2 domain) to upstream signalling molecules and a drug (PD 098059) which inhibits the MEK1 kinase. Both reagents significantly inhibit the response triggered by RPTPκ-Fc, suggesting that this involves the coupling of Grb2 to a MAPK signal transduction cascade.

The type V RPTPζ/β is another RPTP able to control cell adhesion and axonal growth but through a different mechanism to those described above. RPTPζ/β is not expressed by neurons, but instead it is supplied in *trans* by glial cells as a ligand for a large number of proteins such as NCAM, NrCAM, TAG1/Axonin-1, NgCAM/L1, contactin; it also binds tenascin and pleiotrophin (reviewed in Peles *et al.*, 1998). The neurite outgrowth responses to interactions between RPTPζ/β and its ligands are either stimulatory (binding to NrCAM and contactin) or inhibitory (binding to NgCAM/L1). They are dependent on the neuronal cell type studied, probably due to unique receptor complexes in the responding cells since most of the proteins known to interact with RPTPζ/β do interact with other signalling molecules as well. It is worth mentioning that phosphacan, a secreted isoform corresponding to the RPTPζ/β ectodomain, is a chondroitin sulphate proteoglycan expressed at very high levels in the brain and a very potent inhibitor of neurite growth. The nature of signals transmitted into the axonal growth cone following RPTPζ/β binding is still to be characterised. Contactin for example is a GPI-anchored protein which seems to form a co-receptor together with a

large transmembrane protein called Caspr (Peles *et al.*, 1997). Its cytoplasmic domain contains a proline-rich region able to bind SH3 domains of downstream signalling proteins. Another protein that binds contactin in *cis* and seems to be important for neurite extension induced by RPTPζ/β is NrCAM. This associates with ankyrin, a spectrin-binding protein that links the actin cytoskeleton to the plasma membrane. In addition, NrCAM contains a potential binding site for PDZ domain-containing proteins on its C-terminal tail (Peles *et al.*, 1998).

It is difficult to assess at the moment the relevance *in vivo* for all the results listed above. In addition to the *Drosophila* work, mentioned at the beginning of this sub-chapter, several animal models have provided evidence supporting the involvement of RPTPs in axon growth and guidance processes. For instance in *Xenopus* overexpression of a RPTPδ (putative) dominant negative construct inhibited retinal ganglion cell (RGC) axon outgrowth *in vivo*, while similar LAR and CRYPα constructs had no effect (Johnson *et al.*, 2001). In chick however, ectopical expression of a CRYPα ectodomain construct in the developing optic tectum produced a wide panel of phenotypes, including premature stalling and arborisation of RGC fibres, excessive pre-tectal arbor formation and poor convergence onto terminal zones (Rashid-Doubell, McKinnell, Aricescu and Stoker, manuscript submitted). These data support the idea that the interaction between CRYPα and its tectal ligands are necessary for promoting growth of retinal axons over the tectum and for their correct topographic termination. RPTPσ, RPTPδ, RPTPε and LAR-deficient mice, as mentioned above, all have neural defects; some of them may be due to axon growth and/or guidance impairment. Sciatic nerve axons of LAR-deficient mice do regenerate more slowly after crush injuries (Van der Zee *et al.*, 2000; Xie *et al.*, 2001). The RPTPσ mRNA levels are significantly increased following sciatic nerve crush in rats (Haworth *et al.*, 1998); interestingly,

peripheral motor nerve axons of RPTPσ-deficient mice appear to regenerate much faster than controls (M. Tremblay, personal communication).

The above mentioned results are more than sufficient to trigger interest into the role played by RPTPs during neural development and regeneration. However, as stated several times, very little is known about the molecular mechanisms behind their functions. Detailed mapping of the molecular interactions involving RPTPs is badly needed and represents the key for designing molecules able to modulate their functions in pathological conditions.

1.4 The receptor protein tyrosine phosphatase CRYPα

CRYPα (Chick Receptor tYrosine Phosphatase α) is a type IIa RPTP, strongly expressed in both the central and peripheral nervous systems (Stoker, 1994). Its mammalian orthologue, termed RPTPσ, has been identified and cloned in rat (Yan *et al.*, 1993; Pan *et al.*, 1993; Walton *et al.*, 1993; Zhang *et al.*, 1994), mouse (Wagner *et al.*, 1994) and human (Pulido *et al.*, 1995). The human *Ptprs* gene was mapped to chromosome 19p13.3 by FISH analysis (Wagner *et al.*, 1996).

The *CRYPα* gene produces two major transcripts in the embryonic brain (Stoker, 1994) encoding the isoforms termed CRYPα1 and CRYPα2 (Figure 1.3). Several small cDNA fragments have also been identified suggesting that additional isoforms might well be expressed. This seems to be a common feature of type IIa RPTPs, since all their RNAs appear to undergo extensive alternative splicing (Pulido *et al.*, 1995 and references therein). This may have significant functional consequences *in vivo*; however, very little is known about how many of the putative isoforms are really translated and what their expression pattern could be. The two major isoforms mentioned above show that CRYPα is a type I transmembrane protein with a CAM-like ectodomain and a tandem of catalytic (tyrosine phosphatase) domains in the

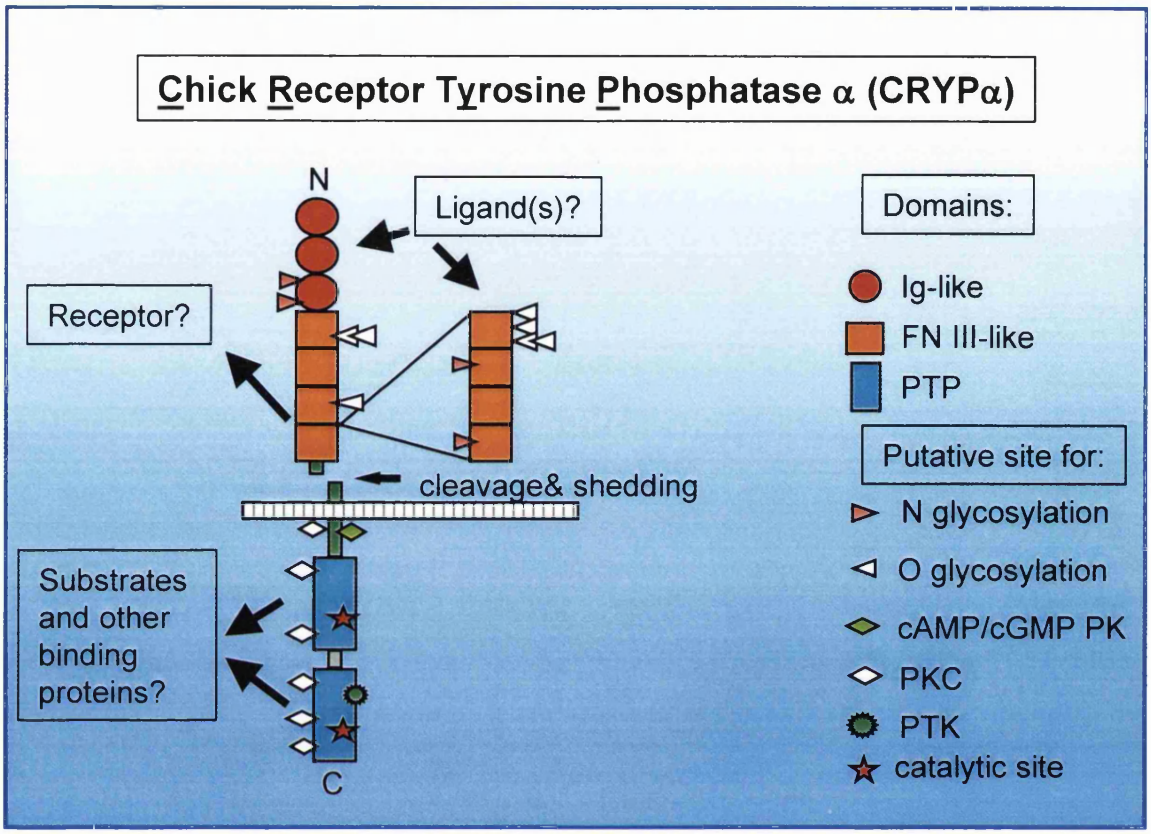

Figure 1.3. CRYPα schematic structure and putative post-translational modifications. The extracellular region of CRYPα1 isoform consists of three Ig-like domain and four FN III-like domains. The CRYPα2 isoform has four additional FN III-like domains (referred to as FN4-FN7) spliced-in. The whole ectodomain can be proteolytically cleaved and shed from the cell surface. The intracellular region consists of a tandem of protein tyrosine phosphatase domains. Various putative sites for N-glycosylation as well as Ser/Thr and Tyr phosphorylation were predicted using the program Prosite (Hofmann *et al.*, 1999). The O-glycosylation sites were predicted by the NetOGlyc 2.0 server (Hansen *et al.*, 1995).

intracellular region. The CRYPα1 isoform contains three Ig-like and four FNIII-like domains in its extracellular region. CRYPα2 contains four additional FNIII-like domains spliced in (Figure 1.3). Northern blot analysis demonstrates that alternative splicing of CRYPα RNA in the brain is developmentally regulated (Stoker, 1994). A 7.7 kb mRNA, corresponding to the CRYPα2 isoform, was detected at highest levels between embryonic day 4 (E4) and E8, then decreases rapidly. A 6.6 kb mRNA, corresponding to the CRYPα1 isoform, appears at low levels before E6, then its amount increases towards E10-E12, followed by stabilisation at an intermediate level after E14. Developmentally regulated expression of CRYPα isoforms has also been observed by *in situ* mRNA hybridisation in the retina (Haj *et al.*, 1999) and in the spinal cord (Chilton and Stoker, 2000). At E6, only CRYPα1 is expressed by the RGC neurons, suggesting that this is the isoform involved in the intraretinal axon growth/guidance events (which take place between E3 and E7). At E8 and E10, however, both isoforms are expressed by RGCs, suggesting that CRYPα2 is upregulated in these cells only after their axons have reached the optic tectum. CRYPα1 but not CRYPα2 is also highly expressed in other retinal cells, such as the amacrine neurons (Haj *et al.*, 1999).

In the spinal cord, a detailed analysis of various developmental stages (E4, E6, E8 and E10) shows that CRYPα1 is specifically expressed in ventral horn motoneurons while CRYPα2 is predominantly expressed in the ventricular/subventricular region, probably being involved in the maturation of nascent neurons and glia (Chilton and Stoker, 2000).

Northern hybridisation at E16 shows that in addition to brain and spinal cord, where CRYPα1 is the major isoform expressed, CRYPα mRNA is also present in the retina, breast muscle, heart, gut and lung (albeit at lower levels and mainly as the CRYPα2 isoform). The signal is extremely weak in the liver and absent in blood RNA (Stoker, 1994).

Immunohistochemical analysis in early embryogenesis has confirmed that CRYPα protein is predominantly expressed in the nervous system and suggests that it may play important roles during neural development. At E3, CRYPα is detected prominently in axons, co-localised with the neurofilament-associated antigen 3A10, in most CNS nerve fibres including segmental nerve roots, the ventral commissure and the lateral spinal cord axons (Stoker *et al.*, 1995). At E4, high-level expression is detected in the segmental nerves, commissural axons, axons in the dorsal and ventral funiculi, and dorsal root ganglia (DRG). This pattern is consistent with the *in situ* hybridisation results at E4 (Stoker, 1994). In cranial regions, CRYPα is detected in various nerve fibre layers of the brain and in the peripheral nerves (Stoker *et al.*, 1995) but also in hindbrain motor nuclei (J. Chilton, personal communication).

In the developing retina, at E6, CRYPα expression is clearly restricted to the RGC fibre layer. Towards E10 and E14, as the retina differentiates, CRYPα expression can also be detected in the inner plexiform layer in addition to the RGC axons (Ledig *et al.*, 1999b). In the optic tectum, the RGC axons' target, the first retinal axons arrive at E6 at the anterior pole and begin to form the superficial "*stratum opticum*". In addition, a deeper network (the circumferential tectobulbar processes) is generated. CRYPα protein can be detected in both these layers.

The axonal localisation of CRYPα is also maintained in tissue culture, where both E7 DRG neurons and E6 RGCs contain high levels of CRYPα along their neurites and on their growth cones, both on lamellipodia and filopodia (Stoker *et al.*, 1995; Ledig *et al.*, 1999a). As mentioned earlier in this chapter, both cell adhesion and signalling by tyrosine phosphorylation are key molecular mechanisms modulating growth cone behaviour. Since CRYPα contains a CAM-like extracellular region, has tyrosine phosphatase enzyme activity and is expressed on the axonal growth cones during key developmental stages, it has all it needs in order to play an important role

during nervous system development, in particular in axon growth and guidance processes. This hypothesis has been recently tested both *in vitro* and *in vivo*. Ledig *et al.* (1999a) have observed, using RGC cultures, that blocking the interaction between CRYPα (endogenously expressed in the growth cones) and its putative ligands (localised in the retinal basal lamina as shown by Haj *et al.*, 1999) results in a strong reduction of axon growth and a significant change in the growth cone morphology, reducing the size of growth cone lamellipodia. These effects were obtained using reagents that interfere either with the "receptor side" (anti-CRYPα antibodies) or with the "ligand side" (the basal laminae were blocked with a soluble form of the CRYPα extracellular region) and, importantly, were strictly substrate-dependent (neither of these reagents significantly affected axon growth or morphology on non-physiological substrates). These results suggest that the interactions between CRYPα and its basal lamina ligand(s) are important for promotion of retinal axon growth and for the maintenance of growth cone lamellipodia.

The *Xenopus* CRYPα has recently been cloned and its expression pattern in the developing retina matches very well the chick description (Johnson and Holt, 2000). Expression of a putative dominant negative mutant, containing only a catalytically inactive intracellular region, had no clear effect on RGC axon growth or guidance *in vivo* (Johnson *et al.*, 2001). However, *in vitro*, the same construct expressed in RGCs significantly enhanced neurite outgrowth in a substrate-dependent manner. This apparently contradicts the findings of Ledig *et al.* (1999).

How can these results fit together? To be honest, I believe that nobody can answer this at the moment, simply because almost nothing is known about the signalling mechanisms in which CRYPα is involved. We know very little about the putative binding partners and we have no clue concerning the regulation of its catalytic activity. Therefore, just a few speculative points will be mentioned below.

Overexpression of the catalytically inactive construct presumably prevents dephosphorylation of CRYPα substrates by competing with or blocking the endogenous enzyme. Interestingly, the "dominant negative" construct has a "growth promoting" effect only on basal laminae which still have the endfeet of Müller glial cells attached. This effect means that the axons grow exactly as well as they normally do on basal laminae from which the endfeet (and indeed a lot of other molecules) are removed by a harsh 2% Triton-X100 wash. CRYPα binds ligands on both the glial endfeet and on the basal lamina itself (Haj *et al.*, 1999; Aricescu *et al.*, submitted). If we accept that CRYPα enzymatic activity is modulated by ligand binding (as it has been suggested for other RPTPs) then it follows that the bare basal lamina ligands maintain CRYPα in an inactive form, thereby allowing efficient axon growth. On basal lamina with glial endfeet, other ligands may activate CRYPα so the expression of the "dominant negative" construct is required to "stimulate" outgrowth. Why does blocking the CRYPα-ligand interaction on basal laminae plus glial endfeet result in growth reduction, as described by Ledig *et al.* (1999)?

First of all, their blocking experiments will prevent CRYPα interacting with ***both*** the basal lamina ***and*** the glial endfeet ligands. Therefore, if those exert opposite effects, the outcome will become unpredictable since their relative "signalling weight" is unknown. The finding that, on basal laminae without glial endfeet, the addition of anti-CRYPα antibody (which blocks ligand binding) results in a significant reduction of neurite outgrowth fits in well with the *Xenopus* story (if we accept that ligand binding induces CRYPα inactivation).

On the other hand, one should keep in mind that the CRYPα ectodomain is CAM-like. It may well be the case that disrupting its interaction with the glial endfeet simply impairs a cell-cell adhesion process, which will subsequently affect growth rate.

The basal lamina ligands, which are not cell adhesion molecules (as described in this thesis), may well be involved in a completely different signalling pathway.

Nevertheless, all these uncertainties clearly show that identifying the ligands, substrates and other interaction partners are key steps towards integrating CRYPα in one or several signalling pathways which will contribute to understanding the functions of this protein *in vitro* and *in vivo*. As mentioned several times in this chapter, *in ovo* experiments on chicken embryos and the analysis of RPTPσ transgenic mice together with gene and protein expression studies show that CRYPα/RPTPσ is an important player during the nervous system development and regeneration.

1.5 The aim of this thesis

It is now well accepted that reversible protein tyrosine phosphorylation is a key signalling mechanism in virtually all major cellular processes in eukaryotic cells. Nervous system development and regeneration, in particular axon growth and guidance, are no exception.

Many RPTPs have a predominantly neural expression pattern, in particular those classified as type IIa (Figure 1.1). These include our molecule of interest, CRYPα. A lot of progress has been made in the last couple of years towards understanding the functional importance of such RPTPs. But how are these functions achieved? What are the molecular mechanisms behind them? What could and should be done to modulate these functions in pathological conditions?

The aim of this thesis is to contribute towards answering these questions by identifying molecules that interact with CRYPα. In particular, most of the research effort was spent finding ligands for CRYPα. This issue represents a major challenge for several research groups in both academic and industrial environments and so it is for our laboratory. Chapter 3 describes a sustained but unsuccessful attempt to identify such

ligands by expression cloning. A detailed analysis of CRYPα ectodomain binding properties and molecular structure has provided the first hints about the nature of (at least a subclass of) physiological ligands. This is described in Chapter 4. Chapter 5 deals with the identification of two such ligands and the characterisation of their interactions with CRYPα. Finally, in Chapter 6, I present the current state of my efforts to identify CRYPα physiological substrates and to understand the significance of these findings *in vivo*.

Chapter 2. **General methods**

2.1 DNA methods

2.1.1 Plasmid DNA preparation – microprep

Principle: Bacterial colonies are disrupted using an alkaline solution and the lysate is directly loaded in an agarose gel, in order to check for the presence of recombinant plasmids. This method is based on the "Rapid disruption of bacterial colonies" method described in Sambrook *et al.* (1989), however it was optimised so that instead of using four separate solutions only one is needed and various incubation intervals have been removed. It allows rapid and simultaneous screening of several dozens of colonies and can easily detect recombinant plasmids that differ by 10-20% in size.

Materials: All chemicals were from Sigma and growth media from Gibco BRL.

- lysis/loading buffer: 10 mM Tris base, 1 mM ethylenediaminetetraacetic acid (EDTA), 10% w/v sucrose, 0.25% w/v sodium dodecyl sulphate (SDS), 100 mM NaOH, 60 mM KCl, 0.05% bromophenol blue. This buffer is stable at -20°C.
- agar plate containing the appropriate medium and selective antibiotic, or sterile 96 well plate containing 100 µl/well liquid medium and selective antibiotic;
- non-sterile 96 well plate for colony lysis;
- agarose gel of desired concentration for nucleic acids separation.

1. Pre-warm the lysis/loading buffer 5 minutes at 65°C.
2. Distribute 15 µl lysis/loading buffer per well in the non-sterile 96 well plate, according to the number of colonies to be screened.

3. Pick a colony using a pipette tip, gently touch the surface of the replica plate or liquid medium in the sterile 96 well plate, then transfer the cells left on the tip to a corresponding well in the plate containing lysis/loading buffer.
4. Mix the lysing cells a couple of times by rotating the tip end in the well, then repeat step 3 until the desired number of colonies has been selected.
5. Load the 15 µl lysates in the agarose gel and separate the nucleic acids by electrophoresis.
6. Cultures from colonies containing recombinant plasmids can now be generated using the replica plate(s).

2.1.2 Plasmid DNA preparation – miniprep

Principle: Plasmid DNA is extracted from cells using an alkaline lysis method (Sambrook *et al.*, 1989) and then purified on a glass fibre matrix column. We currently use the GFX MicroPlasmid Prep Kit (Amersham Pharmacia Biotech), which allows fast production of plasmid DNA suitable for restriction analysis, automated sequencing and transfection in eukaryotic cells. The usual yield for high copy number plasmids is 5-10 µg/ml of culture.

Materials:

- bacterial cultures (5ml), grown overnight;
- GFX MicroPlasmid Prep Kit (Amersham Pharmacia Biotech), containing:
    - solution I: 100 mM Tris.HCl, pH 7.5, 10 mM EDTA, 400 µg/ml RNase I;
    - solution II: 190 mM NaOH, 1% w/v SDS;
    - solution III: a proprietary acetate-buffered solution containing chaotropic salt;
    - wash buffer: 10 mM Tris.HCl, pH 8.0, 1 mM EDTA, 80% v/v ethanol;

- GFX glass fibre matrix spin columns.

The whole procedure is done at room temperature.

1. Transfer 1.5 ml bacterial culture to an Eppendorf tube and pellet the cells by centrifugation, 5 minutes at 13,000 rpm.
2. Discard the supernatant and resuspend the cells (completely) in 150 µl solution I.
3. Add 150 µl solution II and mix the tube content by inversion, 5-6 times. Incubate 5 minutes.
4. Add 300 µl solution III and mix the tube content by inversion, 10-20 times ensuring that the flocculent precipitate is evenly dispersed.
5. Centrifuge the lysate 5 minutes at 13,000 rpm.
6. Transfer the supernatant to a fresh Eppendorf tube and repeat step 5 in order to remove completely all debris.
7. Transfer the supernatant onto a GFX glass fibre column, incubate 1 minute at room temperature and then spin the column 30 sec at 13000 rpm.
8. Wash the column with 400 µl wash buffer by centrifuging 1 minute at 13,000 rpm.
9. Transfer the column to a clean Eppendorf tube. Add 100 µl DNAase/RNAase free water per column, incubate 1 minute, then elute the plasmid DNA by spinning 1 minute at 13,000 rpm. The plasmid prep must be stored at -20°C to avoid degradation.

2.1.3 Plasmid DNA preparation – maxiprep

Principle: Plasmid DNA is extracted from cells using an alkaline lysis method (Sambrook *et al.*, 1989) and then purified on an anion-exchange resin column. We

currently use the Qiagen Maxiprep kit, which allows fast production of large quantities of plasmid DNA (up to 500μg) suitable for restriction analysis, automated sequencing and transfection in eukaryotic cells.

Materials: Common chemicals were from Sigma and growth media from Gibco BRL.

- bacterial cultures (100ml), grown overnight;
- Qiagen Maxiprep kit, containing:
    - buffer P1: 50 mM Tris.Cl, pH 8.0, 10 mM EDTA; 100 μg/ml RNase A;
    - buffer P2: 200 mM NaOH, 1% w/v SDS;
    - buffer P3: 3 M potassium acetate, pH 5.5;
    - QIAGEN-tip 500 anion-exchange resin columns;
    - equilibration buffer (QBT): 50 mM 3-(N-Morpholino)propanesulphonic acid (MOPS), pH 7.0, 750 mM NaCl, 15% v/v isopropanol, 0.15% v/v Triton X-100;
    - wash buffer (QC): 50 mM MOPS, pH 7.0, 1 M NaCl, 15% v/v isopropanol;
    - elution buffer (QF): 50 mM Tris.HCl, pH 8.5, 1.25 M NaCl, 15% v/v isopropanol;
    - 70% v/v ethanol.;
    - TE buffer: 10 mM Tris.HCl, pH 8.0, 1 mM EDTA.

1. Pick a single colony from a fresh agar plate and inoculate a 5ml starter culture in the appropriate liquid medium. Grow for 8 hours at 37°C, with shaking.
2. Transfer the starter culture in 100 ml fresh medium and grow at 37°C, with vigorous shaking, overnight.
3. Collect the bacterial cells by centrifugation, 10 minutes at 7,000 rpm, at 4°C.
4. Discard the supernatant and resuspend the pellet in 10 ml buffer P1.

5. Add 10 ml buffer P2, mix gently (by inversion, 5-6 times) and incubate at room temperature for 5 minutes, for complete lysis.
6. Add 10 ml of ice-cold buffer P3, mix immediately by inversion 5-6 times and incubate on ice 20 minutes to enhance precipitation of bacterial debris.
7. Centrifuge the lysate 30 minutes at 20,000g, at 4°C. Remove the supernatant (containing the plasmid DNA) promptly.
8. Equilibrate a QIAGEN-tip 500 column by applying 10 ml buffer QBT and allow it to empty by gravity flow.
9. Apply the supernatant from step 7 on the column and allow it to pass through by gravity flow.
10. Wash the column twice with 30 ml buffer QC.
11. Elute the bound DNA with 15 ml buffer QF.
12. Precipitate the DNA by adding 10.5 ml isopropanol, at room temperature. Mix thoroughly and centrifuge immediately for 30 minutes at 15,000g, at 4°C.
13. Discard the supernatant and resuspend the DNA pellet in 1 ml 70% ethanol, at room temperature.
14. Centrifuge 5 minutes at 13,000 rpm, room temperature.
15. Discard the supernatant, briefly dry the pellet (let the ethanol to evaporate) and dissolve the DNA in 100 µl buffer TE or sterile, DNAase-RNAase free MilliQ water.
16. Determine the DNA concentration by measuring the absorbance of a 1:300 diluted solution at 260nm. The original sample concentration will be: A_{260} * 50 (µg/ml concentration of a DNA solution whose absorbance at 260nm is 1) * 300 (dilution factor). Store the DNA at -20°C.

2.1.4 Plasmid DNA extraction from fixed mammalian cells

Principle: Mammalian cell lines transformed with an origin-defective SV40 virus (e.g. COS7, 293T) are very good hosts for cDNA expression. These cell lines express the wild-type SV40 large T antigen, therefore they are able to replicate transfected plasmids containing an SV40 virus–derived origin of replication to a very high copy number (10,000 to 100,000 copies/cell). The transfected cells are removed from the growing substrate and lysed in a buffer containing SDS and EDTA. The plasmids thus released are then purified and transformed into bacteria for further amplification.

Materials: All chemicals were purchased from Sigma.

- lysis buffer: 10 mM Tris.Cl, pH 8, 10 mM EDTA, 0.5% w/v SDS, 10 mg/ml proteinase K;
- phenol-chloroform-isoamyl alcohol mix (25:24:1);
- chloroform;
- absolute and 70% v/v ethanol;
- yeast tRNA (carrier);
- 3 M sodium acetate, pH 5.2;
- 19G needles (BDH);
- TE buffer: 10 mM Tris.HCl, pH 8.0, 1 mM EDTA.

1. Fix the transfected cells [either with 4% (w/v) paraformaldehyde or methanol or 60% (v/v) acetone/3% (v/v) formaldehyde] and stain for expression of the protein of interest.
2. Collect the stained cells from the plastic tissue culture dish using a 19G needle (the cells will remain attached to a small piece of plastic but this will not affect further processing).

3. Transfer the cells in 150 µl lysis buffer and incubate 4 hours at 55°C, to allow proteinase K digestion.
4. Add 150 µl phenol-chloroform-isoamyl alcohol and mix well.
5. Centrifuge 10 minutes at 13,000 rpm, at 4°C, and collect the upper (aqueous) layer.
6. Add 150 µl chloroform and mix well.
7. Repeat step 5.
8. Add 10 µg carrier tRNA, then 15 µl sodium acetate solution and 300 µl ice-cold absolute ethanol. Let the nucleic acids precipitate overnight at -20°C.
9. Centrifuge 30 minutes at 13,000 rpm, at 4°C.
10. Discard the supernatant and wash the pellet with 300 µl 70% ethanol.
11. Centrifuge 5 minutes at 13,000 rpm, at 4°C. Remove the ethanol, let the tubes dry briefly and dissolve the nucleic acids in 10 µl TE buffer or sterile, DNAase-RNAase free MilliQ water. The plasmid DNA can be transformed into competent bacteria.

2.1.5 Restriction enzyme cleavage of DNA

Principle: Double-stranded DNA can be cleaved at specific sites by restriction enzymes which recognise, bind and cleave within or adjacent to a particular sequence (for more details see Sambrook *et al.*, 1989). In particular type II restriction nucleases are widely used for cloning purposes, since most of them recognise and cut in a strictly predictable fashion sequences of four, five or six nucleotides in length. A large number of enzymes, requiring different reaction conditions, and purchased from various suppliers, has been used for the experiments described in this thesis, therefore the protocol below is just a general outline.

Materials:

- restriction nuclease specific for the sequence of interest, with appropriate buffer, purchased from the most convenient manufacturer (we currently use Promega, New England Biolabs, Amersham Pharmacia Biotech and Gibco BRL).

1. Prepare a reaction mix containing an aliquot of DNA to be analysed, in the buffer suitable for the restriction enzyme to be used, and 1 unit restriction nuclease per μg of DNA.
2. Incubate the reaction mix at the optimum temperature for the restriction enzyme used, for minimum 2 hours (if complete digestion is required).
3. If necessary, and possible, heat-inactivate the enzyme according to the manufacturer's instructions. If the enzyme cannot be heat-inactivated, it may be removed via phenol extraction (as described in 2.1.4), by using a reaction-cleanup kit or by agarose gel electrophoresis.
4. Check the restriction pattern by agarose gel electrophoresis.

2.1.6 Klenow filling of DNA recessed 3' termini

Principle: The Klenow (large) fragment of the *E. coli* DNA polymerase I has the ability to fill in, in the presence of dNTPs, recessed 3' termini generated by some restriction nucleases. This will result in generation of "blunt ends" which can be ligated with similar blunt-ended DNA fragments.

Materials:

- Klenow fragment of the *E. coli* DNA polymerase I (Promega);
- 1 mM (each) dNTP mix or separate dNTPs, depending on the sequence to be filled (Bioline).

1. When a restriction digestion is complete, add 1 µl dNTPs for each 10 µl reaction mix.
2. Add 1U Klenow fragment of the *E. coli* DNA polymerase I for up to 5 µg DNA in the reaction mix and incubate for 15 minutes at room temperature.
3. Heat-inactivate the Klenow fragment and (possibly) restriction enzyme(s) by incubating 10 minutes at 75°C.

2.1.7 Alkaline phosphatase treatment of DNA fragments

Principle: Alkaline phosphatase removes the 5' phosphate residues from DNA, RNA, dNTPs and rNTPs. This is particularly useful when a cloning vector was opened with a single restriction enzyme or enzymes generating compatible overhangs, in order to prevent vector self-ligation. Calf intestinal alkaline phosphatase is commonly used, however it is very difficult to heat-inactivate it completely (this is absolutely required in order to achieve an efficient ligation later on). Therefore, shrimp alkaline phosphatase is currently used, which is heat-inactivated in 20 minutes at 65°C.

Materials:

- shrimp alkaline phosphatase and buffer, commercially available (Roche Molecular Biochemicals).

1. Add 1U shrimp alkaline phosphatase and the appropriate amount of buffer directly to a restriction reaction containing up to 2 µg of linearised DNA.
2. Incubate 1 hour at 37°C.
3. Heat inactivate the phosphatase (and possibly the restriction enzyme) by incubating 20 minutes at 65°C.

2.1.8 Agarose gel electrophoresis

Principle: DNA molecules, negatively charged at neutral pH, migrate toward the anode in an electric field. DNA fragments between 200 bp and 50 kb in length can migrate through an agarose gel of the desired concentration (usually between 0.3 and 2%) when exposed to an electric field of constant strength and direction (usually in a horizontal configuration) and will separate according to their size and conformation.

Materials: All chemicals were purchased from Sigma.

- agarose, molecular biology grade;
- gel running buffer:
    - Tris-acetate-EDTA (TAE): 40 mM Tris-acetate, pH 7.8, 1 mM EDTA, **or**
    - Tris-borate-EDTA (TBE): 45 mM Tris-borate, pH 7.8, 1 mM EDTA;
- 10 mg/ml ethidium bromide stock solution;
- gel-loading buffer (6x stock): 0.25% bromophenol blue, 0.25% xylene cyanol FF, 40% (w/v) sucrose in water; store at 4°C.

1. Prepare a gel-casting device of a size according to the number of samples to be analysed.
2. Add the required amount of powdered agarose to a glass flask containing TAE or TBE buffer in order to achieve efficient separation for the fragments of interest (for a detailed description see Sambrook *et al.*, 1989). Heat the slurry in a microwave oven until the agarose is completely dissolved.
3. Let the solution cool down to 60°C and add ethidium bromide to a final concentration of 0.5 μg/ml.
4. Pour the warm agarose solution into the casting device and let the gel set, at room temperature.

5. Remove the well-forming comb and place the gel in the electrophoresis apparatus. Cover the gel with a thin (1mm) layer of running buffer.
6. Prepare the DNA samples by mixing the desired amount with gel-loading buffer. Load the samples into the pre-formed wells and apply a voltage of 8V/cm gel.
7. When the dyes from the loading buffer have migrated an appropriate distance, turn off the current and visualise the gel on an ultraviolet transilluminator (302nm).

2.1.9 Purification of DNA fragments from agarose gels

Principle: Glass and silica matrices have the ability to bind DNA very efficiently at high salt concentrations (>3M) and acidic pH (<7.5). The protocol described below (Boyle and Lew, 1995) uses a cheap silica alternative to commonly used "glassmilk" kits (e.g. GeneClean II, Bio-101) and can be easily adapted for "cleaning-up" PCR products or DNA fragments present in other enzymatic reactions.

Materials: All chemicals were purchased from Sigma.

- silica (Sigma Cat. No. S-5631);
- phosphate buffered saline (PBS): 137 mM NaCl, 2.7 mM KCl, 10 mM Na_2HPO_4, 1.76 mM KH_2PO_4;
- 3 M and 6 M sodium iodide solutions;
- wash buffer: 10 mM Tris.HCl, pH 7.5, 50 mM NaCl, 2.5 mM EDTA, 50% v/v ethanol;

1. Prepare the silica suspension (100 mg/ml) by mixing 10 g silica in 100ml PBS and allowing the silica to settle 2 hours at room temperature. The supernatant, containing the fine particulate matter is discarded and the procedure repeated 2 times. Finally resuspend the silica pellet in 3 M NaI at 100 mg/ml (assuming minimal loss of silica

during the washing steps) and keep this suspension at 4°C, in the dark. The binding capacity of 1 mg silica is approximately 5 μg.

2. Isolate the DNA fragment of interest from an agarose gel by excising the gel slice with a sharp scalpel.
3. Add 3 volumes of 6 M NaI to the gel slice and let it melt by incubating for 5 minutes at 55°C, mixing occasionally.
4. Add the appropriate volume of silica suspension, mix and incubate on ice for 10 minutes, mixing occasionally by inversion.
5. Centrifuge 30 sec at 13,000 rpm at room temperature. Discard the supernatant and add 500 μl wash buffer. Gently resuspend the silica pellet.
6. Repeat step 5 twice.
7. Centrifuge 30 sec at 13,000 rpm at room temperature and remove any trace of wash buffer.
8. Add one pellet volume of distilled water and elute the DNA by incubating 1 minute at 55°C. Gently resuspend the silica and incubate another minute at 55°C.
9. Centrifuge 30 sec at 13,000rpm at room temperature and collect the supernatant containing the DNA fragment of interest.

2.1.10 Ligation of DNA fragments

Principle: Double stranded DNA fragments containing either blunt or compatible ends can be ligated by formation of new phosphodiester bonds between phosphate residues located at the 5' termini and adjacent 3'-hydroxyl groups. This reaction is catalysed by DNA ligases (T4 DNA ligase is commonly used) in the presence of ATP.

Materials:

- T4 DNA ligase and buffer (300 mM Tris.HCl, pH 7.8, 100 mM $MgCl_2$, 100 mM DTT, 10 mM ATP), commercially available (Promega).

1. Set up a 10 µl reaction containing: 100-200 ng vector DNA, an equimolar amount (or up to 3 times molar excess) insert DNA, 1 µl of 10x ligase buffer and T4 DNA ligase (0.1 Weiss units).
2. Incubate the reaction at least 10 hours at 16°C.
3. Use 1-2 µl of the reaction to transform competent *E. coli* bacteria.

2.1.11 Preparation of electrocompetent *E. coli*

Principle: Boring series of distilled water washes of bacteria, in order to remove any trace of salt from the culture broth.

Materials: All chemicals were from Sigma and growth media from Gibco BRL.

- 500 ml sterile LB medium (dissolve 5 g bacto-tryptone, 2.5 g bacto-yeast extract and 5 g NaCl in 500ml water, then sterilise by autoclaving 20 minutes at 15 lb/sq.in. on liquid cycle);
- 2x500 ml bottles with sterile MilliQ water, cooled on ice;
- sterile 2 l conical flask;
- 50 ml sterile 10% glycerol solution.

1. Set a 50 ml bacterial culture in LB medium and let it grow overnight at 37°C, with vigorous shaking.
2. Next morning transfer 500 ml sterile LB medium in the 2 l conical flask and inoculate it with the 50 ml overnight culture. The OD_{600} should be approximately 0.2.
3. Incubate the new culture at 37°C, with vigorous shaking.
4. Check the OD_{600} after 2 hours, and every half an hour after that, until it reaches 0.6-0.7.

5. Put the flask on ice for 30 minutes. From now on, **always** keep the cells cold (on ice or in a centrifuge cooled at 4°C.
6. Cool down on ice four 50 ml Falcon tubes and cool the appropriate centrifuge rotor to 4°C. Place the 500 ml sterile water bottles and the 10% glycerol solution on ice.
7. Transfer 50 ml culture in each Falcon tube, centrifuge 10 minutes at 6,000rpm, at 4°C.
8. Discard the supernatant, add again 50 ml culture in each tube and spin down for 10 minutes at 6,000rpm, at 4°C.
9. Discard the supernatant, add 25 ml culture in each tube and spin down for 10 minutes at 6,000rpm, at 4°C.
10. Resuspend the bacterial pellets in 45 ml ice-cold sterile MilliQ water, by vortexing briefly (quite tricky).
11. Centrifuge the tubes for 10 minutes at 6,000rpm, at 4°C.
12. Discard the supernatant, add again 45 ml ice-cold sterile MilliQ water in each tube and resuspend the cells by vortexing briefly (should be much easier now).
13. Centrifuge the tubes for 10 minutes at 6,000 rpm, at 4°C.
14. Discard the supernatant, add again 45 ml ice-cold sterile MilliQ water in each tube and resuspend the cells by vortexing briefly (should be very easy now).
15. Centrifuge the tubes for 10 minutes at 6,000rpm, at 4°C.
16. Discard the supernatant, add 10ml ice-cold 10% glycerol per tube and resuspend the pellet by vortexing. Pool all the cell suspensions together (40 ml in total).
17. Centrifuge the tubes for 10 minutes at 6,000rpm, at 4°C.
18. Discard the supernatant and resuspend the bacterial pellet in 2 ml ice-cold 10% glycerol.
19. Place 40 1.5ml Eppendorf tubes on dry ice. Aliquot 80 µl bacterial suspension in each tube, place it back on dry ice and then store at -70°C.

2.1.12 Transformation of bacteria by electroporation

Principle: Electroporation is a method of introducing macromolecules such as DNA into cells by using a brief electrical pulse to cause transient membrane pore formation. This method usually produces better results than chemical transformation. The conditions described below are optimised for the Electroporator II (Invitrogen).

Materials: Growth media were purchased from Gibco BRL.

- electrocompetent bacteria;
- DNA to be transformed;
- LB liquid medium;
- LB-agar bacterial plates, with selective antibiotic.

1. Thaw the required number of electrocompetent cell aliquots on ice. Also place on ice the equivalent number of electroporation cuvettes (0.1cm wide).
2. Check that the electroporator is set as follows: armed; 1800V; 150Ω; pulse.
3. Check that the power supply is OFF. Connect the electroporator. Turn ON the power supply and set it to: 1500V, 25mA, 25W.
4. Set the charge/pulse switch to CHARGE and allow the unit to develop a full charge (30 seconds).
5. Leaving the arm/disarm dial in the ARMED position, charge and discharge the unit twice (by pressing PULSE) without a cuvette in place.
6. Recharge the unit.
7. Mix the DNA (1-4μl) with the cells and transfer the mixture in the cuvette. Replace cap and dry the cuvette surface. Set the arm/disarm dial to DISARMED and insert the cuvette into the unit. Switch the arm/disarm dial back to ARMED.

8. Flip the charge/pulse switch to PULSE position. At this step the bacteria are transformed.

9. Remove the cuvette and immediately add 1ml LB, at room temperature. Transfer the suspension in a 2059 Falcon tube and incubate it at 37°C, with shaking, for 30 minutes in order to allow the expression of the antibiotic resistance gene(s).

10. Plate aliquots of transformed bacteria on selective agar plates.

2.1.13 Polymerase Chain Reaction (PCR)

Principle: "Classic" PCR is used to amplify a DNA segment flanked by two regions of known sequence for which complementary oligonucleotides (primers) can be designed and synthesised. A thermostable, primer dependent, DNA polymerase will synthesise, in the presence of deoxynucleotides, the sequence of interest, as defined by the chosen primer pair. A cycle of DNA thermal denaturation (generating single-stranded templates), annealing (when the primers attach to the complementary sequence in the template) and DNA synthesis is then repeated around 30 times. The products from a reaction cycle will serve as templates for the next one, therefore each cycle will double the amount of the desired product.

Materials:

- thermostable DNA polymerase and the corresponding buffer, many types commercially available (e.g. Stratagene);
- dNTPs mix, 12.5mM each (Bioline);
- template-specific oligonucleotides (usually 20-25 bp long) (Hybaid);
- template DNA.

1. Prepare the reaction mix containing 2 ng DNA template, 200 μM dNTPs, 1 μM primers (each), reaction buffer and the appropriate number of units of DNA

polymerase, according to manufacturer's instructions. Use molecular biology grade water to adjust the final volume to 50 µl. Cover the reaction mix with a thin layer of mineral oil if using a thermal cycler not equipped with a heated lid.

2. Set the parameters (temperature and duration) for the 3 steps of the reaction cycle, according to the primers, template, size of the fragment to be amplified and polymerase used.
3. Check the reaction product by electrophoresis in an agarose gel in order to determine its size.

2.1.14 Site-directed mutagenesis

Principle: Oligonucleotide-based site directed mutagenesis is performed directly on a supercoiled double-stranded DNA plasmid template by using a pair oligonucleotides, complementary to each other and to opposite strands of the vector and containing the desired mutation in a central position. The oligonucleotides are extended during temperature cycling by using the *Pfu Turbo* DNA polymerase, generating mutated plasmids. The "parental" templates are subsequently digested with *Dpn*I, a restriction nuclease specific for methylated and hemimethylated DNA (as the template and hybrid molecules will be if isolated from a standard *E. coli* strain).

Materials:

- mutagenic oligonucleotides, 35-40 bp long, >60% GC, T_m>78°C (Hybaid);
- DNA plasmid template, ideally purified using the maxiprep method;
- *Pfu Turbo* DNA polymerase and buffer (Stratagene);
- dNTPs mix, 12.5 mM each (Bioline);
- *Dpn*I restriction nuclease (Promega, New England Biolabs);
- electrocompetent bacteria;
- LB-agar plates with selective antibiotic.

1. Prepare the reaction mix containing 20 ng DNA template, 125 ng each oligonucleotide, 200 μM (each) dNTP mix, reaction buffer and adjust the final volume to 50μl with molecular biology grade water. Mix and add 2.5 U *Pfu Turbo* DNA polymerase. Cover with mineral oil if necessary.
2. Transfer the reaction in a thermal cycler and run the following program: 1x(95°C, 1 minute), 18x(95°C, 50 sec; 60°C, 50 sec; 68°C, 2 minutes/kb plasmid length), 1x(68°C, 7 minutes).
3. Place the reactions on ice, 2 minutes.
4. Add 10 U *Dpn*I per reaction. Incubate 1-3 hours at 37°C.
5. Use 1-3 μl to transform electrocompetent bacteria.

2.1.15 DNA sequencing

Principle: Sequencing reactions were performed using the *ABI Prism dGTP BigDye Terminator Ready Reaction Kit*, using a cycle sequencing protocol. The basic chemistry relies on the Sanger method of dideoxy-mediated chain termination. In this kit the dideoxy terminators are fluorescently labelled, each nucleotide type with a different fluorochrome, so that the sequence can be read in one lane using an ABI Prism 377 DNA Sequencer (Perkin-Elmer Applied Biosystems).

Materials: Common chemicals were from Sigma.

- *ABI Prism dGTP BigDye Terminator Ready Reaction Kit* (PE Applied Biosystems), containing in a single mix: fluorochrome labelled dideoxy terminators, dNTPs, AmpliTaq DNA polymerase, r*Tth* pyrophosphatase, $MgCl_2$ and Tris.HCl buffer, pH 9.
- DNA template and sequencing primer;
- denaturing gel loading buffer: 5:1 ratio of (deionised formamide) : (25 mM EDTA, pH 8, with 50 mg/ml blue dextran).

1. Prepare a 20 µl reaction mix containing 500 ng-1µg DNA template, 3.2 pmol primer and 4 µl terminator ready sequencing mix. Mix well and spin briefly. Cover with mineral oil if necessary.
2. Transfer the reaction in a thermal cycler and run the following program: 1x(96°C, 2 minutes), 25x(96°C, 30 sec; 50°C, 20 sec; 60°C, 4 minutes), 1x(4°C, ∞).
3. Transfer the 20 µl reaction mix in a 1.5 ml Eppendorf tube, avoiding contamination with mineral oil. Add 80 µl of 75% isopropanol. Mix well.
4. Leave the tubes 15 minutes at room temperature to precipitate the extension products.
5. Centrifuge 20 minutes at 14,000 rpm, at room temperature.
6. Discard the supernatant and wash the pellet with 250 µl of 75% isopropanol. Vortex briefly and centrifuge 5 minutes at 14,000 rpm, at room temperature.
7. Carefully aspirate the supernatants and dry the samples 1 minute at 90°C. The samples can be stored dry, at -20°C.
8. Resuspend the pellet in 5 µl gel-loading buffer. Vortex and spin briefly.
9. Heat the samples at 95°C for 2 minutes. Place on ice until ready to load in a vertical polyacrylamide gel, in an ABI Prism 377 DNA Sequencer.

2.1.16 Preparation of DNA linkers

Principle: Complementary oligonucleotides are mixed in equimolar amounts, heat denatured and let to anneal by slowly decreasing the temperature. They were used to introduce multiple cloning sites in plasmid vectors or to attach various peptide tags to fusion proteins.

Materials:

- complementary oligonucleotides (15-40bp) (Hybaid);

- buffer solution (New England Biolabs #1): 10mM Bis Tris Propane-HCl, pH 7.0, 10mM $MgCl_2$, 1mM DTT;
- 50mM $MgCl_2$.

1. Prepare a mix containing: 1µl of 1mM oligonucleotide (each, if non-palindromic, or 2µl if palindromic), 2.5µl NEB buffer #1, 5µl of 50mM $MgCl_2$ solution and 15.5µl molecular biology-grade water.
2. Transfer the reaction in a thermal cycler and run the following program: 1x(95°C, 5 minutes), 1x(down to 4°C @ 0.1°C/30 sec), 1x(4°C, ∞).
3. The linker can be stored frozen at -20°C.

2.2 RNA methods

2.2.1 Total RNA isolation from tissue samples

Principle: The *Perfect*RNA Total RNA isolation kit (Maxi Scale) from 5'→3', Inc. has been used to purify total RNA from snap-frozen tissue samples (chick embryo retina and optic tectum). The kit uses a chaotropic guanidinium isothiocyanate solution for cell lysis and rapid inactivation of RNAases. The total RNA in the lysate is subsequently bound to a proprietary matrix, washed to remove contaminants and eluted in RNAase free water. Up to 3 mg total RNA per gram of tissue have been obtained.

Materials:

- *Perfect*RNA Total RNA isolation kit (Maxi Scale) from 5'→3', Inc. Detailed recipies for solutions are not disclosed...;
- ethanol, absolute and 70% v/v.

1. Lyse 200 mg to 1 g tissue by adding 9 ml lysis solution and homogenising with a Ultra-Turrax T25 (IKA) apparatus.
2. Add an additional 9 ml lysis solution and vortex vigorously. Incubate the lysate for 5 minutes at room temperature.
3. Add 18 ml 70% ethanol to the lysate and mix thoroughly but very gently, by repeated inversion.
4. Add 4 ml *Perfect*RNA binding matrix solution and mix by inversion.
5. Place two *Perfect*RNA spin columns in 50 ml centrifuge tubes and evenly distribute 20 ml of the above mixture between the two columns. Centrifuge 10 minutes at 2,000g. Discard the filtrate.
6. Add 10 ml wash solution I and centrifuge the assemblies for 5 minutes at 2,000g. Transfer the columns to fresh 50ml tubes.
7. Add 10 ml wash solution II and centrifuge the assemblies for 5 minutes at 2,000g. Transfer the columns to 30 ml collection tubes and add 1 ml molecular biology-grade water to each column.
8. Incubate in a 50°C water bath for 5 minutes. Vortex 5 seconds and centrifuge the assemblies for 5 minutes at 2,000g.
9. Store recovered total RNA at -80°C.

2.2.2 Poly(A)$^+$ mRNA purification

Principle: Poly(A)$^+$ mRNA binds specifically to an oligo(dT) cellulose matrix and is eluted in hot Tris.Cl/EDTA buffer. Total RNA prepared as described above has been used as the source of poly(A)$^+$ mRNA. Up to 15 μg mRNA per mg of total RNA have been obtained.

Materials:

- The mini-oligo(dT) cellulose spin column kit from 5'→3', Inc. has been used. It contains:
    - oligo(dT) cellulose spin columns;
    - loading buffer: 100 mM Tris.Cl, pH 7.5, 5 mM EDTA, 2.5 M NaCl;
    - wash buffer I: 20 mM Tris.Cl, pH 7.5, 1 mM EDTA, 0.5 M NaCl;
    - wash buffer II: 20 mM Tris.Cl, pH 7.5, 1 mM EDTA, 0.1 M NaCl;
    - elution buffer: 10 mM Tris.Cl, pH 7.5, 1 mM EDTA;
    - 3 M sodium acetate, pH 5.2;
    - 1mg/ml mussel glycogen, in molecular biology-grade water;
- ethanol, absolute and 70% v/v.

1. Equilibrate the mini-oligo(dT) cellulose spin column(s) by washing once with wash buffer I.
2. Prepare the RNA sample(s), dissolved in 1 ml water, by heating 5 minutes at 65°C; then add 0.25 ml loading buffer, mix and cool on ice.
3. Preheat the elution buffer to 65°C. Apply the RNA sample to an equilibrated oligo(dT) cellulose spin column, cap the column and mix the content.
4. Incubate 15 minutes at room temperature with mixing at 2-3 minutes interval.
5. Remove the caps and centrifuge the column 10 sec (at speed) at 200 g. Discard the flow through.
6. Apply 1 ml of wash buffer I to the column and centrifuge 10 sec (at speed) at 200 g.
7. Apply 1 ml of wash buffer II to the column and centrifuge 10 sec (at speed) at 200 g.
8. Apply another 1ml of wash buffer II to the column and centrifuge 10 sec (at speed) at 200 g.

9. Elute the poly(A)$^+$ mRNA by applying 0.5 ml of 65°C elution buffer and immediately centrifuge 10 sec (at speed) at 200 g.
10. Repeat step 9 and pool together the two 0.5 ml elution fractions.
11. Add 20 µl of the 1mg/ml mussel glycogen as carrier, 100 µl of 3 M sodium acetate and 2.8 ml ice-cold absolute ethanol in order to precipitate the mRNA.
12. Incubate at -20°C overnight.
13. Collect the mRNA precipitate by centrifugation for 30 minutes at 16,000 g, at 4°C.
14. Wash the pellet twice with 70% ethanol and once with absolute ethanol, then air dry. Resuspend the mRNA in the desired volume of molecular biology-grade water.

2.2.3 RNA electrophoresis in agarose gels

Principle: RNA molecules can be separated in agarose gels as described above for DNA, however, for better resolution, the RNA secondary structures are denatured in the presence of formaldehyde.

Materials: All chemicals were purchased from Sigma.

- DEPC-treated and autoclaved MilliQ water;
- RNAase-free agarose;
- 10X MOPS buffer: 400 mM MOPS, pH 7.0, 100 mM sodium acetate, 10 mM EDTA;
- 12.3 M formaldehyde (37% solution);
- sample buffer (fresh): 100 µl 10X MOPS buffer, 175 µl formaldehyde; 500 µl deionised formamide, 75 µl water;
- RNA dye: 50% v/v glycerol, 1 mM EDTA, 0.4% w/v bromophenol blue, 0.4% w/v xylene cyanole, in RNAase-free water;
- 10 mg/ml ethidium bromide stock, in RNAase-free water.

1. Soak the gel caster and combs in diluted bleach, overnight, then rinse thoroughly with DEPC-treated water.
2. Prepare a 1% agarose gel in 85 ml DEPC-treated water, add 10 ml of 10X MOPS buffer. Heat the solution until the agarose is dissolved, then let it cool to 60°C and add 5.4ml formaldehyde.
3. Prepare the gel running buffer: 1X MOPS buffer and 0.66 M formaldehyde.
4. Prepare the samples by mixing 3 µl RNA (5-10 µg of total RNA) with 8.5 µl sample buffer. Heat 10 minutes at 55°C, then cool the samples on ice. Add 1.5 µl of a 13:2 mixture of RNA dye and 10 mg/ml ethidium bromide and load the samples in the gel.
5. Run the gel at 4 V/cm until the bromophenol blue has migrated 8 cm and visualise the samples on a UV transilluminator.

2.3 Protein methods

2.3.1 Protein quantitation using bicinchoninic acid

Principle: The BCA Protein Assay kit (Pierce) is a detergent-compatible method based on bicinchoninic acid (BCA) for the colorimetric detection and quantitation of proteins. It combines the biuret reaction (reduction of Cu^{+2} to Cu^{+1} by peptide bonds in an alkaline medium) with sensitive and selective colorimetric detection of Cu^{+1} by BCA. This complex has a strong absorbance at 562 nm that is linear for protein concentrations between 20 µg/ml and 2,000 µg/ml.

Materials:

- BCA Protein Assay kit (Pierce), containing:
    - reagent A (contains sodium carbonate, sodium bicarbonate, BCA and sodium tartrate in 0.2 N NaOH);

- reagent B: 4% cupric sulphate;
- 2 mg/ml bovine serum albumin standard;

- 96-well plate.

1. Mix 50 parts reagent A with 1 part reagent B. 200 µl per sample are required.
2. Adjust the protein samples to 25 µl. Prepare BSA standard samples at 25, 50, 100, 200, 400 and 800 µg/ml. Also use a suitable blank solution. Place the samples in the 96-well plate.
3. Add 200 µl reagent mix per well and mix thoroughly.
4. Cover the plate and incubate 30 minutes at 37°C.
5. Cool the plate at room temperature and measure the absorbance at 562 nm in a plate reader.
6. Subtract the blank reading from the samples and plot a standard curve using the BSA readings. Then, determine the protein concentration for each unknown sample.

2.3.2 Filter paper dye-binding assay for protein quantitation

Principle: This represents a modification (Minamide and Bamburg, 1990) of the classical Bradford assay, the dye-binding being performed on a strip of filter paper rather than in solution. Methanol washing of the paper strip, on which the protein samples are applied, ensures removal of contaminants (ammonium sulfate, urea, thiol-reducing agents, amino acids, DNA, ionic and nonionic detergents) which otherwise interfere with the assay. The assay is based on the equilibrium between three forms of Coomassie Blue G dye. Under strongly acid conditions, the dye is most stable as a doubly-protonated red form. Upon binding to protein, however, it is most stable as an unprotonated, blue form. This assay is linear for 100 ng-20 µg protein/spot.

Materials: All chemicals were purchased from Sigma.

- filter paper (Whatman, no. 1);

- absolute methanol;

- dye solution: 0.5% w/v Coomassie brilliant blue G in 7% acetic acid, filtered;

- destain solution: 7% acetic acid;

- extraction buffer: 66% methanol, 33% water, 1% ammonium hydroxide.

1. Cut 5 mm filter paper stripes and mark on them 5 mm squares with a pencil.
2. Apply 2 µl sample per square and allow to air dry. Include also BSA standard samples in a range of 50 ng-1 µg per spot and keep blank spots.
3. Rinse the strip in absolute methanol for 20 seconds. Allow it to air dry.
4. Place the strip in dye solution (enough to be well covered) and incubate 30 minutes at room temperature, with continuous agitation.
5. Destain the strip in 7% acetic acid, with agitation, until the background is reduced (0.5-3 hours).
6. Air dry the strip. Cut the squares containing samples and transfer them in 1.5 ml Eppendorf tubes containing 200 µl extraction buffer. Vortex well. Incubate for 5 minutes at room temperature, then vortex again.
7. Transfer 150 µl extract in a 96-well plate and read OD_{600}-OD_{405}.
8. Subtract the blank readings from the samples and plot a standard curve using the BSA values. Then, determine the protein concentration for each unknown sample.

2.3.3 Sodium Dodecyl Sulphate – Polyacrylamide Gel Electrophoresis (SDS-PAGE)

Principle: A protein mixture can be separated for analytical or preparative purposes in polyacrylamide gels under conditions that ensure dissociation into individual peptide chains. The strongly anionic detergent sodium dodecyl sulphate (SDS) is commonly

used in combination with a reducing agent and heat to treat the protein samples before they are loaded on the gel. The denatured proteins bind SDS, an amount directly proportional to their molecular weight, and became negatively charged. Therefore they will migrate in an electric field towards the anode and will be separated in the polyacrylamide gel according to their size by sieving.

Materials: All chemicals were purchased from Sigma.

- monomers stock solution: 29% w/v acrylamide, 1% w/v *N,N'*-methylenebisacrilamide prepared in deionised water;
- 10% w/v SDS stock solution;
- TEMED (N,N,N',N'-tetramethylethylenediamine);
- 10% ammonium persulfate solution;
- tank buffer: 25 mM Tris base, 192 mM glycine, pH 8.3, 0.1% w/v SDS;
- 4x resolving gel buffer: 1.5 M Tris base, pH 8.8 adjusted with HCl;
- 4x stacking gel buffer: 0.5 M Tris base, pH 6.8 adjusted with HCl;
- 2x loading buffer: 125 mM Tris, pH 6.8, 4% w/v SDS, 20% v/v glycerol, 200 mM dithiothreitol (add just before use), 0.02% bromophenol blue.

1. Assemble the glass plates according to the manufacturer's instructions.
2. Prepare the resolving gel mix including the concentration of acrylamide appropriate for the size of the protein(s) of interest. A guideline (for 18 ml gel) is given below:

	Acrylamide concentration:				
	6%	8%	10%	12%	15%
Monomers (ml)	3.6	4.8	6	7.2	9
4x resolving gel buffer (ml)	4.5	4.5	4.5	4.5	4.5
10% SDS (µl)	180	180	180	180	180
Deionised water (ml)	9.6	8.4	7.2	6	4.2
10% Ammonium persulphate (µl)	100	100	90	90	80
TEMED (µl)	11	10	8	8	7

3. Pour the gel mix into the casting device, leaving space for the stacking gel (length of comb teeth plus 1 cm). Carefully overlay the gel surface with water or 0.1% SDS. Let the gel polymerise for 1 hour at room temperature.
4. Prepare the stacking gel mix, containing 4% acrylamide, following the guideline (for 5ml) given below:

Monomers (ml)	0.65
4x stacking gel buffer (ml)	1.25
10% SDS (µl)	50
Deionised water (ml)	3
10% Ammonium persulphate (µl)	25
TEMED (µl)	5

5. Pour the stacking gel on top of the resolving gel and carefully insert the comb. Let the gel polymerise 30 minutes at room temperature.
6. Mix the protein samples with an equal volume of 2x loading buffer and heat them for 5 minutes at 100°C.
7. Remove the comb from the gel, assemble the electrophoresis apparatus and add the tank buffer. Remove any air bubbles trapped at the bottom of the gel.
8. Load an amount of sample according to the well size and protein concentration, in order to be able later on to detect the protein of interest by the staining method of choice.
9. Attach the apparatus to a power supply and apply a current of 10mA per 8cm gel length. Run the gel until the bromophenol blue reaches the bottom of the resolving gel. After that, process the gel for protein detection.

2.3.4 Staining SDS-PAGE gels with Coomassie Brilliant Blue

Principle: SDS-PAGE gels are fixed with methanol:trichloroacetic acid and subsequently stained under acidic conditions with the Coomassie Brilliant Blue R250 dye which binds to proteins. A series of washes will allow the excess of dye to diffuse from the gel and the protein bands become clearly visible.

Materials: All chemicals were purchased from Sigma.

- fixing solution: 10% w/v trichloroacetic acid, 40% v/v methanol;
- staining solution: 0.1% w/v Coomassie Brilliant Blue R250, 40% v/v methanol, 10% v/v glacial acetic acid. Filter the solution through Whatman no. 1 paper to remove any particulate matter.
- destaining solution: 50% v/v methanol, 10% v/v acetic acid.

1. Immerse the gel into the fix solution for 20 minutes at room temperature.
2. Decant the fix solution (can be reused several times) and cover the gel with staining solution. Incubate (with gentle shaking) 20 minutes at room temperature, if the staining solution is fresh, or up to 1 hour otherwise. Decant and re-use the staining solution.
3. Cover the gel with destaining solution and incubate (with gentle shaking) 20 minutes at room temperature. Add fresh destaining solution and incubate as above, until the background is removed. If the gel is left overnight, the destaining solution must be diluted 1:4 with water. The destaining solution can be reused after filtering through active charcoal.
4. The gels can be stored indefinitely in water containing 20% glycerol or dried on filter paper, on a heated gel dryer.

2.3.5 Staining SDS-PAGE gels with silver nitrate

Principle: This process is based on the differential reduction of silver ions bound to the side chains of amino acids, from the proteins precipitated within the gel, to metallic silver.

Materials: All chemicals were purchased from Sigma.

- fixing solution: 50% v/v methanol, 12% v/v acetic acid;
- 50% ethanol;
- 1.25 mM $Na_2S_2O_3$ (sodium thiosulphate) solution;
- 0.6 M silver nitrate stock solution;
- 12.3 M formaldehyde (37% solution);
- developing solution: 0.56 M Na_2CO_3, 0.02% formaldehyde, 25 μM $Na_2S_2O_3$.

1. Incubate the gel in fixing solution 1 hour – overnight at room temperature.
2. Discard the fixing solution and cover the gel with 50% ethanol. Incubate the gel for 20 minutes at room temperature, with gentle shaking.
3. Repeat step 2 twice.
4. Discard the ethanol and incubate the gel 1 minute in the sodium thiosulphate solution.
5. Wash the gel 3 times, 20 seconds each, with distilled water.
6. Dilute the silver nitrate stock solution 1:50 with water and add formaldehyde to 0.03% final concentration. Prepare enough to cover the gel. Incubate the gel in this solution for 30 minutes at room temperature with gentle shaking.
7. Wash the gel briefly with water.
8. Cover the gel with developing solution and incubate with gentle agitation until the desired signal (and contrast) is obtained (usually a couple of minutes).
9. Wash the gel briefly with water and then quench the reaction by incubating the gel in fixing solution for 15 minutes.

10. Soak the gel in water 30 minutes. The gels can be stored indefinitely in water containing 20% glycerol or dried on filter paper, on a heated gel dryer.

2.3.6 Western immunoblotting

Principle: Electrophoretically separated proteins are electrotransferred from a polyacrylamide gel to a membrane (nitrocellulose or polyvinylidene difluoride usually) and probed with antibodies that recognise epitopes displayed on their surface. Bound antibodies are detected subsequently by using a reporter enzyme (horseradish peroxidase or alkaline phosphatase usually) crosslinked either to the primary antibody or to a secondary one.

Materials: All chemicals were purchased from Sigma.

- nitrocellulose or polyvinylidene difluoride (PVDF) membrane (Amersham Pharmacia Biotech or Stratagene);
- transfer buffer:
    - for semi-dry transfer: 48 mM Tris base, 39 mM glycine, 0.037% w/v SDS, 20% v/v methanol;
    - for wet transfer: 50 mM Tris base, 380 mM glycine, 0.1% w/v SDS, 20% v/v methanol;
- Ponceau S solution: 2 g Ponceau S, 30 g trichloroacetic acid, 30 g sulfosalicylic acid, water to 100 ml;
- blocking buffer: 5% w/v nonfat dried milk in PBS, pH 7.4;
- antibody dilution buffer: 5% w/v nonfat dried milk, 0.1% Tween-20 in PBS, pH 7.4;
- wash buffer: 0.1% Tween-20 in PBS, pH 7.4.

Note: If using anti-phosphotyrosine antibodies, replace the nonfat dried milk with bovine serum albumin and PBS with TBS (25 mM Tris base, 137 mM NaCl, adjust pH to 7.6 with HCl).

1. Cut six filter paper pieces and a piece of membrane to the exact size of the SDS-polyacrylamide gel. Equilibrate them in transfer buffer for 15 minutes. If PVDF membrane is used, it has to be soaked 5 seconds in absolute methanol and then rinsed well with water before being put in transfer buffer.
2. Arrange the following "sandwich", from anode: 3 layers of filter paper, the membrane, the polyacrylamide gel, 3 layers of filter paper. Align them exactly and remove any trapped air bubbles. Submerge this under transfer buffer (for wet transfer).
3. Connect the blotting apparatus to the power supply and set the current at 0.65 mA/cm^2 of gel, run for 1 hour (semi-dry transfer), or set the voltage to 60 V and run for 16 hours (wet transfer, with cooling).
4. Remove the membrane from the stack and stain it a couple of minutes with Ponceau S solution. Mark the positions of the molecular weight markers with a pencil.
5. Wash the membrane twice with water and cover it with blocking buffer. Incubate overnight at 4°C or one hour at room temperature.
6. Wash the membrane 5 minutes at room temperature in wash buffer.
6. Place the membrane in a plastic bag, add the primary antibody diluted as necessary in the antibody dilution buffer, seal the bag and incubate 1 hour at room temperature, with shaking.
7. Wash the membrane 3 times for 5 minutes each at room temperature in wash buffer.
8. If necessary, place the membrane in a plastic bag, add the secondary antibody diluted as appropriate in the antibody dilution buffer, seal the bag and incubate 1 hour at room temperature, with shaking.
9. Wash the membrane 3 times for 5 minutes each at room temperature in wash buffer.

10. Detect the bound (and labelled) antibody as appropriate for the reporter enzyme used. We normally use horseradish peroxidase-conjugated antibodies and detect them by chemiluminescence using the ECL Plus kit from Amersham Pharmacia Biotech, according to the manufacturer's instructions.

2.3.7 Blot-overlay assay

Principle: This technique is very similar to western immunobloting (described above), the only difference being that, instead of using a primary antibody for identifying antigens immobilised on the membrane, one uses a tagged form of the protein for which binding partners (ligands) present on the membrane are sought after. The washing and dilution buffers must be adjusted to reflect the particular properties of the interaction analysed (e.g. sensitivity to various reagents present in the buffers).

2.3.8 Immunoprecipitation of target proteins

Principle: Proteins of interest present in a mixture (e.g. cell lysate) can be isolated and analysed if specific antibodies directed against them or a stable interaction partner are available. Following antibody binding, in solution, the complex is isolated with Protein A/G/L or secondary antibody immobilised on beads, and further analysed. The method described below exemplifies immunoprecipitation of proteins from mammalian cell lysates.

Materials: All chemicals were purchased from Sigma.

- RIPA buffer: 50 mM Tris.Cl, pH 8, 150 mM NaCl, 1% Nonidet P-40 (NP-40), 0.5% sodium deoxycolate, 0.1% SDS, 100 μg/ml phenylmethylsulfonyl fluoride (PMSF), 1μg/ml aprotinin.
- primary antibody against the protein of interest;
- protein A/G/L or secondary antibodies immobilised on beads;

- NET-gel buffer: 50 mM Tris.Cl, pH 7.5, 150 mM NaCl, 0.1% Nonidet P-40, 1 mM EDTA, 0.25% gelatin (from a sterile 2.5% w/v stock, melted just before use).

1. Wash the cell culture dish briefly with PBS, then add 0.25 ml ice-cold RIPA buffer per 3.5 mm dish. Incubate on ice for 30 minutes.
2. Scrape the cells to one side of the dish and transfer the lysate to a chilled centrifuge tube. Centrifuge 5 minutes at 13,000 g, at 4°C.
3. Transfer the supernatant to a fresh centrifuge tube and adjust the volume to 1 ml with cold NET-gel buffer. Split the lysate in two equal parts, add antibody against the target protein to one half, and a control antibody to the other half.
4. Incubate the lysates for 1 hour at 0-4°C, with gentle rocking.
5. Add the protein A/G/L or secondary antibody immobilised on beads, enough to precipitate the primary antibody. Incubate the lysates for 1 hour at 4°C, with gentle rocking.
6. Collect the beads by centrifugation, 20 seconds at 12,000 g, at 4°C. Carefully remove the supernatants and resuspend the beads in 1 ml RIPA buffer. Incubate 15 minutes at 4°C, with gentle rocking.
7. Repeat step 6 twice.
8. Add 30 µl SDS-PAGE 2x gel loading buffer (see above) and analyse the sample by electrophoresis and western blotting.

2.4 Cell culture methods

2.4.1 Basic cell culture procedures

Cell lines: All the cell lines used for various experiments (293T, COS7, NIH/3T3) were obtained from the Dunn School Cell Bank (Department of Pathology, University of

Oxford). They were grown in Dulbecco's Modified Eagle's Medium (DMEM) with 10% v/v heat inactivated foetal bovine serum and 1% v/v penicillin-streptomycin solution (10,000 units penicillin and 10 mg streptomycin per ml), in a humidified 37°C incubator, with 5% CO_2. All reagents commonly used for cell culture were obtained from Sigma.

Culture splitting (adherent cells): All solutions were pre-warmed at 37°C. The cells were briefly washed with PBS (without $CaCl_2$ and $MgCl_2$) and then detached by adding a few drops of trypsin-EDTA solution (0.05% porcine trypsin and 0.02% EDTA·4Na) and incubating at room temperature as necessary. The trypsin was inactivated by adding 2 ml growth medium. The cells were centrifuged 5 minutes at 1,000 rpm, at room temperature, and the supernatant was discarded. Then the cells were resuspended in the desired amount of fresh growth medium and seeded in plastic dishes.

Cell freezing/thawing: Frozen stocks of cells can be kept indefinitely in liquid nitrogen. Adherent cells were split with trypsin, centrifuged and resuspended in the appropriate amount of fresh growth medium containing 10% dimethyl sulfoxide (DMSO). 1 ml aliquots (containing approximately 10^6 cells) were transferred into cryovials and frozen slowly to -70°C. 24 hours later the vials were transferred to liquid nitrogen. For thawing, vials recovered from liquid nitrogen were immediately transferred to a water bath pre-warmed to 37°C for 1 minute, then the cells were transferred into a centrifuge tube containing 5 ml fresh growth medium. Following a 5 minutes centrifugation at 1,000 rpm the supernatant was discarded, the cells resuspended in the desired amount of growth medium and seeded in plastic dishes.

2.4.2 Line 0 chick embryo fibroblasts (CEF) primary cultures

Principle: Line 0 eggs were obtained from highly inbred, retrovirus-free chickens. Fibroblasts, isolated by proteolytic digestion from ten days old (E10) line 0 embryos, can be effectively transfected with retroviral DNA and then they will produce viral particles, at high titers, which can easily spread in the whole culture.

Materials: All chemicals were purchased from Sigma.

- line 0 eggs (supplied by the Institute for Animal Health, Newbury, Berks);
- sterile PBS;
- sterile dissociation medium: F10 medium, 0.12% w/v sodium bicarbonate, 10 mM HEPES, pH 7.4, 1 mg/ml trypsin, 1.5 mg/ml collagenase;
- growth medium: DMEM, 10% v/v heat inactivated foetal bovine serum, 2% v/v heat inactivated chick serum, 100 U/ml penicillin, 100 μg/ml streptomycin;
- dimethyl sulfoxide.

All the procedure is done under sterile conditions, in a laminar flow sterile cabinet. All the solutions must be pre-warmed at 37°C.

1. Collect E10 chick embryos from the eggs, immerse in PBS in a plastic dish and remove the head, limbs and viscera.
2. Mince the trunks with a sterile blade and transfer them into a 50 ml centrifuge tube containing 10 ml dissociation buffer (roughly enough for 2 trunks).
3. Incubate 20 minutes at room temperature with gentle shaking.
4. Dissociate the large tissue clumps by repeated pipetting with a 10ml serological pipette and incubate 30 more minutes at room temperature.
5. Place the tube in a vertical position and allow the cell clumps to settle for 5 minutes.

6. Transfer the supernatant into a fresh centrifuge tube and spin 5 minutes at 1,000 rpm at room temperature. Discard the supernatant and resuspend the cells in 5 ml growth medium. Count them using a haemocytometer and adjust the final volume to have $2x10^6$ cells/ml. The cells can be seeded directly on plastic dishes or frozen as described above.

2.4.3 Retinal glial cell primary cultures

Principle: Müller glial cells are the most abundant non-neuronal cells in the vertebrate retina. They can be isolated from chick embryo retinas by proteolytic digestion and maintained in culture, for a limited number of passages, for cell biological and biochemical studies.

Materials: All chemicals were purchased from Sigma.

- white Leghorn eggs, supplied by Needle Farm, Herts;
- sterile PBS, without $CaCl_2$ and $MgCl_2$;
- sterile dissociation medium: F10 medium, 0.12% w/v sodium bicarbonate, 10 mM HEPES, pH 7.4, 1 mg/ml trypsin;,1.5 mg/ml collagenase;
- growth medium: DMEM, 10% v/v heat inactivated foetal bovine serum, 2% v/v heat inactivated chick serum, 100 U/ml penicillin, 100 µg/ml streptomycin.

The procedure (except initial dissection) is done under sterile conditions, in a laminar flow cabinet. All the solutions must be pre-warmed at 37°C.

1. Dissect E7 chick retinas (six will usually be enough) in sterile PBS, completely removing the pigmented epithelial layer. Transfer the retinas to a 15 ml centrifuge tube containing fresh PBS, without $CaCl_2$ and $MgCl_2$, and incubate 10 minutes at room temperature.

2. Carefully remove the PBS and add 5ml dissociation medium. Incubate 10 minutes at room temperature.
3. Gently dissociate tissue clumps by repetitive pipetting. Let the tube stand vertically 5 minutes and transfer the supernatant to a fresh tube. Centrifuge 5 minutes at 1,000 rpm, at room temperature.
4. Discard the supernatant and resuspend the pellet in 5ml growth medium. Count the cells and seed them in plastic dishes at the desired cell density.

2.4.4 Retinal explant cultures

Principle: Retinal ganglion cells are able to extend robust neurites *in vitro*, when grown on a growth permissive substrate, such as laminin or retinal basal laminae. Dissected retinae were flatmounted on a nitrocellulose filter and 280 μm wide strips were cut with a tissue chopper. The strips are then placed on various growth substrates and the influence of various reagents on axon growth can be measured. This protocol is based on Halfter *et al.*, (1987).

Materials: All chemicals were purchased from Sigma.

- white Leghorn eggs, supplied by Needle Farm, Herts;
- sterile PBS;
- 13 mm glass coverslips;
- 90% nitric acid;
- absolute methanol;
- 0.01% poly-L-lysine (PLL) solution;
- growth medium: F12 nutrient mixture, 10% v/v heat inactivated foetal bovine serum, 2% v/v heat inactivated chick serum, 100 U/ml penicillin, 100 μg/ml streptomycin;
- nitrocellulose filters (Millipore);

- metal bars (8x1.5x1.5 mm);

Coverslip preparation:

1. Place 1-200 glass coverslips in a glass Petri dish and cover them with nitric acid. Incubate 30 minutes at room temperature with slow shaking.
2. Discard the nitric acid and wash the coverslips in distilled water, 30 minutes at room temperature with slow shaking.
3. Discard the water and wash the coverslips in absolute methanol, 30 minutes at room temperature with slow shaking.
4. Air dry the coverslips and sterilise them by baking 4 hours at 150°C.
5. Coat the desired number of coverslips with 150 µl PLL solution, 30 minutes at room temperature.
6. Aspirate the PLL and allow the coverslips to air-dry (in a laminar flow sterile cabinet) for 30 minutes-1 hour. They can be stored at 4°C for up to a week.

7. (Optional) Coat the coverslips with 150 µl solution of various extracellular matrix components (e.g. laminin 50 µg/ml, fibronectin 50 µg/ml), incubate 30 minutes at room temperature. Then aspirate the solution and leave the coverslips to air-dry 45 minutes.

Dissection and flatmounting of retinae:

1. Remove the eyes of an E7 embryo by careful circling a closed pair of forceps around the eye. The dissection is performed in sterile growth medium.
2. Peel off the connective tissue and then the pigmented epithelial layer. Remove the lens and the vitreous body.
3. Cut a 1 cm^2 piece of a nitrocellulose filter and slide it underneath the retina. Carefully unroll the retina and pin it down on the filter, vitreal side up.
4. Wash the filter in clean medium to remove any dissection debris attached.

Basal lamina coating of glass coverslips:

1. Take a fresh flatmounted retina and briefly dry the supporting filter on a paper tissue to remove excess of liquid.
2. Placed the retina (vitreal side down) on a PLL coated coverslip. Place three metal bars on the filter and add a drop of medium just to keep the filter moist.
3. Incubate 15 minutes at 37°C in a humidified incubator.
4. Remove the metal bars and slowly peel off the filter with retina attached and discard it. Basal lamina should stick to the coverslip.
5. Cover the coverslip with medium and keep in the incubator until needed (no longer than a couple of hours).

Retinal explants culture:

1. Flatmount a retina as described above and cut the filter into 280 μm strips using a tissue chopper. Orient the retina so that the optic fissure is perpendicular to the blade, since the cells in this region produce the most axons.
2. Place two strips (retina face down) on the basal lamina coated coverslips. Hold down with two metal bars across the ends of the strips.
3. Add a few drops of growth medium and incubate 15 minutes in the 37°C, humidified incubator, to allow the strips to attach.
4. Add the rest of growth medium (according to the dish size) and culture overnight in the incubator.

2.4.5 Transient transfection of adherent cells

Principle: DNA constructs are introduced (transfected) into cultured eukaryotic cells for various functional studies and for recombinant protein production. The transfection

is usually achieved by using DNA precipitation reagents (e.g. calcium phosphate, DEAE-dextran), liposomes, positively charged dendrimer reagents or by electroporation. When the cells are transfected transiently, the DNA of interest is introduced into the cell nucleus but does not integrate into chromosomes. Many copies of the gene of interest are present (if it is cloned into a plasmid able to replicate episomally) therefore allowing high level of protein expression. We currently use the Superfect reagent (Qiagen), a spherical activated dendrimer terminating at charged amino groups, for most transient transfections.

Materials:

- serum/antibiotic free and complete growth medium, specific for the cell line transfected;
- sterile DNA, 1 μg/μl stock;
- sterile PBS;
- Superfect transfection reagent (Qiagen).

The media and PBS solutions should be pre-warmed at 37°C.

1. One or maximum 2 days in advance, seed the cells to be transfected in a plastic dish so that they will be 50-80% confluent on the day of transfection. Grow them at 37°C, 5% CO_2, in a humidified incubator.
2. Dilute the DNA of interest to 0.03 μg/μl in serum/antibiotic free medium, the final volume depending on the dish size (150 μl for a 60 mm dish). Mix briefly.
3. Add 4 μl Superfect reagent per μg DNA, mix well and incubate 10 minutes at room temperature to allow complex formation.
4. While the complex is forming, aspirate the growth medium from the cells and briefly wash with PBS.

5. Add complete growth medium to the complex, just enough to cover the cells (the volume depends on the dish size, for example 1 ml for a 60 mm dish), mix by pipetting twice and immediately transfer the mixture to the cells.
6. Incubate the cells at 37°C, 5% CO_2, in a humidified incubator, for 3 hours.
7. Remove the medium containing the Superfect-DNA complex, wash the cells once with PBS and cover them with the appropriate amount of complete growth medium.
8. Assay for gene expression 24-48 hours post-transfection.

2.5 Histology/cytology methods

2.5.1 Preparation of tissue cryosections

Principle: Tissue samples (pre-fixed or not) are frozen, cut into thin sections using a cryostat, mounted on glass microscope slides and stored at -70°C indefinitely.

Materials:

- glass microscope slides;
- industrial methylated spirits (IMS);
- 2% 3-aminopropyltriethoxysilane (Sigma) in IMS;
- 4% paraformaldehyde in PBS;
- 30% sucrose in PBS;
- OCT tissue freezing compound (Tissue Tek).

Preparation of glass microscope slides:

1. Place the slides in plastic racks and immerse in IMS for 5 minutes.
2. Transfer the racks in 2% 3-aminopropyltriethoxysilane (Sigma) in IMS and incubate 5 minutes.

3. Wash the slides twice in deionised water, then briefly dehydrate in IMS. Place them on a paper towel to dry, for 60 minutes, then bake at 65°C for two hours. Store in an air-tight box.

Preparation of tissue samples and sectioning:

1. Tissue samples are either frozen immediately after surgical decapitation or fixed overnight in 4% paraformaldehyde in PBS and cryoprotected in 30% sucrose in PBS for another 24 hours.
2. Place the tissue in a mould with OCT compound and orient it in the desired position. Then transfer it on a dry ice/pentane bath until frozen. Store at -70°C.
3. For section, warm the frozen tissue pieces to -20°C and cut 10-12 μm thick sections in a cryostat (Bright Instrument Company).
4. Place the freshly-cut sections on a glass slide, let them air-dry, incubate 2 hours at 37°C and then wrap the slides in aluminium foil and store at -70°C.

2.5.2 Immunohistochemistry and immunocytochemistry

Principle: Antibody detection of specific antigens exposed in tissue sections or expressed by adherent cells. This example illustrates the use of an unlabelled primary antibody and fluorochrome-labelled secondary antibody. When horseradish peroxidase-labelled secondary antibodies were used, they were localised using diaminobenzidine and hydrogen peroxide as substrates.

Materials:

- tissue sections mounted on glass microscope slides OR adherent cells grown on extracellular matrix components-coated glass coverslips;
- humidified plastic chamber for incubations;
- fixative: ice-cold absolute methanol or fresh 4% paraformaldehyde in PBS, pH 7.5;

- pre-block solution: 1% w/v bovine serum albumin (BSA), 0.2% Triton X-100 in PBS;
- antibody dilution solution: 3% w/v BSA, 0.05% Triton X-100 in PBS;
- wash solution: 0.1% w/v BSA, 0.05% Triton X-100 in PBS;
- antibodies (unlabelled primary, fluorochrome-labelled secondary);
- mounting reagent: Fluorosave (Calbiochem).

1. Rinse the slides/coverslips briefly in PBS.
2. Fix the tissue sections/cells either with 4% paraformaldehyde, 5 minutes at room temperature or with ice-cold absolute methanol, 1-5 minutes at -20°C (The fixation method depends on the antigen sensitivity).
3. Rinse the slides/coverslips briefly in PBS, twice. If using microscope slides, draw around the sections of interest a hydrophobic circle using a wax pen, to prevent leakage of antibody solutions.
4. Block non-specific binding sites by covering the tissue sections/cells with pre-block solution. Incubate 15 minutes at room temperature.
5. Remove the pre-block solution and incubate the tissue sections/cells with the primary antibody, adjusted to the working concentration with dilution solution. Incubate 1 hour at room temperature or overnight at 4°C.
6. Wash the slides/coverslips in wash solution 3 times, 5 minutes each, with shaking, at room temperature.
7. Incubate the tissue sections/cells with the secondary (labelled) antibody adjusted to the working concentration with dilution solution. Incubate 1 hour at room temperature. At this step other staining reagents (e.g. phalloidin-TRITC) can be added.
8. Repeat step 6.
9. Rinse the slides/coverslips briefly in distilled water.

10. Mount them in Fluorosave, allow the reagent to solidify 1 hour at room temperature and then store the slides up to two weeks, in dark, at 4°C.

2.5.3 Receptor Affinity Probe (RAP) *in situ*

Principle: Cell-surface receptors usually bind their ligands with high affinity and specificity. Therefore, soluble receptor ectodomains, usually tagged at their carboxy terminus, can be used as probes to detect their ligands in various assay formats. The heat-stable human placental alkaline phosphatase (AP) is commonly being used as a C terminus tag (Flanagan *et al.*, 2000). It has the advantage of possessing an intrinsic enzymatic activity that allows easy detection and accurate quantification.

Materials: All common chemicals were purchased from Sigma.

- tissue sections mounted on glass microscope slides OR adherent cells grown on extracellular matrix components-coated glass coverslips;
- AP fusion protein: 7-day conditioned medium obtained from 293T cells transiently transfected with a plasmid encoding the construct of interest; this medium is buffered with 10mM HEPES, pH 7, sterile filtered (0.45 μm), and stored at 4°C;
- humidified plastic chamber for incubations;
- fixatives: ice-cold absolute methanol and fresh 4% paraformaldehyde in PBS, pH 7.5;
- HBAH buffer: Hanks' balanced salt solution, 20 mM HEPES, pH 7.0, 0.5 mg/ml bovine serum albumin, 0.1% w/v NaN_3;
- HBS buffer: 10 mM HEPES, pH 7.0, 150 mM NaCl;
- AP buffer: 100 mM Tris.HCl, pH 9.5, 5 mM $MgCl_2$, 100 mM NaCl;
- NBT/BCIP (nitroblue tetrazolium / bromochloro-indolyl phosphate) substrate mix (Roche Molecular Biochemicals).

1. Rinse the slides/coverslips 2 minutes in HBS, at room temperature.

2. (Optional) Fix the tissue sections/cells either with ice-cold absolute methanol, 2 minutes at -20°C or with 4% paraformaldehyde, 5 minutes at room temperature (The fixation method should be tested and optimised for each receptor/ligand pair).

3. Rinse twice, 90 sec each, in HBAH buffer.

4. Add AP fusion protein to cover the tissue sections/cells and incubate 90 minutes at room temperature

5. Wash the slides/coverslips six times, 90 sec each, in cold HBAH buffer.

6. Fix in 4% paraformaldehyde, 90 sec at room temperature.

7. Wash the slides/coverslips twice, 90 sec each, in HBS.

8. Incubate the sections/coverslips in pre-heated HBS, in a 65°C waterbath, for 30 minutes – 1 hour.

9. Wash the slides/coverslips in AP buffer, 5 minutes.

10. Add AP buffer containing NBT/BCIP to cover the tissue sections/cells and incubate at room temperature in a dark humidified plastic chamber. Monitor the reaction periodically until the desired signal intensity is achieved.

11. Stop the reaction by washing briefly with distilled water and mount the slides/coverslips.

2.6 Chick embryo manipulation methods

2.6.1 *In ovo* electroporation

Principle: Electroporation (permeabilisation of cell membranes by application of short-duration electric field pulses) is an increasingly popular method for gene transfer into neurons *in vivo* (Haas *et al.*, 2001). For chick *in ovo* electroporation, fertile eggs are incubated to the desired developmental stage, then a window is cut in the shell allowing visualisation of the embryo. A solution containing the macromolecule of interest (e.g.

DNA) is injected into the target organ and two electrodes connected to an electric pulse generator are placed so that the electric field will open pores in the cell membranes in the region of interest and charged molecules will be carried by electrophoresis into these cells. The egg is sealed and the embryo is left to develop to a stage when the phenotypic effect can be assessed.

Materials: All common chemicals were purchased from Sigma.

- fertile eggs (White Leghorn, from Needle farm, Herts);
- DNA to be electroporated, 2 μg/μl, dissolved in 10 mM Tris.HCl, pH 8, 1mM EDTA;
- 0.1% w/v fast green dye (0.22 μm push-filtered and boiled 20 minutes);
- antibiotic/antimycotic solution (100U penicillin, 0.1 mg streptomycin and 250 ng amphotericin B per ml);
- glass microneedles (pulled glass capilaries).

The protocol shown below was optimised for the Electro Square Porator ECM 830 (BTX).

1. Place the eggs horizontally at 38°C in a humidified incubator. Allow them to reach embryo stage 10 (approx. 33 hours, Hamburger and Hamilton, 1992).
2. Using a 19G needle connected to a syringe, made a small hole at the blunt end of the egg in order to release the air in the air sac, and a similar hole at the pointed end of the egg. Remove 5ml of albumin in order to lower the embryo.
3. Cover the "upper" side of the shell (as the eggs were incubated), including the two holes, with a strip of scotch tape.
4. Mix 3 μl DNA solution with 0.2 μl fast green stock, and transfer it, using a Microloader pipette tip (Eppendorf) into a glass microneedle. Connect it with a

compressed air supply [controlled by a PM1000 Microinjector (MicroData Instrument Inc.)].

5. Open a 2-3 cm long, 1 cm wide window in the top surface of one egg, through the scotch tape, in order to minimise shell cracking.
6. Localise the embryo and carefully insert the glass needle in the target organ. Inject a desired amount of DNA.
7. Retract the glass needle and place a pair of electrodes (gold coated Genetrodes, BTX) either side of the target region. For electroporation of the optic primordium, one of the electrodes was replaced with a sharp tungsten wire placed inside the prosencephalon.
8. Apply a series of 4 pulses, 50 msec each, with 950 msec intervals, at 10 V (for the optic primordium, optimum conditions for other organs need to be tested).
9. Retract the electrodes, cover the embryo with a few drops of antibiotic/antimycotic solution, re-seal the egg with scotch tape and place it into the incubator.
10. Observe the phenotype at the desired stage.

Chapter 3. **Expression cloning attempts to identify CRYPα ligands**

3.1 Introduction

An increasing number of experimental data, reviewed in chapter 1.4, support the hypothesis that CRYPα and its mammalian orthologue RPTPσ play important functional roles during nervous system development and regeneration. This fact has prompted us and other research groups to try to identify interaction partners for CRYPα in order to understand the molecular mechanisms behind its functions and to provide starting points in designing molecules able to modulate them. The "receptor-like" (type I transmembrane protein) structure of CRYPα and the presence of CAM-like domains in its extracellular region suggest that it should be able to bind extracellular ligands. Indeed, preliminary studies using the receptor affinity probe technique (RAP *in situ*; Flanagan *et al.*, 2000) suggest the existence of at least three classes of CRYPα ligands: one in the extracellular matrix (basement membranes of the retina, optic stalk, optic chiasm and optic tectum, all representing physiological substrates on which the retinal ganglion cell axons grow), a second one on the endfeet of radial glial cells (situated just below the retinal and tectal basement membranes) and a third one on retinal and tectobulbar axons themselves (Haj *et al.*, 1999). In addition, Haj *et al.* (1999) have demonstrated that neither CRYPα1 nor CRYPα2 isoforms bind in a homophilic manner, as suggested for other type II RPTPs such as HmLAR, RPTPδ, RPTPμ and RPTPκ (see chapter 1.3.2).

A variety of biochemical and molecular biology tools for the identification and characterisation of protein-protein interactions have been developed. These include "classical" co-immunoprecipitation, receptor affinity chromatography, phage display of peptide libraries, various two-hybrid system formats and expression cloning. We

decided to choose expression cloning (Seed, 1995) for both theoretical and practical considerations.

Theoretical reasons include:

- *the nature of CRYPα receptor*: CRYPα is a transmembrane protein and its ectodomain is membrane-attached; it contains Ig-like domains which require disulfide bond formation for correct folding; the ectodomain is likely to be glycosylated, which may be relevant for correct folding or ligand binding and therefore only a mammalian expression system is appropriate.
- *the expected nature of its ligands*: RAP *in situ* results predicted that some ligands are cell surface-attached (on glia and neurons; Haj *et al.*, 1999); the ligands themselves might have stringent requirements for correct folding and post-translational processing, therefore their expression in mammalian cells is the most appropriate; the particular expression cloning strategy employed here does not permit identification of secreted ligands.

The practical issues considered were:

- *the very limited amount of CRYPα1 or CRYPα2 ectodomains* we were able to produce: repeated attempts to obtain stable cell lines secreting CRYPα ectodomain constructs have failed (F. Haj, I. McKinnell and A. Stoker, unpublished data). The transient transfection procedure we use for expressing CRYPα constructs in 293T cells, after years of optimisation, does not produce more than a few tens of micrograms per litre of conditioned medium - clearly insufficient for classical biochemical approaches. Attempts to scale-up production by transfecting a very large number of cells were not financially realistic.
- *the fact that CRYPα-AP fusion proteins, even expressed at such low levels, were sufficient to detect ligands by RAP-in situ* (Haj *et al.*, 1999). Indeed, this method is

extremely sensitive, with detection limits into the subfemtomole range (Flanagan and Cheng, 2000).

- *the successful application of this method (expression cloning and screening with AP-fused constructs) to identify several receptor/ligand pairs* such as neuropilin-1/semaphorin III (He and Tessier-Lavigne, 1997; Kolodkin *et al.*, 1997), OB-R/leptin (Tartaglia *et al.*, 1995), EphA3/ephrin-A2 and EphA4/ephrin-A2 (Cheng and Flanagan, 1994) and c-kit/stem cell factor (Flanagan and Leder, 1990).

A successful expression cloning procedure largely relies on using a suitable cDNA expression library. Based on the ligand expression pattern (as judged from RAP *in situ* experiments on tissue sections; Haj *et al.*, 1999) we thought that the chick optic tectum would represent a good source of RNA. The developmental stage selected was E7, a day after the RGC axons reach the optic tectum and presumably bind to ligands expressed there. Therefore, I generated an E7 chicken optic tectum directional cDNA expression library, placed under a CMV promoter in a plasmid containing the SV40 origin of replication. Control constructs cloned in this vector were expressed at high levels in several cell lines. After optimising transfection, expression and screening conditions, the library was transfected into COS7 cells for expression cloning. Although small numbers of "positive" cells were routinely obtained, no enrichment was observed during consecutive rounds of selection. Therefore, a CRYPα ligand could not be identified using this procedure. Experimental details and possible reasons leading to this outcome will be discussed below.

3.2 Experimental procedures

cDNA library construction. E7 chick embryo heads were dissected in ice-cold PBS and the optic tectum was cut from each embryo and snap-frozen immediately in liquid nitrogen. One gram of frozen tissue was crushed to obtain a fine powder by using

a mortar and pestle (cooled on a dry ice/IMS bath). Total RNA was extracted using the *Perfect*RNA kit (5'-->3', Inc.) as described in chapter 2.2.1. Poly(A)$^+$ mRNA was prepared by two rounds of oligo(dT) cellulose purification from 1 mg total RNA, using the Mini-oligo(dT) cellulose spin column kit (5'-->3', Inc.) as described in chapter 2.2.2. Double-stranded cDNA was obtained using the pCMV-Script XR cDNA library construction kit (Stratagene). First strand synthesis was primed with an eighteen-base poly(dT) oligo, also containing a *Xho*I restriction site and a 5' "GAGA" protective sequence. *Eco*RI adapters were added at the ends of blunted double-stranded cDNA molecules, followed *Xho*I digestion. The use of 5-methyl dCTP during first strand synthesis protects endogenous *Xho*I sites from being digested. *Eco*RI -*Xho*I cDNA fragments were size-fractionated on a Sepharose CL-2B gel filtration column and aliquots of the fractions collected were radiolabelled with [α-^{32}P]dCTP using Klenow DNA polymerase (taking advantage of the *Xho*I restriction site sequence) and separated by agarose gel electrophoresis. Fractions containing fragments larger than 2 kb were pooled and cloned into the pCMV-Script expression vector (Stratagene). This library was named LTc1R. Before screening, the library was amplified using the semi-solid amplification method (Hanahan *et al.*, 1991) in two 500 ml bottles with 2xLB agarose (for 1 litre: 20 g tryptone, 10 g yeast extract, 10 g NaCl and 3 g SeaPrep agarose).

Expression of the CRYPα-AP fusion proteins. A *Hin*dIII - *Xho*I insert from the APtag-2 plasmid (Flanagan and Leder, 1990), which encodes for the heat-stable human placental alkaline phosphatase (AP) lacking its secretion signal, was subcloned into the pcDNA 3.1 eukaryotic expression vector (Invitrogen). The resulting plasmid was called pBG and represents the backbone vector in which several CRYPα constructs described in this thesis were cloned. The ectodomains of CRYPα1 (amino acids 1 to 721; pBG-CRYPα1-AP, created by I. McKinnell) and CRYPα2 (amino acids 1 to 1124;

pBG-CRYPα2-AP, created by I. McKinnell) were subcloned in the *Hin*dIII site of pBG in frame with the AP. CRYPα1-AP and CRYPα2-AP fusion proteins were expressed by transient transfection in 293T cells. Conditioned media were collected after six to eight days, 0.45 μm filtered, buffered with 20mM HEPES (pH 7) and stored at 4°C.

An *Xba*I fragment from the pBG-CRYPα1-AP plasmid, encoding for the CRYPα1-AP fusion protein, was subcloned into the "shuttle" vector pCS3N (see chapter 6.2), removed by *Cla*I and *Acl*I digestion and finally ligated into the *Cla*I-opened RCAX (A. Stoker, unpublished) avian replication-defective retrovirus. The resulting construct was named RX-CRYPα1-AP. RCAX is derived from the RCAS(A) avian retrovirus (Hughes *et al.*, 1987) by removal of the *gag* and *pol* genes in order to allow subcloning of larger inserts (up to 5 kb). RCAX and derivatives are replication-incompetent, therefore co-transfection with a helper virus such as RIAS (Chen *et al.*, 1999) is required for viral particle production and spreading into chick or quail cell cultures. RX-CRYPα1-AP and RIAS were co-transfected into the QT6 fibroblast cell line and the cells were passaged every 96 hours. Twenty-four hours later, cells were stained for AP activity, thus monitoring the expression of fusion proteins and virus spreading.

Screening of the expression library. The 10 cm tissue culture dishes of COS7 cells (approx. 10^6 cells/dish) were transiently transfected with 10 μg of LTc1R plasmid DNA each, using Superfect (see chapter 2.4.5). When the procedure was scaled-up, fifteen 15 cm tissue culture dishes with COS7 cells (approx. $2.5x10^6$ cells/dish) were transfected using the DEAE-dextran method (Arrufo, 1997). In control experiments, the DEAE-dextran transfection method was found to be as efficient as the Superfect when using COS7 cells (data not shown) and is much cheaper. Forty-eight hours post-transfection the cells were stained by RAP *in situ* as described in chapter 2.5.3. AP

staining was monitored against a white background under a dissecting microscope. After identification of positive (stained) cells, the plasmid DNA was extracted as described in chapter 2.1.4, purified, transformed by electroporation in *E. coli* XL10 Gold bacteria (see chapter 2.1.12) and amplified. Two 10 cm plates with COS7 cells were transfected for the following round of selection as described above.

3.3 Results

3.3.1 Construction of an E7 chicken optic tectum expression cDNA library

The chick embryo optic tectum represents a major site of expression for CRYPα ligands, as detected by RAP *in situ* (Haj *et al.*, 1999). Therefore, we decided to use this tissue as the RNA source for constructing an expression library, thus (hopefully) enriching the representation of the target molecule(s). Approximately 3 mg of total RNA per gram of tissue were obtained ($OD_{260/280}$=2). The poly(A)$^+$ mRNA yield, after two rounds of purification on oligo(dT)-cellulose, was approximately 15 μg per milligram of total RNA. 5 μg poly(A)$^+$ mRNA were then used as template for cDNA synthesis with a poly(dT) primer in order to increase the chance of obtaining full-length cDNAs. Indeed, agarose gel electrophoresis of size-fractionated double-stranded cDNA fragments demonstrates that products up to 9 kb were obtained (data not shown). Fractions containing cDNAs of 2 kb or longer were then directionally subcloned into the pCMV-Script eukaryotic expression vector, orienting the 5' end towards the promoter.

Test ligations of aliquots from each selected fraction have predicted a library size of at least 10^6 independent clones (colony forming units, "cfu"). After scaling-up the ligations and transformations a primary library of approximately $5x10^6$ independent clones was obtained. This library was then amplified in a weak LB-agarose gel which allows three-dimensional, uniform colony growth and reduces the potential for under-

representation of particular clones due to neighbouring colonies overgrowth, commonly seen during direct plating methods. The final amplified library, termed LTc1R, has a titer of $3.6x10^{10}$ cfu. Sixty clones were randomly selected and analysed by agarose gel electrophoresis and about 90% had inserts ranging in size from 2 to 5 kb. As an additional test, PCR amplification was used to check whether the library contains CRYPα cDNA, which should be represented at E7 in the optic tectum. Various primer pairs were used to amplify fragments specific for both CRYPα1 and CRYPα2 isoforms and bands of the expected size were obtained. It is worth mentioning that CRYPα2 cDNA is almost 6 kb, which further demonstrates that LTc1R library contains large inserts and there is a good chance to contain a full-length cDNA encoding for a CRYPα ligand.

3.3.2 Retroviral expression of the CRYPα1-AP fusion protein

The amount of fusion protein available for library screening ultimately determines the design of the expression cloning strategy and therefore may be a crucial factor for the final outcome. Only small amounts of CRYPα1-AP can be produced by transient transfection in 293T cells. Trying to overcome this limitation, I constructed a replication-incompetent avian retrovirus termed RX-CRYPα1-AP which, co-transfected with a helper virus, should readily spread in chick or quail fibroblast cultures and it should stably integrate into their genome. In addition, the strong viral promoter should lead to high expression levels of the CRYPα1-AP fusion protein in conditioned media. Figure 3.1 shows that a control virus expressing the alkaline phosphatase alone has indeed the ability to spread into QT6 cultures when co-transfected with the RIAS helper and that high expression levels are maintained during successive passages. In contrast, the virus expressing CRYPα1-AP did not spread and after four passages the expression was completely lost. This seems to be due to the intrinsic nature of the

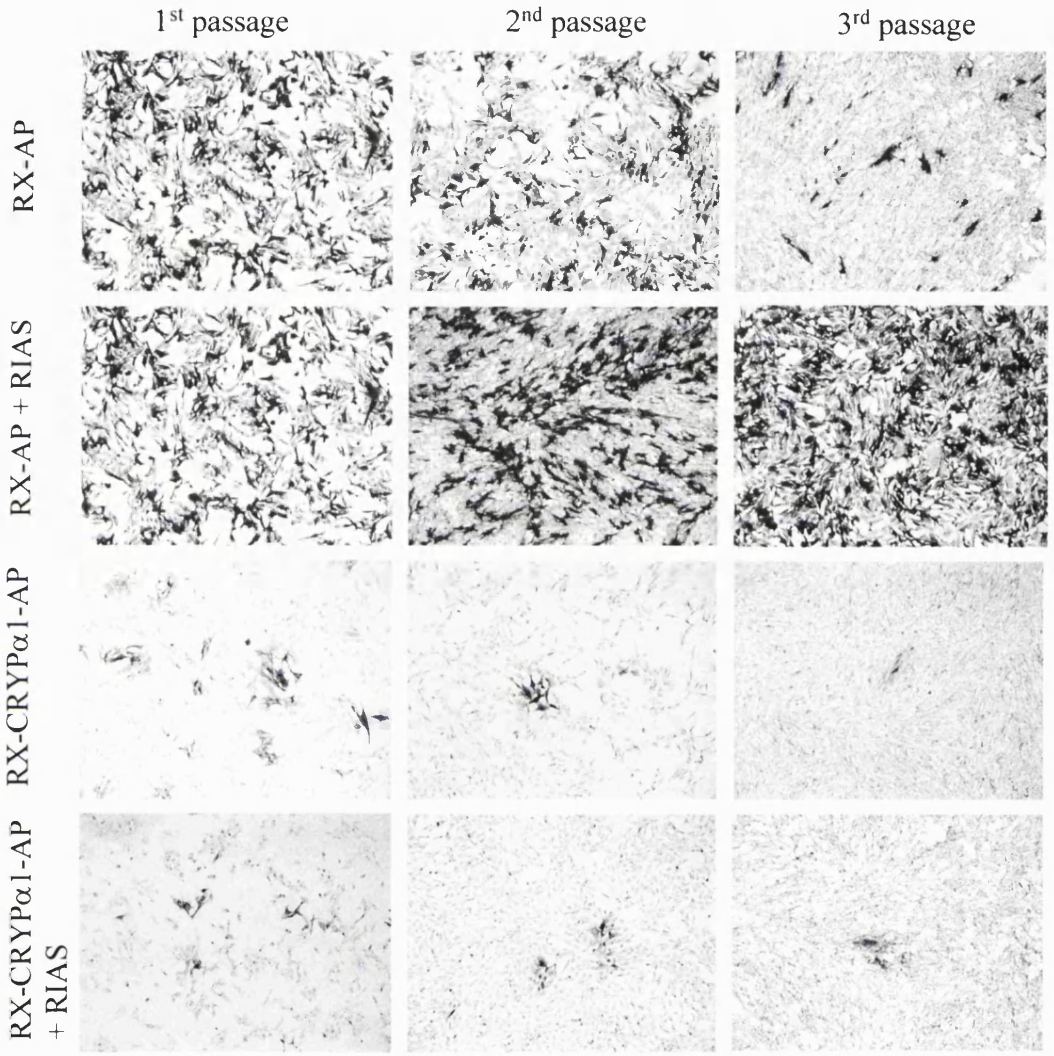

Figure 3.1. Expression of alkaline phosphatase and CRYPα1-AP fusion protein in the quail fibroblast cell line QT6. Replication defective retroviral vectors (RX) encoding either AP (RX-AP) or the CRYPα1-AP fusion protein (RX-CRYPα1-AP) were transfected into QT6 cells with or without addition of helper virus (RIAS). The cells were split every 96 hours and 24 hours post-splitting each plate was stained for AP activity. AP expression from RX-AP is well maintained in the presence of helper virus, however CRYPα1-AP expression is lost irrespective of helper virus addition after just a couple of passages.

CRYPα1-AP fusion protein since previous attempts to establish stable NIH 3T3 cell lines expressing it have also failed (F. Haj, I. McKinnell and A. Stoker, unpublished results). Therefore, the expression library screening detailed below was performed using conditioned media obtained from transient transfections.

3.3.3 Expresison cloning attempts

Plasmid vectors having a SV40 origin of replication, such as pCMV-Script, are amplified episomally with high efficiency (to more than 100,000 copies/cell) in cell lines expressing the SV40 large T antigen, such as COS7 or 293T (Mellon *et al.*, 1981). This would represent an advantage for the recombinant protein (encoded by the library) expression levels but also would allow efficient extraction and purification of the plasmid DNA from "positive" cells (expressing putative CRYPα ligands). Therefore, I first tested by RAP *in situ* whether these two cell lines are appropriate for our expression cloning strategy. The main concern was to avoid a high background level, i.e. binding of the fusion protein constructs either non-specifically or due to the expression of a endogenous ligand, which would mask a novel receptor-ligand interaction. 293T cells were found to be completely unsuitable, binding very high amounts of both CRYPα1-AP and CRYPα2-AP (not shown). COS7 cells, however, did not bind the CRYPα1-AP construct at all (Figure 3.2A) but did bind CRYPα2-AP (Figure 3.2B). Interestingly, when a 1:1 mixture of CRYPα1-AP and CRYPα2-AP was tested, "non-specific" binding was significantly increased (Figure 3.2C). In all three cases the total quantity of fusion protein (measured by the AP activity level) was kept constant, which suggests that the CRYPα1 and CRYPα2 isoforms might associate with each other or binding of CRYPα2 facilitates subsequent binding of CRYPα1 via an unknown mechanism. Nevertheless, these preliminary tests have established that the COS7 cell line is suitable for expression cloning of CRYPα1 ligands.

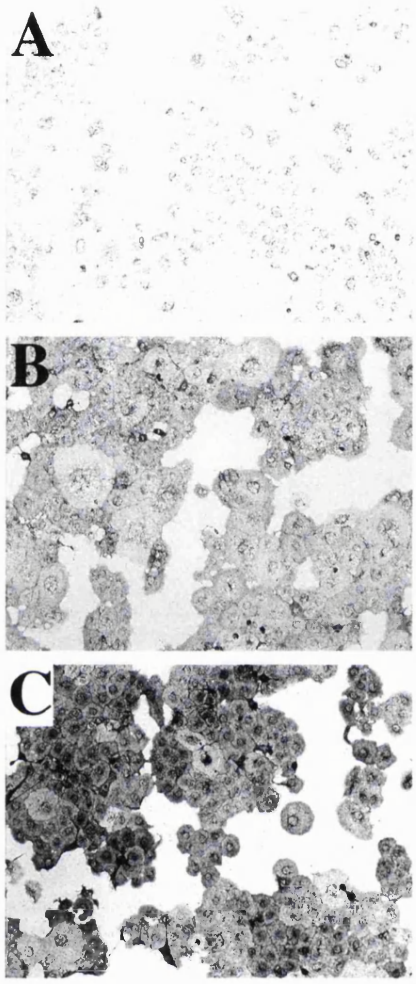

Figure 3.2. RAP *in situ* staining of non-transfected COS-7 cells in culture. COS-7 cells were incubated with CRYPα1-AP (A), CRYPα2-AP (B) and a 1:1 mixture of CRYPα1-AP and CRYPα2-AP (C) conditioned media. Non-specific binding is detected when CRYPα2-AP conditioned medium is used, either alone or (much stronger) mixed with CRYPα1-AP. However, this is not the case when CRYPα1-AP alone is used.

A second problem to be considered was the occurrence of a very small number of AP-stained cells in non-transfected cultures. This was particularly observed in areas of high cell density and may reflect incomplete heat-inactivation of endogenous phosphatases. Therefore, various heat-inactivation times (15, 30, 45, 60 and 100 minutes at 65°C) and fixatives (4% w/v paraformaldehyde; 60% v/v acetone/3% v/v formaldehyde; 1.8% v/v formaldehyde) were tested in order to identify the optimal heat inactivation and fixation conditions. Best results were obtained for 30 seconds fixation in 60% acetone - 3% formaldehyde followed by 45 minutes heat inactivation, whereby usually no stained cells were detected.

Transfection of the LTc1R cDNA library in COS7 cells produced variable results during the first round of screening, when rare positive cells (approx. 2 in 10^6) could be observed after only 3 hours staining (Figure 3.3). It is worth mentioning that, as expected, these cells appear to have a membrane staining pattern. Overnight incubation led to detection of 5-6 additional positive cells per 10^6, presumably expressing weak binders or low levels of ligand or simply being false positives. These results compare well to similar experiments reported (Nastuk *et al.*, 1998; Davis *et al.*, 1996). Plasmid DNA was rescued from each stained cell, purified, electroporated into bacterial cells and amplified to produce a "ligand enriched pool" of much lower complexity than the original library. Each of these primary plasmid pools was then used to transfect COS7 cells. It was expected that a significantly larger number of positive cells would be detected by RAP *in situ* at this stage. However, the number of "positives" observed was just similar to the first screening round. Unfortunately, no enrichment was observed after two further rounds of selection, which suggests that the observed staining is non-specific. Similar "positive" cells were occasionally observed in control experiments, further underlining the above conclusion.

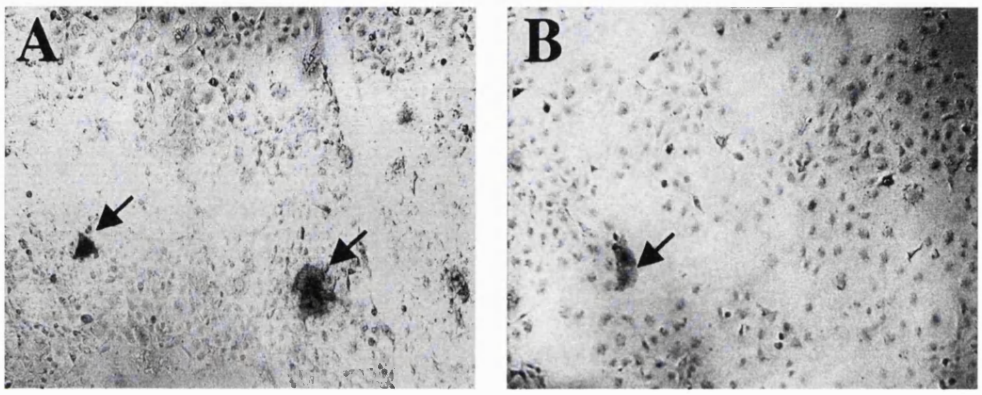

Figure 3.3. CRYPα1-AP screening of the LTc1R expression library transfected in COS-7 cells. Rare cells with membrane staining were detected after the first screening round (A). No significant enrichment in the number of stained cells can be detected at the second round of screening (B). The arrows indicate "positive" cells.

According to published protocols, the scale of transfection used for a library of LTc1R size should have been sufficient for a successful outcome. Nevertheless, the whole procedure was then scaled-up nearly tenfold but this did not change the results.

3.4 Discussion

Expression cloning is a powerful method for identification of novel proteins interacting with a known molecule. Its major advantage is the direct linkage between a functional assay (e.g. receptor-ligand interaction) and the cloning of the (full-length) cDNA encoding the novel protein. This allows rapid identification of its primary structure (by DNA sequencing) and, usually, straightforward high level expression in the system of choice for further biochemical or functional studies. Expression cloning in mammalian cells is particularly useful for identification and functional characterisation of novel membrane proteins (reviewed in Flanagan and Cheng, 2000; Seed, 1995). More problematic would be to identify secreted proteins using such a system, although a successful case has been reported (Davis *et al.*, 1996). On the other hand, proteins that undergo specific post-translational modifications essential for their activity, which cannot take place in the cell lines commonly used, require extensive adaptations of the standard protocols.

Very little is known about type II RPTP ligands. A particular isoform of LAR binds to the laminin-nidogen complex, both extracellular matrix proteins (O'Grady *et al.*, 1998). RPTPμ, RPTPκ, RPTPδ and HmLAR ectodomains can bind in a homophilic manner (detailed in chapters 1.2.2 and 1.3.2). CRYPα, however, cannot bind homophilically and RAP *in situ* studies suggest that heterotypic ligands are expressed in the basement membranes, on the axonal surface and on radial glia endfeet (Haj *et al.*, 1999; Ledig *et al.*, 1999a). Based on the RAP *in situ* patterns described by Haj *et al.*, (1999) and repeatedly confirmed in our laboratory, we decided to use the chick embryo

optic tectum as an RNA source for constructing a directional cDNA expression library. It was hoped that, by using this library in an expression cloning approach, it would be possible to identify at least the membrane-attached ligand(s) expressed on axonal and glial surfaces. We had no indication concerning the molecular nature of these putative ligands or, indeed, any of their binding properties. The particular expression cloning procedure I used can be successful only if a series of minimal conditions are fulfilled:

- the ligand is a protein;
- its full-length cDNA is present in the LTc1R library I constructed; (The first strand synthesis was primed with an oligo(dT) primer, therefore the library was not enriched in 5' cDNA regions, and the pCMV-Script backbone vector does not provide a start codon.);
- ligand binding to CRYPα does not require post-translational modifications that cannot take place in COS7 cells;
- the ligand itself is a transmembrane or GPI-anchored protein, therefore it will remain attached to the cell's plasma membrane *without* requiring another anchoring protein which may not be expressed in COS7 cells;
- the ligand can be expressed in COS7 cells at a level sufficient for detection.

Probably the main problem I encountered during the whole ligand identification project was the very limited amount of CRYPα protein we were able to produce. As mentioned in the introduction, attempts to obtain stable cell lines producing the CRYPα ectodomain have repeatedly failed. In a different approach, I cloned AP-fused CRYPα ectodomain constructs in avian retroviruses hoping to obtain conditioned media from infected chick and quail fibroblast cultures. However, cells expressing the constructs were specifically eliminated (or switched off expression) after only three passages required by the retrovirus to spread in the culture. The reason for this remains unclear.

The limited amount of CRYPα1-AP conditioned medium that can be obtained in transient transfection experiments did not allow further scaling-up of the expression cloning procedure. It also contributed to the decision to find an alternative to the screening strategy commonly used. Specifically, most authors recommend splitting the original library in pools of maximum 1000-2000 clones (e.g. Flanagan and Cheng, 2000; He and Tessier-Lavigne, 1997; Kolodkin *et al.*, 1997) which are then individually transfected in 10 cm tissue culture dishes with COS cells. For a library of LTc1R's size ($5x10^6$ primary cfu) theoretically this requires a large number of tissue culture dishes, which is not cost-effective.

Therefore, a different strategy known as the "single cell" expression cloning approach (Davis *et al.*, 1994) has been used. In this technique the whole library was transfected in a limited number of cells and very rare positive cells (1-2 in 10^6) were isolated and the small amount of plasmid DNA they contain was extracted, purified and amplified in *E. coli*. This method has been used successfully in the past in similar experiments (Davis *et al.*, 1996; Nastuk *et al.*, 1998) and obviously provides considerable simplification over the traditional technique of screening library pools. Interestingly, a recent paper describes a mathematical model to determine the number of cells required to successfully screen cDNA libraries by expression cloning (Wu and Gu, 2000). According to their model, the number of cells I used should be enough for a library of LTc1R size but ***only*** if the library was first diluted about 1:30 with a non-replicable plasmid. When very complex DNA mixtures are used, COS cells are efficiently transfected with a large number of different plasmids expressing different constructs therefore most of these will be present at levels below the detection limit. A non-replicable plasmid will compete during transfection but not for episomal replication and therefore will allow higher copy number of the library plasmids per cell which

results in higher expression levels of the proteins encoded. Maybe it is worth testing this model in the future.

One of the possible criticisms regarding the expression cloning experiments is that I did not include a positive control for the screening step. However, since we did not have any information regarding the molecular nature of the CRYPα ligands, it is difficult to say how exactly an appropriate positive control could have been designed.

The library itself contained large inserts including the long cDNA of the CRYPα2 isoform, as observed by PCR tests. The transfection steps were very efficient, as confirmed by using control plasmids encoding AP as a reporter gene. Plasmid isolation from "positive" COS cells was again efficient, regularly over 500 clones/positive cell were obtained after electroporation in *E. coli* XL10 Gold bacteria. No clones were obtained in control experiments using DNA purified from non-transfected COS cells. It is difficult to say exactly what was the cause for the expression cloning approach failure. Fortunately, alternative approaches subsequently proved to be more fruitful, as discussed in the following chapters.

Chapter 4. **CRYPα is a heparin-binding protein**

4.1 Introduction

The outcome of the expression cloning experiments prompted me to find alternative solutions for identification of CRYPα ligands. First, I carefully reviewed all the information we had about CRYPα itself and its binding properties.

CRYPα-ligand interactions could be detected in two systems: RAP *in situ* (Haj *et al.*, 1999) and blot overlay assays (Aricescu *et al.*, submitted). They share principial similarities and suggest that, whatever the CRYPα ligand is, we are looking at an extremely robust interaction: it can resist fixation with both methanol and formaldehyde, but also protein denaturation during SDS-PAGE. Two more predictions can therefore be advanced about the ligand properties: the CRYPα binding epitope appears to be linear and amino groups on the ligand surface may not be determinantly involved in this interaction.

As previously discussed, ligands recognised by RAP *in situ* probes appear to be both secreted (basement membrane constituents) and membrane-attached (on glia and neurons surface). In addition, another ligand seems to be expressed on muscular fibres or their basement membranes (J. Chilton, F. Haj, A. Stoker, unpublished observation). Which one of these putative ligands might have relevance *in vivo*? Ledig *et al.* (1999a) have shown that the ligand(s) present on the radial glia endfeet and/or the retinal basal lamina can promote neurite outgrowth by interacting with CRYPα. *In vivo*, the intraretinal axon outgrowth in chicken embryos takes place between E3 and E7 (Halfter and von Boxberg, 1992). During this period RGCs express only the CRYPα1 isoform and the main ligand(s) detected in the retina by RAP *in situ*, is (are) the ones located in the basal lamina (Haj *et al.*, 1999). On the other hand, we recently confirmed that

CRYPα1 can also bind to the retinal basal lamina *in vivo* (Aricescu *et al.*, submitted). An avian retrovirus that encodes for a CRYPα1 ectodomain construct fused with the VSV peptide tag can readily infect the whole retina by E6. The CRYPα1-VSV fusion protein, produced by the infected retinal cells, binds to its ligand(s) on the basal lamina. Together, these experiments suggest that the CRYPα1 interaction with basal lamina ligands has physiological significance and is not simply a RAP *in situ* artefact.

As mentioned in chapter 1.4, CRYPα is expressed as two major isoforms: CRYPα1 has three Ig-like and four FNIII-like (FN 1-3 and 8) domains; CRYPα2 ectodomain has four additional FNIII domains spliced in (FN 4-7). Protein database alignments show that the CRYPα ectodomain has closest similarities with the other type IIa RPTPs: 78% identity with human RPTPσ, 62% identity with human RPTPδ, 58% identity with human LAR and 46% identity to *Drosophila* DLAR. Such values are useful indicators for protein classification but they tell little about biochemical properties. On the other hand, irrespective of how complicated the 3D structure of a given protein is, interactions with ligands necessarily happen in discrete areas. Such sites usually involve residues coming from one or several solvent-exposed loops (surfaces). Therefore, molecular modelling and database mining approaches can potentially provide valuable information regarding putative functional interactions.

Experiments described in this chapter demonstrate that this interaction appears to be ionic in nature and heparin competition effectively abolished it. A CRYPα1–AP construct binds heparin with very high affinity in solid-phase assays. Molecular modelling of individual domains in the extracellular region and site-directed mutagenesis led to the identification of the heparin-binding site on CRYPα surface. Importantly, mutant constructs with little or no heparin-binding ability cannot bind retinal basal lamina ligands either. The results shown below suggest that the heparin-binding site of CRYPα1 coincides with its retinal basal lamina-binding site and, since

free heparin has not been described in the retina, the basal lamina ligands might be heparan sulphate proteoglycans. On the other hand, retinal glial cells appear to express an additional class of ligands.

4.2. Experimental procedures

Expression constructs, fusion protein production and site-directed mutagenesis. CRYPα1-AP conditioned medium was obtained by transient transfection of the pBG-CRYPα1-AP plasmid in 293T cells, as described in chapter 3.2. When necessary, batches expressing low levels of fusion proteins were concentrated on Centricon-30 ultrafiltration units (Amicon). An *Xba*I fragment encoding for a CRYPα1 extracellular construct lacking the membrane-proximal FNIII-like domain and fused with alkaline phosphatase at the C-terminus ("FN3Δ-AP") was removed from the pBG-FN3Δ-AP plasmid (created by J. Chilton) and subcloned into the pCS3N expression vector (see chapter 6.2). The resulting plasmid, termed pCS3N-FN3Δ-AP, was used to express the FN3Δ-AP fusion protein in 293T cells as described above but also represented the template for site-directed mutagenesis. Various CRYPα mutants were created following the protocol described in chapter 2.1.14, using the primer pairs described below:

- for M1 (K67,68A): CACGAGTCACCTGGAACGCGGCCGGGAAGAAAGTGAACTC and GAGTTCACTTTCTTCCCGGCCGCGTTCCAGGTGACTCGTG;

- for M2 (K70,71A): CACCTGGAACAAGAAAGGGGCGGCCGTGAACTCTCAGAGG and CCTCTGAGAGTTCACGGCCGCCCCTTTCTTGTTCCAGGTG;

- for M3 (K67,68,70,71A): CGAGTCACCTGGAACGCGGCCGGGGCGGCCGTGAACTCTCAGAGG and CCTCTGAGAGTTCACGGCCGCCCCGGCCGCGTTCCAGGTGACTCG;

- for M4 (R96,99A): GGATCCAGCCGCTCGCGACTCCCGCGGATGAGAACATTTATG and CATAAATGTTCTCATCCGCGGGAGTCGCGAGCGGCTGGATCC;

- for M5 (R182,187A/K184A):

GCACGAGCAATGGGGCAATTGCGCAGCTGGCATCAGGTGGCCTGC and

GCAGGCCACCTGATGCCAGCTGCGCAATTGCCCCATTGCTCGTGC;

- for M6 (R225,227,228A): GCAAACCTTTACGTGGCAGTTGCGGCCGTGGCCCCTCGC and

GCGAGGGGCCACGGCCGCAACTGCCACGTAAAGGTTTGC.

All mutant constructs were verified by DNA sequencing (carried out by C. Patternote on an ABI Prism 377 DNA Sequencer), transfected into 293T cells and conditioned media collected and stored as described in chapter 3.2.

RAP *in situ*. The *in situ* localisation of CRYPα ligands on E6 chicken head cryosections was performed using 293T conditioned media containing various fusion protein constructs, as described in chapter 2.5.3. In modified RAP assays the sections were pre-treated for one hour at room temperature with the following group-selective chemical modification reagents (Kramer *et al.*, 1990; Britten and Bird, 1997): N-ethylmaleimide (NEM; cysteine-selective), dithionitrobenzene (DTNB; cysteine selective), phenylglyoxal (PGO; arginine-selective), diethylpyrocarbonate (DEPC; histidine-selective), 1-acetylimidazole (NAI, tyrosine-selective) and N,N'-dicyclohexylcarbodiimide (DCCD; carboxyl group-selective). Stock solutions were prepared in either PBS (NEM), methanol (DTNB, PGO, NAI) or ethanol (DCCD, DEPC) and 0.1mM, 1mM and 10mM working solutions were prepared in PBS. The pH of the dilution buffer was 7.4, except for DEPC (pH 6.4, in order to achieve histidine specificity). All reagents were purchased from Sigma, except NAI (Aldrich). For heparin competition experiments conditioned media samples were pre-incubated 1 hour at room temperature with 100μg/ml heparin (Sigma) before addition to the cryosections, glial cell cultures or flat-mounted basal laminae. To test whether ionic strength variations can influence CRYPα1-AP binding on tissue sections, sodium chloride was

added to a final concentration of 500 mM to conditioned media samples used for RAP *in situ*. Glial cell cultures were prepared as described in chapter 2.4.3 and retinal basal laminae were isolated and attached to glass coverslips as described in chapter 2.4.4.

Homology modelling of CRYPα domains. Individual domains of the extracellular region of CRYPα were defined using the Pfam server (http://www.sanger.ac.uk/Pfam; Bateman *et al.*, 2000). The corresponding sequences were submitted to the SWISS-MODEL v3.5 protein modelling server (http://www.expasy.ch/swissmod/SWISS-MODEL.html; Guex *et al.*, 1999) for analysis. Suitable modelling templates were identified in the ExNRL-3D database using SWISS-MODEL Blast. The sequence alignments obtained were analysed and the most appropriate ExPDB (http://www.expasy.org/swissmod/SM_Check_ExPDB.html) entries were selected as templates. All the models generated were quality checked by the WHAT IF verification routines (WHAT-CHECK; Hooft *et al.*, 1996) and the Biotech protein validation suite (http://biotech.embl-heidelberg.de:8400/). Energy minimisation was done with the GROMOS implementation of Swiss-PdbViewer v3.6b2 (http://www.expasy.ch/spdbv/; Guex and Peitsch, 1997).

Solid-phase binding assays. Heparin-albumin (Sigma) was immobilised on microtiter plates at a concentration of 5 μg/ml, for 2 hours at room temperature. Remaining binding sites were saturated by overnight incubation at 4°C in PBS buffer containing 3% (w/v) bovine serum albumin (BSA). Wells were incubated with 293T conditioned media containing AP fusion protein constructs for 3 hours at room temperature. After four washes in PBS and one wash in SEAP buffer (0.5 mM $MgCl_2$, 1 M diethanolamine, pH 9.8), the bound AP activity was determined by adding 200 μl SEAP buffer containing 10 mM p-nitrophenyl phosphate. Progress curves were

recorded for 1h at 405nm, at room temperature, in a Dynex MRX *Revelation* microplate reader and the initial rates were determined using the SigmaPlot 4.01 software (SPSS Inc.). Each data point represents the average of triplicate wells ± SD. Non-specific binding was determined from CRYPα1-AP bound to BSA (immobilised at a concentration of 3 mg/ml) and was subtracted from each data point.

In order to determine the equilibrium dissociation constants, I used the analytical solution of the following equation to fit the saturation curve by nonlinear regression:

$b^*_{tot}{}^2 - b^*_{tot}[\beta(K_d + L^*_{tot}) + r_{tot}] + \beta L^*_{tot} r_{tot} = 0,$

where b^*_{tot} is the total amount of bound ligand (CRYPα1-AP) expressed in OD/min; β is the specific AP activity expressed in (OD/min)/molar units; K_d is the equilibrium dissociation constant; L^*_{tot} is the total ligand (CRYPα1-AP) concentration and r_{tot} is the maximal specific binding expressed in OD/min.

This equation takes into account significant ligand depletion (since more than 10% of the initial AP activity was bound on heparin-albumin), with negligible non-specific binding (Swillens, 1995). The specific activity used for CRYPα1-AP fusion protein was 0.47 (OD/min)/nM.

4.3 Results

4.3.1. The molecular nature of the retinal basal lamina ligand(s)

RAP *in situ* experiments using the CRYPα1-AP fusion protein demonstrate that major binding partners exist in the basement membranes of the developing chicken retinotectal system (Haj *et al.*, 1999). The interaction with the retinal basal lamina ligand(s) appears to have functional relevance (Ledig *et al.*, 1999a) and occurs *in vivo* (Aricescu *et al.*, submitted). Therefore, we set out to identify this (these) ligand(s). The first step was to gain information about the chemical properties of this interaction. One set of experiments (I. McKinnell, unpublished) had suggested that the RAP *in situ*

binding is not affected by the addition of various amounts of EDTA or Nonidet P-40. This shows that the interaction does not require divalent cations and does not appear to be hydrophobic. In contrast, increasing concentrations of sodium chloride affected CRYPα1-AP binding to the basal lamina, abolishing it completely at 500 mM (Figure 4.1).

This observation prompted another question: is this a protein-protein interaction? If so, chemical reagents commonly used for protein modification may be able to modulate it. Therefore, E6 chick retina cryosections were pretreated with NEM and DTNB (cysteine-specific), PGO (arginine-specific), DEPC (histidine-specific), NAI (tyrosine-specific) and DCCD (carboxyl group-specific), according to the conditions described in Kramer *et al.* (1990) and Britten and Bird (1997). Although under such circumstances the reactions were expected to be efficiently completed, none of the reagents tested could significantly impair CRYPα1-AP binding to retinal basal laminae (Figure 4.1).

Considering the effect of sodium chloride addition mentioned above, I tested next heparin, a highly charged polyanionic molecule. This proved to be a very efficient competitor, completely abolishing CRYPα1-AP binding. This could happen either by masking the CRYPα binding site on the basal lamina ligand surface or by blocking the ligand-binding site on CRYPα itself.

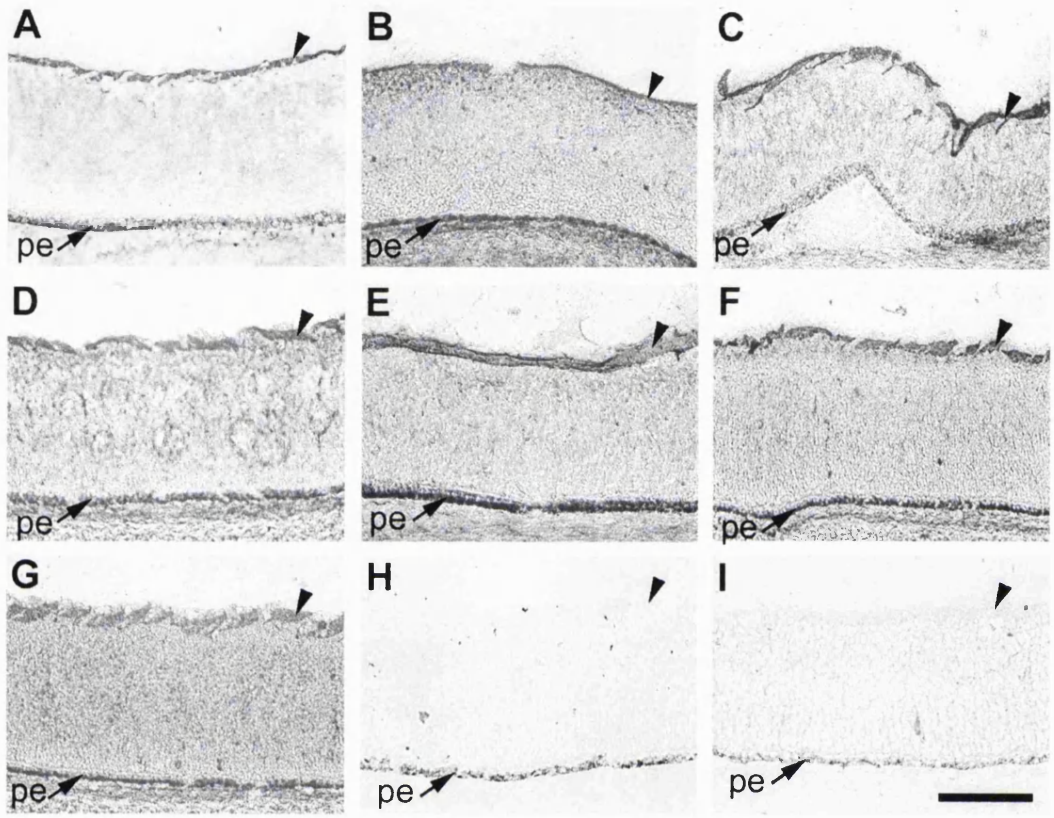

Figure 4.1. The effect of protein modification reagents, sodium chloride and heparin on CRYPα binding to its basal lamina ligand(s). Receptor affinity probe assays on E6 chicken retina cryosections were performed using CRYPα1-AP conditioned medium. Sections were either untreated (A, H, I) or pre-treated with the following reagents: N-ethylmaleimide (B), dithionitrobenzene (C), phenylglyoxal (D), diethylpyrocarbonate (E), 1-acetylimidazole (F) or N,N'-dicyclohexylcarbodiimide (G). Sodium chloride or heparin were added to the conditioned medium prior to incubation with the tissue sections (in H and I, respectively). The basal lamina staining indicates fusion protein binding. No effect is observed after pre-treatment with chemical modification reagents, however sodium chloride and heparin effectively abolish CRYPα binding. Arrowheads indicate the retinal basal lamina; pe, pigmented epithelium. Scalebar, 0.1 mm.

4.3.2. CRYPα is a heparin-binding protein

293T conditioned media containing either CRYPα1-AP, AP alone or an AP fusion of the RPTPμ extracellular region were tested in solid-phase binding assays for their ability to bind immobilised heparin. CRYPα1-AP does indeed bind heparin-albumin at picomolar to low nanomolar concentrations (Figure 4.2). An equilibrium dissociation constant (K_d) value of 0.29±0.02 nM was measured, which demonstrates that CRYPα binds heparin with very high affinity. Neither AP alone nor an RPTPμ-AP construct, used as controls, could bind to heparin-albumin in similar assays (not shown). In addition, the non-specific binding of CRYPα1-AP on wells coated just with albumin was negligible (not shown). Therefore, I conclude that the CRYPα1-AP construct binds heparin via the extracellular region of CRYPα.

4.3.3. The first Ig-like domain of CRYPα contains a putative heparin-binding site

To gain further insight into the CRYPα-HSPG interactions at the molecular level, I searched for putative heparin-binding sites in the extracellular region of CRYPα1. Specifically, basic amino acid clusters located on the surface of extracellular domains are likely to bind polyanionic glycosaminoglycan (GAG) chains (for review see Hileman *et al.*, 1998). Using the SWISS-MODEL (v3.5) automated protein modelling server (Guex *et al.*, 1999), I obtained 3D models for all the Ig domains and three out of four FNIII domains. It was not possible to build a model for the FNIII-4 domain since it has less than 30% identity to any 3D structure in the Protein Data Bank (PDB) (Table 4.1). Several small, positively charged, clusters were observed on the molecular surfaces (computed using the Swiss-PdbViewer v3.6b2 program; Guex and Peitsch, 1997), the most prominent being in the Ig-1 domain (Figure 4.3A). This cluster

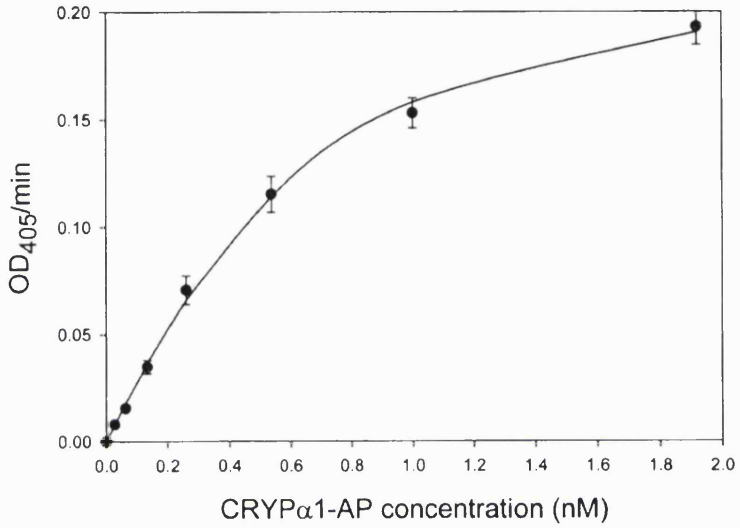

Figure 4.2. Solid-phase binding of CRYPα to heparin. Heparin-albumin was coated on microtiter plates and incubated with a range of CRYPα1-AP concentrations. Curves were fitted by nonlinear regression analysis as described under Experimental procedures. Each value represents the mean ± standard deviation of three measurements.

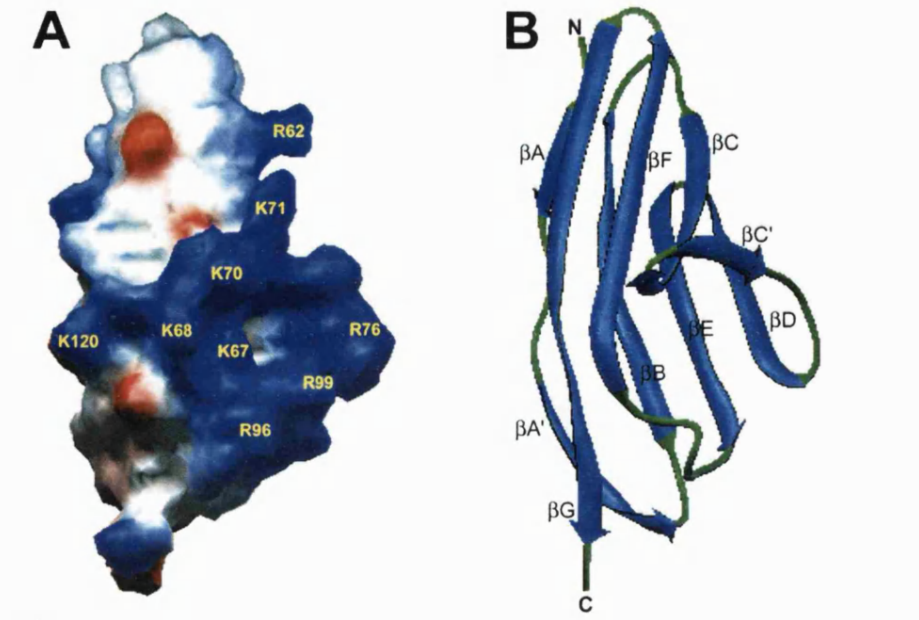

C

```
Telokin      40   VKFYFTKTI- ---LDMDIVE GSAARFDCKI EGYLDDETMV FKDDNPIKES

CRYPα-Ig1    30   SPIVITKKP- ---VDQIGVS GGVASFVCQA TGDPKPRVTW NKKGKKVNSQ
mRPTPσ       30   EPPRFIREP- ---KDQIGVS GGVASFVCQA TGDPKPRVTW NKKGKKVNSQ
hRPTPσ       30   EPPRFIKEP- ---KDQIGVS GGVASFVCQA TGDPKPRVTW NKKGKKVNSQ
NCAM-Ig2     97   QKLMFKNAP- ---TPQEFKE GEDAVIVCDV VSSLPPTIIW KHKGRDVILK
FGFR1-Ig2   151   VAPYWTSPEK MEKKLHAVPA AKTVKFKCPS SGTPQPTLRW LKNGKEFKPD

Telokin      86   ---RIPQIDY DEEGNFSFTI SEICGDD-DA KYTCKVVASL --GEATCTAE ILVE

CRYPα-Ig1    76   ---RFETIEF DESAGAVIRI QPLRTPRDEN IYECVAQNSV --GEVTVHAK LTVL
mRPTPσ       76   ---RFETIDF DESSGAVLRI QPLRTPRDEN VYECVAQNSV --GEITIHAK LTVL
hRPTPσ       76   ---RFETIEF DESAGAVLRI QPLRTPRDEN VYECVAQNSV --GEITVHAK LTVL
NCAM-Ig2    143   -KDVNFIVLS ----NNYLQI RGIKKTD-EG TYRCEGRILA RGEINFKDIQ VIVV
FGFR1-Ig2   201   HRIGGYKVRY A---TWSIIM DSVVPSD-KG NYTCIVENEY --GSINHTYQ LDVV
```

Figure 4.3. Structural model of the Ig-1 domain of CRYPα and sequence alignment with the Ig domains of telokin, NCAM (Ig-2) and FGFR1 (Ig-2). (A) Electrostatic surface representation of the Ig-1 domain of CRYPα; blue and red represent positive and negative electrostatic potential, respectively. The large positive potential patch represents the putative heparin-binding site. Basic residues are labelled in yellow and numbered according to Stoker (1994). (B) Ribbon view of the predicted folding - the orientation is the same as in (A). N and C denote the amino and carboxyl termini. The β strands are labelled, from A to G, according to the telokin fold. (C) Structure-based sequence alignment between telokin (the template used for modelling) and the heparin-binding Ig domains of CRYPα, NCAM and FGFR1. The corresponding sequences of the CRYPα mouse and human orthologues (mRPTPσ and hRPTPσ) have also been included. The heparin-binding sites are highlighted in blue (proposed site for CRYPα/ RPTPσ). The telokin key structural residues and their conserved equivalents in CRYPα are highlighted in green. The β strands are underlined. The secondary structure definitions were reported as follows: for telokin in (Holden *et al.*, 1992), for NCAM in (Kasper *et al.*, 2000) and for FGFR1 in (Plotnikov *et al.*, 1999). This figure was made using the Swiss-PdbViewer v3.6b2 (Guex and Peitsch, 1997).

consists mainly of a β-hairpin formed by strands βC and βC' (Figure 4.3B) and contains the sequence R^{62}VTWNKKGKKVNSQR^{76}, plus the side chains of Arg96 and Arg99 from a loop between the βE and βF strands. The Ig-1 domain homology model was generated using telokin as a template (39.3% identity, PDB codes 1FHG and 1TLK), a typical Ig superfamily I-set structure. Twenty-four out of the 35 key structural residues as defined by Bateman *et al.* (1996) are identical, representing all the major secondary structures and most of the peripheral regions (Figure 4.3C).

The cluster described above in the CRYPα Ig-1 domain contains a BBxBB motif suggested to interact optimally with heparan sulphate chains (where B represents Arg or Lys; Hileman *et al.*, 1998). Other proteins containing heparin/heparan sulphate binding sites located in I-set Ig domains have been described, including the "classical" examples: neural cell adhesion molecule (NCAM) and fibroblast growth factor receptors (FGFRs). High-resolution 3D structures of both NCAM (1EPF, X-ray structure; Kasper *et al.*, 2000) and FGFR1 (1CVS, X-ray structure; Plotnikov *et al.*, 1999) have recently been published, and these were aligned with the CRYPα Ig-1 model using Swiss-PdbViewer (Figure 4.3C). The proposed heparin-binding site of CRYPα is perfectly conserved in its mouse and human orthologues and aligns well with the heparin-binding site found in NCAM (Cole and Akeson, 1989). However, the location of the FGFR1 heparin-binding site does not seem to overlap, suggesting a different molecular architecture of the FGFR1-heparin complex.

Table 4.1. Modelling templates for individual CRYPα1 domains. The acceptable threshold value for modelling is 30% identity.

Domain	Template	Identity	PDB ID
Ig-1	- Telokin - N-terminal fragment of chicken axonin-1	39.3% 39%	1FHG, 1TLK 1CS6
Ig-2	- Telokin - N-terminal fragment of chicken axonin-1	42.8% 37%	1FHG, 1TLK 1CS6
Ig-3	- N-terminal fragment of chicken axonin-1 - Third Ig-like domain of FGFR1	31% 30.7%	1CS6 1CVS
FNIII-1	- 10th type III cell adhesion module of human fibronectin	35.4%	1FNA
FNIII-2	- FNIII domain from the cytoplasmic tail of integrin α6β4	36.4%	1QG3
FNIII-3	- 14th type III cell adhesion module of human fibronectin - second FNIII domain of the cytokine-binding region of gp130	42% 36.8%	1FNH 1BQUA
FNIII-4	- no suitable template	-	-

4.3.4. The heparin-binding site of CRYPα is essential for binding to the retinal basal lamina

To test the accuracy of the molecular modelling prediction, I mutated the charged amino acids in the putative heparin-binding site of the Ig-1 domain and, as controls, other basic clusters present in CRYPα Ig domains 2 and 3. Several basic clusters are also present in the membrane-proximal FNIII-4 domain. A CRYPα1 extracellular construct lacking this FNIII-4 domain, termed FN3Δ-AP, bound similarly to full length CRYPα1 by RAP *in situ* (Figure 4.5A and B). Therefore FNIII-4 does not contain the basal lamina binding site. The FN3Δ-AP construct was used as a backbone to incorporate further mutations, as shown in Figure 4.4A. Mutations M1, M2, M3 and M4 are all directed to the charged amino acids from the putative heparin/heparan sulphate-binding site in Ig-1. Mutation M5 targets a basic cluster in Ig-2 and M6 targets a similar cluster in the loop connecting Ig-2 and Ig-3. All constructs were transfected into 293T cells and essentially equal amounts of fusion protein were secreted in the conditioned media, quantified by measuring the heat-stable alkaline phosphatase activity (data not shown). All the mutations directed at the large basic cluster in Ig-1 (Figure 4.3A) showed impaired heparin binding in solid-phase assays (Figure 4.4B). Binding of M5 and M6 constructs was not significantly affected.

The mutated constructs were tested on E6 chick retina sections by RAP *in situ*. The basal lamina binding pattern observed correlated with the solid-phase heparin binding profile (Figure 4.5). Therefore I conclude that the heparin/heparan sulphate-binding site was correctly predicted by molecular modelling. This site is essential for the binding of CRYPα1 ectodomains to the basal lamina ligands.

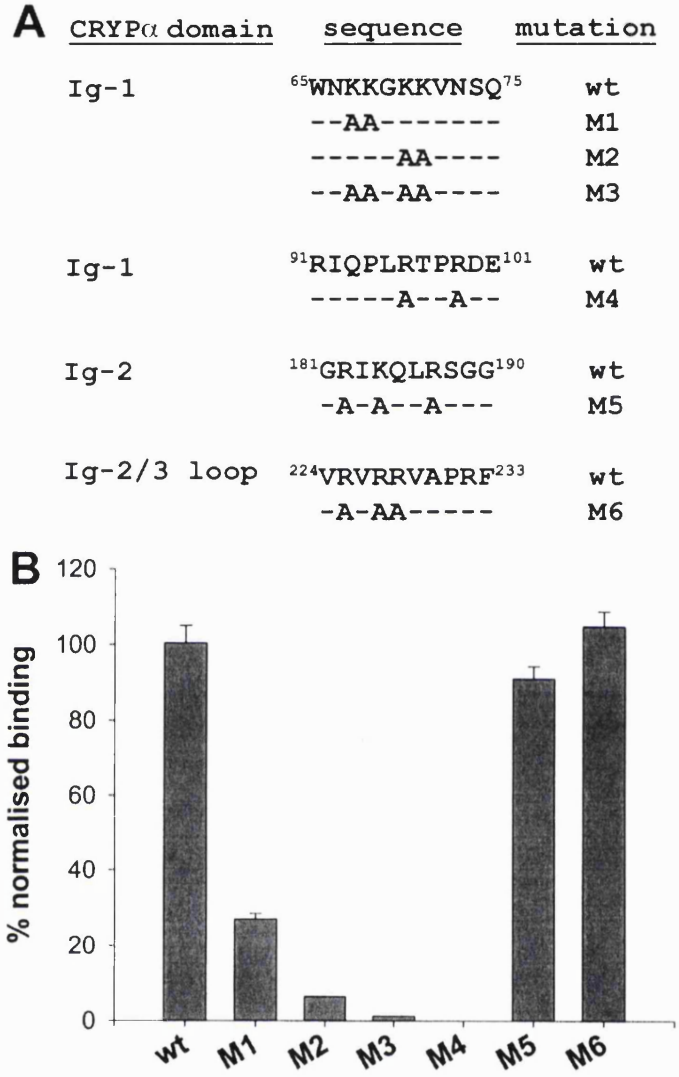

Figure 4.4. Identification of the CRYPα heparin-binding site by site-directed mutagenesis. (A) Basic residues in the heparin-binding site in domain Ig-1 (mutations M1, M2, M3 and M4), another cluster in Ig-2 (mutation M5) or in the loop connecting Ig-2 and Ig-3 (mutation M6) were replaced with alanine. "wt" corresponds to the original CRYPα sequence. (B) The mutated proteins were tested in solid-phase binding assays for binding to heparin-BSA. Bars represent means ± standard errors of three determinations.

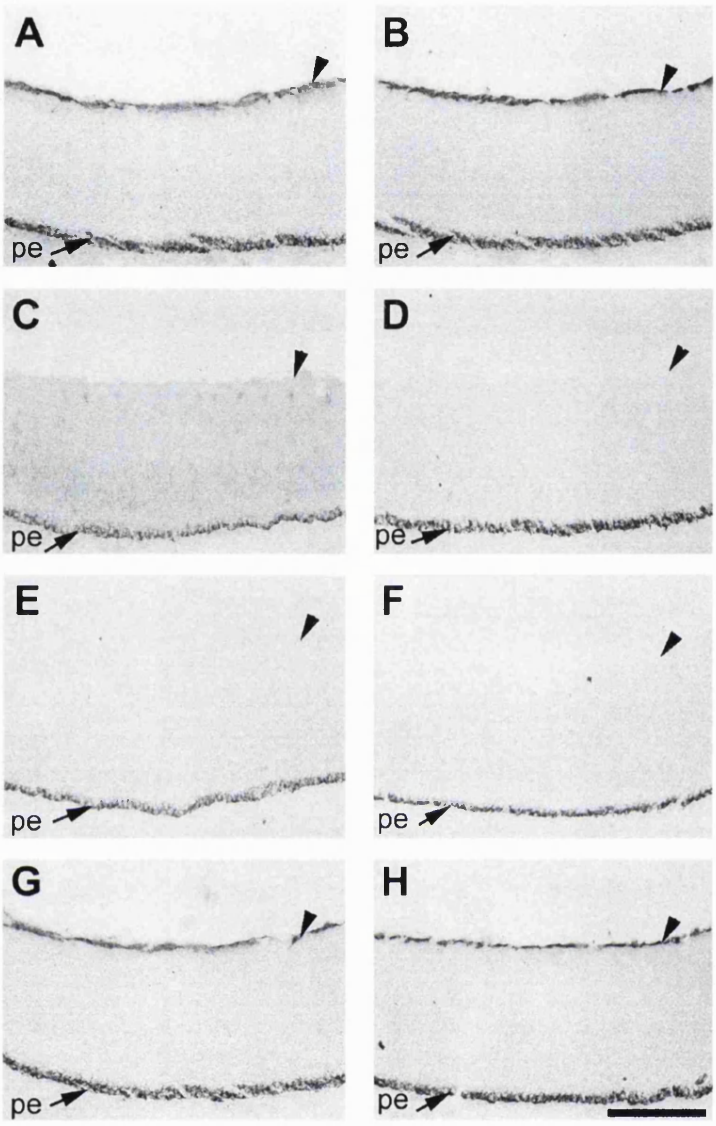

Figure 4.5. The heparin/heparan sulphate binding site in domain Ig-1 is essential for retinal basal lamina binding. Receptor affinity probe assays were performed using CRYPα1-AP (A), FN3Δ-AP (B), M1 (C), M2 (D), M3 (E), M4 (F), M5 (G) and M6 (H) conditioned media, respectively. The basal lamina staining indicates fusion protein binding. Arrowheads indicate the retinal basal lamina; pe, pigmented epithelium. Scalebar, 0.1 mm.

4.3.5. Radial glial cells (appear to) express two classes of CRYPα ligands

Radial glial cells ("Müller glia") are the only non-neuronal cell type in the chicken retina. RAP *in situ* experiments (Haj *et al.*, 1999; Ledig *et al.*, 1999a) demonstrate that, in addition to the basal lamina ligand(s), CRYPα binds very strongly to radial glia endfeet. This is particularly obvious on basal lamina flat-mounted preparations (Figure 4.7A) and appears to have physiological relevance during the intraretinal axon growth stage. I first questioned whether CRYPα has the ability to bind on the surface of cultured Müller glial cells. Primary retinal cell cultures were maintained for up to 3 weeks in medium without nerve growth factor and subjected to repeated passaging in order to remove most of the neurons. The glial cells kept dividing and maintained their typical, flat, well-spread morphology (Stier and Schlosshauer, 1998). RAP *in situ* experiments using CRYPα1-AP conditioned medium revealed strong binding on glial cell membranes (Figure 4.6A). This binding was abolished in the presence of 0.5 M sodium chloride (Figure 4.6C) and also by the addition of 100 μg/ml heparin (Figure 4.6E). All these observations agree with the results obtained on retina cryosections and described above.

However, similar experiments performed on flat-mounted basal laminae do not provide such clear-cut results. As shown in Figure 4.7, heparin addition can diminish CRYPα1-AP binding on glial endfeet but, unlike on cryosections or cultured Müller glia, this interaction is not blocked completely. In addition, several CRYPα1 mutant constructs exhibited reduced binding to the glial endfeet (Figure 4.7) but again the difference is less drastic compared to the results obtained on retinal cryosections (Figure 4.5).

Altogether these observations suggest that the glial endfeet, a highly differentiated area of the Müller glia, may express an additional, heparin-insensitive

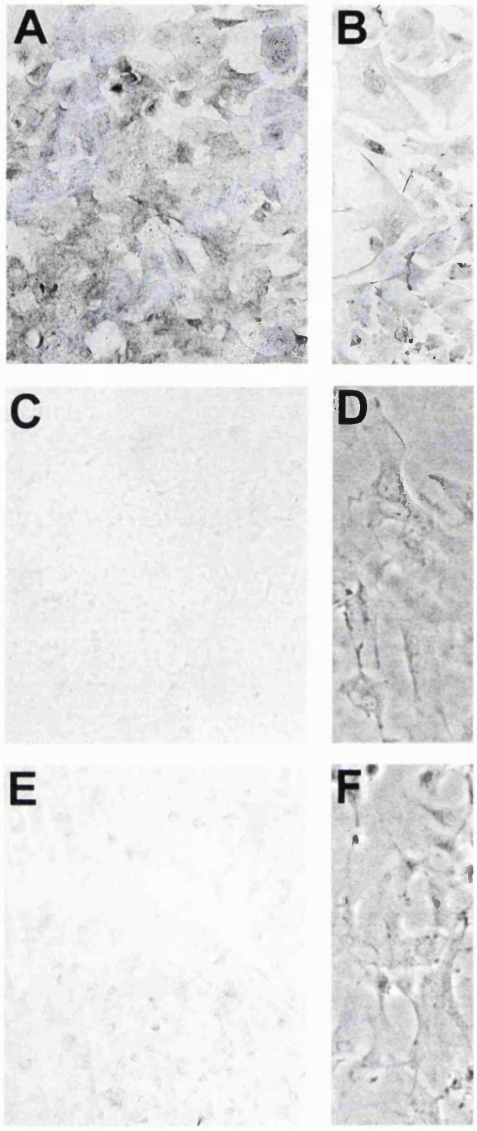

Figure 4.6. Sodium chloride and heparin abolish CRYPα binding to cultured retinal cells. RAP *in situ* assays using CRYPα1-AP conditioned medium demonstrate that these cells express a CRYPα ligand (A). Sodium chloride (C) or heparin (E) addition to conditioned media can prevent CRYPα binding to cultured cells. Phase-contrast images of the cultures shown in (C) and (E) are shown in (D) and (F) respectively. Anti-GFAP antibody staining (B) shows that primary retinal cell cultures contain mainly Müller glia after three successive passages.

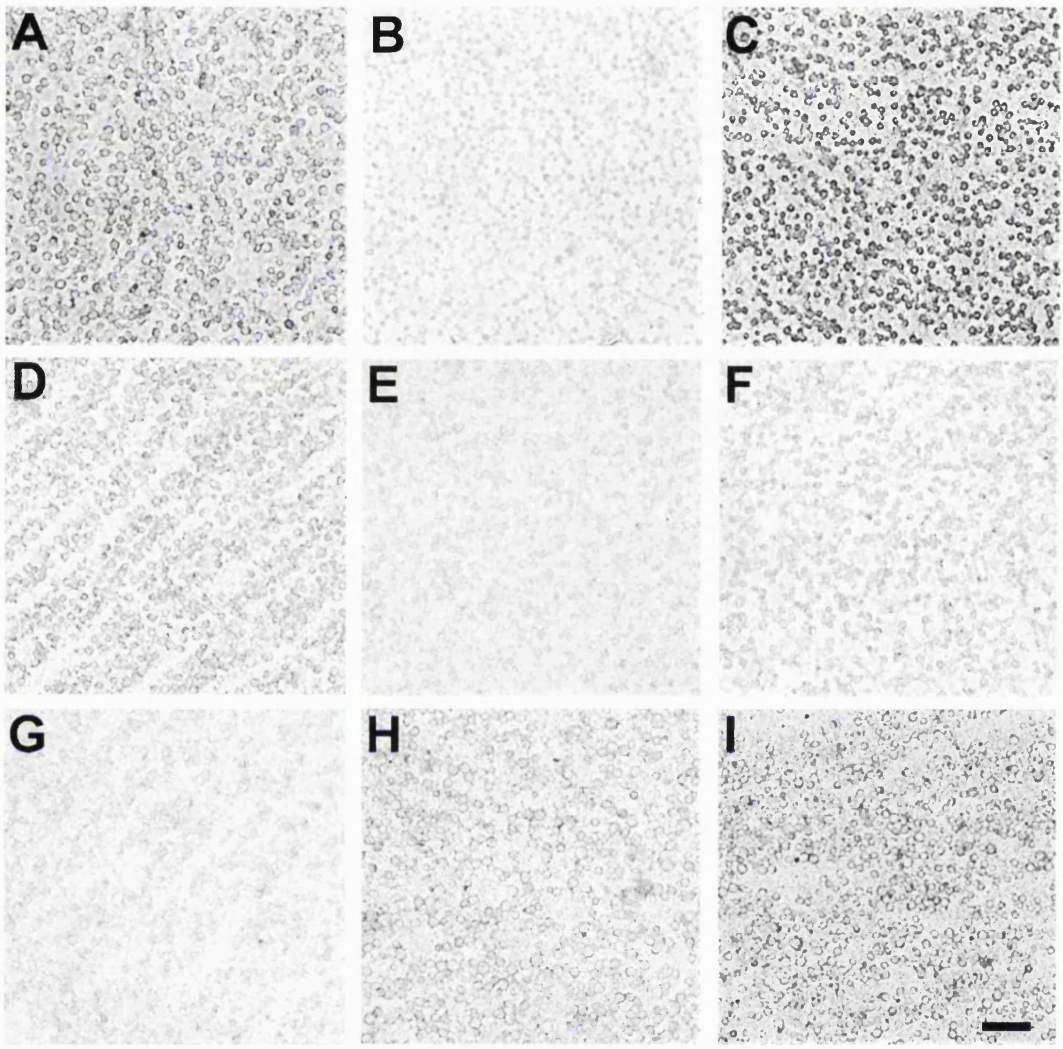

Figure 4.7. CRYPα binding to its glial endfeet ligand(s) cannot be completely abolished by heparin or mutations in the heparin-binding site. Retinal basal lamina with glial endfeet attached were flat-mounted on glass coverslips and probed by RAP *in situ* with conditioned media containing CRYPα1-AP (A, B), FN3Δ-AP (C), M1 (D), M2 (E), M3 (F), M4 (G), M5 (H) or M6 (I) fusion protein constructs. Heparin was added to the experiment shown in (B). Scalebar, 10 μm.

class of CRYPα ligands. Alternatively, a crucial part of a binding complex is downregulated or lost in culture and somehow disrupted/degraded on cryosections but sufficiently well maintained in the flat-mount BL preparations.

4.4 Discussion

The molecular architecture of CRYPα suggests that it has extracellular ligands and these ligands should modulate its phosphatase activity in order to exert a physiological function.

The main ligand detection system we have so far, *in vitro*, is the RAP *in situ* technique using soluble CRYPα ectodomain constructs fused with AP as probes. Putative ligands seem to be localised, among other places, in the chicken retino-tectal system (on the basement membranes, neuronal and glial cell surfaces; Haj *et al.*, 1999; Ledig *et al.*, 1999a). This is one of the most extensively studied neural development systems and therefore it was chosen to assess the functional role of CRYPα *in vitro* (Ledig *et al.*, 1999a; Johnson *et al.*, 2001) and *in vivo* (Johnson *et al.*, 2001; Rashid-Doubell *et al.*, submitted). It emerged that CRYPα-ligand interactions are important for controlling growth and possibly targeting of retinal ganglion cells' axons. The interactions required for the above-mentioned functions match very well the RAP *in situ* results. In addition, we have recently been able to demonstrate that CRYPα can bind to the retinal basal lamina *in vivo* (Aricescu *et al.*, submitted).

My main target was to identify these putative ligands. Therefore, having a high degree of confidence that the RAP *in situ* results are relevant, I set out to characterise this interaction at the molecular level. The major CRYPα binding site in the E6 chicken retina is the basal lamina (inner limiting membrane). Various chemicals used to modulate this interaction have led to a surprising conclusion: the CRYPα basal lamina ligand appears not to be a protein, or rather, this appears not to be a protein-protein

interaction. Instead, it seems that CRYPα may bind glycosaminoglycans, abundantly present in basement membranes. Clearly, CRYPα binding on RAP *in situ* is prevented by the addition of heparin. Moreover, CRYPα itself can bind heparin with a very high affinity. The significance of this finding will be discussed below.

Heparin is a highly sulphated polysaccharide, made up of repetitive disaccharide units containing an uronic acid residue (either D-glucuronic acid or L-iduronic acid) and D-glucosamine, which is either N-sulphated or N-acetylated. The disaccharides may be further O-sulphated at C6 and/or C3 of the D-glucosamine and at C2 of the uronic acid residue. More than 100 heparin-binding proteins have been described to date and this number is increasing (reviewed in Conrad, 1998). These include growth factors and their receptors, extracellular matrix proteins, cell adhesion molecules, proteins involved in lipid metabolism, in blood coagulation and fibrinolysis. How many of these interactions are physiologically relevant? If we consider that heparin, as such, is an intracellular product found in the secretory granules of mast cells in complex with basic proteases, and gets secreted only following degranulation, the situation doesn't look promising at all. However, another glycosaminoglycan structurally similar to heparin, termed heparan sulphate, is present on the surface of most if not all animal cells, attached to a protein core molecule. Both the protein core and the heparan sulphate chains present a high variability, thus defining a large family of molecules called heparan sulphate proteoglycans (HSPG). Despite the overall structural homology between heparin and heparan sulphate, many chemical variations have been described and the classification of various "heparinoid" fractions is still highly controversial (Conrad, 1998). Generally speaking heparan sulphate is less sulphated than heparin and shows a higher variability in the saccharide building blocks sequence. In fact, following recent advances in the glycan sequencing technology, the concept of "heparanome" has been recently proposed to reflect the wide variability of heparan sulphate sequences

expressed by particular cells or tissues and involved in specific functional roles (Turnbull *et al.*, 2001). A detailed presentation of HSPG classification and their developmental functions will be given in the following chapter. Nevertheless, it is worth mentioning here that a growing body of experimental evidence demonstrates that HSPGs are involved in modulating axon growth and guidance events and are important neurite outgrowth-promoting molecules. Considering that some HSPGs represent major constituents of basement membranes, including the retinal basal lamina, they are placed in a prime position as CRYPα candidate ligands.

Molecular modelling and site-directed mutagenesis experiments led to the identification of the CRYPα heparin-binding site in the N-terminus Ig domain. There are at least two well-characterised examples of type I membrane proteins able to bind heparin via their Ig domains: fibroblast growth factor (FGF) receptors and NCAM. Over ten years of research lie behind one of the key dogmas of cell signalling, namely that heparin (heparan sulphate *in vivo*) is required for functional binding of FGF to its receptors. In the early 1990s it was demonstrated that FGFR1 can bind heparin in a FGF-independent manner and that the intact Ig domain concerned, together with the associated heparin or HSPG molecule, is essential for efficient binding of FGF (Kan *et al.*, 1993). Since then, various FGFs and receptor constructs have represented favourite targets for the structural biologists, culminating in the recent determination of FGF-FGFR-heparin ternary complex structures (Schlessinger *et al.*, 2000; Pellegrini *et al.*, 2000). Ironically, the two structures reported are significantly different and so are the models proposed for heparin involvement in FGF signalling. Nevertheless, both the "two-ends" model (based on a 2:2:2 FGF:FGFR:heparin stoichiometry; Schlessinger *et al.*, 2000) and the "asymmetric heteropentamer" model (based on a 2:2:1 FGF:FGFR:heparin stoichiometry; Pellegrini *et al.*, 2000) are carefully arranged to agree with the available biochemical data which postulate a key function for

heparin/HSPGs in the molecular association between FGF and its receptor and for their biological activity.

NCAM, a well-characterised cell adhesion molecule, is known to be involved in both homophilic and heterophilic interactions. Its heterophilic partners include cell surface and extracellular matrix HSPGs (Storms *et al.*, 1996a,b). The importance of heparan sulphate binding to NCAM has been proven by the ability of exogenous heparin or heparan sulphate to inhibit completely neural cell adhesion to an NCAM substratum (Cole and Glaser, 1986) or to a monolayer of dissociated retinal cells (Cole *et al.*, 1986). The issue of whether heparin binding to NCAM is required for homophilic binding has been controversial. Only recently, the crystal structure of the NCAM first two Ig domains, which seem to be responsible for both heparin and homophilic binding, has been reported (Kasper *et al.*, 2000). It appears that the homophilic binding interface is localised away from the heparin-binding loop and therefore NCAM association with heparin probably does not interfere with homophilic binding and both processes may occur simultaneously. The predicted heparin-binding site of CRYPα matches very well the NCAM model and it would be interesting to analyse a crystal structure of the CRYPα ectodomain complexed with heparin (and of an NCAM-heparin complex too). Does heparin promote or stabilise a CRYPα dimer? If so, this may have significant functional consequences, as described in chapter 1.4.

An intriguing observation described in this chapter is the apparent presence of a heparin-independent interaction of CRYPα with radial glia endfeet, in addition to the proposed one involving HSPGs. Heparin efficiently competes with CRYPα binding on cultured Müller glia. Why is this not happening on the glial endfeet as well? Several studies support the idea that radial glial endfeet, both in the retina and optic tectum, are highly differentiated structures (Stier and Schlosshauer, 1998; Braisted *et al.*, 1997). Probably their direct contacts with the basement membranes trigger specific signalling

pathways and determine synthesis and local accumulation of specific molecules, otherwise absent from the glial cells' surface. In the tectal endfeet for example, a specific accumulation of ephrin B1 has been detected (Braisted *et al.*, 1997). Axon outgrowth experiments *in vitro* also demonstrate that retinal Müller glia are highly polarised: the cell bodies (glial somata) express a heat-sensitive repellent molecule while the endfeet are growth permissive (Stier and Schlosshauer, 1998). Unfortunately, what the authors call a "pure glial endfeet preparation" in fact means glial endfeet attached to the retinal basal lamina, as we used in our experiments. It is wrong to ignore the significant neurite outgrowth promoting potential of the basal lamina itself since it is well known that it represents a much better growth substrate than basal lamina with endfeet attached. Probably, as Ledig *et al.* (1999a) suggest, the glial endfeet contain a balance of positive and negative cues. The outcome of these factors, including the basal lamina influence, is indeed permissive since, in chicken, retina ganglion cell axons extend exclusively into the optic fibre layer and not into the outer retina, both *in vitro* and *in vivo*.

In conclusion, the fact that CRYPα binds heparin *in vitro* strongly suggests that it will bind HSPGs *in vivo*. Their location in the retinal basal lamina and their demonstrated role in modulating axon growth events make HSPGs prime candidates for CRYPα ligands. This possibility will be analysed in the following chapter.

Chapter 5. **Heparan sulphate proteoglycans are ligands for CRYPα**

5.1. Introduction

Proteoglycans are molecules that carry long, unbranched sugar polymers, termed glycosaminoglycans (GAGs), attached to specific serine residues of a protein core. GAGs are typically composed of ~50-200 disaccharide units (~25-100 kDa). Depending on the disaccharide structures, GAGs can be grouped into chondroitin sulphate (CS), dermatan sulphate (DS), heparin/heparan sulphate (HS) and keratan sulphate (KS). In addition, hyaluronan, which in contrast to the GAGs mentioned above is not sulphated, exists as a protein-free polysaccharide on cell surfaces and in the extracellular matrix (reviewed in Bandtlow and Zimmerman, 2000).

Heparan sulphate proteoglycans (HSPGs) can be very abundant. At the epithelial cell surface for example, it has been estimated that there may be as many as a million syndecan-1 molecules (Perrimon and Bernfield, 2001). Each protein core can have between one and eight HS chains attached. Considering that each HS chain, which adopts an extended helical coil conformation, can measure 40-160 nm in length, it appears that HSPGs are definitely a dominant feature of the cell surfaces. HSPGs can be transmembrane molecules (i.e. syndecans, 4 families in vertebrates), attached to the cell surface via a glycosylphosphatidylinositol (GPI) anchor (i.e. glypicans, 6 families in vertebrates) or can be secreted into the extracellular matrix to become key elements of basement membranes (perlecan, agrin and collagen XVIII). In addition, the syndecan and glypican core proteins can be proteolytically cleaved near the cell surface by matrix metalloproteinases and the ectodomains are released with all the HS chains of the parent molecule attached (Perrimon and Bernfield, 2000 and references therein).

"Traditionally", these highly abundant, strongly anionic molecules have been considered to interact non-specifically with secreted growth factors and extracellular matrix proteins, sequestering them in basement membranes or on cell surfaces in order to be presented to their "real" receptors. Recent insights from genetic studies in *Drosophila* and mice have strongly challenged this view (see below). Moreover, it is now understood that HSPGs have a rapid turnover rate, cells can alter the HS structures they make in response to extracellular stimuli and, more importantly, HS chain sequences are highly variable and at the same time cell- and tissue-specific (reviewed in Turnbull *et al.*, 2001). This sequence specificity is mainly due to cell- and tissue-specific expression of the HS modifying enzymes and formation of specialised enzyme complexes. The biosynthesis of HS involves a complex set of enzymatic reactions that first creates a non-sulphated polysaccharide chain precursor and then modifies it to generate a specific pattern of sulphation at selective positions (Turnbull *et al.*, 2001). Two key observations must be added: the HS synthesis seems not to be template-driven and the enzymes involved do not modify all the available sugars in the chain. It appears that regions of 10-16 highly modified disaccharides alternate with larger regions of relatively unmodified disaccharides, thus maybe creating discrete and specific binding sites. The fact that at least 32 possible unique disaccharide units have been described demonstrates an enormous potential for variability even in short sequences. In fact HS has been described as one of the most information-dense molecules in biology (Nugent, 2000). Current HS sequencing methods can only cope with saccharides up to about 12-16 sugar units in size (Turnbull *et al.*, 2001). A great effort is now being spent to improve the technology, and undoubtedly this will lead to a better understanding of the HS-protein binding specificity.

The identification and analysis of Drosophila and mice mutants deficient in enzymes involved in HS chain biosynthesis or in HSPG core proteins have revealed a

remarkable degree of HSPG specificity in developmental processes (reviewed in Perrimon and Bernfield, 2000). For example, the *Drosophila* gene *tout velu* (*ttv*) encodes for an enzyme involved in the production of HS chains (an HS polymerase that transfers a D-glucuronic acid on an N-acetyl-D-glucosamine unit to generate the initial HS chain precursor). Surprisingly, the *ttv* mutant only affects the Hedgehog (Hh) signalling pathway, leading to the inability of the membrane-targeted cholesterol-modified Hh molecule to move through cell fields (Bellaiche *et al.*, 1998). The human homologues of *ttv*, members of the *EXT* gene family, are implicated in the multiple exostoses syndrome, characterised by bone outgrowth and tumours. On the other hand, *Drosophila* mutants in the UDP-D-glucose dehydrogenase, called *sugarless* (*sgl*), and in the N-deacetylase/N-sulphotransferase (NDST), termed *sulfateless* (*sfl*), show more widespread phenotypes, affecting the Wingless (Wg), FGF and Hh signalling pathways. It is worth mentioning that the phenotypes observed are very severe, corresponding to a complete loss of activity of these pathways, which indicates that HSPGs are absolutely required for these molecules' signalling (reviewed in Perrimon and Bernfield, 2000). In mice, animals deficient in the gene encoding HS 2-O-sulphotransferase show multiple developmental abnormalities, renal agenesis being the most obvious one (Bullock *et al.*, 1998). On the other hand, targeted disruption of one of the four known NDST genes prevents mast cell biosynthesis of heparin chains but does not affect biosynthesis of other HS chains (Forsberg *et al.*, 1999; Humphries *et al.*, 1999).

Genes encoding HSPG core proteins have also specific developmental roles. For example, genetic analysis of the *dally Drosophila* mutant (affecting a glypican gene) suggests its involvement in both Wg and Decapentaplegic (Dpp) signalling. Dally appears to act as a co-receptor for Wg, in conjunction with Frizzled2 (Tsuda *et al.*, 1999). The *dally* mutant phenotype is reminiscent of the loss of the Wg activity. Interestingly, Dally is also involved in the Dpp signalling but only in imaginal disks

(Jackson *et al.*, 1997). Although Dpp is expressed during the embryonic stages, *dally* mutants show no defects related to the early function of Dpp in the establishment of dorso-ventral embryonic polarity. This provides an interesting example of a developmentally regulated HSPG function.

Proteoglycans are also important regulators of axon growth and guidance processes (reviewed in Bovolenta and Fernaud-Espinosa, 2000; Yamaguchi, 2001). In particular, there is strong experimental evidence that HSPGs act (indirectly) as promotors of neurite outgrowth. Experiments *in vitro* demonstrate that HSPGs can significantly enhance the growth-promoting abilities of a variety of molecules such as laminin (Lander *et al.*, 1985), NCAM (Cole *et al.*, 1986) or FGF2 (Chai and Morris, 1999). On the other hand, the interaction between Slit2 protein and its Robo1 receptor is significantly enhanced by cell-surface HSPGs and enzymatic removal of HS abolishes the chemorepulsive response to Slit2 shown by both migrating neurons and growing axons (Hu, 2001).

Further evidence for the role played by HS in axon guidance has been obtained from experiments *in vivo*. Wang and Denburg (1992) observed that exogenously added HS causes pathfinding errors in the Ti1 pioneer axons of cockroach embryos. Similar errors were detected in heparinase III-treated embryos, while chondroitinase or hyaluronidase treatments had no obvious effects. HS and heparitinase can also disrupt the trajectory of Fe2, another pioneer axon in the cockroach embryo (Rajan and Denburg, 1997). Analysis of the developing retinotectal system in *Xenopus* provided additional data regarding putative molecular mechanisms involving HSPGs during axon guidance. Walz *et al.* (1997) found that an HS fraction that preferentially binds FGF2 could prevent retinal axons from entering the optic tectum when added to an "exposed brain" preparation. In contrast, an HS fraction that preferentially binds FGF1 did not have such an effect, which further underlines the specificity of HS binding. Heparitinase

removal of the native HS chains at the beginning of optic tract formation caused retardation of retinal axon elongation. Although addition of FGF2 restored axon growth, they completely lost directionality. Interestingly, heparitinase treatment or HS competition caused a phenotype similar to the one obtained when a dominant negative FGF receptor was expressed in retinal ganglion cells (McFarlane *et al.*, 1996). Later on, Nyhus and Denburg (1998) found that anti-FGF2 antibodies and heparitinase treatment cause similar guidance errors in cockroach embryos. All these experiments demonstrate that heparan sulphate is involved in axon growth and guidance through modulation of FGF2 signalling. The identity of the HSPG involved in these events is not yet known. Nevertheless, this is not the only signalling pathway relevant for axon extension and pathfinding in which HSPGs are involved. For example, glypican-1 binds Slit2 (Liang *et al.*, 1999) and, as mentioned above, this appears to play a key role in mediating its repulsive effect (Hu, 2001). Syndecan-3 (N-syndecan) is a cell-surface receptor for heparin-binding growth-associated molecule (HB-GAM, better known as pleiotrophin), a well-characterised neurite outgrowth promoting factor (Raulo *et al.*, 1994).

In addition to cell surfaces, the extracellular matrix is also rich in HSPGs and represents a key component of the growth cone environment. The retinal basal lamina (BL), for example, a major growth substrate for the retinal ganglion cells, has a very complex structure. At least 20-30 different proteins can be electrophoretically separated after extensive detergent washing of the cell debris and most of the associated soluble proteins (Halfter and Von Boxberg, 1992). These include collagen IV, laminins, nidogen, HSPGs (agrin, collagen XVIII, perlecan) and chondroitin sulphate proteoglycans. Among HSPGs, the retinal BL is unique in that it expresses only trace levels of perlecan, otherwise very abundant in other basement membranes (Halfter *et al.*, 2000). Instead, agrin and collagen XVIII are the major HSPGs in the BL.

Agrin was originally isolated from the muscle basal lamina based on its ability to induce clustering of the acetylcholine receptors in cultured myotubes. Further studies firmly established agrin as a key regulator of synaptogenesis in the developing and regenerating neuromuscular junction (reviewed in Ruegg and Bixby, 1998). Alternative splicing (Figure 5.1) yields agrin isoforms that vary slightly in primary sequence but significantly in function. The so-called neural isoforms are unique to neurons and contain inserts of 4 and 8 (and/or 11) amino acids at two sites towards the C-terminus of the molecule (reviewed in Hagiwara and Fallon, 2001). Splice isoforms lacking the 8/11 amino acid inserts are termed "muscle" agrin, although they are highly expressed in other tissues such as brain, and in the lung and kidney basement membranes. Despite its abundance, agrin's function in the brain is not clear yet. Immunohistochemical studies revealed a striking pattern of expression along the developing axonal pathways including the optic pathway, the tecto-bulbar tract and the presumptive white matter of the spinal cord (Tsen *et al.*, 1995; Kroger, 1997; Halfter *et al.*, 1997). This expression pattern correlates with the active axonal growth and guidance stages in the developing nervous system. In addition, agrin was localised by electron microscopy on the surface of growing retinal ganglion cells in the developing optic pathway (Halfter *et al.*, 1997).

Collagen XVIII is a ubiquitous constituent of embryonic and adult basement membranes (Halfter *et al.*, 1998). Initially cloned during a screen for new genes containing collagen-like motifs (Oh *et al.*, 1994), collagen XVIII became an extensively studied molecule following the discovery that an 18 kDa anti-angiogenic peptide termed endostatin (ES) is in fact derived by proteolytical cleavage of its C-terminal domain (O'Reilly *et al.*, 1997). In addition, a mutation in the human *COL18A1* gene has been identified as causing the Knobloch syndrome, an autosomal recessive disorder characterised by retinal and neural tube closure defects (Sertie *et al.*, 2000). Kuo *et al.* (2001) have shown that a C-terminal fragment termed NC1/endostatin (NC11-end of

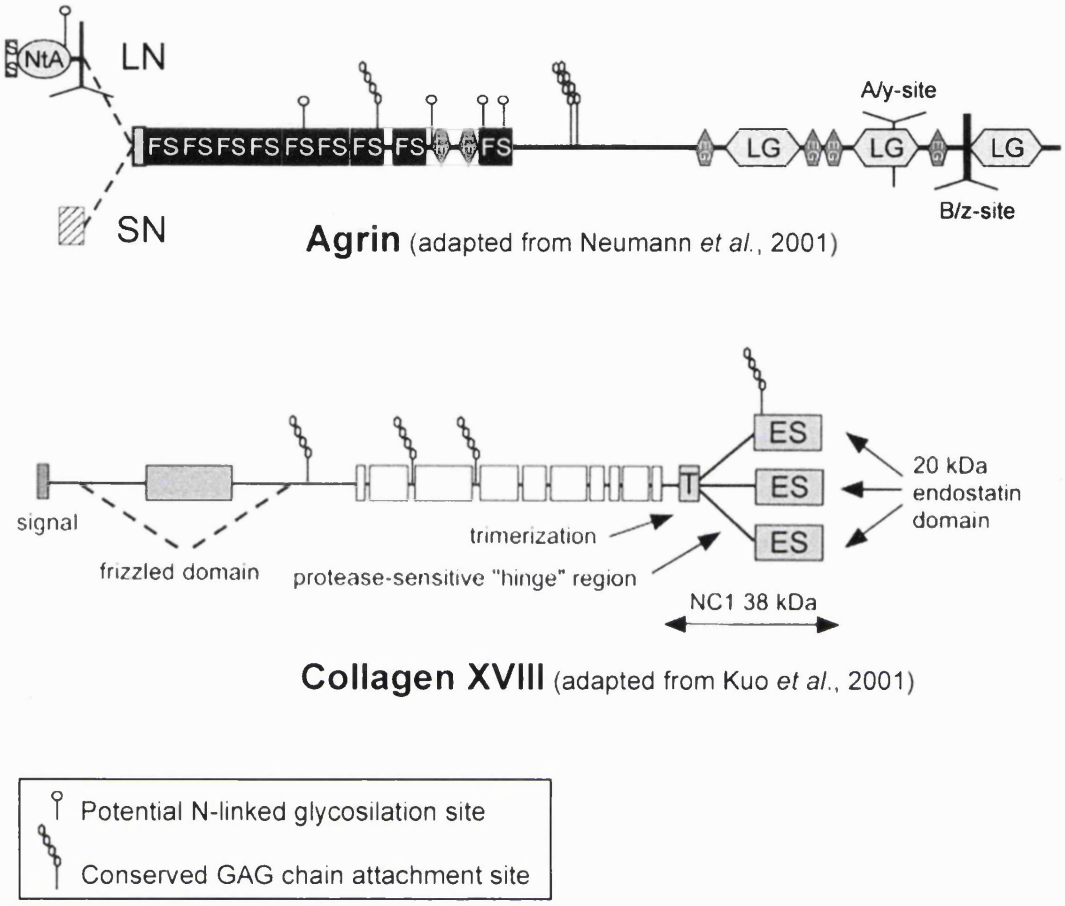

Figure 5.1. Schematic representation of agrin and collagen XVIII HSPGs.
Alternative promoter usage and N-terminus splicing of agrin results in two neuronal isoforms. The isoform termed LN contains a signal sequence (SS) followed by the NtA domain (necessary for binding laminin-1 in basement membranes), while the isoform termed SN contains a shorter N-terminus sequence responsible for membrane anchoring in a type II topology. The common part of the molecule contains follistatin-like domains (FS), laminin EGF-like domains (LE), EGF-like domains (EG) and laminin G-like domains (LG). Sites of alternative mRNA splicing are marked by ⊥. The second LG domain binds to heparin if a 4 amino acid insert is present at the A/y site. The third LG domain, in conjunction with the B/z site (which may contain inserts of 8, 11 or 19 amino acids) is sufficient to induce aggregation of the ACh receptors on myotubes.
Collagen XVIII contains ten triple helical regions (white boxes), a trimerisation motif (T) and an endostatin (ES) domain. The frizzled domain is present only in the liver-specific isoform.

molecule in Figure 5.1) has the ability to promote motility of various cell types in a manner strictly requiring oligomerisation of the ES domain and the activities of the small GTPases Rac and Cdc42 and the mitogen-activated protein kinase (MAPK) pathway. Furthermore, the *C. elegans* homologue of collagen XVIII, termed CLE-1 is similarly found in basement membranes and, at high levels, in the nervous system (Ackley *et al.*, 2001). Interestingly, deletion of the *cle-1* region encoding the "NC1" domain (NC11 in Figure 5.1) results in multiple cell migration and axon guidance defects.

Therefore, retinal basal lamina HSPGs and in particular agrin and collagen XVIII are expressed in the right place at the right time to bind CRYPα and possibly modulate its activity. In this chapter, I demonstrate that CRYPα binds the basal lamina HSPGs via their HS chains *in vitro*. Solid-phase binding assays using immunopurified agrin and collagen XVIII shows that CRYPα can bind these HSPGs with very high affinity. Their overlapping expression patterns suggest that such interactions can happen *in vivo* as well. On the other hand, further arguments are provided supporting the idea that Müller glia endfeet express an additional, non-HSPG (class of) ligand(s).

5.2. Experimental procedures

RAP *in situ*. The *in situ* localisation of CRYPα ligands on E6 tissue sections, primary retinal cell cultures and flat-mounted retinal basal laminae were performed using CRYPα1-AP conditioned medium as previously described (chapter 2.5.3). In modified RAP assays the CRYPα1-AP probe was pre-incubated with 100μg/ml heparin (Sigma), bovine kidney heparan sulphate (Sigma) or chondroitin sulphate (Calbiochem) for 1h at room temperature, then added to cryosections (see chapter 2.5.1), cells (see chapter 2.4.3) or basal laminae (see chapter 2.4.4). Alternatively, the sections, cells or basal laminae were pre-treated for 2 hours at 37°C with 0.5 U heparitinase (heparinase

III, Sigma) in 50 µl PBS, pH 7.4 containing 0.1% w/v BSA or with 0.1 U chondroitinase ABC (Sigma) in 50 µl Tris-acetate buffer, pH 8. The protease inhibitor 4-(2-Aminoethyl)-benzenesulfonyl fluoride was added to both reactions to a final concentration of 2 mM.

Single-chain variable fragment (scFv) antibodies selected against skeletal muscle basal lamina HSs were a gift from A. Oosterhof (University of Nijmegen; Jenniskens *et al.*, 2000). E6 chicken embryo cryosections were pre-blocked for 20 min in PBS with 0.1% w/v BSA. Periplasmic fractions of IPTG-induced *E. coli* HB2151 cultures (clones RB4EA12, HS4C3, AO4B08, EV3C3 and HS4E4) containing scFv antibodies were diluted 1:5 in PBS with 0.1% (w/v) BSA and incubated 90 min at room temperature with the sections. Anti-agrin (clone 6D2; Halfter, 1993) and anti-collagen XVIII (clone 6C4; Halfter *et al.*, 1998) monoclonal antibodies were diluted 1:20 in PBS containing 0.1% (w/v) BSA and incubated with the tissue sections as described above. After 3 x 10 min washes in PBS, the sections were incubated with CRYPα1-AP conditioned medium following the standard RAP *in situ* protocol described in chapter 2.5.3.

Solid-phase binding assays. Agrin, purified as described in Halfter *et al.* (1997), and collagen XVIII, purified as described in Halfter *et al.* (1998), were kindly provided by W. Halfter (University of Pittsburgh). Aliquots of 100 µl were bound on 96-well microtiter plates at a protein concentration of 5 µg/ml, for 2 hours at room temperature, then the remaining binding sites were blocked by overnight incubation at 4°C in PBS containing 3% (w/v) BSA. Conditioned media containing various concentrations of CRYPα1-AP were incubated with the coated wells for 3 hours at room temperature. Bound CRYPα1-AP quantification and K_D determinations were performed as described in chapter 4.2.

Expression constructs and fusion protein production. CRYPα1-AP conditioned medium was obtained by transient transfection of the pBG-CRYPα1-AP plasmid in 293T cells, as described in chapter 2.3. The pα1-VST expression vector was constructed by subcloning the *Hin* dIII fragment coding for CRYPα1 extracellular region into the pCS3N-VST shuttle vector (Aricescu and Stoker, unpublished), which contains a *Hin* dIII site, a linker coding for the VSV peptide tag, a short spacer sequence and an *Acl* I site, all flanked by two *Not* I sites. pα1-VST was used to express the secreted CRYPα1-VSV fusion protein in 293T cells as described above or, for higher expression levels, the CRYPα1-VSV coding fragment was transferred into the RCAS(A) avian retrovirus (Hughes *et al.*, 1987) in two steps, as follows: pα1-VST was linearised with *Acl* I and ligated into the *Cla* I opened RCAS(A); the shuttle vector backbone was then removed via *Not* I digestion and self-ligation, resulting in the RCAS-α1VST retrovirus. This construct was transfected into line 0 chick embryo fibroblasts (grown in DMEM plus 10% v/v foetal calf serum plus 2% v/v chick serum) using Superfect (Qiagen). After 6 passages the conditioned medium containing CRYPα1-VSV was collected, sterile filtered, and buffered to pH 7.4 with 20 mM HEPES.

Immunoblotting and blot-overlay assays. An HSPG-enriched fraction (HfV) from E9 chick embryo vitreous bodies homogenised in Ca^{2+}/Mg^{2+} free Hanks' balanced salt solution, pH 7.3 (CMF) was partially purified by ion-exchange chromatography as follows. The vitreous homogenate was supplemented with 1:100 protease inhibitors cocktail with no metal chelators (Sigma) and centrifuged at 12,000 g for 30 min at 4°C to remove debris. The supernatant was applied on a Q-Sepharose Fast Flow column (Amersham Pharmacia Biotech), washed with 0.5 M NaCl in CMF, and the HfV

fraction was eluted with 1.5 M NaCl in CMF. Eluted fractions were concentrated using Centricon YM-30 (Amicon) centrifugal filter units and the buffer changed to CMF. Aliquots of the HfV, as well as 100 ng immunopurified agrin and collagen XVIII (as described in Halfter *et al.*, 1997; Halfter *et al.*, 1998) were pre-incubated for 2 h at 37°C with either 0.5 U heparinase III, 0.1 U chondroitinase ABC or 0.1 U collagenase (Sigma type VII) in PBS, pH 7.4, containing 2 mM 4-(2-Aminoethyl)-benzenesulfonyl fluoride.

For immunoblotting the reactions were mixed with equal volumes of Laemmli sample loading buffer (62 mM Tris, pH 6.8, 2% SDS, 10% glycerol, 5% β-mercaptoethanol, 0.001% Bromophenol Blue), boiled and separated by 6% SDS-polyacrylamide gel electrophoresis. Proteins were transferred onto Hybond-C Extra nitrocellulose membranes (Amersham Pharmacia Biotech), blocked overnight at 4°C in 5% w/v non-fat milk (Marvel) in PBS, and probed for 1 hour at room temperature with anti-agrin (6D2, 1:20; Halfter, 1993) or anti-collagen XVIII (6C4, 1:20; Halfter *et al.*, 1998) monoclonal antibodies. The secondary antibody used was HRP-conjugated rabbit anti-mouse (Dako) diluted at 1:2000. Chemiluminescent detection was performed using the ECL Western blotting kit (Amersham Pharmacia Biotech).

For blot-overlay assays the samples were processed as above except that, following overnight blocking, the membranes were incubated for 3 hours at room temperature with CRYPα1-VSV conditioned medium supplemented with 0.5% Igepal CA-630 (Sigma). The membranes were then washed 3 times with PBS containing 0.5% Igepal CA-630 and bound CRYPα1-VSV was detected using the anti-VSV monoclonal antibody (P5D4, 1:1000; Sigma) as described above.

Immunohistochemistry and immunocytochemistry. E6 or E10 chick embryo heads were fixed in 4% paraformaldehyde in PBS, cryoprotected in 30% sucrose in PBS and frozen in OCT compound (TissueTek). Cryosections (10-12 μm) were mounted on

3-aminopropyltriethoxysilane coated glass slides. For immunohistochemistry, sections were blocked with 1% w/v BSA, 0.25% Triton X-100 in PBS for 15 min at room temperature. Primary antibodies used were IG2 (anti-CRYPα rabbit polyclonal, Stoker *et al.*, 1995) diluted at 1:500; P5D4 (anti-VSV glycoprotein monoclonal, Sigma) at 1:500; 6D2 (anti-agrin monoclonal; Halfter, 1993) at 1:20 and 6C4 (anti-collagen XVIII monoclonal; Halfter *et al.*, 1998) at 1:20, all in 3% w/v BSA, 0.25% TritonX-100 in PBS. After 1 hour incubation at room temperature the sections were washed three times in 0.1% w/v BSA, 0.05% TritonX-100 in PBS and secondary antibodies were added for 1 hour at room temperature, as follows: HRP-conjugated goat anti-rabbit (Promega), diluted at 1:100; HRP-conjugated rabbit anti-mouse (Promega), at 1:100; FITC-conjugated goat anti-mouse (Jackson Labs), at 1:200. After three final washes the peroxidase reactions were performed using the DAB substrate kit (Vector Laboratories) and the FITC-labelled sections were mounted in Fluorsave (Calbiochem).

All the anti-HS antibodies previously used for RAP *in situ* competition are VSV-tagged and therefore, after binding on cryosections as described above, they were detected with the P5D4 monoclonal antibody (diluted at 1:200; Sigma) following the standard procedure described above.

Primary retinal cell cultures were fixed in cold methanol for 2 min at -20°C and blocked 15 minutes at room temperature in PBS containing 1% w/v BSA and 0.1% Triton X100. A rabbit polyclonal anti-GFAP (glial fibrillary acidic protein) antibody (Sigma), diluted at 1:200 in PBS containing 3% w/v BSA and 0.05% Triton X-100, was then incubated with the cells for 1 hour at room temperature. The excess antibody was removed by 3 x 10 min washes in PBS containing 0.05% Triton X-100 and the secondary antibody (HRP-conjugated goat anti-rabbit, Promega) was added at 1:200 dilution for 1 hour at room temperature. The peroxidase reaction was performed as described above.

All sections and cell preparations were analysed using an Axiophot fluorescence microscope (Zeiss).

5.3. Results

5.3.1. CRYPα binds to retinal HSPGs

CRYPα is a heparin-binding protein, as shown in chapter 4.3.2. In addition, heparin is able to abolish CRYPα binding on retinal BL ligands and on cultured retinal cells (see chapters 4.3.1. and 4.3.5). In those experiments, heparin can either compete with the BL ligand(s) for the same binding site on CRYPα or, alternatively, it can compete with CRYPα for the same binding site on the BL. Site-directed mutagenesis experiments (see chapter 4.3.4) targeting the heparin-binding site of CRYPα suggest that heparin-like molecules in the basal lamina are indeed the ligands detected by RAP *in situ*. The obvious candidates are the polyanionic glycosaminoglycan chains attached to basal lamina proteoglycans.

RAP *in situ* competition experiments demonstrate that charge alone is not sufficient to modulate this interaction. Heparan sulphate (Figure 5.2 C), like heparin (Figure 5.2 B), efficiently competes for CRYPα binding, while the same amount of chondroitin sulphate has no effect (Figure 5.2 D). On the other hand, specific digestion of basal lamina heparan sulphate chains by heparinase III results in complete loss of CRYPα binding (Figure 5.2 E), while chondroitinase ABC pre-treatment had no effect (Figure 5.2 F).

In addition, a panel of five monoclonal scFv antibodies raised against HS chains (Jenniskens *et al.*, 2000) was tested for their ability to bind the E6 chick retinal BL. As

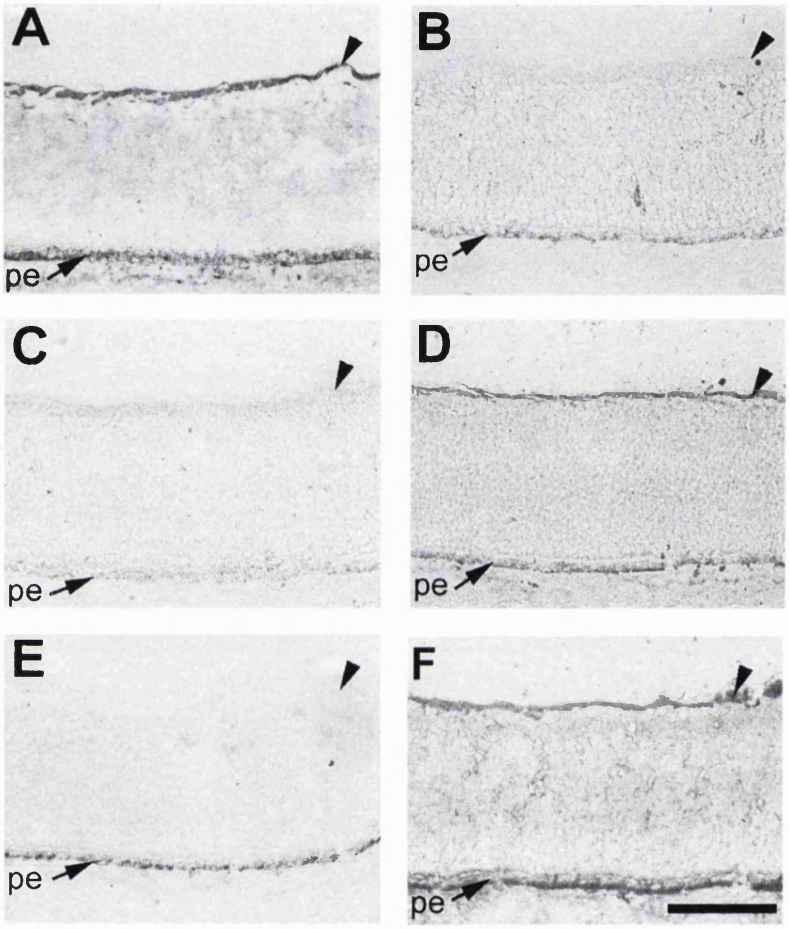

Figure 5.2. CRYPα binding to the E6 chick retinal basal lamina is mediated by heparan sulphate chains. (A) to (F): Receptor affinity probe assays using the extracellular region of CRYPα1 fused to alkaline phosphatase. Retina sections were untreated (A-D), or pre-treated with heparinase III (E) or chondroitinase ABC (F). CRYPα1-AP conditioned medium was used alone (A), or pre-incubated with heparin (B), heparan sulphate (C) or chondroitin sulphate (D). The basal lamina staining indicates CRYPα1-AP binding. Arrowheads indicate the retinal basal lamina; pe, pigmented epithelium. Scalebar, 0.1 mm.

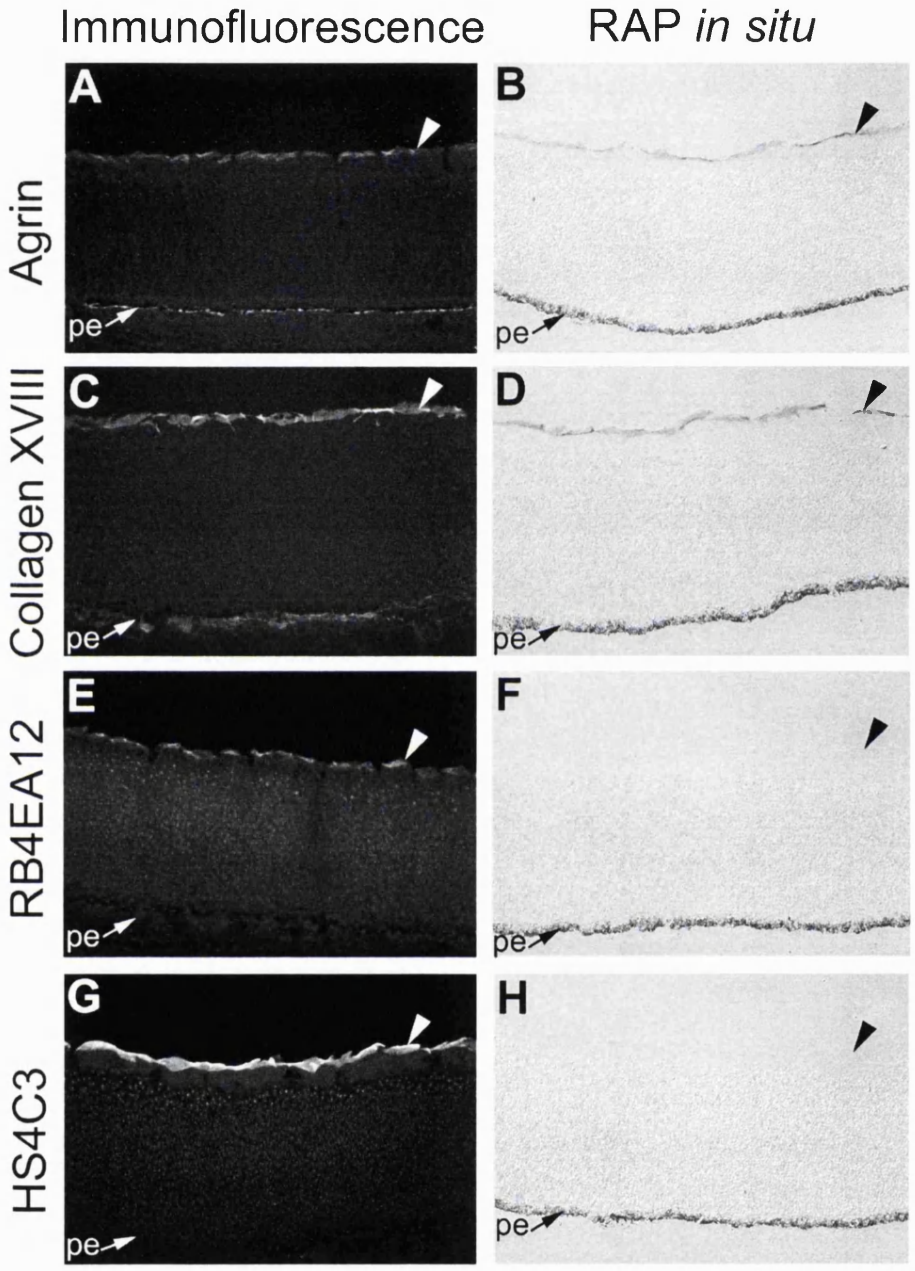

Figure 5.3. (Continued on the next page)

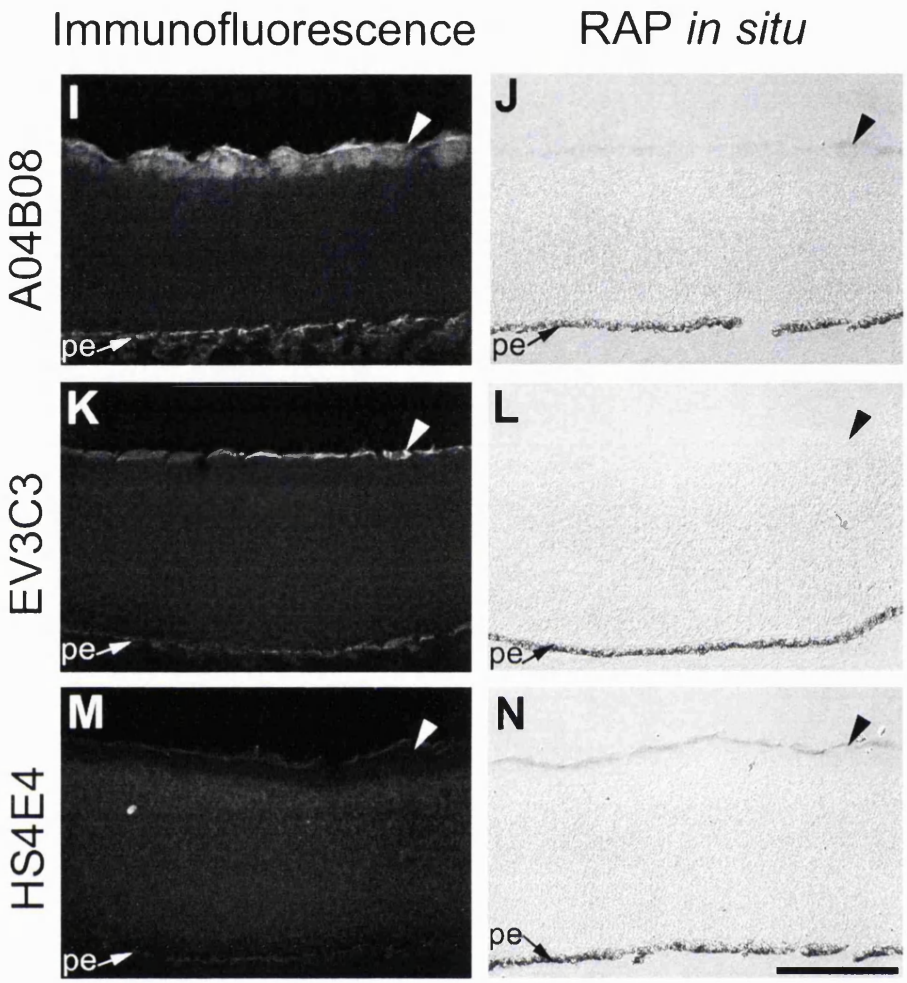

Figure 5.3. (Continued from previous page) Various anti-HSPG monoclonal antibodies affect CRYPα binding to the retinal BL in a differential manner. Immunofluorescent staining of E6 chick retina sections with monoclonal antibodies against the agrin protein core (A), collagen XVIII protein core (C) and various scFv antibodies against basement membrane HS chains (E, G, I, K, M) reveal specific staining patterns. All antibodies except HS4C3 (M) bind to the retinal basal lamina (white arrowheads). RAP *in situ* using CRYPα1-AP conditioned medium demonstrates that all anti-HS antibodies that are able to bind to the retinal BL can effectively compete with CRYPα binding (F, H, J, L). However, antibodies against agrin (B) or collagen XVIII (D) protein cores as well as HS4C3 cannot abolish the RAP *in situ* signal.
Arrowheads indicate the retinal basal lamina; pe, pigmented epithelium. Scalebar, 0.1 mm.

seen in figure 5.3, most of them bind, with various degrees of specificity. HS4C3 and EV3C3 clearly label the BL (Figure 5.3 G and K), as do the control monoclonal antibodies directed against the protein cores of the main retinal HSPG constituents (agrin and collagen XVIII, Figure 5.3 A and B, respectively). RB4EA12 and, to a lesser extent, HS4C3 have additional binding sites in or around the retinal cells' nuclei (Figure 5.3 E and G), as previously described in cultured CHO cells by Jenniskens *et al.* (2000). AO4B08 also labels the retinal ganglion cell axons forming the outer fibre layer, as well as the basal lamina (Figure 5.3 I). In contrast, HS4E4 did not bind at all on the retinal basal lamina (Figure 5.3 M).

The ability of various antibodies to bind HS chains in the basal lamina correlates with their ability to block CRYPα binding in RAP *in situ* experiments. The anti-agrin and anti-collagen XVIII antibodies did not affect CRYPα binding significantly, neither did HS4E4 (Figure 5.3 B, D and N). On the other hand, RB4EA12, HS4C3 and EV3C3 blocked this interaction completely (Figure 5.3 F, H and L) and only a very weak signal could be detected when AO4B08 was used (Figure 5.3 J).

Together, the experiments mentioned above support two conclusions: the retinal BL ligands for CRYPα detected by RAP *in situ* on cryosections are HSPGs and this interaction is mediated by their HS chains rather than the core protein.

5.3.2. CRYPα binds to the extracellular matrix HSPGs agrin and collagen XVIII.

The major HSPGs present in the retinal basal lamina are agrin and collagen XVIII (Halfter *et al.*, 2000). Perlecan can also be detected but is much less abundant. Agrin and collagen XVIII samples immunopurified from the vitreous body (gift of W. Halfter, University of Pittsburgh; Halfter *et al.*, 1997; Halfter *et al.*, 1998) were tested as candidate CRYPα ligands in solid-phase binding assays. CRYPα1-AP bound at picomolar concentrations to both agrin and collagen XVIII (Figure 5.4 A and B). The

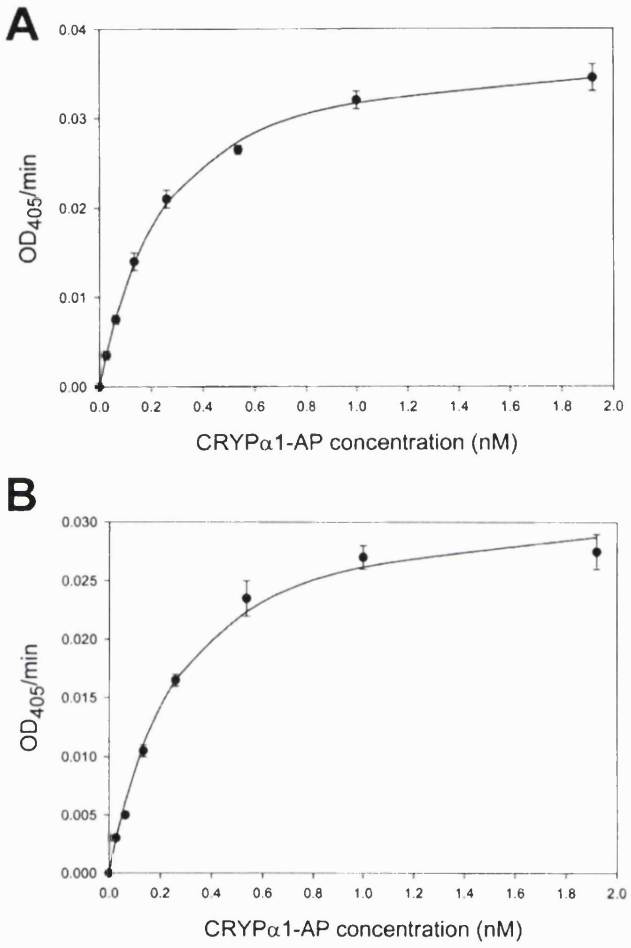

Figure 5.4. Solid-phase binding of CRYPα to agrin and collagen XVIII. Agrin (A) and collagen XVIII (B) were coated on microtiter plates and incubated with a range of CRYPα1-AP concentrations. Curves were fitted by nonlinear regression analysis as described under Materials and Methods. Each value represents the mean ± standard deviation of three measurements.

dissociation constants measured were 0.18±0.01 nM for agrin and 0.21±0.02 nM for collagen XVIII, demonstrating that CRYPα binds these HSPGs with very high affinity. This experiment shows that native agrin and collagen XVIII can function as ligands for CRYPα, at least *in vitro*.

These interactions were investigated in a further assay to determine whether CRYPα-proteoglycan interactions occur mainly via the HS chain, as predicted above. An HSPG-enriched (HfV) fraction from E9 chick embryo vitreous bodies was prepared by ion-exchange chromatography and, together with pure agrin and collagen XVIII, was tested on a blot-overlay assay. As shown in Figure 5.5 A, the HfV fraction contains both agrin and collagen XVIII. Agrin, a large proteoglycan with an apparent molecular mass of 500 kDa, appears undegraded in the HfV fraction and was not digested by treatment with collagenase (lane c) or chondroitinase ABC (lane d). However, treatment with heparinase III (lane b) reduced agrin's size to 250 kDa, corresponding to its core protein. Similarly, the molecular mass of collagen XVIII was reduced from around 300 kDa to the 180 kDa core protein (lane f). Chondroitinase ABC treatment had no effect (lane h), whereas collagenase removed any trace of collagen XVIII (lane g). When the same HfV samples were probed with the CRYPα1-VSV conditioned medium in the blot-overlay assay, two bands, corresponding in size to agrin and collagen XVIII, were observed in the untreated (lane i) and chondroitinase ABC treated (lane l) samples. Heparinase III digestion (lane j) completely removed any signal on the blot overlay, showing that CRYPα binding requires the presence of HS chains. This agrees with the RAP *in situ* results described above. Finally, collagenase pre-incubation (lane k) specifically removed the lower molecular weight band, corresponding to collagen XVIII.

The same patterns were obtained when purified agrin (Figure 5.5 B) or purified collagen XVIII (Figure 5.5 C) samples were enzyme-treated and probed in immunoblots or blot-

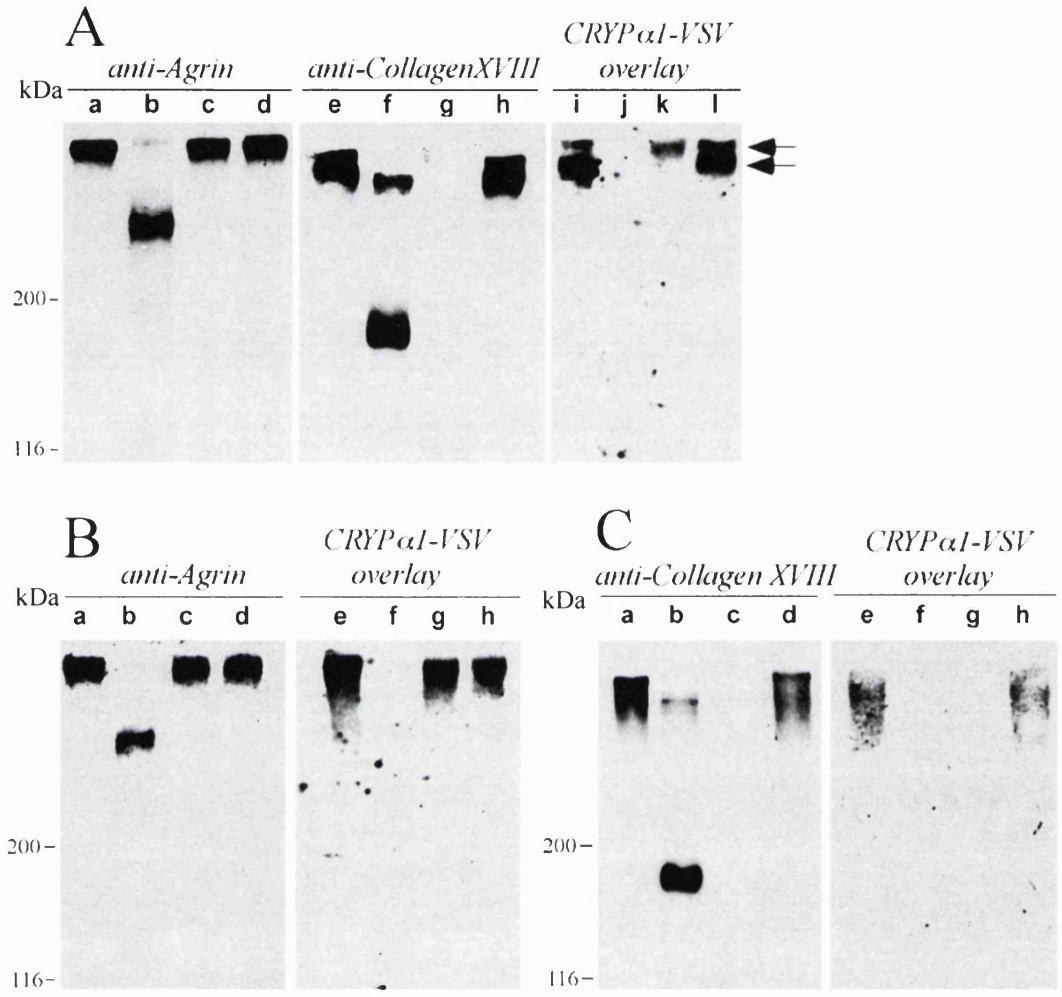

Figure 5.5. CRYPα binds the extracellular matrix proteoglycans agrin and collagen XVIII via their heparan sulphate chains. An HSPG-enriched fraction from chick embryo vitreous bodies (A), purified agrin (B) and purified collagen XVIII (C) samples, separated by 6% SDS-PAGE, were transferred on nitrocellulose membranes and probed with anti-agrin mAb 6D2, anti-collagen XVIII mAb 6C4 or CRYPα1-VSV conditioned medium. Bound CRYPα1-VSV was detected using an anti-VSV mAb. Samples were either untreated with enzymes (lanes a, e, i) or pre-digested with heparinase III (lanes b, f, j), collagenase (lanes c, g, k) or chondroitinase ABC (lanes d, h, l). Arrows in (A) indicate the two bands corresponding in molecular mass to agrin (upper) and collagen XVIII (lower) observed in the blot-overlay assay.

overlay assays. The collagen XVIII blots (Fig. 4C) appear smearier than in the fresh HfV samples, presumably due to partial degradation during the purification steps.

Altogether, these data suggest that agrin and collagen XVIII can act as ligands for CRYPα, irrespective of the CRYPα–fusion tag used (AP or VSV), and that these interactions occur necessarily via their HS chains.

5.3.3. Overlapping expression patterns of CRYPα, agrin and collagen XVIII in the developing chick retina.

It has been previously shown that CRYPα, agrin and collagen XVIII are expressed in the embryonic nervous system in a developmentally regulated manner (Stoker *et al.*, 1995; Ledig *et al.*, 1999b; Halfter *et al.*, 1997; Halfter *et al.*, 1998). Here I examined whether the expression patterns of CRYPα and the proposed ligands are juxtaposed, as would be expected if they were to be interacting *in vivo*. At E6 CRYPα is localised in retinal axons in the optic fibre layer (OFL) in close contact with the BL (Figure 5.6 A). Agrin (Figure 5.6 C) and collagen XVIII (Figure 5.6 E) are localised at E6 mainly in the basal lamina, which forms part of the complex substrate on which the RGCs extend their axons towards the optic nerve head. At E10, when the retinal plexiform layers have formed, CRYPα is mainly localised in the OFL and in the inner plexiform layer (IPL) (Figure 5.6 B). Agrin, produced like CRYPα by the RGCs, is present in the OFL and IPL, but also accumulates in large amounts in the BL (Figure 5.6 D). Collagen XVIII however, produced by the ciliary body (Halfter *et al.*, 2000) is only present on the retina inner surface, representing the BL (Figure 5.6 F).

The expression patterns described above suggest that CRYPα would indeed be able to interact with both agrin and collagen XVIII during eye development.

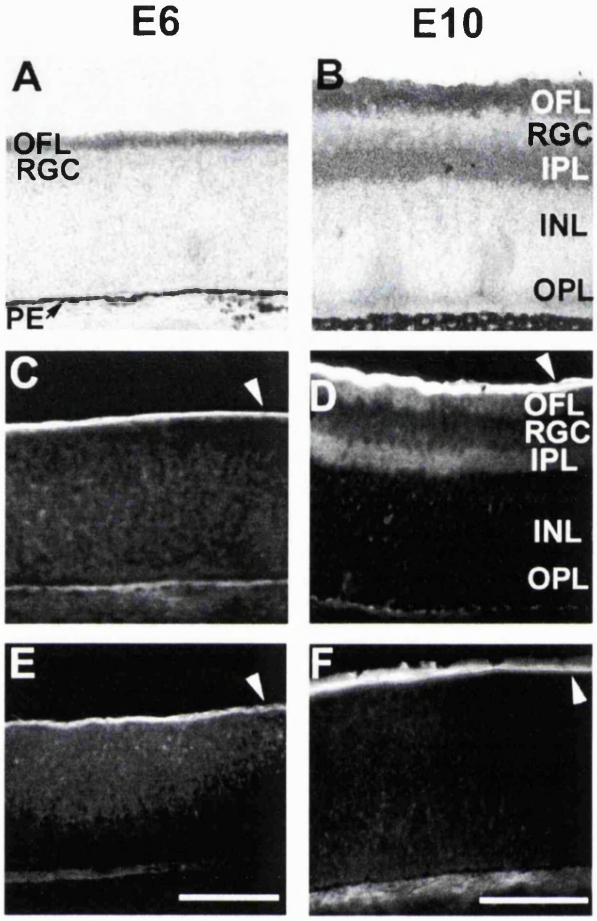

Figure 5.6. Expression patterns of CRYPα, agrin and collagen XVIII in the developing chick retina. E6 (A, C, E) and E10 (B, D, F) chick retina sections were probed with antibodies anti- CRYPα (A,B), anti-agrin (C,D) and anti-collagen XVIII (E, F). At E6, CRYPα is strongly expressed in the retinal axons (outer fibre layer, OFL) while both agrin and collagen XVIII show strong expression in the juxtaposed basal lamina (white arrows), the substrate for RGC axon growth. At E10 the retinal layers are better differentiated and CRYPα shows strong expression mainly in neurite layers: OFL and IPL (inner plexiform layer). The agrin expression pattern is overlapping and also shows that, together with collagen XVIII, agrin is a major constituent of the retinal basal lamina. RGC, retinal ganglion cells layer; INL, inner nuclear layer; OPL, outer plexiform layer; PE, pigmented epithelium. Scalebar, 0.1 mm.

5.3.4. A non-HSPG class of ligands appears to be expressed on Müller glia endfeet

RAP *in situ* experiments described in chapter 4.3.5 demonstrate that CRYPα binding to Müller glia endfeet is not entirely heparin-sensitive. In contrast, binding to primary retinal cells in culture is completely abolished by heparin or sodium chloride. These observations suggest that the Müller glia may express two classes of ligands. In order to further analyse this hypothesis, primary retinal cells in culture and flat-mounted retinal basal laminae were tested by modified RAP *in situ* experiments as described in chapter 5.3.1. Heparinase III treatment prevents CRYPα binding on cells (Figure 5.7 D), however its effect on glial endfeet is less pronounced (Figure 5.8 C). On the other hand, neither chondroitin sulphate nor chondroitinase ABC pre-treatment could impair the interaction between CRYPα and its ligands expressed on cultured cells (Figure 5.7 E and F) or glial endfeet (Figure 5.8 D and E).

These results demonstrate that glial cell surface HSPGs and not CSPGs are responsible for CRYPα binding observed by RAP *in situ* and that the HS chains are essential for this interaction. This seems not to be the case on glial endfeet where, although both heparin and heparinase III treatment can reduce binding to some extent, an additional, non-HSPG, ligand appears to be present.

5.4. Discussion

The HS chains contain binding sites for a variety of extracellular proteins such as matrix constituents, proteases and their inhibitors, lipases, lipoproteins, growth factors and their receptors, cytokines and anti-microbial peptides (Park *et al.*, 2000). These molecules are involved in essential processes including morphogenesis, tissue repair, energy balance and host defence. In addition, pathogens like herpes simplex virus, *Neisseria* and *Plasmodium* bind to the cell surface via HS chains (Rostand and Esko, 1997). A complex biosynthetic process is responsible for the large structural

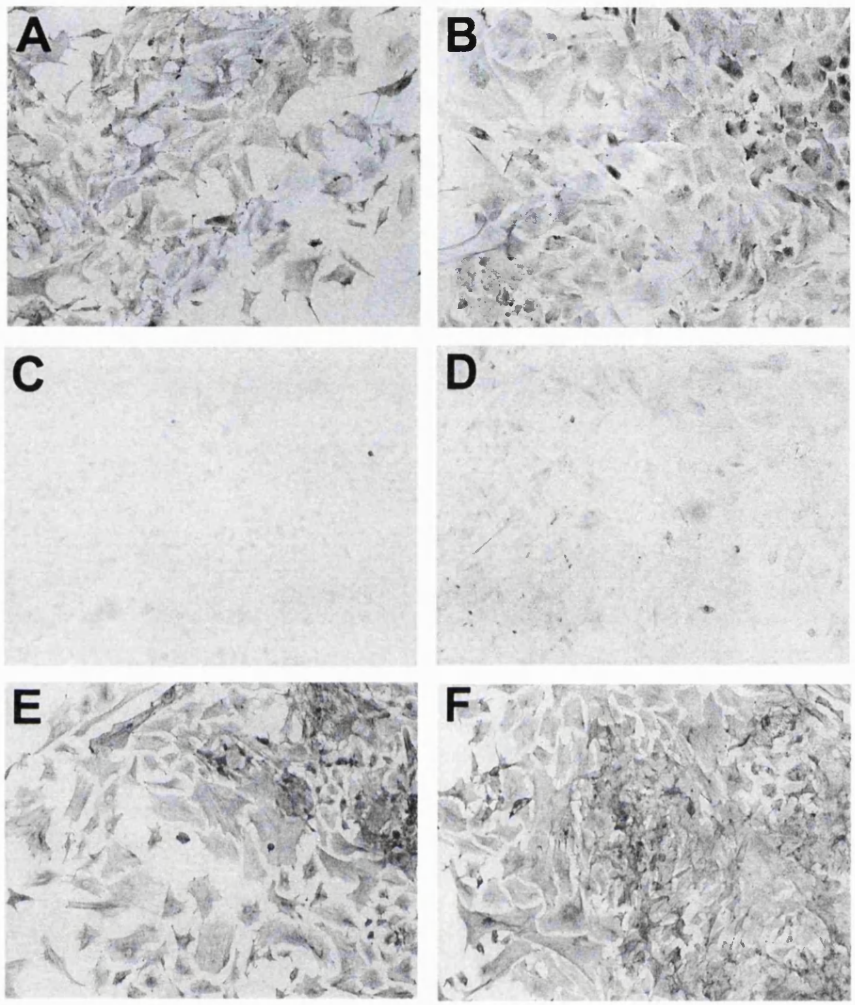

Figure 5.7. Retinal cells in culture express an HSPG ligand for CRYPα. CRYPα1-AP binds efficiently to primary retinal cell cultures in RAP *in situ* assays (A). Heparin addition (C) or heparinase III pre-treatment of the cultured cells (D) significantly reduce CRYPα binding. However, neither chondroitin sulphate addition (E) nor chondroitinase ABC pre-treatment of cells (F) can affect this interaction. Anti-GFAP antibody staining (B) shows that the cultures contain mainly Müller glia after three successive passages.

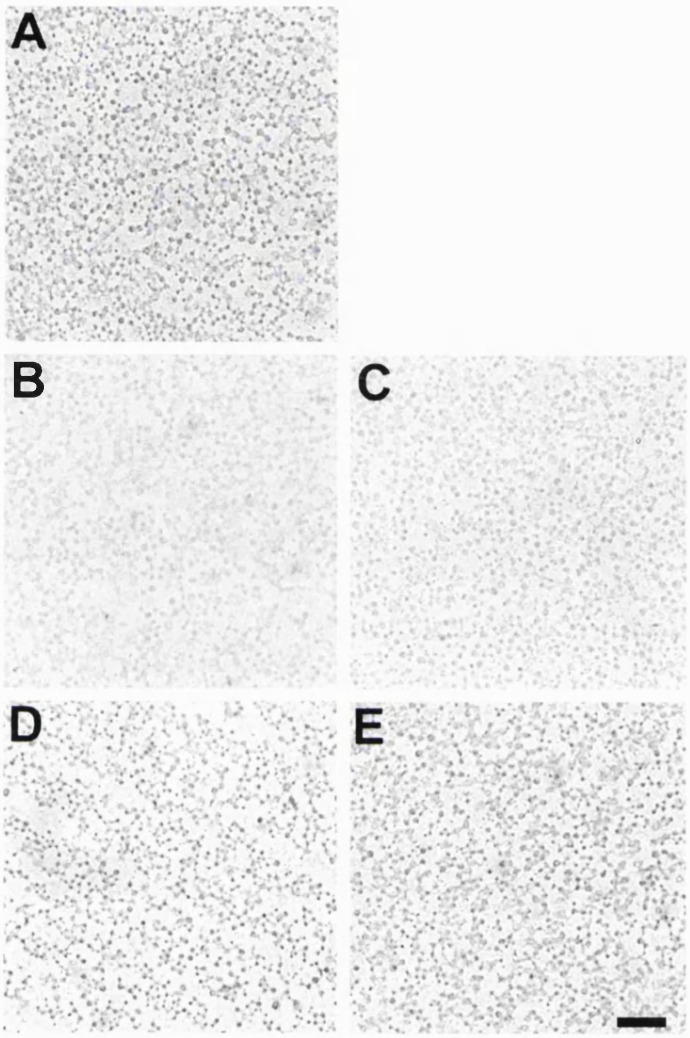

Figure 5.8. Müller glia endfeet appear to express two classes of CRYPα ligands. Retinal basal laminae with glial endfeet attached were flat-mounted on glass coverslips and probed by RAP *in situ* with conditioned medium containing CRYPα1-AP alone. Heparin addition (B) or heparinase III pre-treatment (C) reduce binding compared to the control experiment (A) but cannot abolish it completely. Chondroitin sulphate addition (D) or chondroitinase ABC pre-treatment (E) do not affect CRYPα binding. Scalebar, 10 μm.

diversity of HS polymers (reviewed in Turnbull *et al.*, 2001), which, in turn, accounts for their selectivity and specificity in protein binding. Results obtained using recent advances in complex polysaccharide sequencing methods (Venkataraman *et al.*, 1999; Keiser *et al.*, 2001) clearly support the hypothesis that the protein-glycosaminoglycan interactions involve sequence and structure specificity for both partners.

Putative, heterotypic, ligands for CRYPα have been previously described on retinal BL, RGC neurites and Müller glia endfeet (Haj *et al.*, 1999; Ledig *et al.*, 1999a). Experiments described in this chapter show that CRYPα can also bind Müller glia in culture. On the other hand, I demonstrated that HSPGs represent a major class of ligands both in the retinal BL and on retinal cell surfaces in culture (largely glia but small numbers of neurons were still present). Since both heparin competition and heparinase III treatment, but not chondroitin sulphate competition or chondroitinase ABC treatment, can abolish CRYPα-ligand binding, it results that the interaction observed in RAP *in situ* experiments is mediated by HS chains. Both agrin and collagen XVIII, the major retinal BL HSPGs, have the ability to bind CRYPα *in vitro* with high affinity via their HS chains. The neuronal and glial cell surface HSPG ligands have not been characterised yet but, most probably, they include members of either syndecan or glypican families. Agrin itself also represents a strong candidate for the CRYPα ligand (or maybe co-receptor?) present on the neuronal surface since two recent studies report the identification of a neuronal-specific isoform attached to the plasma membrane as a type II protein (Burgess *et al.*, 2000; Neumann *et al.*, 2001).

CRYPα binding to glial endfeet appears to be mediated by both HSPGs and an additional (class of) ligand(s). As discussed in chapter 4.4, the glial endfeet are structures differentiated as a consequence of the direct contact with the BL. It would be interesting to identify this elusive ligand, but technically challenging since the glial cells do not produce similar endfeet in culture. Growing glial cells in culture on basal lamina

substrates may allow endfeet differentiation and ultimately cloning (or purification) of the CRYPα endfeet-specific ligand.

CRYPα, like many other RPTPs, is referred to as an "orphan receptor", since no ligands have been described to date. In fact, the basal lamina HSPGs (agrin and collagen XVIII) are the first heterotypic binding partners described for a neural isoform of a type IIa RPTP. These interactions can bring further insight to understanding the molecular mechanisms behind currently known CRYPα functions, which include the neurite outgrowth modulatory ability and maintenance of growth cone cytoskeletal architecture, but also suggest new potential functions for CRYPα. Agrin, for example, is very abundant in axonal pathways of the chick central nervous system, such as the optic nerve and the tecto-bulbar pathway (Halfter *et al.*, 1997). The temporal coincidence of its expression with axonal outgrowth stages suggests a growth-promoting role for agrin, as it has been proposed for CRYPα too (Ledig *et al.*, 1999a). Surprisingly though, purified agrin displayed an inhibitory activity when used as a substrate for neurite outgrowth *in vitro* (Halfter *et al.*, 1997). At least two points can be raised regarding this experiment. Firstly, one can never find, *in vivo*, pure agrin as such. A large variety of molecules bind to agrin via its HS chains, protein core, or both, including laminin-1, thrombospondin, fibronectin, FGF2, merosin (laminin-2) and pleiotrophin. All these are potent substrates for neurite extension and their binding to HSPGs is important for modulating this activity. A functional interaction between agrin and CRYPα may be independent of such molecules or not. Secondly, as mentioned above, agrin is expressed in several isoforms. Alternative promoter and first (N-terminal) exon usage defines a long ("LN") and short ("SN") isoforms (Burgess *et al.*, 2000; Neuman *et al.*, 2001). The LN is the isoform secreted and incorporated into the BL, while SN remains attached on the neuronal surface. The antibody used by Halfter *et al.* (1997) cannot discriminate between the two isoforms although, on the other hand, the purified agrin used as a

substrate for axon growth experiments *in vitro* was the LN one. It is possible therefore that the agrin detected in axonal tracts and involved in neurite outgrowth modulation is of SN type. Both isoforms mentioned above can interact with CRYPα either as a ligand (LN agrin) or as a co-receptor on the neuronal surface (SN agrin). Which one of these interactions has functional consequences is still to be determined.

It is worth mentioning here that the best-characterised function for agrin relates to its ability to induce acetylcholine receptor clustering at the skeletal neuromuscular junctions. In addition, transgenic animals provided convincing evidence for the essential role of neural agrin in triggering synaptic differentiation (reviewed in Hagiwara and Fallon, 2001). Interestingly, Burgess *et al.* (2001) demonstrate that LN agrin is the functional isoform at the neuromuscular junction. The insertion of a gene trap construct in the mouse genome between the LN and SN exons, which abolishes expression of LN but has no effect on SN agrin, produces a neuromuscular phenotype similar to mice lacking all isoforms of agrin. CRYPα1 is expressed on motor neurons and can bind muscles in RAP *in situ* experiments (J. Chilton, F. Haj and A. Stoker, unpublished). Therefore, it would be worth testing whether CRYPα plays any role at the neuromuscular junctions.

In the avian retina, *agrin* mRNA was detected in the RGCs, being the only BL protein synthesised by the neural retina (Halfter *et al.*, 2000). Agrin is found mainly in the BL and retinal plexiform layers (from E8 onwards; Halfter, 1993; Kroger *et al.*, 1996), consistent with a possible involvement of an agrin isoform in interneuronal synapse formation (Kroger, 1997). The fact that CRYPα is present at high levels in the inner plexiform layer (Stoker *et al.*, 1995) and, as reported here, it binds to agrin, raises the interesting possibility that CRYPα might be involved in retinal synaptogenesis. There is evidence already that RPTPδ may be involved in modulating synaptic plasticity (Uetani *et al.*, 2000).

Despite the large amount of data supporting the role of agrin at neuromuscular junctions, little is known about its roles in the brain, where it represents a major HSPG. Recent reports (Cotman *et al.*, 2000; Donahue *et al.*, 1999), have revealed a very interesting role played by agrin in Alzheimer's disease (AD) brains. AD is a progressive neurodegenerative disorder characterised by pathological lesions which include senile plaques and neurofibrillary tangles (reviewed in Lee *et al.*, 2001). The β-amyloid peptide (Aβ), derived by proteolytic processing of the amyloid precursor protein (APP), accumulates as a multimeric aggregate with a fibrillar appearance in senile plaques and cerebrovascular deposits. Cotman *et al.* (2000) have found that Aβ binds to the HS chains of agrin *in vitro*, which leads to the acceleration of Aβ fibril formation. In addition, agrin is localised to Aβ deposits in Alzheimer's disease brains. Interestingly, senile plaques have the ability to promote neurite outgrowth and usually contain numerous dystrophic neurites. Previous studies suggest that FGF2, which can associate with agrin's HS chains as mentioned above, may attract neurites into plaques (Cummings *et al.*, 1992). It would be interesting to see whether RPTPσ plays any role in this process.

The other basal lamina ligand for CRYPα described here, collagen XVIII, has recently emerged as a molecule involved in modulating cell migration and axon guidance (Ackley *et al.*, 2001). As mentioned above, a mutation in the human *COL18A1* gene causes the Knobloch syndrome (Sertie *et al.*, 2000). A 38 kDa C-terminal fragment termed NC1, containing a trimerisation domain, a proteolytically sensitive hinge region and the endostatin domain, appears to be responsible for stimulating cell and axon migration (Ackley *et al.*, 2001). Although this fragment has heparin-binding ability, its neuronal receptor has not been identified yet. This fragment itself contains a putative O-glycosylation site although it is not clear yet whether it is glycosylated *in vivo*. As described in this chapter, I found that CRYPα binding to collagen XVIII is dependent

on the integrity of its HS chains, at least in blot-overlay assays. I cannot rule out the possibility that direct protein-protein interactions occur as well, and it is possible that such contacts can also take place if the HS chain is supplied by another HSPG on the cell surface. It is very tempting to speculate about the possibility of CRYPα/RPTPσ being a receptor for NC1/endostatin, considering its involvement in neurite growth and guidance. In addition, one cannot ignore the huge interest this molecule has attracted due to its anti-angiogenic properties and potential for being used in cancer therapy (O'Reilly *et al.*, 1997).

The functional relevance of the interactions between CRYPα and its HSPG ligands described here represents an important experimental target to be studied. On the other hand, identification of the specific HS sequence recognised by CRYPα would facilitate the design of small molecules able to modulate this interaction, which can be tested *in vivo* to gain further functional insights. Finally, once a CRYPα substrate will be identified, it will be possible to study the effect of HSPG binding on the phosphatase activity, which represents one of the major questions still to be answered. In the following chapter I will describe preliminary attempts to identify a substrate as well as other interactions partners for CRYPα.

Chapter 6. **Putative interaction partners for the intracellular region of CRYPα**

6.1. Introduction

Heparan sulphate proteoglycans, in particular agrin and collagen XVIII, are ligands for CRYPα *in vitro*, as shown in the previous chapters. The analysis of their developmentally regulated expression patterns, together with the functional data available so far, suggests that such interactions could also have functional significance *in vivo*. At molecular level, HSPGs could possibly modulate the enzymatic activity of CRYPα, extend its half-life on the neuronal surface, control its distribution in the membrane plane or facilitate its interaction with additional ligands, substrates and other interaction partners in a receptor complex. Each of these mechanisms would ultimately affect the signalling properties of CRYPα and can control the activation state of downstream signalling molecules. However, for many RPTPs, including CRYPα, the identity of such downstream molecules is not known yet. Therefore, identifying substrates or indeed other binding partners is essential for understanding the role played by these receptor enzymes.

Type IIa RPTPs display a common overall molecular architecture (Figure 1.1) but also a remarkable degree of conservation at their primary structure level. As seen in Figure 6.1, the three human representatives (hLAR, hRPTPσ and hRPTPδ) share about 70% overall amino acid identity and up to 90% identity in their intracellular regions. Most probably they are derivatives of a unique "DLAR-like" ancestor. CRYPα appears to be the chick orthologue of RPTPσ, while full-length avian orthologues of RPTPδ and LAR are still to be cloned. When the two phosphatase domains (D1 and D2) are individually aligned, it emerges that D1, usually considered to account for 99% of the

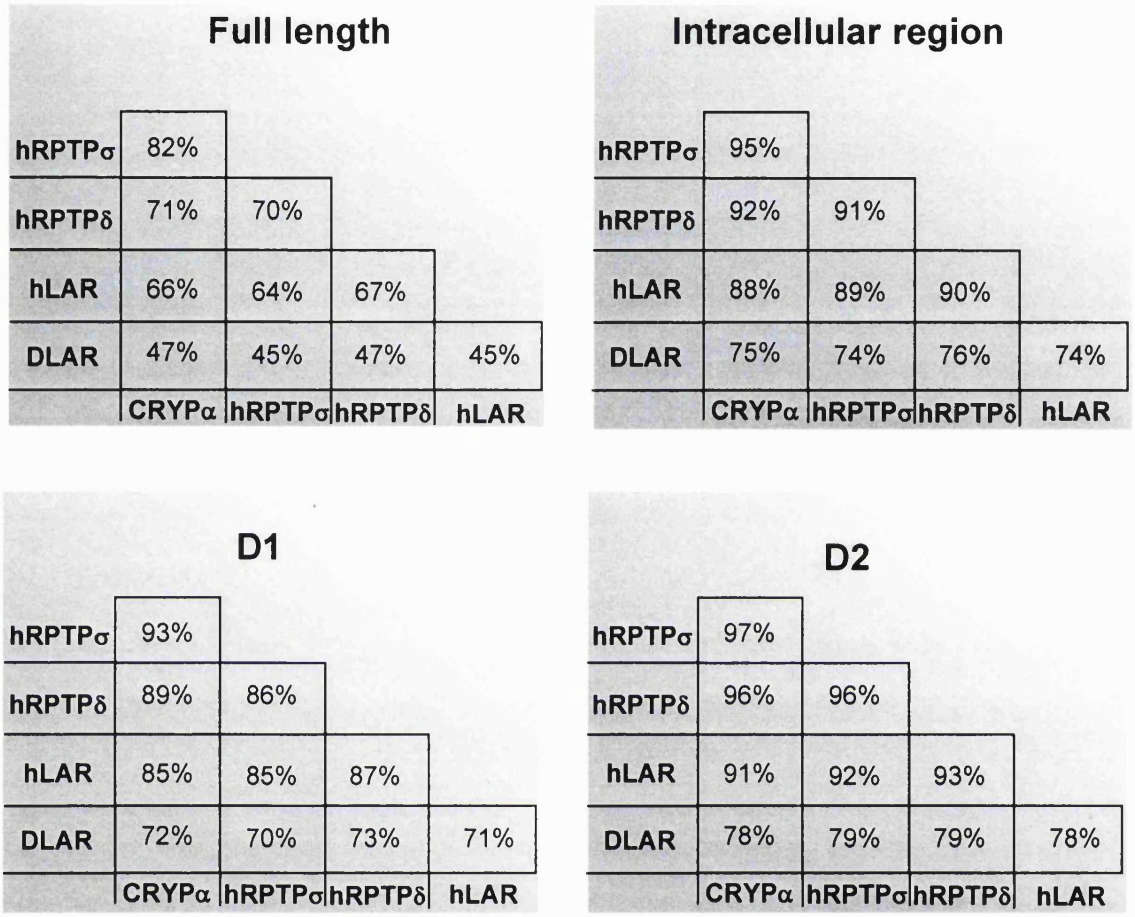

Figure 6.1. Sequence alignment results (percentage identity) for various regions of the typeII RPTP family members. All three human representatives (hRPTPσ, hRPTPδ and hLAR) seem to be derived from a common ancestor similar to the *Drosophila* DLAR. CRYPα is the chick orthologue of hRPTPσ. Interestingly, the intracellular regions appear to be better conserved than the extracellular ones, and the second (membrane distal) phosphatase domain better conserved than the first one.

enzyme activity (Streuli *et al.*, 1990), is slightly more divergent than D2. Nevertheless, an obvious question would be how one can achieve any specificity at these levels of conservation. Firstly, as mentioned in chapter 4.1 and also it results from Figure 6.1, the extracellular regions of type IIa RPTPs are more divergent. Therefore they may respond to distinct environmental cues. Secondly, they may not all be expressed simultaneously in the same cell at the same moment. Indeed, a detailed analysis of their expression patterns in mouse embryos (Schaapveld *et al.*, 1998) shows largely overlapping patterns for RPTPσ and RPTPδ while for LAR it appears to be more divergent. Similarly, within the developing *Xenopus* retina, overlapping but distinct expression patterns have been described (Johnson and Holt, 2000). For instance, all three type IIa RPTPs are expressed in the retinal ganglion cells while in other layers there are significant differences at various developmental stages.

The high degree of conservation in the intracellular region suggests, nevertheless, that they can share common substrates and may interact with the same (or similar) adapter or regulatory proteins. Indeed, this seems to be the case for α-liprins, a subfamily of coiled coil proteins shown to interact with LAR at focal adhesion sites (Serra-Pages *et al.*, 1995). Interaction trap assays demonstrate that α-liprins bind to the D2 domains of LAR, RPTPδ and RPTPσ but not RPTPμ or CD45 (Serra-Pages *et al.*, 1998). The multi-domain protein Trio, an important cytoskeletal regulator (Dickson, 2001), which contains (among others) Rac1 and RhoA guanine nucleotide exchange factor (GEF) domains and a protein serine/threonine kinase (PSK) domain, can interact with the D2 phosphatase domain of LAR (Debant *et al.*, 1996). It is not known yet whether the other type IIa RPTPs can bind Trio but if this is the case it may have functional significance considering the proposed role played by RPTPs in modulating the actin cytoskeleton. Neither liprins nor Trio are tyrosine phosphorylated, therefore they cannot represent substrates for RPTPs. In PC12 cells, however, type IIa RPTPs (at

least LAR and RPTPδ) associate with the cadherin-catenin complex via β-catenin and appear to modulate its tyrosine phosphorylation state, thereby possibly controlling the cadherins' adhesive function during processes such as neurite outgrowth (Kypta *et al.*, 1996).

A particularly interesting feature of RPTPs, not fully understood yet in functional terms, is their ability to associate both homotypically and heterotypically via their extra- and/or intracellular regions. As discussed in chapter 1.2.3, several PTP domain crystals obtained to date reveal protein dimers. The D1 catalytic domain of RPTPα forms a symmetrical, inhibited, dimer in which a helix-turn-helix wedge element from one monomer is inserted into the catalytic site of the other monomer (Bilwes *et al.*, 1996). If such a dimerisation can indeed happen *in vivo*, as a consequence of ligand binding for example, it would cause inhibition of the phosphatase activity. Elegant experiments *in vivo* support this model. RPTPα dimerisation, induced by Cys substitution of residues at certain positions in the ectodomain juxtamembrane region, inhibited its phosphatase activity in a wedge-dependent manner (Jiang *et al.*, 1999). Similarly, when the CD45 ectodomain was substituted with the EGF receptor extracellular region, its PTP activity was inhibited by EGF-induced dimerization (Desai *et al.*, 1993), in a wedge-dependent manner (Majeti *et al.*, 1998). Furthermore, a single point mutation that disrupts the inhibitory wedge of CD45 in transgenic mice causes polyclonal lymphocyte activation leading to lymphoproliferation and severe autoimmunity, which demonstrates the importance *in vivo* of negative CD45 regulation by dimerization (Majeti *et al.*, 2000). On the other hand, the crystal structures of RPTPμ-D1 (Hoffman *et al.*, 1997), LAR-D1D2 (Nam *et al.*, 1999) and PTP-SL/BR7 phosphatase domains (Szedlacsek *et al.*, 2001), all containing the equivalent wedge structure, reveal monomeric proteins and unhindered catalytic sites (the RPTPμ-D1

dimer in the crystal appears to be artefactual). This triggers caution in extrapolating the RPTPα and CD45 results as a general RPTP regulatory mechanism.

Wallace *et al.* (1998) suggested that heterodimerisation can also be a significant RPTP regulatory mechanism since the D2 domain of RPTPδ can bind to and inhibit the PTP activity of the D1 domain of RPTPσ. This interaction is specific, since the RPTPσ D2 cannot bind RPTPδ D1. Moreover, the intracellular region of RPTPα was found to bind with different affinities, via its D1 wedge, to a variety of PTP domains such as RPTPσ-D2, RPTPα-D2, LAR-D2, RPTPδ-D2 and RPTPμ-D2. These interactions were confirmed in multiple assay systems such as yeast two-hybrid, glutathione-S-transferase pull-down and co-immunoprecipitation (Blanchetot and den Hertog, 2000). This observation was recently expanded for type I, II and IV RPTPs, resulting in a complex matrix of interactions between RPTPs and various D2 domains (C. Blanchetot, personal communication). In particular, RPTPσ D2 was able to bind the D1 domains of all RPTPs tested, namely CD45, RPTPσ, RPTPδ, LAR, RPTPμ, RPTPα and RPTPε.

Several substrates for type II RPTPs have been identified to date. These include Abl and Ena (for DLAR, see chapter 1.3.2), the focal adhesion adapter protein p130^{cas} (for LAR; Weng *et al.*, 1999) and the insulin receptor substrates 1 and 2 (for LAR; Zhang *et al.*, 1996; Li *et al.*, 1996). CRYPα may be able to dephosphorylate these proteins, however, most probably, novel and specific substrates exist as well. A technique commonly used for identification of RPTP substrates is based on the construction of "substrate trapping" mutants (Flint *et al.*, 1997). Enzyme kinetics studies, together with the significant number of phosphatase domains analysed by X-ray crystallography, have allowed a very good understanding of the PTP catalytic mechanism and the identification of key residues involved in catalysis (see chapter 1.2.1). Therefore, mutant constructs still having the ability to bind substrates efficiently but not to hydrolyse phosphotyrosine can be easily designed and have been successfully

used for both receptor (Buist *et al.*, 2000; Kawachi *et al.*, 2001) and intracellular RPTPs (Flint *et al.*, 1997; Tiganis *et al.*, 1998; Zhang *et al.* 1999; Tiganis *et al.*, 1999).

In this chapter I describe the construction of a CRYPα "substrate trapping" mutant and the identification of a 75 kDa putative substrate. Preliminary data indicating that CRYPα may interact with the multidomain Trio protein are also presented. Ideally, the significance of any interaction between CRYPα and its substrates or binding partners should ultimately be tested *in vivo*, in the native tissues where this RPTP is expressed and at the appropriate developmental stage. In principle, various CRYPα constructs can be introduced into retinal ganglion cells by *in ovo* electroporation and their effects on axon growth and guidance may then be monitored *in vitro* and *in vivo*. Preliminary experiments aimed at optimising this technique will also be described.

6.2. Experimental procedures

Expression constructs and fusion protein production. The pCS3N expression vector was created using the pCMV-Script (Stratagene) plasmid backbone and substituting its multiple cloning site with a DNA fragment containing the following restriction sites: *Sac*I-*Not*I-*Sma*I-*Pst*I-*Eco*RI-*Eco*RV-*Hin*dIII-*Cla*I-*Xba*I-*Acl*I-*Bst*XI-*Not*I-*Xho*I-*Kpn*I. A *Hin*dIII fragment encoding the CRYPα extracellular region (amino acids 1-721) was subcloned from the pBG-CRYPα1-AP vector (described in chapter 3.2) into pCS3N resulting the pCS3Nα1 plasmid. This vector contains two *Xba*I sites; the one located just before the CRYPα1 start codon was destroyed by restriction, blunting with Klenow DNA polymerase and self-ligation and the resulting construct was named pCS3Nα1dX.

A *Bam*HI-*Xba*I fragment containing the CRYPα secretion signal (amino acids 1-33) followed by the Myc tag, the transmembrane and the intracellular regions (amino acids 835-1499 according to CRYPα1 isoform numbering; Stoker, 1995) was isolated

from the RCAS-D1 vector (D. Breikreutz and A. Stoker, unpublished) and subcloned into the pUCα19 plasmid (Gibco BRL). The resulting construct, termed α19-ICC/BX was partially digested with *Nco*I and the synthetic linker CATGTATACAGACATAGAGATGAACCGACTTGGAAAGCTC was inserted upstream of the Myc tag. This linker encodes for the VSV glycoprotein tag (YTDIEMNRLGKL). The new construct obtained, called α19-VSV-ICC/BX, was cut with *Bam*HI and *Xba*I and the fragment encoding for the VSV-tagged CRYPα transmembrane-intracellular regions was then subcloned into the *Bam*HI-*Xba*I cut pCS3Nα1dX vector described above. This led to the replacement of the CRYPα1 ectodomain in pCS3Nα1dX with the VSV-tagged intracellular region and it re-created the functional N-terminus CRYPα secretion signal upstream of the VSV tag. This vector, termed pCS3N-VSVICC, allows the expression of a membrane-anchored CRYPα intracellular region construct exposing its VSV tag on the cell surface.

Two rounds of site-directed mutagenesis were performed on pCS3N-VSVICC, as described in chapter 2.1.14, in order to correct an unwanted 1bp deletion in the VSV tag and to replace an *Acl*I restriction site in the first phosphatase domain with *Bgl*II, without affecting the amino acid sequence. This mutated construct, termed pCS3N-VSVICCM3_A→B, encodes the CRYPα construct schematically represented in Figure 6.2 and labelled "wt". One additional round of site-directed mutagenesis was used to replace an aspartate residue (1109 according to CRYPα1 isoform numbering), resulting the plasmid pCS3N-VSVICCM3_A→B_TrapD→A which encodes the construct labelled "trap" in figure 6.2. All clones resulted from the mutagenesis experiments were sequenced (by C. Paternotte) to confirm the absence of unwanted mutations. The "wt" and "trap" constructs were also subcloned via *Not*I digestion into the pCAβ vector (a gift from J. Gilthorpe, King's College, London) for expression under the strong chicken β-actin promoter.

All the mammalian expression vectors mentioned above were transiently transfected into the 293T cell line, as described in chapter 2.4.5, and 24-48 hours later analysed by western blotting.

Immunoprecipitation and immunoblotting. Immunoprecipitation reactions were performed as described in chapter 2.3.8, except that the cells were lysed on ice in the following buffer: 50mM HEPES, pH 7.4, 150 mM NaCl, 1 mM $MgCl_2$, 10% glycerol, 1% Triton X-100, 5mM iodoacetic acid, supplemented with a protease inhibitor cocktail (Sigma) containing 4-(2-aminoethyl)benzenesulfonyl fluoride (AEBSF), pepstatin A, trans-epoxysuccinyl-L-leucylamido(4-guanidino)butane (E-64), bestatin, leupeptin, and aprotinin. After the addition of 10 mM dithiothreitol to inactivate unreacted iodoacetic acid, the lysates were pre-cleared with rabbit anti-mouse antibodies covalently bound to agarose beads (Sigma) and then an anti-VSV monoclonal antibody (clone P5D4, Sigma) was added (6 μg/ml lysate). After incubating 1 hour at 4°C, the immune complexes were precipitated using agarose beads coated with rabbit anti-mouse antibodies, washed 3x 20 min with lysis buffer without iodoacetic acid, mixed with an equal volume of 2x SDS-PAGE loading buffer and separated in 8% and 10% polyacrilamide gels. The proteins were transferred on PVDF membranes and further processed as described in chapter 2.3.6. The anti-VSV monoclonal antibody (P5D4, diluted at 1:3000) and peroxidase-labelled anti-phosphotyrosine monoclonal antibody (4G10, Upstate Biotech, diluted at 1:1000) were used as primary antibodies. Bound anti-VSV antibodies were detected using a peroxidase-labelled rabbit anti-mouse secondary antibody (Dako, diluted at 1:2000). Chemiluminescent detection was performed using the ECL Plus Western blotting kit (Amersham Pharmacia Biotech). Coomassie staining was performed as described in chapter 2.3.4.

Phosphatase activity assays. The phosphatase activity of the CRYPα intracellular constructs was assayed by monitoring the p-nitrophenolate absorbance at 410 nm using a Dynex MRXII microplate reader. Assays were performed in duplicate at 37°C in a 200µl reaction mixture containing 30mM acetate buffer, pH 5.4, 2 mM DTT, 5 mM EDTA and 10 mM p-nitrophenyl phosphate (pNPP). Reactions were started by the addition of 20µl agarose beads coated with CRYPα constructs immunoprecipitated from 0.5 ml cell lysates as described above. A correction was made for the non-enzymatic hydrolysis of the substrate.

Yeast two-hybrid assays. CRYPα fragments were amplified by PCR and cloned between the *Bam*HI and *Xho*I sites of the pEG202 plasmid (gift from A. Debant, CNRS Montpellier; Gyuris *et al.*, 1993) in frame with the LexA peptide (amino acids 1-202) as follows: D1 contains the first phosphatase domain, amino acids 877-1234; D2 contains the second phosphatase domain, amino acids 1228-1499; D1D2 contains both phosphatase domains, amino acids 877-1499, ΔD1D2 contains both phosphatase domains as above except the last 46 residues at the C-terminal end.

The yeast two-hybrid assays were carried out by S. Schmidt (CNRS Montpellier) using the CRYPα baits described above and a Trio interactor (Cl.1G0, Trio amino acids 2450-2861) containing the Ig-like and the protein serine/threonine kinase domains cloned into the pJG4-5 plasmid, as described in Debant *et al.* (1996) and Gyuris *et al.* (1993).

***In ovo* electroporation.** This technique was performed following the protocol described in chapter 2.6.1. The DNA constructs tested were pCAβ-EGFPm5 (gift from J. Gilthorpe, King's College, London), encoding a modified green fluorescent protein

construct under the strong chick β-actin promoter, and AP-70 plasmid, constructed by subcloning the *Cla*I insert from the RCAS-AP vector (Chen *et al.*, 1999) into the pCS3N vector described above and thus encoding a GPI-anchored form of the heat-stable human placental alkaline phosphatase expressed under the CMV promoter. Twenty-four and 48 hours later the embryos were dissected and either analysed directly using an Axiophot fluorescence microscope (for EGFP expression) or fixed 30 min at room temperature in 4% paraformaldehyde, washed 3x 20 min in PBS containing 0.1% Triton X-100, incubated 3 hours at 65°C to inactivate the background alkaline phosphatase activity and stained with NBT/BCIP as described in chapter 2.5.3.

6.3. Results

6.3.1. Efficient expression of CRYPα intracellular region constructs in 293T cells.

Flint *et al.* (1997) have found that a single amino acid substitution (D181A) in the phosphatase domain of PTP1B renders an enzyme whose catalytic activity is drastically reduced (10^5-fold) but still able to bind substrates as efficiently as the wild type form. Such a mutant construct, termed "substrate trapping", forms enzyme-substrate complexes stable enough to withstand isolation. Therefore, in order to identify putative CRYPα substrates, I generated an equivalent CRYPα construct by mutating the corresponding Asp residue to Ala (D1109A). This construct (termed "trap") as well as its wild-type ("wt") equivalent contains the entire intracellular region of CRYPα but also its secretion signal and transmembrane region, in order to achieve a correct subcellular localisation. Both constructs are N-terminal tagged with the VSV-G peptide (Figure 6.2 A).

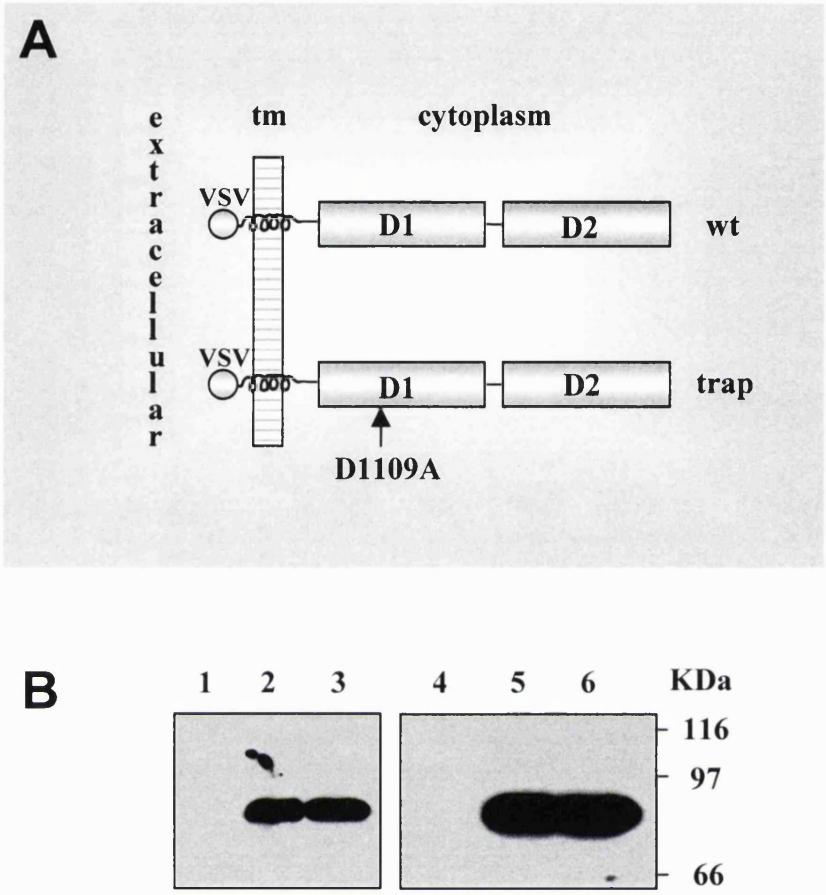

Figure 6.2. Expression of recombinant CRYPα intracellular region constructs. (A) Schematic representation of the CRYPα constructs, containing the VSV peptide tag at the N-terminus, followed by the transmembrane region and the two phosphatase domains. The "trap" construct contains a point mutation in the catalytic site of the first phosphatase domain where the general acid Asp residue was replaced with Ala. (B) Efficient expression of both "wt" (lanes 2, 5) and "trap" (lanes 3, 6) constructs in 293T cells was driven by either the CMV promoter (lanes 2, 3) or the chick β-actin promoter (lanes 5, 6). The CRYPα constructs were transiently transfected in 293T cells and lysates were separated by SDS-PAGE, transferred onto a PVDF membrane and probed with an anti-VSV antibody. Lysates from mock transfections were run on lanes 1 and 4.

Western blot assays demonstrate that both "wt" and "trap" CRYPα constructs can be efficiently expressed, in equal amounts, in 293T cells by transient transfection (Figure 6.2. B). The expression driven by the chick β-actin promoter allows production of significantly higher levels of fusion proteins, therefore this system was used for subsequent experiments.

The tyrosine phosphatase activity of the two CRYPα constructs, immunoprecipitated from 293T cell lysates, was determined using the artificial substrate p-nitrophenyl phosphate (Figure 6.3). Since the measurements were made using proteins attached to agarose beads coated with primary and secondary antibodies, an accurate quantification of CRYPα constructs' kinetic parameters was not performed. Nevertheless, figure 6.3 demonstrates that the "wt" construct is catalytically active while the activity of the "trap" mutant is almost completely abolished.

6.3.2. CRYPα can be tyrosine phosphorylated *in vivo*

Both the "wt" and "trap" CRYPα constructs immunoprecipitated from untreated 293T cells display low levels of tyrosine phosphorylation, as detected by western blotting (Figure 6.4). This appears to be independent of the intrinsic PTPase activity of CRYPα since the "wt" construct appears unable to autodephosphorylate at this (these) particular site(s). Alternatively, this may simply represent an artefactual signal due to the relatively high amounts of protein loaded in the gel (see the Coomassie staining panels, Figure 6.4).

On the other hand, stimulation of the 293T cells with 6mM H_2O_2 leads to a significant increase in the overall phosphotyrosine levels (data not shown), most probably due to the inactivation of cellular PTPases (Denu and Tanner, 1998). As a consequence, high levels of phosphotyrosine can be detected on the immunoprecipitated

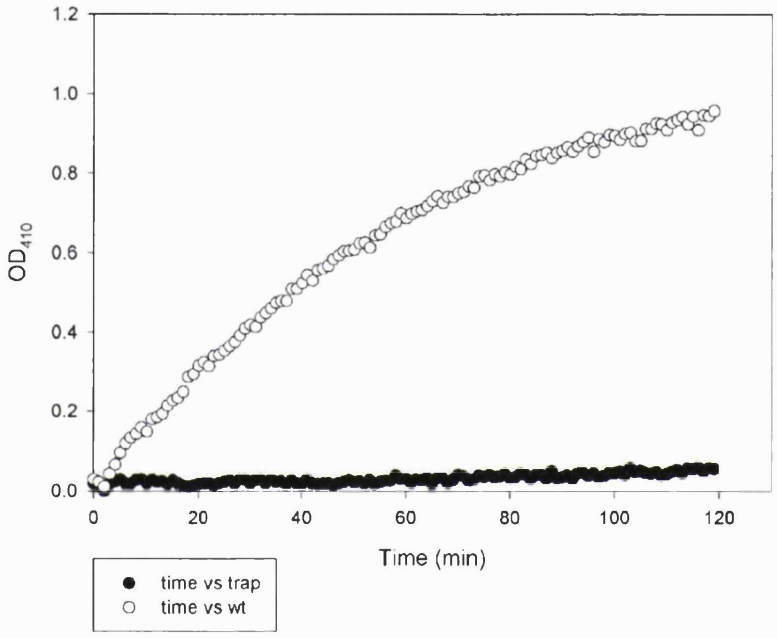

Figure 6.3. Kinetic assay of the CRYPα intracellular constructs. Both "wt" and "trap" constructs were transiently expressed in 293T cells, immunoprecipitated from 293T cell lysates using an anti-VSV monoclonal antibody and bound on agarose beads. Progress curves of the pNPP dephosphorylation were recorded and plotted after subtraction of the non-enzymatic substrate hydrolysis. Equal amounts of enzyme were used in each reaction, as judged from western blotting assays.

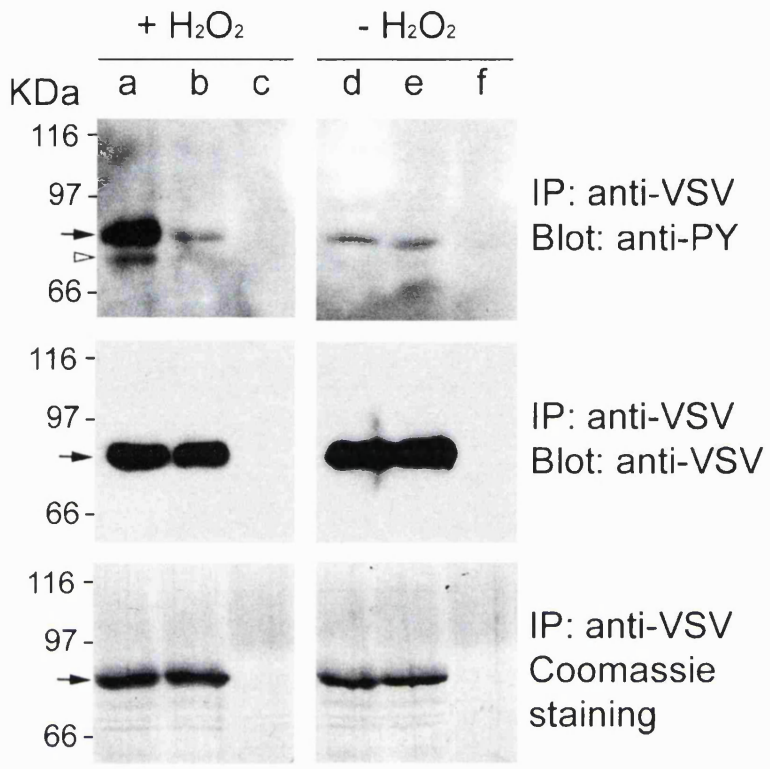

Figure 6.4. CRYPα is tyrosine phosphorylated *in vivo* and it dephosphorylates a putative 75 kDa substrate. 293T cells were transiently transfected with either the "trap" construct (lanes a and d), the "wt" construct (lanes b and e) or mock transfected (lanes c and f). Relatively equal amounts of recombinant proteins were immunoprecipitated with an anti-VSV antibody, as revealed by Coomassie staining and anti-VSV western blotting, irrespective of the hydrogen peroxide treatment. A low-level tyrosine phosphorylation can be detected on the CRYPα constructs from the untreated cultures (lanes d and e). Incubation with 6mM H_2O_2 for 15 minutes, just before cell lysis, strongly increases the tyrosine phosphorylation level of the "trap" construct (lane a) but it does not affect the "wt" construct (lane b). In addition, the "trap" construct co-precipitates with a 75 kDa putative substrate (lane a, white arrowhead). Black arrows indicate the CRYPα constructs.

CRYPα "trap" construct (Figure 6.4, lane a, black arrow). Interestingly though, no significant increase in tyrosine phosphorylation could be detected on the "wt" construct (Figure 6.4, compare lanes b and e), suggesting that this construct has the ability to autodephosphorylate very efficiently. Since the thiolate group of the catalytic Cys residue of "wt" itself is expected to be rapidly (but reversibly) oxidised by the hydrogen peroxide to the sulfenic acid of cysteine, it results that, most probably, the autodephosphorylation reaction occurs during the long immunoprecipitation procedure in the presence of dithiothreitol. It is important to underline that cysteine oxidation prevents its alkylation by iodoacetic acid (Lee *et al.*, 1998), thereby allowing enzyme reactivation by dithiothreitol.

Altogether, these results suggest that CRYPα can be tyrosine phosphorylated *in vivo* and that it also has the ability to autodephosphorylate via an intra- or intermolecular mechanism.

6.3.3. A putative substrate for CRYPα

As mentioned above, one can construct mutant PTP domains inactive catalytically but still able to bind tyrosine-phosphorylated substrates with high affinity. The most commonly used mutagenesis targets are either the nucleophilic Cys residue from the phosphatase catalytic site or the general acid Asp residue from the so-called "WPD" loop. The "trap" construct described above, a "WPD" loop mutant, could not co-precipitate detectable levels of any putative substrate when overexpressed in untreated 293T cells (Figure 6.4, lane d). Hydrogen peroxide treatment of the 293T cells promotes both a significant increase in the overall cellular phosphotyrosine levels and the reversible oxidation of the strong nucleophilic thiolate group from cysteine residues to sulfenic acid. Under these conditions, the "trap" construct specifically co-precipitates with an ~75 kDa phosphoprotein (Figure 6.4, lane a, open arrowhead). This protein

therefore represents a putative CRYPα substrate. This experiment gave reproducible results but it needs to be further scaled-up in order to obtain sufficient amounts of protein required for mass spectrometry/protein sequencing analysis, since an equivalent band could not be detected on the Coomassie stained blot (Figure 6.4, lane 1). On the other hand, various competitors still need to be tested in order to confirm that the "trap" construct interacts via its catalytic site with the 75 kDa phosphoprotein.

6.3.4. CRYPα interacts with the multifunctional protein Trio in yeast two-hybrid assays

Recent studies have established Trio as a key regulator of the small GTPases of the Rho family (Rac, Cdc42 and Rho) and modulator of the growth cone morphology and guidance (reviewed in Dickson, 2001). The RPTP LAR appears to be (one of) the receptor(s) acting upstream of Trio, as suggested by biochemical and genetic experiments (Debant *et al.*, 1996; Bateman *et al.*, 2000). Considering the high identity between the LAR and CRYPα intracellular regions (88%, figure 6.1) and the fact that CRYPα regulates the growth cone's morphology (Ledig *et al.*, 1999a) we sought to analyse whether Trio can also interact with the intracellular region of CRYPα and thereby mediate its signalling function.

Various CRYPα constructs (Figure 6.5 A) were cloned as baits and tested for interaction with Trio in yeast two-hybrid assays. The Trio interactor used has been previously shown to bind the second phosphatase domain (D2) of LAR (Debant *et al.*, 1996). As shown in figure 6.5 B, our experiments confirm that the full-length CRYPα intracellular region (D1D2) can interact with Trio. Unlike LAR, however, the D1 domain of CRYPα can bind the Trio fragment as well. Interestingly, sequence

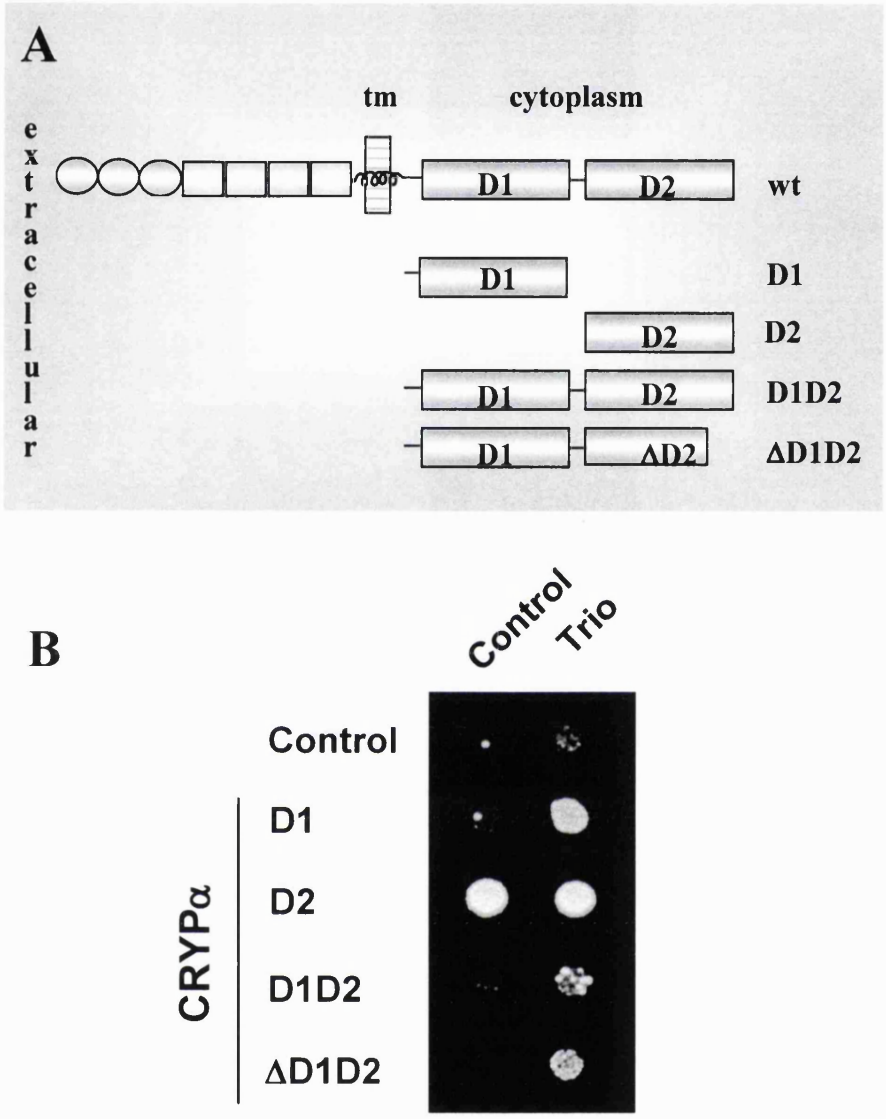

Figure 6.5. CRYPα can interact with the multidomain protein Trio in yeast two-hybrid assays. The CRYPα constructs tested in this assay are schematically represented in (A). Interactions between D1, D1D2, ΔD1D2 and Trio can be detected (B), which suggests that the D1 domain is sufficient for Trio binding. The interaction between D2 and Trio appears to be artefactual, due to a high non-specific binding with the activation domain encoded by the control plasmid.

alignments reveal a higher identity between the D1 domain of CRYPα and LAR D2 (48%) compared to the identity between the LAR D1 and D2 (45%). Since the exact Trio binding site in LAR D2 is not known yet, it may be interesting to test whether amino acids conserved in LAR D2 and CRYPα D1 but absent in LAR D1 are involved in this interaction.

Unfortunately we could not confirm whether CRYPα D1 contains or not the unique Trio interaction site since D2 alone gave a strong non-specific interaction with the transcription activation domain encoded by the empty (control) vector. This is probably caused by an artificial binding site created at the LexA-D2 junction, or exposed on D2 after D1 removal, since the other CRYPα constructs containing D2 usually exhibit a weaker interaction with Trio (Figure 6.5 B). In addition, deletion of the C-terminal 46 amino acids of D2 (ΔD1D2 construct), which form the final two α-helices and a short β-strand involved in interdomain hydrogen bonding with D1, does not appear to disrupt the interaction with Trio.

It is difficult to draw a definitive conclusion from this experiment, considering the non-specific interaction of the LexA-D2 construct. At the most one can say that CRYPα intracellular region can bind Trio and the D2 domain does not appear to be required for this interaction, at least in the yeast two-hybrid assays.

6.4. Technical appendix: Efficient gene transfer in the developing chick retina by *in ovo* electroporation

As discussed in chapter 1.4, there is increasing experimental evidence supporting the involvement of CRYPα in modulating retinal axon growth *in vitro* (Ledig *et al.*, 1999a; Johnson *et al.*, 2001). In particular, these results suggest an important role for CRYPα at the intra-retinal axon growth stage. Targeted expression of various CRYPα constructs described in this thesis, containing the secreted or

membrane-bound ectodomain as well as the "wild-type" and "substrate trapping" intracellular region, into the developing retinal ganglion cells can contribute to a better understanding of the role played by this RPTP *in vivo*.

Chick embryos represent an excellent model for developmental biology studies due to their accessibility, ease of tissue manipulation and *in ovo* culture. However, in the absence of established methods for genetic manipulations (such as transgenic analysis), ectopic gene expression relies primarily on transfer systems using retroviral vectors. Although useful, such systems have several disadvantages such as the strict DNA size constraints (2 kb), delayed expression of the transgene (approx. 18 hours) and time-consuming procedures for high titer retrovirus production. Therefore, the recent development of the *in ovo* electroporation technique represents a long-awaited step forward (reviewed in Itasaki *et al.*, 1999; Momose *et al.*, 1999; Nakamura *et al.*, 2001). This simple and effective method requires cloning of the DNA of interest into an appropriate plasmid, injection of this plasmid in the target tissue of the chick embryo and application of several short electric pulses in order to introduce the negatively charged DNA in the recipient cells. By this method, translation products of the inserted genes can be detected as early as 2 hours after electroporation and the DNA size limitations have been removed. Nevertheless, difficulties still remain in controlling the precision and efficiency of DNA insertion into the target tissue.

Therefore I set out to identify the optimum conditions required for targeted expression of a gene of interest into the developing retina, using two reporter gene constructs: the heat-stable human placental alkaline phosphatase and a modified green fluorescent protein. The basic method used (described in chapter 2.6.1) was derived from the one described by Momose *et al.* (1999). The DNA constructs were injected into Hamburger-Hamilton stage 10 chick embryos (~33 hours) in the prosencephalon (Figure 6.6 A) and the electrodes placed as shown in Figure 6.6 B. A technical detail

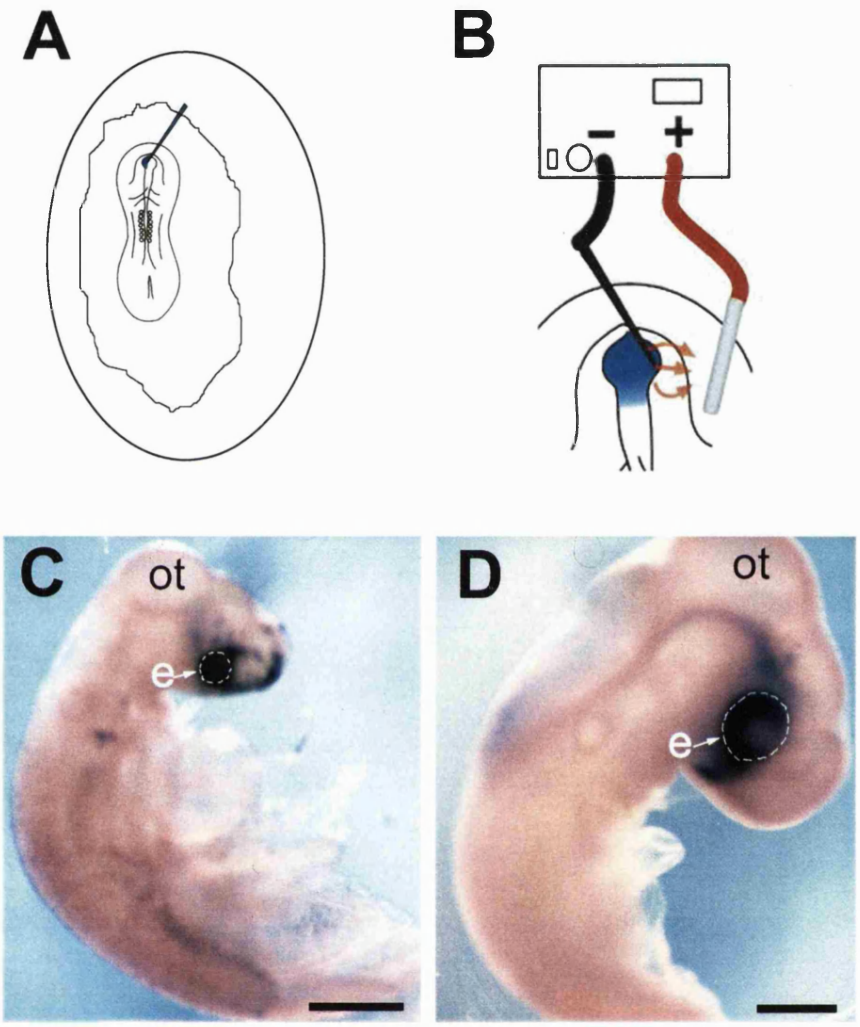

Figure 6.6. *In ovo* electroporation of stage 10 chick embryos optic primordium and reporter gene expression analysis. The DNA of interest is microinjected with a fine glass capillary into the target tissue, in this case the prosencephalon (A). A sharp tungsten needle, connected to the cathode, is then inserted into the prosencephalon and a thicker gold electrode, connected to the anode, is placed outside the embryo (B). The DNA is inserted into the target cells by application of several electric pulses. The time-course of a heat-stable human placental alkaline phosphatase reporter construct expression in the electroporated embryos was then analysed. At E2.5 (C) and E3.5 (D) the reporter gene is mainly expressed into the eye. e = eye; ot = optic tectum. Scalebars, 1mm.

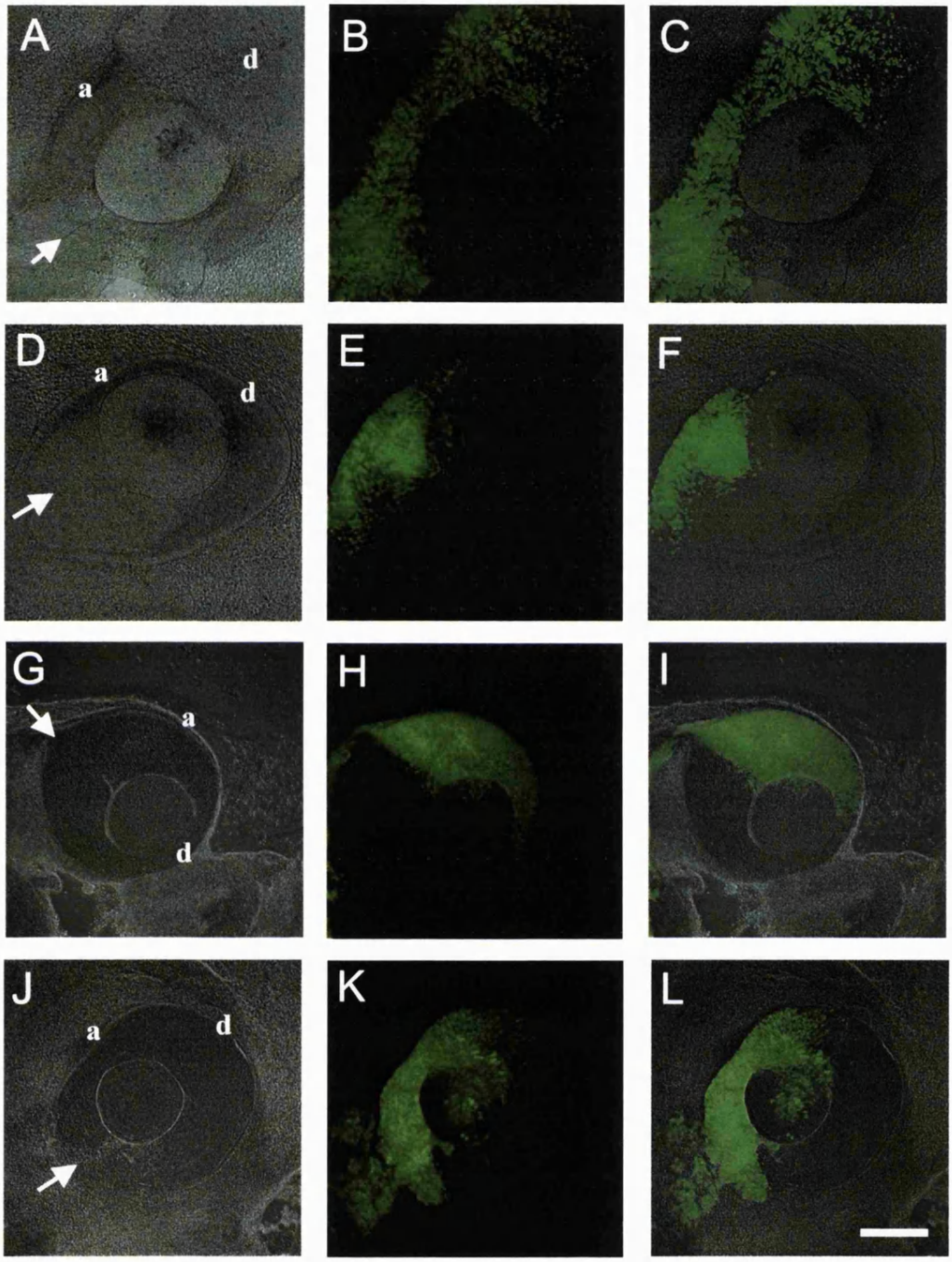

Figure 6.7. Enhanced green fluorescent protein (EGFP) expression into E4.5 chick embryo eyes. The embryos were electroporated at stage 10 with an EGFP expression vector, left to develop *in ovo* up to this stage and then photographed using a fluorescence microscope. A,D,G,J: bright field images; B,E,H,K: fluorescence images; C,F,I,L: overlapped images. In this experiment, a typical example, 24 embryos were electroporated, out of which 5 were analysed at E4.5. One of these did not express the EGFP and the remaining 4 cases are shown in this figure. White arrows indicate the closing ventral choroid fissure. a = anterior; d = dorsal. Scalebar: 1mm.

greatly influencing the electroporation efficiency, embryo viability and absence of head malformations was the use of a particular type of cathode, an electrolytically-sharpened tungsten needle (prepared by G. Sajnani-Perez, Institute of Child Health, London). This was inserted into the prosencephalon, ideally via the neuropore, in close proximity with the lateral wall of an optic vesicle. Alternative orientations and electrode shapes were tested, with limited success. In addition, other parameters were optimised including the number of pulses, pulse length, voltage and DNA solubilisation buffer.

Another critical parameter to be considered is the time window in which the target tissue is easily accessible and "permissive" but also appropriate for the developmental events under study. The optimum time window for efficient retinal expression of foreign genes was found to be stage 10-11 (~33-36 hours). Repeated attempts to electroporate the optic cup or, later on, the neural retina have failed since the embryos, although viable, did not express the transgene (G. Sajnani-Perez, personal communication). The particular process I was interested in, the intra-retinal axon growth stage, takes place between E3 and E7 in chick (Halfter and von Boxberg, 1992). Therefore, I have analysed the expression of reporter genes at various time points during this interval. Very efficient expression of the alkaline phosphatase reporter can be detected in the developing eye at E2.5 (stage 16, Figure 6.6 C) and E3.5 (stage 21, Figure 6.6 D) but also up to E5 (not shown). The EGFP reporter can also be detected in the developing eye up to E4.5 (Figure 6.7). I was unable to detect efficient expression of reporter genes at later stages, although sporadically labelled neurons could be observed up to E7, the stage we normally use for retinal ganglion cell cultures. Therefore, data involving the various CRYPα constructs cannot be presented at this moment since further optimisation of the technique is required.

Nevertheless, very recent results obtained in our laboratory demonstrate that efficient gene expression can be achieved in E7 retinal ganglion cells (G. Sajnani-Perez,

personal communication), and therefore the functional analysis of CRYPα *in vivo* using *in ovo* electroporation will soon become technically feasible.

6.5. Discussion

A receptor enzyme usually has a multi-modular molecular architecture, consisting of structurally unrelated domains "fused" in a single entity. CRYPα for instance contains cell adhesion molecule-like modules in its extracellular region (such as Ig-like and FN III-like) linked, via a transmembrane segment, with two protein tyrosine phosphatase domains. Such a molecule has the ability to receive extracellular signals, transmit them across the plasma membrane and finally convert them into a chemical message relevant for the intracellular environment.

An attempt to understand the molecular mechanisms underlying CRYPα's recently described functions should therefore question the identity of both extra- and intracellular interaction partners, be they signal or scaffolding molecules, adapters or substrates. Since a signalling complex at the plasma membrane is expected to be highly dynamic, rapid and reversible post-translational modifications (such as tyrosine phosphorylation and thiol oxidation) can significantly alter the pattern of intramolecular interactions. Therefore, following the identification of extracellular ligands mentioned in the previous chapter, I have described here preliminary attempts aimed at characterising the intracellular interactors of CRYPα. The results presented demonstrate that CRYPα can be tyrosine phosphorylated *in vivo* and also suggest the existence of a putative ~75 kDa substrate. In addition, the first catalytic domain of CRYPα appears to interact with Trio, a key cytoskeletal regulatory molecule.

As previously mentioned, the regulation of many fundamental cellular processes is associated with a reversible phosphorylation of specific tyrosine residues on the proteins involved. Interestingly, the PTPs, enzymes directly involved in controlling the

cellular phosphotyrosine levels, appear to be themselves regulated by the same mechanism. Early reports by Vogel *et al.* (1993) and Feng *et al.* (1993) have shown that PTP1D (also known as Syp, SHP-2 etc.) is phosphorylated on tyrosine following PDGF and EGF stimulation and this causes an enhancement of its catalytic activity. PTP1B, an intracellular PTP now emerging as an important regulator of insulin signalling, appears to be involved in a very interesting regulatory loop with the insulin receptor kinase. Insulin stimulation generates a burst of intracellular hydrogen peroxide which can reversibly oxidise the thiol group of the PTP1B (and presumably other PTPs) catalytic cysteine, leading to its rapid inactivation (Mahadev *et al.*, 2001). The insulin receptor kinase can directly tyrosine phosphorylate PTP1B, both *in vivo* and *in vitro* (Tao *et al.*, 2001; Dadke *et al.*, 2001). Tao *et al.* (2001) have observed a simultaneous decrease of PTP1B activity in immunoprecipitates from insulin-treated cells and suggested that this may be a consequence of tyrosine phosphorylation. However, Dadke *et al.* (2001) have shown *in vitro* that tyrosine phosphorylation of PTP1B by the insulin receptor kinase results in enzyme activation. Therefore, it appears that most probably the decrease in PTP1B activity reported by Tao *et al.* (2001) is due to cysteine oxidation and, on the other hand, PTP1B tyrosine phosphorylation alone does indeed increase its catalytic activity. Finally, PTP1B negatively regulates insulin signalling by dephosphorylating the tandem phosphotyrosine residues of the insulin receptor kinase activation segment (a process described at the structural level by Salmeen *et al.*, 2000).

RPTPs can also be regulated by tyrosine phosphorylation. For example, CD45 is phosphorylated by the p50csk kinase on two tyrosine residues, one of them identified as Tyr1193, thereby creating a binding site for another kinase, p56lck, and also increasing the PTPase activity (Autero *et al.*, 1994). Tyrosine phosphorylation of RPTPα and RPTPε creates a binding site for the adapter protein Grb2 (den Hertog *et al.*, 1994; den Hertog and Hunter, 1996; Su *et al.*, 1996; Toledano-Katchalski and Elson, 1999),

suggesting that, in addition to direct regulation of the PTP catalytic activity, such a modification can control the assembly of signalling complexes involving RPTPs.

Regarding CRYPα, it is not known yet which or at least how many tyrosine residues are phosphorylated and what is the functional consequence of CRYPα phosphorylation. A PROSITE (http://ca.expasy.org/prosite/) analysis of the CRYPα sequence led to the identification of only one putative tyrosine phosphorylation site, Tyr1287 according to CRYPα1 isoform numbering, in the second phosphatase domain (Figure 6.8). Since this residue appears to be located away from the catalytic site in a 3D structural model, and since any catalytic activity of CRYPα-D2 still remains to be demonstrated, one can speculate that phosphorylation of Tyr1287 would create a binding site for a protein containing a phosphotyrosine binding domain rather than directly influence the catalytic activity of CRYPα. My results also suggest that, like many other PTPs analysed, CRYPα can auto-dephosphorylate, either via an intra- or intermolecular interaction. Interestingly, the D1109A "trap" mutant is not over-phosphorylated when expressed in 293T cells in the presence of serum. Since this construct appears to be catalytically inactive, it results that either the endogenous RPTPσ or other PTPs are able to dephosphorylate it efficiently. This is important since an equivalent D→A mutant of PTPH1 loses its trapping ability when over-expressed in 293T cells due to phosphorylation on a Tyr residue close to its catalytic site, which most probably prevents substrate binding (Zhang *et al.*, 1999).

A brief incubation in the presence of hydrogen peroxide before cell lysis, however, triggers a dramatic increase in the cellular phosphotyrosine level due to the reversible oxidation of the PTPs' catalytic Cys residues. Under these conditions the "trap" construct can be recovered in a phosphorylated form, unlike the "wt" construct which most probably auto-dephosphorylates during the immunoprecipitation in the presence of dithiothreitol.

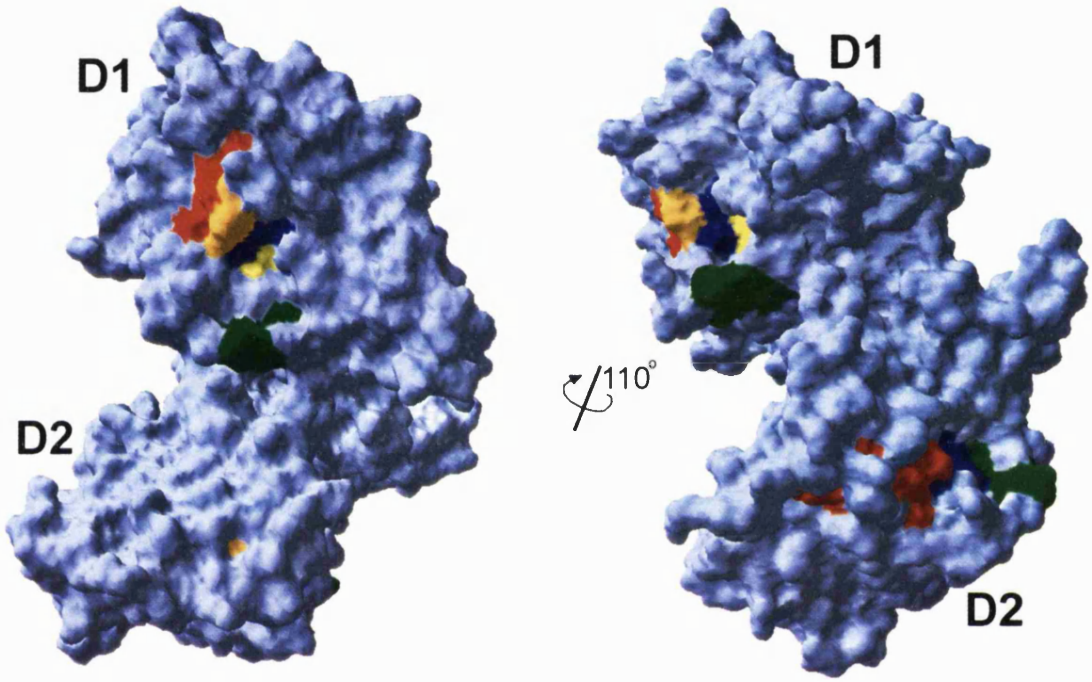

Figure 6.8. 3D model of the intracellular region of CRYPα. This model is based on the recently published structure of LAR intracellular region (PDB entry 1LAR, Nam *et al.*, 1999) which has 88% identity with CRYPα. The three loops forming the catalytic site of each phosphatase domain are coloured in red (substrate recognition loop), blue (phosphatase motif loop) and green (WPD loop). The catalytic Cys residue in D1 is shown in yellow. Putative phosphorylation sites, coloured in orange correspond to Tyr1287 (in domain D2, predicted with PROSITE) and Tyr974 (in domain D1, corresponding to the one described for PTPH1, see text for details). This figure was created with Swiss-PdbViewer v3.6b2 (Guex and Peitsch, 1997).

On the other hand, under these conditions the "trap" construct co-precipitates with a ~75 kDa tyrosine phosphorylated protein. This may represent a putative substrate, although further experiments are clearly required to confirm this hypothesis. Firstly, one must confirm that this "trapping" interaction involves the catalytic site of CRYPα. If this is indeed the case, competitive inhibitors such as vanadate, phosphate or p-nitrophenol should be able to disrupt this interaction. Secondly, additional mutations in the catalytic site such as Cys→Ser, frequently used in substrate trapping experiments, may be tested. Thirdly, the whole experiment should be scaled-up or re-designed by expressing the intracellular CRYPα constructs in bacteria, as GST fusion proteins, and performing a pull-down assay from 293T but also from additional cell lines (Buist *et al.*, 2000). This should hopefully allow the isolation of a phosphorylated substrate under regular cell culture conditions. Although several attempts were made, as mentioned above, a putative substrate could not be trapped unless the cells were pre-treated with hydrogen peroxide. One may wonder whether, under such conditions, the CRYPα construct can indeed maintain its trapping ability. As discussed by Denu and Tanner (1998), membrane-permeant oxidants can irreversibly inactivate PTPs *in vivo* and *in vitro* by oxidising the thiol group of the catalytic Cys residue to either sulfinic acid (Cys-SO_2H) or sulfonic acid (Cys-SO_3H). Hydrogen peroxide, on the other hand, has been shown to oxidise the catalytic Cys only to sulfenic acid (Cys-SOH), which can be fully reduced back to the active thiolate by thiols such as reduced glutathione, dithiothreitol and β-mercaptoethanol (Denu and Tanner, 1998). Obviously, if PTPs are controlled by cellular redox mechanisms it is highly unlikely that they will be irreversibly inactivated during downregulation. Oxidation of the catalytic Cys residue to sulfenic acid is in fact very similar to a Cys-Ser point mutation. However, further oxidation beyond this step would result in bulky and negatively charged groups occupying the catalytic site, which most probably will abolish any substrate trapping

ability. Interestingly, Gross *et al.* (1999) demonstrate that UV irradiation of cells causes inactivation of several PTPs, including RPTPα and RPTPσ. Their results suggest that this involves a thiol group and presumably an oxidative process. Furthermore, UV-irradiation provoked the generation of a "substrate trapping configuration" of RPTPα, similarly to that caused by the Cys→Ser mutation. The fact that I could not detect any putative tyrosine phosphorylated substrate trapped by the "wt" CRYPα construct, even after peroxide treatment, is most probably due to the reduction of its Cys residue during the immunoprecipitation, as mentioned above.

In an attempt to suggest putative identities for the ~75 kDa protein which co-precipitated with the "trap" construct, I performed an *Entrez* Protein Database search for 70-80 kDa proteins. This resulted in 5033 entries for the human subset alone. However, considering the ability of CRYPα to modulate axonal growth cone's cytoskeleton (Ledig *et al.*, 1999a), a query restricted to actin-binding proteins resulted in only 28 entries. Amongst them, drebrin 1, synapsin I, radixin, ezrin, moesin and paxillin are known to be expressed in growth cones and modulate neurite outgrowth and also they can be tyrosine phosphorylated. In a similar situation are isoforms of other cytoskeletal-related proteins such as gigaxonin, limatin, vinculin and the kinases Pak5 and Arg (Abl2). It is probably worth testing these proteins as putative CRYPα substrates, irrespective of the final outcome of scaled-up trapping experiments. For example, proteins of the ERM (ezrin-radixin-moesin) family are well characterised modulators of the growth cone morphology. Microscale chromophore-assisted laser inactivation (micro-CALI) of radixin in chick dorsal root ganglion growth cones causes a significant reduction of the lamellipodial area (Castelo and Jay, 1999), a phenotype similar to the one observed in CRYPα-ligand interaction perturbation experiments (Ledig *et al.*, 1999a). Furthermore, antisense oligonucleotide suppression of both radixin and moesin expression in cultured neurons results in the reduction of growth cone size, retraction of

the lamellipodial veil and disorganisation of the actin filaments in the central region of the growth cone where they co-localise with microtubules (Paglini *et al.*, 1998). Although it is well established that Thr phosphorylation of ERM proteins plays an important role for their transition between active and inactive conformations (Gautreau *et al.*, 2000; Ishikawa *et al.*, 2001), these proteins can be tyrosine phosphorylated (Fazioli *et al.*, 1993) and this may have functional significance.

The interaction between CRYPα and the multidomain protein Trio is still far from being definitely demonstrated by our experiments. First of all, one should understand and eliminate the cause for the non-specific interaction observed with the LexA-D2 construct. One could try the insertion of a flexible peptide linker between the two fusion partners, or shifting the N-terminal end of the D2 construct. Secondly, the yeast two-hybrid experiments need to be confirmed by pull-down and co-immunoprecipitation assays. It is worth mentioning that even in the original paper (Debant *et al.*, 1996), a direct physical interaction between endogenous LAR and Trio proteins could not be detected. The initial yeast two-hybrid results suggesting an interaction between LAR-D2 and Trio appear to be supported by genetic data in *Drosophila*. Mutations in the LAR orthologue, *Dlar*, disrupt the projections of many axons that are also affected in *trio* mutants (Krueger *et al.*, 1997; Bateman *et al.*, 2000). Similarly, mutants of the type IIa RPTP *Dptp69A* have an axonal phenotype resembling that of *trio* in loss-of-function mutant retinas (Garrity *et al.*, 1999). However, it is unclear whether a direct LAR-Trio physical interaction can occur in *Drosophila*, or even in *C. elegans*, since the C-terminal domains of Trio responsible for the human orthologues interaction are not conserved (Debant *et al.*, 1996). Nevertheless, the phenotypes caused by *Dlar* mutations are exacerbated by loss of either *trio* or *Drac1*, which suggests that the Trio/Rac pathway is important for LAR signalling (Kaufmann *et al.*, 1998; Bateman *et al.*, 2000). It has been suggested that *Drosophila* RPTPs may

signal through Trio via some intermediate partners, such as the PTK Abl (Bateman and van Vactor, 2001) or even that they function in separate pathways (Dickson, 2001). That CRYPα does indeed interact with Trio *in vivo* still remains to be tested, but nevertheless their signalling pathways still appear to converge towards regulation of the actin cytoskeleton.

In conclusion, the experiments described in this chapter provide preliminary hints towards putative intracellular interaction partners for CRYPα. Once their identities are confirmed by further studies and a detailed phenotypic analysis of various CRYPα constructs electroporated into the developing retina are available, one should be able to appreciate the functional significance of the interactions proposed here.

Chapter 7. **Concluding remarks**

One may think that focusing a PhD thesis on a single protein is a rather risky business, since the smaller the target, the greater the chance to miss it. In particular, this protein being a rather unknown membrane receptor. Nevertheless, as discussed in Chapter 1.4, CRYPα/RPTPσ is part of a "new wave" of molecules emerging as important regulators of neural development, specifically axon growth and guidance, and nerve repair. In addition, it still holds several fundamental questions to be answered: What sort of signals does it respond to? How does it function, i.e. perform signal transduction? What are its direct intracellular molecular targets? The work described in this thesis is, broadly speaking, aimed at tackling these issues.

Once the target and a working strategy are set, a biochemical study of CRYPα implies overcoming at least one more problem: getting sufficient amounts of it. This is one of the reasons why the functional studies have moved faster. But this can also explain why the nature of CRYPα (or indeed most RPTP) ligands remained "elusive" for such a long time, despite numerous attempts to identify them.

The classical expression cloning experiment described in Chapter 3 appeared to work very well, but only until it reached the final screening step. This may be due to the intrinsic nature of CRYPα ligands, such as the secreted HSPGs found later on. Nevertheless, as suggested in Chapters 4 and 5, but also by experiments reported in Ledig *et al.* (1999a) and Johnson *et al.* (2001), Müller glia endfeet appear to express an additional class of membrane-bound ligands. I did try to identify such a ligand by crosslinking CRYPα with proteins on the membrane surface of radioactively labelled rat Müller glia cell cultures, unsuccessfully though (data not included in this thesis). Only later on I understood that such a putative ligand seems to be specifically expressed on glial endfeet. Therefore, I think that it would be worth repeating this experiment

using cells grown on a vitreous body extract substrate, which contains most basal lamina constituents, if one can prove that it induces endfeet differentiation. In this case, it may also be worth trying to screen a new cDNA library generated from cells grown under such conditions. This could also be combined with a more powerful screening method such as fluorescence-activated cell sorting.

The turning point in this thesis' fortunes was probably the simple observation that sodium chloride and heparin impair CRYPα binding on the retinal basal lamina in RAP *in situ* experiments. From this, the presence of a heparin-binding site in the CRYPα ectodomain, identified by molecular modelling and confirmed by site-directed mutagenesis, together with the highly reproducible RAP *in situ* experiments, suggested basal lamina HSPGs as putative ligands. The retinal basal lamina, in particular, is a structure characterised biochemically in great detail and it contains two major HSPGs, namely agrin and collagen XVIII. CRYPα binds to both of them, as well as heparin, with very high affinity. One may also question the specificity of this interaction. This still remains to be determined, since I could not obtain a pure HSPG sample to which CRYPα does not bind. Interestingly however, recent results suggest that the EV3C3 single-chain antibody, which can efficiently block CRYPα binding to the retinal basal lamina (Chapter 5), does not bind perlecan (Toin van Kuppevelt, personal communication). On the other hand, as mentioned in chapter 5, there are numerous circumstances in which CRYPα and agrin or collagen XVIII can functionally overlap. Alternatively, maybe the exact nature of the HSPG ligand is not as important as the exact HS sequence to which CRYPα binds. Do various proteins bind HS chains with the same degree of specificity to which, for example, restriction endonucleases bind DNA sequences? It may well be the case, although this still remains to be demonstrated.

The interaction between CRYPα and HSPGs appears to be mediated by their HS chains. The exact role(s) of such an interaction is (are) still unclear and one can

speculate on several possibilities. For example, HSPGs may directly modulate the enzymatic activity of CRYPα and therefore represent "genuine" ligands. As mentioned several times in this thesis, the control of RPTPs' dimerisation state appears to be an important, although not ubiquitous, regulatory mechanism. The relative subunit orientation is critically important for receptor dimer regulation (Jiang and Hunter, 1999; Jiang *et al.*, 1999), and the HS chain may well play an important role in orienting a putative CRYPα dimer. This may ultimately control the signalling ability of CRYPα, either by holding the receptor in a catalytically active conformation, in which it will actively dephosphorylate its endogenous substrates, or by inducing an "inactive" conformation in which CRYPα may become tyrosine phosphorylated (this possibility being suggested by experiments described in chapter 6). CRYPα "silencing" and tyrosine phosphorylation in itself may trigger signal transduction, by allowing adapter proteins to bind and organise a signalling complex.

On the other hand, HSPGs are known to bind a plethora of small proteins, such as growth factors and cytokines. One cannot exclude the possibility that such a small heparin-binding molecule may represent a ligand for CRYPα and therefore the HSPG may play a co-receptor function. Testing proteins able to bind the HS chains of agrin and collagen XVIII may lead to the characterisation of additional CRYPα ligands.

Another interesting possibility relates to a particular feature of RPTPs, including CRYPα (Stoker *et al.*, 1995), namely ectodomain shedding. It is still unclear in which circumstances this occurs and what is the functional significance of this process. Ectodomain shedding may attenuate signalling through the receptor, by triggering redistribution and internalisation of the cytoplasmic (P) region (Aicher *et al.*, 1997). The soluble ectodomain may, for instance, remain attached to the cell surface via HSPGs and be presented as a ligand to another receptor.

Understanding the functional significance of the interaction between CRYPα and HSPGs, or indeed any other ligand which may be discovered, is impossible without the knowledge of downstream (intracellular) interacting partners and signalling pathways related to this RPTP. In this thesis I could only very briefly address this issue and further experiments are needed to confirm the physiological significance of CRYPα tyrosine phosphorylation, the identity of the putative ~75 kDa substrate and the suggested interaction with Trio. In addition, recent improvements in the *in ovo* electroporation technique will definitely allow a detailed analysis of the CRYPα function *in vivo*, by expressing a variety of mutant constructs.

In conclusion, the results presented in this thesis demonstrate that CRYPα has a novel, heparin-binding activity and that its interaction with the retinal basal lamina is mediated by the HS chains of extracellular matrix HSPGs. I also describe the first identification of heterotypic ligands for a type II neural RPTP, namely agrin and collagen XVIII. These molecules have a considerable functional plasticity and therefore can offer novel clues towards understanding the complex role played by CRYPα, and possibly other RPTPs, in neural development and repair. Modulating the enzymatic activity of RPTPs such as CRYPα might have a direct clinical relevance, for example in stimulating post-traumatic nerve regrowth and regeneration of functional synaptic connections, in Alzheimer's disease and cancer therapy. Since heparin mimetics are currently being considered as putative growth factor receptor modulators, a similar approach might be considered for RPTPs, assuming that indeed the protein-HS interaction is highly specific. If this is not the case, the results presented here are equally important by revealing a major interference risk.

This thesis provides multiple starting points for further experiments and offers a new perspective for understanding the complex biological functions of RPTPs.

References

Ackley, B.D., J.R. Crew, H. Elamaa, T. Pihlajaniemi, C.J. Kuo, and J.M. Kramer. (2001). The NC1/endostatin domain of Caenorhabditis elegans type XVIII collagen affects cell migration and axon guidance. *J Cell Biol.* **152**:1219-1232.

Aicher, B., M.M. Lerch, T. Muller, J. Schilling, and A. Ullrich. (1997). Cellular redistribution of protein tyrosine phosphatases LAR and PTPsigma by inducible proteolytic processing. *J Cell Biol.* **138**:681-696.

Alexander, D.R. (2000). The CD45 tyrosine phosphatase: a positive and negative regulator of immune cell function. *Semin Immunol.* **12**:349-359.

Angers-Loustau, A., J.F. Cote, A. Charest, D. Dowbenko, S. Spencer, L.A. Lasky, and M.L. Tremblay. (1999). Protein tyrosine phosphatase-PEST regulates focal adhesion disassembly, migration, and cytokinesis in fibroblasts. *J Cell Biol.* **144**:1019-31.

Aricescu, A.R., T.A. Fulga, V. Cismasiu, R.S. Goody, and S.E. Szedlacsek. (2001). Intramolecular interactions in protein tyrosine phosphatase RPTPmu: kinetic evidence. *Biochem Biophys Res Commun.* **280**:319-327.

Aruffo, A. (1997). *In* Current Protocols in Molecular Biology. 16.13.1-16.13.7.

Autero, M., J. Saharinen, T. Pessa-Morikawa, M. Soula-Rothhut, C. Oetken, M. Gassmann, M. Bergman, K. Alitalo, P. Burn, C.G. Gahmberg, and et al. (1994). Tyrosine phosphorylation of CD45 phosphotyrosine phosphatase by p50csk kinase creates a binding site for p56lck tyrosine kinase and activates the phosphatase. *Mol Cell Biol.* **14**:1308-1321.

Baker, M.W., and E.R. Macagno. (2000). The role of a LAR-like receptor tyrosine phosphatase in growth cone collapse and mutual-avoidance by sibling processes. *J Neurobiol.* **44**:194-203.

Bandtlow, C.E., and D.R. Zimmermann. (2000). Proteoglycans in the developing brain: new conceptual insights for old proteins. *Physiol Rev.* **80**:1267-1290.

Barbacid, M. (1995). Neurotrophic factors and their receptors. *Curr Opin Cell Biol.* **7**:148-155.

Barford, D., A.J. Flint, and N.K. Tonks. (1994). Crystal structure of human protein tyrosine phosphatase 1B. *Science.* **263**:1397-1404.

Barford, D., A.K. Das, and M.P. Egloff. (1998). The structure and mechanism of protein phosphatases: insights into catalysis and regulation. *Annu Rev Biophys Biomol Struct.* **27**:133-164.

Bashaw, G.J., T. Kidd, D. Murray, T. Pawson, and C.S. Goodman. (2000). Repulsive axon guidance: Abelson and Enabled play opposing roles downstream of the roundabout receptor. *Cell.* **101**:703-15.

Bateman, A., E. Birney, R. Durbin, S.R. Eddy, K.L. Howe, and E.L. Sonnhammer. (2000). The Pfam protein families database. *Nucleic Acids Res.* **28**:263-266.

Bateman, J., H. Shu, and D. Van Vactor. (2000). The guanine nucleotide exchange factor trio mediates axonal development in the Drosophila embryo. *Neuron.* **26**:93-106.

Bateman, J., and D. Van Vactor. (2001). The Trio family of guanine-nucleotide-exchange factors: regulators of axon guidance. *J Cell Sci.* **114**:1973-1980.

Baum, P.D., and G. Garriga. (1997). Neuronal migrations and axon fasciculation are disrupted in ina-1 integrin mutants. *Neuron.* **19**:51-62.

Bellaiche, Y., I. The, and N. Perrimon. (1998). Tout-velu is a Drosophila homologue of the putative tumour suppressor EXT-1 and is needed for Hh diffusion. *Nature.* **394**:85-88.

Bilwes, A.M., J. den Hertog, T. Hunter, and J.P. Noel. (1996). Structural basis for inhibition of receptor protein-tyrosine phosphatase-alpha by dimerization. *Nature.* **382**:555-559.

Bixby, J.L., and P. Jhabvala. (1992). Inhibition of tyrosine phosphorylation potentiates substrate-induced neurite growth. *Journal of Neurobiology.* **23**:468-480.

Blanchetot, C., and J. den Hertog. (2000). Multiple interactions between receptor protein-tyrosine phosphatase (RPTP) alpha and membrane-distal protein-tyrosine phosphatase domains of various RPTPs. *J Biol Chem.* **275**:12446-12452.

Blanchetot, C., and J. den Hertog. (2000). Antibody-induced dimerization of HARPTPalpha-EGFR chimera suggests a ligand dependent mechanism of regulation for RPTPalpha. *FEBS Lett.* **484**:235-240.

Bovolenta, P., and I. Fernaud-Espinosa. (2000). Nervous system proteoglycans as modulators of neurite outgrowth. *Prog Neurobiol.* **61**:113-132.

Boyle, J.S., and A.M. Lew. (1995). An inexpensive alternative to glassmilk for DNA purification. *Trends Genet.* **11**:8.

Brady-Kalnay, S.M., A.J. Flint, and N.K. Tonks. (1993). Homophilic binding of PTPm, a receptor-type protein tyrosine phosphatase, can mediate cell-cell aggregation. *J. Cell Biol.* **122**:961-972.

Brady-Kalnay, S.M., T. Mourton, J.P. Nixon, G.E. Pietz, M. Kinch, H. Chen, R. Brackenbury, D.L. Rimm, R.L. Del Vecchio, and N.K. Tonks. (1998). Dynamic

Interaction of PTPmu with Multiple Cadherins In Vivo. *J Cell Biol.* **141**:287-96.

Braisted, J.E., T. McLaughlin, H.U. Wang, G.C. Friedman, D.J. Anderson, and D. O'Leary D. (1997). Graded and lamina-specific distributions of ligands of EphB receptor tyrosine kinases in the developing retinotectal system. *Dev Biol.* **191**:14-28.

Bregman, B.S., E. Kunkel-Bagden, L. Schnell, H.N. Dai, D. Gao, and M.E. Schwab. (1995). Recovery from spinal cord injury mediated by antibodies to neurite growth inhibitors. *Nature.* **378**:498-501.

Britten, C.J., and M.I. Bird. (1997). Chemical modification of an alpha 3-fucosyltransferase; definition of amino acid residues essential for enzyme activity. *Biochim Biophys Acta.* **1334**:57-64.

Brittis, P.A., and J.G. Flanagan. (2001). Nogo domains and a Nogo receptor: implications for axon regeneration. *Neuron.* **30**:11-14.

Brose, K., and M. Tessier-Lavigne. (2000). Slit proteins: key regulators of axon guidance, axonal branching, and cell migration. *Curr Opin Neurobiol.* **10**:95-102.

Buist, A., Y.L. Zhang, Y.F. Keng, L. Wu, Z.Y. Zhang, and J. den Hertog. (1999). Restoration of potent protein-tyrosine phosphatase activity into the membrane-distal domain of receptor protein-tyrosine phosphatase alpha. *Biochemistry.* **38**:914-922.

Buist, A., C. Blanchetot, L.G. Tertoolen, and J. den Hertog. (2000). Identification of p130cas as an in vivo substrate of receptor protein- tyrosine phosphatase alpha. *J Biol Chem.* **275**:20754-20761.

Bullock, S.L., J.M. Fletcher, R.S. Beddington, and V.A. Wilson. (1998). Renal agenesis in mice homozygous for a gene trap mutation in the gene encoding heparan sulfate 2-sulfotransferase. *Genes Dev.* **12**:1894-1906.

Burden-Gulley, S.M., and S.M. Brady-Kalnay. (1999). PTPmu Regulates N-Cadherin-dependent Neurite Outgrowth. *J Cell Biol.* **144**:1323-1336.

Burgess, R.W., W.C. Skarnes, and J.R. Sanes. (2000). Agrin isoforms with distinct amino termini: differential expression, localization, and function. *J Cell Biol.* **151**:41-52.

Callahan, C.A., M.G. Muralidhar, S.E. Lundgren, A.L. Scully, and J.B. Thomas. (1995). Control of neuronal pathway selection by a Drosophila receptor protein-tyrosine kinase family member. *Nature.* **376**:171-4.

Caras, I.W. (1997). A link between axon guidance and axon fasciculation suggested by studies of the tyrosine kinase receptor EphA5/REK7 and its ligand ephrin-A5/AL-1. *Cell Tissue Res.* **290**:261-4.

Castelo, L., and D.G. Jay. (1999). Radixin is involved in lamellipodial stability during

nerve growth cone motility. *Mol Biol Cell.* **10**:1511-1520.

Chai, L., and J.E. Morris. (1999). Heparan sulfate in the inner limiting membrane of embryonic chicken retina binds basic fibroblast growth factor to promote axonal outgrowth. *Exp Neurol.* **160**:175-185.

Chen, C.A., D.M. Smith, M.A. Peters, M.E. Samson, J. Zitz, C.J. Tabin, and C.L. Cepko. (1999). Production and design of more effective avian replication-incompetent retroviral vectors. *Dev Biol.* **214**:370-84.

Chen, M.S., A.B. Huber, M.E. van der Haar, M. Frank, L. Schnell, A.A. Spillmann, F. Christ, and M.E. Schwab. (2000). Nogo-A is a myelin-associated neurite outgrowth inhibitor and an antigen for monoclonal antibody IN-1. *Nature.* **403**:434-439.

Cheng, H.J., and J.G. Flanagan. (1994). Identification and cloning of ELF-1, a developmentally expressed ligand for the Mek4 and Sek receptor tyrosine kinases. *Cell.* **79**:157-68.

Chiarugi, P., M.L. Taddei, P. Cirri, D. Talini, F. Buricchi, G. Camici, G. Manao, G. Raugei, and G. Ramponi. (2000). Low molecular weight protein-tyrosine phosphatase controls the rate and the strength of NIH-3T3 cells adhesion through its phosphorylation on tyrosine 131 or 132. *J Biol Chem.* **275**:37619-37627.

Chilton, J.K., and A.W. Stoker. (2000). Expression of receptor protein tyrosine phosphatases in embryonic chick spinal cord. *Mol Cell Neurosci.* **16**:470-80.

Chisholm, A., and M. Tessier-Lavigne. (1999). Conservation and divergence of axon guidance mechanisms. *Curr Opin Neurobiol.* **9**:603-15.

Clark, E.A., and J.S. Brugge. (1995). Integrins and signal transduction pathways: the road taken. *Science.* **268**:233-9.

Colamarino, S.A., and M. Tessier-Lavigne. (1995). The axonal chemoattractant netrin-1 is also a chemorepellent for trochlear motor axons. *Cell.* **81**:621-629.

Cole, G.J., A. Loewy, and L. Glaser. (1986). Neuronal cell-cell adhesion depends on interactions of N-CAM with heparin-like molecules. *Nature.* **320**:445-447.

Cole, G.J., and L. Glaser. (1986). A heparin-binding domain from N-CAM is involved in neural cell- substratum adhesion. *J Cell Biol.* **102**:403-412.

Cole, G.J., and R. Akeson. (1989). Identification of a heparin binding domain of the neural cell adhesion molecule N-CAM using synthetic peptides. *Neuron.* **2**:1157-1165.

Conrad, H.E. (1998). Heparin-binding proteins. Academic Press, San Diego, CA.

Consortium, I.H.G.S. (2001). Initial sequencing and analysis of the human genome.

Nature. **409**:860-921.

Cotman, S.L., W. Halfter, and G.J. Cole. (2000). Agrin binds to beta-amyloid (Abeta), accelerates abeta fibril formation, and is localized to Abeta deposits in Alzheimer's disease brain. *Mol Cell Neurosci.* **15**:183-198.

Cummings, B.J., J.H. Su, and C.W. Cotman. (1993). Neuritic involvement within bFGF immunopositive plaques of Alzheimer's disease. *Exp Neurol.* **124**:315-325.

Davis, S., N.W. Gale, T.H. Aldrich, P.C. Maisonpierre, V. Lhotak, T. Pawson, M. Goldfarb, and G.D. Yancopoulos. (1994). Ligands for EPH-related receptor tyrosine kinases that require membrane attachment or clustering for activity. *Science.* **266**:816-819.

Davis, S., T.H. Aldrich, P.F. Jones, A. Acheson, D.L. Compton, V. Jain, T.E. Ryan, J. Bruno, C. Radziejewski, P.C. Maisonpierre, and G.D. Yancopoulos. (1996). Isolation of angiopoietin-1, a ligand for the TIE2 receptor, by secretion-trap expression cloning. *Cell.* **87**:1161-1169.

Davy, A., N.W. Gale, E.W. Murray, R.A. Klinghoffer, P. Soriano, C. Feuerstein, and S.M. Robbins. (1999). Compartmentalized signaling by GPI-anchored ephrin-A5 requires the Fyn tyrosine kinase to regulate cellular adhesion. *Genes Dev.* **13**:3125-3135.

Debant, A., C. Serra-Pages, K. Seipel, S. O'Brien, M. Tang, S.H. Park, and M. Streuli. (1996). The multidomain protein Trio binds the LAR transmembrane tyrosine phosphatase, contains a protein kinase domain, and has separate rac- specific and rho-specific guanine nucleotide exchange factor domains. *Proc Natl Acad Sci U S A.* **93**:5466-5471.

Deiner, M.S., T.E. Kennedy, A. Fazeli, T. Serafini, M. Tessier-Lavigne, and D.W. Sretavan. (1997). Netrin-1 and DCC mediate axon guidance locally at the optic disc: loss of function leads to optic nerve hypoplasia. *Neuron.* **19**:575-89.

den Hertog, J., C.E. Pals, M.P. Peppelenbosch, L.G. Tertoolen, S.W. de Laat, and W. Kruijer. (1993). Receptor protein tyrosine phosphatase alpha activates pp60c-src and is involved in neuronal differentiation. *Embo J.* **12**:3789-3798.

den Hertog, J., S. Tracy, and T. Hunter. (1994). Phosphorylation of receptor protein-tyrosine phosphatase alpha on Tyr789, a binding site for the SH3-SH2-SH3 adaptor protein GRB-2 in vivo. *Embo J.* **13**:3020-3032.

den Hertog, J., J. Sap, C.E. Pals, J. Schlessinger, and W. Kruijer. (1995). Stimulation of receptor protein-tyrosine phosphatase alpha activity and phosphorylation by phorbol ester. *Cell Growth Differ.* **6**:303-307.

den Hertog, J., and T. Hunter. (1996). Tight association of GRB2 with receptor protein-tyrosine phosphatase alpha is mediated by the SH2 and C-terminal SH3 domains. *Embo J.* **15**:3016-3027.

den Hertog, J., C. Blanchetot, A. Buist, J. Overvoorde, A. van der Sar, and L.G. Tertoolen. (1999). Receptor protein-tyrosine phosphatase signalling in development. *Int J Dev Biol.* **43**:723-33.

Denu, J.M., and K.G. Tanner. (1998). Specific and reversible inactivation of protein tyrosine phosphatases by hydrogen peroxide: evidence for a sulfenic acid intermediate and implications for redox regulation. *Biochemistry.* **37**:5633-5642.

Denu, J.M., and J.E. Dixon. (1998). Protein tyrosine phosphatases: mechanisms of catalysis and regulation. *Curr Opin Chem Biol.* **2**:633-641.

Desai, D.M., J. Sap, J. Schlessinger, and A. Weiss. (1993). Ligand-mediated negative regulation of a chimeric transmembrane receptor tyrosine phosphatase. *Cell.* **73**:541-554.

Desai, C.J., J.G. Gindhart, Jr., L.S. Goldstein, and K. Zinn. (1996). Receptor tyrosine phosphatases are required for motor axon guidance in the Drosophila embryo. *Cell.* **84**:599-609.

Desai, C.J., Q. Sun, and K. Zinn. (1997). Tyrosine phosphorylation and axon guidance: of mice and flies. *Curr Opin Neurobiol.* **7**:70-4.

Desai, C., N. Krueger, H. Saito, and K. Zinn. (1997). Competition and cooperation among receptor tyrosine phosphatases control motoneuron growth cone guidance in Drosophila. *Development.* **124**:1941-52.

Dickson, B.J. (2001). Rho GTPases in growth cone guidance. *Curr Opin Neurobiol.* **11**:103-110.

Doherty, P., G. Williams, and E.J. Williams. (2000). CAMs and axonal growth: a critical evaluation of the role of calcium and the MAPK cascade. *Mol Cell Neurosci.* **16**:283-295.

Donahue, J.E., T.M. Berzin, M.S. Rafii, D.J. Glass, G.D. Yancopoulos, J.R. Fallon, and E.G. Stopa. (1999). Agrin in Alzheimer's disease: altered solubility and abnormal distribution within microvasculature and brain parenchyma. *Proc Natl Acad Sci U S A.* **96**:6468-6472.

Drescher, U. (1997). The Eph family in the patterning of neural development. *Curr Biol.* **7**:R799-807.

Driessens, M.H., H. Hu, C.D. Nobes, A. Self, I. Jordens, C.S. Goodman, and A. Hall. (2001). Plexin-B semaphorin receptors interact directly with active Rac and

regulate the actin cytoskeleton by activating Rho. *Curr Biol.* **11**:339-344.

Drosopoulos, N.E., F.S. Walsh, and P. Doherty. (1999). A Soluble Version of the Receptor-like Protein Tyrosine Phosphatase kappa Stimulates Neurite Outgrowth via a Grb2/MEK1-Dependent Signaling Cascade. *Mol Cell Neurosci.* **13**:441-449.

Elchebly, M., J. Wagner, T.E. Kennedy, C. Lanctot, E. Michaliszyn, A. Itie, J. Drouin, and M.L. Tremblay. (1999). Neuroendocrine dysplasia in mice lacking protein tyrosine phosphatase sigma. *Nat Genet.* **21**:330-333.

Erskine, L., S.E. Williams, K. Brose, T. Kidd, R.A. Rachel, C.S. Goodman, M. Tessier-Lavigne, and C.A. Mason. (2000). Retinal ganglion cell axon guidance in the mouse optic chiasm: expression and function of robos and slits. *J Neurosci.* **20**:4975-4982.

Fan, J., and J.A. Raper. (1995). Localized collapsing cues can steer growth cones without inducing their full collapse. *Neuron.* **14**:263-274.

Fauman, E.B., J.P. Cogswell, B. Lovejoy, W.J. Rocque, W. Holmes, V.G. Montana, H. Piwnica-Worms, M.J. Rink, and M.A. Saper. (1998). Crystal structure of the catalytic domain of the human cell cycle control phosphatase, Cdc25A. *Cell.* **93**:617-625.

Fazioli, F., W.T. Wong, S.J. Ullrich, K. Sakaguchi, E. Appella, and P.P. Di Fiore. (1993). The ezrin-like family of tyrosine kinase substrates: receptor-specific pattern of tyrosine phosphorylation and relationship to malignant transformation. *Oncogene.* **8**:1335-1345.

Feiken, E., I. van Etten, M.F. Gebbink, W.H. Moolenaar, and G.C. Zondag. (2000). Intramolecular interactions between the juxtamembrane domain and phosphatase domains of receptor protein-tyrosine phosphatase RPTPmu. Regulation of catalytic activity. *J Biol Chem.* **275**:15350-15356.

Felberg, J., and P. Johnson. (2000). Stable interdomain interaction within the cytoplasmic domain of CD45 increases enzyme stability. *Biochem Biophys Res Commun.* **271**:292-298.

Feng, G.S., C.C. Hui, and T. Pawson. (1993). SH2-containing phosphotyrosine phosphatase as a target of protein- tyrosine kinases. *Science.* **259**:1607-1611.

Fischer, E.H. (1999). Cell signaling by protein tyrosine phosphorylation. *Adv Enzyme Regul.* **39**:359-369.

Flanagan, J.G., and P. Leder. (1990). The kit ligand: a cell surface molecule altered in steel mutant fibroblasts. *Cell.* **63**:185-94.

Flanagan, J.G., and P. Vanderhaeghen. (1998). The ephrins and Eph receptors in

neural development. *Annu Rev Neurosci.* **21**:309-345.

Flanagan, J.G., and H.J. Cheng. (2000). Alkaline phosphatase fusion proteins for molecular characterization and cloning of receptors and their ligands. *Methods Enzymol.* **327**:198-210.

Flanagan, J.G., H.J. Cheng, D.A. Feldheim, M. Hattori, Q. Lu, and P. Vanderhaeghen. (2000). Alkaline phosphatase fusions of ligands or receptors as in situ probes for staining of cells, tissues, and embryos. *Methods Enzymol.* **327**:19-35.

Flint, A.J., T. Tiganis, D. Barford, and N.K. Tonks. (1997). Development of "substrate-trapping" mutants to identify physiological substrates of protein tyrosine phosphatases. *Proc Natl Acad Sci U S A.* **94**:1680-1685.

Forsberg, E., G. Pejler, M. Ringvall, C. Lunderius, B. Tomasini-Johansson, M. Kusche-Gullberg, I. Eriksson, J. Ledin, L. Hellman, and L. Kjellen. (1999). Abnormal mast cells in mice deficient in a heparin-synthesizing enzyme. *Nature.* **400**:773-776.

Fournier, A.E., T. GrandPre, and S.M. Strittmatter. (2001). Identification of a receptor mediating Nogo-66 inhibition of axonal regeneration. *Nature.* **409**:341-346.

Frearson, J.A., and D.R. Alexander. (1997). The role of phosphotyrosine phosphatases in haematopoietic cell signal transduction. *Bioessays.* **19**:417-427.

Fuchs, M., H. Wang, T. Ciossek, Z. Chen, and A. Ullrich. (1998). Differential expression of MAM-subfamily protein tyrosine phosphatases during mouse development. *Mech Dev.* **70**:91-109.

Garrity, P.A., C.H. Lee, I. Salecker, H.C. Robertson, C.J. Desai, K. Zinn, and S.L. Zipursky. (1999). Retinal axon target selection in Drosophila is regulated by a receptor protein tyrosine phosphatase. *Neuron.* **22**:707-17.

Gautreau, A., D. Louvard, and M. Arpin. (2000). Morphogenic effects of ezrin require a phosphorylation-induced transition from oligomers to monomers at the plasma membrane. *J Cell Biol.* **150**:193-203.

Gebbink, M.F.B.G., G.C.M. Zondag, R.W. Wubbolts, R.L. Beijersbergen, I. Van_Etten, and W.H. Moolenaar. (1993). Cell-cell adhesion mediated by a receptor-like protein tyrosine phosphatase. *J Biol Chem.* **268**:16101-16104.

Gebbink, M.F., G.C. Zondag, G.M. Koningstein, E. Feiken, R.W. Wubbolts, and W.H. Moolenaar. (1995). Cell surface expression of receptor protein tyrosine phosphatase RPTP mu is regulated by cell-cell contact. *J Cell Biol.* **131**:251-260.

Gershon, T., M. Baker, M. Nitabach, and E. Macagno. (1998). The leech receptor protein tyrosine phosphatase HmLAR2 is concentrated in growth cones and is

involved in process outgrowth. *Development.* **125**:1183-90.

Goldstein, B.J., A. Bittner-Kowalczyk, M.F. White, and M. Harbeck. (2000). Tyrosine dephosphorylation and deactivation of insulin receptor substrate-1 by protein-tyrosine phosphatase 1B. Possible facilitation by the formation of a ternary complex with the Grb2 adaptor protein. *J Biol Chem.* **275**:4283-4289.

GrandPre, T., F. Nakamura, T. Vartanian, and S.M. Strittmatter. (2000). Identification of the Nogo inhibitor of axon regeneration as a Reticulon protein. *Nature.* **403**:439-444.

Gross, S., A. Knebel, T. Tenev, A. Neininger, M. Gaestel, P. Herrlich, and F.D. Bohmer. (1999). Inactivation of protein-tyrosine phosphatases as mechanism of UV-induced signal transduction. *J Biol Chem.* **274**:26378-26386.

Guex, N., and M.C. Peitsch. (1997). SWISS-MODEL and the Swiss-PdbViewer: an environment for comparative protein modeling. *Electrophoresis.* **18**:2714-2723.

Guex, N., A. Diemand, and M.C. Peitsch. (1999). Protein modelling for all. *Trends Biochem Sci.* **24**:364-367.

Gyuris, J., E. Golemis, H. Chertkov, and R. Brent. (1993). Cdi1, a human G1 and S phase protein phosphatase that associates with Cdk2. *Cell.* **75**:791-803.

Haas, K., W.C. Sin, A. Javaherian, Z. Li, and H.T. Cline. (2001). Single-cell electroporation for gene transfer in vivo. *Neuron.* **29**:583-91.

Hagiwara, H., and J.R. Fallon. (2001). Shaping membrane architecture: agrins in and out of the synapse. *J Cell Biol.* **153**:F39-42.

Haj, F., I. McKinnell, and A. Stoker. (1999). Retinotectal Ligands for the Receptor Tyrosine Phosphatase CRYPalpha. *Mol Cell Neurosci.* **14**:225-240.

Halfter, W., W. Reckhaus, and S. Kroger. (1987). Nondirected axonal growth on basal lamina from avian embryonic neural retina. *J Neurosci.* **7**:3712-22.

Halfter, W., and Y. von Boxberg. (1992). Axonal growth on solubilised and reconstituted matrix from the embryonic chicken retina inner limiting membrane. *Eur. J. Neurosci.* **4**:840-852.

Halfter, W. (1993). A heparan sulfate proteoglycan in developing avian axonal tracts. *J Neurosci.* **13**:2863-2873.

Halfter, W., B. Schurer, J. Yip, L. Yip, G. Tsen, J.A. Lee, and G.J. Cole. (1997). Distribution and substrate properties of agrin, a heparan sulfate proteoglycan of developing axonal pathways. *J Comp Neurol.* **383**:1-17.

Halfter, W., S. Dong, B. Schurer, and G.J. Cole. (1998). Collagen XVIII is a basement membrane heparan sulfate proteoglycan. *J Biol Chem.* **273**:25404-25412.

Halfter, W., S. Dong, B. Schurer, A. Osanger, W. Schneider, M. Ruegg, and G.J. Cole. (2000). Composition, synthesis, and assembly of the embryonic chick retinal basal lamina. *Dev Biol.* **220**:111-128.

Hamburger, V., and H.L. Hamilton. (1992). A series of normal stages in the development of the chick embryo. 1951. *Dev Dyn.* **195**:231-72.

Hanahan, D., J. Jessee, and F.R. Bloom. (1991). Plasmid transformation of Escherichia coli and other bacteria. *Methods Enzymol.* **204**:63-113.

Harroch, S., M. Palmeri, J. Rosenbluth, A. Custer, M. Okigaki, P. Shrager, M. Blum, J.D. Buxbaum, and J. Schlessinger. (2000). No obvious abnormality in mice deficient in receptor protein tyrosine phosphatase beta. *Mol Cell Biol.* **20**:7706-7715.

Haworth, K., K.K. Shu, A. Stokes, R. Morris, and A. Stoker. (1998). The expression of receptor tyrosine phosphatases is responsive to sciatic nerve crush. *Mol. Cell. Neurosci.* **12**:93-104.

He, Z., and M. Tessier-Lavigne. (1997). Neuropilin is a receptor for the axonal chemorepellent Semaphorin III. *Cell.* **90**:739-751.

Hileman, R.E., J.R. Fromm, J.M. Weiler, and R.J. Linhardt. (1998). Glycosaminoglycan-protein interactions: definition of consensus sites in glycosaminoglycan binding proteins. *Bioessays.* **20**:156-167.

Hoffmann, K.M., N.K. Tonks, and D. Barford. (1997). The crystal structure of domain 1 of receptor protein-tyrosine phosphatase mu. *J Biol Chem.* **272**:27505-27508.

Holden, H.M., M. Ito, D.J. Hartshorne, and I. Rayment. (1992). X-ray structure determination of telokin, the C-terminal domain of myosin light chain kinase, at 2.8 A resolution. *J Mol Biol.* **227**:840-851.

Holmberg, J., D.L. Clarke, and J. Frisen. (2000). Regulation of repulsion versus adhesion by different splice forms of an Eph receptor. *Nature.* **408**:203-206.

Hooft, R.W., G. Vriend, C. Sander, and E.E. Abola. (1996). Errors in protein structures. *Nature.* **381**:272.

Hopker, V.H., D. Shewan, M. Tessier-Lavigne, M. Poo, and C. Holt. (1999). Growth-cone attraction to netrin-1 is converted to repulsion by laminin- 1. *Nature.* **401**:69-73.

Hu, H. (2001). Cell-surface heparan sulfate is involved in the repulsive guidance activities of Slit2 protein. *Nat Neurosci.* **4**:695-701.

Hughes, S.H., J.J. Greenhouse, C.J. Petropoulos, and P. Sutrave. (1987). Adaptor plasmids simplify the insertion of foreign DNA into helper- independent retroviral

vectors. *J Virol.* **61**:3004-12.

Humphries, D.E., G.W. Wong, D.S. Friend, M.F. Gurish, W.T. Qiu, C. Huang, A.H. Sharpe, and R.L. Stevens. (1999). Heparin is essential for the storage of specific granule proteases in mast cells. *Nature.* **400**:769-772.

Humphries, M.J. (2000). Integrin structure. *Biochem. Soc. Trans.* **28**: 311-319.

Hunter, T., and B.M. Sefton. (1980). Transforming gene product of Rous sarcoma virus phosphorylates tyrosine. *Proc Natl Acad Sci U S A.* **77**:1311-1315.

Hunter, T. (1998). The Croonian Lecture 1997. The phosphorylation of proteins on tyrosine: its role in cell growth and disease. *Philos Trans R Soc Lond B Biol Sci.* **353**:583-605.

Ishikawa, H., A. Tamura, T. Matsui, H. Sasaki, T. Hakoshima, and S. Tsukita. (2001). Structural conversion between open and closed forms of radixin: low- angle shadowing electron microscopy. *J Mol Biol.* **310**:973-978.

Itasaki, N., S. Bel-Vialar, and R. Krumlauf. (1999). 'Shocking' developments in chick embryology: electroporation and in ovo gene expression. *Nat Cell Biol.* **1**:E203-207.

Jackson, S.M., H. Nakato, M. Sugiura, A. Jannuzi, R. Oakes, V. Kaluza, C. Golden, and S.B. Selleck. (1997). dally, a Drosophila glypican, controls cellular responses to the TGF- beta-related morphogen, Dpp. *Development.* **124**:4113-4120.

Jenniskens, G.J., A. Oosterhof, R. Brandwijk, J.H. Veerkamp, and T.H. van Kuppevelt. (2000). Heparan sulfate heterogeneity in skeletal muscle basal lamina: demonstration by phage display-derived antibodies. *J Neurosci.* **20**:4099-4111.

Jiang, G., J. den Hertog, J. Su, J. Noel, J. Sap, and T. Hunter. (1999). Dimerization inhibits the activity of receptor-like protein-tyrosine phosphatase-alpha. *Nature.* **401**:606-610.

Jiang, G., and T. Hunter. (1999). Receptor signaling: when dimerization is not enough. *Curr Biol.* **9**:R568-571.

Johnson, K.G., and C.E. Holt. (2000). Expression of CRYP-alpha, LAR, PTP-delta, and PTP-rho in the developing Xenopus visual system. *Mech Dev.* **92**:291-4.

Johnson, K.G., I.W. McKinnell, A.W. Stoker, and C.E. Holt. (2001). Receptor protein tyrosine phosphatases regulate retinal ganglion cell axon outgrowth in the developing Xenopus visual system. *J Neurobiol.* **49**:99-117.

Kalo, M.S., and E.B. Pasquale. (1999). Multiple in vivo tyrosine phosphorylation sites in EphB receptors. *Biochemistry.* **38**:14396-14408.

Kan, M., F. Wang, J. Xu, J.W. Crabb, J. Hou, and W.L. McKeehan. (1993). An essential heparin-binding domain in the fibroblast growth factor receptor kinase.

Science. **259**:1918-1921.

Kasper, C., H. Rasmussen, J.S. Kastrup, S. Ikemizu, E.Y. Jones, V. Berezin, E. Bock, and I.K. Larsen. (2000). Structural basis of cell-cell adhesion by NCAM. *Nat Struct Biol.* 7:389-393.

Kaufmann, N., Z.P. Wills, and D. Van Vactor. (1998). Drosophila Rac1 controls motor axon guidance. *Development.* **125**:453-461.

Kawachi, H., A. Fujikawa, N. Maeda, and M. Noda. (2001). Identification of GIT1/Cat-1 as a substrate molecule of protein tyrosine phosphatase zeta /beta by the yeast substrate-trapping system. *Proc Natl Acad Sci U S A.* **98**:6593-6598.

Keiser, N., G. Venkataraman, Z. Shriver, and R. Sasisekharan. (2001). Direct isolation and sequencing of specific protein-binding glycosaminoglycans. *Nat Med.* 7:123-128.

Kerbel, R.S. (2000). Tumor angiogenesis: past, present and the near future. *Carcinogenesis.* **21**:505-515.

Kishihara, K., J. Penninger, V.A. Wallace, T.M. Kundig, K. Kawai, A. Wakeham, E. Timms, K. Pfeffer, P.S. Ohashi, M.L. Thomas, and et al. (1993). Normal B lymphocyte development but impaired T cell maturation in CD45- exon6 protein tyrosine phosphatase-deficient mice. *Cell.* **74**:143-156.

Knebel, A., H.J. Rahmsdorf, A. Ullrich, and P. Herrlich. (1996). Dephosphorylation of receptor tyrosine kinases as target of regulation by radiation, oxidants or alkylating agents. *Embo J.* **15**:5314-5325.

Kolodkin, A.L., D.V. Levengood, E.G. Rowe, Y.T. Tai, R.J. Giger, and D.D. Ginty. (1997). Neuropilin is a semaphorin III receptor. *Cell.* **90**:753-762.

Korey, C.A., and D. Van Vactor. (2000). From the growth cone surface to the cytoskeleton: one journey, many paths. *J Neurobiol.* **44**:184-193.

Kozma, R., S. Sarner, S. Ahmed, and L. Lim. (1997). Rho family GTPases and neuronal growth cone remodelling: relationship between increased complexity induced by Cdc42Hs, Rac1, and acetylcholine and collapse induced by RhoA and lysophosphatidic acid. *Mol Cell Biol.* **17**:1201-11.

Kramer, W., W. Durckheimer, F. Girbig, U. Gutjahr, I. Leipe, and R. Oekonomopulos. (1990). Influence of amino acid side-chain modification on the uptake system for beta-lactam antibiotics and dipeptides from rabbit small intestine. *Biochim Biophys Acta.* **1028**:174-182.

Kroger, S., S.E. Horton, and L.S. Honig. (1996). The developing avian retina expresses agrin isoforms during synaptogenesis. *J Neurobiol.* **29**:165-182.

Kroger, S. (1997). Differential distribution of agrin isoforms in the developing and adult avian retina. *Mol Cell Neurosci.* **10**:149-161.

Krueger, N.X., D. Van Vactor, H.I. Wan, W.M. Gelbart, C.S. Goodman, and H. Saito. (1996). The transmembrane tyrosine phosphatase DLAR controls motor axon guidance in Drosophila. *Cell.* **84**:611-22.

Kuo, C.J., K.R. LaMontagne, Jr., G. Garcia-Cardena, B.D. Ackley, D. Kalman, S. Park, R. Christofferson, J. Kamihara, Y.H. Ding, K.M. Lo, S. Gillies, J. Folkman, R.C. Mulligan, and K. Javaherian. (2001). Oligomerization-dependent regulation of motility and morphogenesis by the collagen XVIII NC1/endostatin domain. *J Cell Biol.* **152**:1233-1246.

Kypta, R.M., H. Su, and L.F. Reichardt. (1996). Association between a transmembrane protein tyrosine phosphatase and the cadherin-catenin complex. *J Cell Biol.* **134**:1519-1529.

Lander, A.D., D.K. Fujii, and L.F. Reichardt. (1985). Purification of a factor that promotes neurite outgrowth: isolation of laminin and associated molecules. *J Cell Biol.* **101**:898-913.

Lanier, L.M., and F.B. Gertler. (2000). From Abl to actin: Abl tyrosine kinase and associated proteins in growth cone motility. *Curr Opin Neurobiol.* **10**:80-7.

Ledig, M., F. Haj, I. McKinnell, A.W. Stoker, and B. Mueller. (1999). The receptor tyrosine phosphatase CRYPalpha promotes intraretinal axon growth. *J. Cell Biol.* **147**:375-388.

Ledig, M.M., I.W. McKinnell, T. Mrsic-Flogel, J. Wang, C. Alvares, I. Mason, J.L. Bixby, B.K. Mueller, and A.W. Stoker. (1999). Expression of receptor tyrosine phosphatases during development of the retinotectal projection of the chick. *J Neurobiol.* **39**:81-96.

Lee, S.R., K.S. Kwon, S.R. Kim, and S.G. Rhee. (1998). Reversible inactivation of protein-tyrosine phosphatase 1B in A431 cells stimulated with epidermal growth factor. *J Biol Chem.* **273**:15366-15372.

Lee, V.M., M. Goedert, and J.Q. Trojanowski. (2001). Neurodegenerative tauopathies. *Annu Rev Neurosci.* **24**:1121-1159.

Li, P.M., W.R. Zhang, and B.J. Goldstein. (1996). Suppression of insulin receptor activation by overexpression of the protein-tyrosine phosphatase LAR in hepatoma cells. *Cell Signal.* **8**:467-73.

Li, L., and J.E. Dixon. (2000). Form, function, and regulation of protein tyrosine phosphatases and their involvement in human diseases. *Semin Immunol.* **12**:75-84.

Liang, Y., R.S. Annan, S.A. Carr, S. Popp, M. Mevissen, R.K. Margolis, and R.U. Margolis. (1999). Mammalian homologues of the Drosophila slit protein are ligands of the heparan sulfate proteoglycan glypican-1 in brain. *J Biol Chem.* **274**:17885-17892.

Lu, J., A.L. Notkins, and M.S. Lan. (1994). Isolation, sequence and expression of a novel mouse brain cDNA, mIA-2, and its relatedness to members of the protein tyrosine phosphatase family. *Biochem Biophys Res Commun.* **204**:930-936.

Maeda, N., T. Nishiwaki, T. Shintani, H. Hamanaka, and M. Noda. (1996). 6B4 proteoglycan/phosphacan, an extracellular variant of receptor-like protein-tyrosine phosphatase zeta/RPTPbeta, binds pleiotrophin/heparin- binding growth-associated molecule (HB-GAM). *J Biol Chem.* **271**:21446-21452.

Maeda, N., K. Ichihara-Tanaka, T. Kimura, K. Kadomatsu, T. Muramatsu, and M. Noda. (1999). A receptor-like protein-tyrosine phosphatase PTPzeta/RPTPbeta binds a heparin-binding growth factor midkine. Involvement of arginine 78 of midkine in the high affinity binding to PTPzeta. *J Biol Chem.* **274**:12474-12479.

Maehama, T., and J.E. Dixon. (1998). The tumor suppressor, PTEN/MMAC1, dephosphorylates the lipid second messenger, phosphatidylinositol 3,4,5-trisphosphate. *J Biol Chem.* **273**:13375-13378.

Mahadev, K., A. Zilbering, L. Zhu, and B.J. Goldstein. (2001). Insulin-stimulated hydrogen peroxide reversibly inhibits protein- tyrosine phosphatase 1b in vivo and enhances the early insulin action cascade. *J Biol Chem.* **276**:21938-21942.

Majeti, R., A.M. Bilwes, J.P. Noel, T. Hunter, and A. Weiss. (1998). Dimerization-induced inhibition of receptor protein tyrosine phosphatase function through an inhibitory wedge. *Science.* **279**:88-91.

Majeti, R., Z. Xu, T.G. Parslow, J.L. Olson, D.I. Daikh, N. Killeen, and A. Weiss. (2000). An inactivating point mutation in the inhibitory wedge of CD45 causes lymphoproliferation and autoimmunity. *Cell.* **103**:1059-1070.

McFarlane, S., L. McNeill, and C.E. Holt. (1995). FGF signaling and target recognition in the developing Xenopus visual system. *Neuron.* **15**:1017-28.

McFarlane, S., E. Cornel, E. Amaya, and C.E. Holt. (1996). Inhibition of FGF receptor activity in retinal ganglion cell axons causes errors in target recognition. *Neuron.* **17**:245-54.

Mellitzer, G., Q. Xu, and D.G. Wilkinson. (2000). Control of cell behaviour by signalling through Eph receptors and ephrins. *Curr Opin Neurobiol.* **10**:400-408.

Mellon, P., V. Parker, Y. Gluzman, and T. Maniatis. (1981). Identification of DNA

sequences required for transcription of the human alpha 1-globin gene in a new SV40 host-vector system. *Cell.* **27**:279-288.

Meng, K., A. Rodriguez-Pena, T. Dimitrov, W. Chen, M. Yamin, M. Noda, and T.F. Deuel. (2000). Pleiotrophin signals increased tyrosine phosphorylation of beta beta- catenin through inactivation of the intrinsic catalytic activity of the receptor-type protein tyrosine phosphatase beta/zeta. *Proc Natl Acad Sci U S A.* **97**:2603-2608.

Merkler, D., G.A. Metz, O. Raineteau, V. Dietz, M.E. Schwab, and K. Fouad. (2001). Locomotor recovery in spinal cord-injured rats treated with an antibody neutralizing the myelin-associated neurite growth inhibitor Nogo-A. *J Neurosci.* **21**:3665-3673.

Milev, P., D.R. Friedlander, T. Sakurai, L. Karthikeyan, M. Flad, R.K. Margolis, M. Grumet, and R.U. Margolis. (1994). Interactions of the chondroitin sulfate proteoglycan phosphacan, the extracellular domain of a receptor-type protein tyrosine phosphatase, with neurons, glia, and neural cell adhesion molecules. *J Cell Biol.* **127**:1703-1715.

Milev, P., P. Maurel, M. Haring, R.K. Margolis, and R.U. Margolis. (1996). TAG-1/axonin-1 is a high-affinity ligand of neurocan, phosphacan/protein-tyrosine phosphatase-zeta/beta, and N-CAM. *J Biol Chem.* **271**:15716-15723.

Minamide, L.S., and J.R. Bamburg. (1990). A filter paper dye-binding assay for quantitative determination of protein without interference from reducing agents or detergents. *Anal Biochem.* **190**:66-70.

Ming, G.L., H.J. Song, B. Berninger, C.E. Holt, M. Tessier-Lavigne, and M.M. Poo. (1997). cAMP-dependent growth cone guidance by netrin-1. *Neuron.* **19**:1225-35.

Momose, T., A. Tonegawa, J. Takeuchi, H. Ogawa, K. Umesono, and K. Yasuda. (1999). Efficient targeting of gene expression in chick embryos by microelectroporation. *Dev Growth Differ.* **41**:335-344.

Morrison, D.K., M.S. Murakami, and V. Cleghon. (2000). Protein kinases and phosphatases in the drosophila genome. *J Cell Biol.* **150**:F57-62.

Mueller, B.K. (1999). Growth cone guidance: first steps towards a deeper understanding. *Annu Rev Neurosci.* **22**:351-388.

Mustelin, T., K.M. Coggeshall, and A. Altman. (1989). Rapid activation of the T-cell tyrosine protein kinase pp56lck by the CD45 phosphotyrosine phosphatase. *Proc Natl Acad Sci U S A.* **86**:6302-6306.

Nakamura, F., M. Tanaka, T. Takahashi, R.G. Kalb, and S.M. Strittmatter. (1998). Neuropilin-1 extracellular domains mediate semaphorin D/III-induced growth cone collapse. *Neuron.* **21**:1093-100.

Nakamura, F., R.G. Kalb, and S.M. Strittmatter. (2000). Molecular basis of semaphorin-mediated axon guidance. *J Neurobiol.* **44**:219-229.

Nakamura, H., and J. Funahashi. (2001). Introduction of DNA into chick embryos by in ovo electroporation. *Methods.* **24**:43-48.

Nam, H.J., F. Poy, N.X. Krueger, H. Saito, and C.A. Frederick. (1999). Crystal structure of the tandem phosphatase domains of RPTP LAR. *Cell.* **97**:449-457.

Nastuk, M.A., S. Davis, G.D. Yancopoulos, and J.R. Fallon. (1998). Expression cloning and characterization of NSIST, a novel sulfotransferase expressed by a subset of neurons and postsynaptic targets. *J Neurosci.* **18**:7167-7177.

Neel, B.G. (1993). Structure and function of SH2-domain containing tyrosine phosphatases. *Semin Cell Biol.* **4**:419-432.

Neumann, F.R., G. Bittcher, M. Annies, B. Schumacher, S. Kroger, and M.A. Ruegg. (2001). An alternative amino-terminus expressed in the central nervous system converts agrin to a type II transmembrane protein. *Mol Cell Neurosci.* **17**:208-225.

Newsome, T.P., B. Asling, and B.J. Dickson. (2000). Analysis of drosophila photoreceptor axon guidance in eye-specific mosaics. *Development.* **127**:851-60.

Nugent, M.A. (2000). Heparin sequencing brings structure to the function of complex oligosaccharides. *Proc Natl Acad Sci U S A.* **97**:10301-10303.

Nyhus, J.K., and J.L. Denburg. (1998). The in vivo regulation of pioneer axon growth by FGF-2 and heparan sulfate proteoglycans in cultured embryos of the cockroach. *Mol Cell Neurosci.* **11**:305-323.

O'Grady, P., N.X. Krueger, M. Streuli, and H. Saito. (1994). Genomic organization of the human LAR protein tyrosine phosphatase gene and alternative splicing in the extracellular fibronectin type-III domains. *Journal of Biological Chemistry.* **269**:25193-25199.

O'Grady, P., T.C. Thai, and H. Saito. (1998). The laminin-nidogen complex is a ligand for a specific splice isoform of the transmembrane protein tyrosine phosphatase LAR. *J Cell Biol.* **141**:1675-1684.

O'Reilly, M.S., T. Boehm, Y. Shing, N. Fukai, G. Vasios, W.S. Lane, E. Flynn, J.R. Birkhead, B.R. Olsen, and J. Folkman. (1997). Endostatin: an endogenous inhibitor of angiogenesis and tumor growth. *Cell.* **88**:277-285.

Oh, S.P., Y. Kamagata, Y. Muragaki, S. Timmons, A. Ooshima, and B.R. Olsen. (1994). Isolation and sequencing of cDNAs for proteins with multiple domains of Gly-Xaa-Yaa repeats identify a distinct family of collagenous proteins. *Proc Natl Acad Sci U S A.* **91**:4229-4233.

Ostergaard, H.L., D.A. Shackelford, T.R. Hurley, P. Johnson, R. Hyman, B.M. Sefton, and I.S. Trowbridge. (1989). Expression of CD45 alters phosphorylation of the lck-encoded tyrosine protein kinase in murine lymphoma T-cell lines. *Proc Natl Acad Sci U S A.* **86**:8959-8963.

Ostergaard, H.L., and I.S. Trowbridge. (1991). Negative regulation of CD45 protein tyrosine phosphatase activity by ionomycin in T cells. *Science.* **253**:1423-1425.

Paglini, G., P. Kunda, S. Quiroga, K. Kosik, and A. Caceres. (1998). Suppression of radixin and moesin alters growth cone morphology, motility, and process formation in primary cultured neurons. *J Cell Biol.* **143**:443-455.

Pan, M.-G., C. Rim, K.P. Lu, T. Florio, and P.J.S. Stork. (1993). Cloning and expression of two structurally distinct receptor-linked protein-tyrosine phosphatases generated by RNA processing from a single gene. *J. Biol. Chem.* **268**:19284-19291.

Park, P.W., O. Reizes, and M. Bernfield. (2000). Cell surface heparan sulfate proteoglycans: selective regulators of ligand-receptor encounters. *J Biol Chem.* **275**:29923-29926.

Peles, E., M. Nativ, P.L. Campbell, T. Sakurai, R. Martinez, S. Lev, D.O. Clary, J. Schilling, G. Barnea, G.D. Plowman, and et al. (1995). The carbonic anhydrase domain of receptor tyrosine phosphatase beta is a functional ligand for the axonal cell recognition molecule contactin. *Cell.* **82**:251-260.

Peles, E., M. Nativ, M. Lustig, M. Grumet, J. Schilling, R. Martinez, G.D. Plowman, and J. Schlessinger. (1997). Identification of a novel contactin-associated transmembrane receptor with multiple domains implicated in protein-protein interactions. *Embo J.* **16**:978-88.

Peles, E., J. Schlessinger, and M. Grumet. (1998). Multi-ligand interactions with receptor-like protein tyrosine phosphatase beta: implications for intercellular signaling. *Trends Biochem Sci.* **23**:121-4.

Pellegrini, L., D.F. Burke, F. von Delft, B. Mulloy, and T.L. Blundell. (2000). Crystal structure of fibroblast growth factor receptor ectodomain bound to ligand and heparin. *Nature.* **407**:1029-1034.

Peluso, J.J. (2000). N-cadherin-mediated cell contact regulates ovarian surface epithelial cell survival. *Biol Signals Recept.* **9**:115-121.

Peretz, A., H. Gil-Henn, A. Sobko, V. Shinder, B. Attali, and A. Elson. (2000). Hypomyelination and increased activity of voltage-gated K(+) channels in mice lacking protein tyrosine phosphatase epsilon. *Embo J.* **19**:4036-4045.

Perrimon, N., and M. Bernfield. (2000). Specificities of heparan sulphate proteoglycans in developmental processes. *Nature.* **404**:725-728.

Perrimon, N., and M. Bernfield. (2001). Cellular functions of proteoglycans--an overview. *Semin Cell Dev Biol.* **12**:65-67.

Plotnikov, A.N., J. Schlessinger, S.R. Hubbard, and M. Mohammadi. (1999). Structural basis for FGF receptor dimerization and activation. *Cell.* **98**:641-650.

Poon, R.Y., and T. Hunter. (1995). Dephosphorylation of Cdk2 Thr160 by the cyclin-dependent kinase- interacting phosphatase KAP in the absence of cyclin. *Science.* **270**:90-93.

Pot, D.A., T.A. Woodford, E. Remboutsika, R.S. Haun, and J.E. Dixon. (1991). Cloning, bacterial expression, purification, and characterization of the cytoplasmic domain of rat LAR, a receptor-like protein tyrosine phosphatase. *J Biol Chem.* **266**:19688-19696.

Prinjha, R., S.E. Moore, M. Vinson, S. Blake, R. Morrow, G. Christie, D. Michalovich, D.L. Simmons, and F.S. Walsh. (2000). Inhibitor of neurite outgrowth in humans. *Nature.* **403**:383-384.

Pulido, R., C. Serra Pages, M. Tang, and M. Streuli. (1995). The LAR/PTP delta/PTP sigma subfamily of transmembrane protein-tyrosine-phosphatases: multiple human LAR, PTP delta, and PTP sigma isoforms are expressed in a tissue-specific manner and associate with the LAR-interacting protein LIP.1. *Proc Natl Acad Sci U S A.* **92**:11686-90.

Pulido, R., N.X. Krueger, C. Serra-Pages, H. Saito, and M. Streuli. (1995). Molecular characterization of the human transmembrane protein-tyrosine phosphatase delta. Evidence for tissue-specific expression of alternative human transmembrane protein-tyrosine phosphatase delta isoforms. *J Biol Chem.* **270**:6722-6728.

Rajan, I., and J.L. Denburg. (1997). Mesodermal guidance of pioneer axon growth. *Dev Biol.* **190**:214-228.

Rauch, U., P. Gao, A. Janetzko, A. Flaccus, L. Hilgenberg, H. Tekotte, R.K. Margolis, and R.U. Margolis. (1991). Isolation and characterization of developmentally regulated chondroitin sulfate and chondroitin/keratan sulfate

proteoglycans of brain identified with monoclonal antibodies. *J Biol Chem.* **266**:14785-14801.

Raulo, E., M.A. Chernousov, D.J. Carey, R. Nolo, and H. Rauvala. (1994). Isolation of a neuronal cell surface receptor of heparin binding growth- associated molecule (HB-GAM). Identification as N-syndecan (syndecan-3). *J Biol Chem.* **269**:12999-13004.

Ringstedt, T., J.E. Braisted, K. Brose, T. Kidd, C. Goodman, M. Tessier-Lavigne, and D.D. O'Leary. (2000). Slit inhibition of retinal axon growth and its role in retinal axon pathfinding and innervation patterns in the diencephalon. *J Neurosci.* **20**:4983-91.

Rostand, K.S., and J.D. Esko. (1997). Microbial adherence to and invasion through proteoglycans. *Infect Immun.* **65**:1-8.

Ruegg, M.A., and J.L. Bixby. (1998). Agrin orchestrates synaptic differentiation at the vertebrate neuromuscular junction. *Trends Neurosci.* **21**:22-27.

Rutishauser, U., and L. Landmesser. (1996). Polysialic acid in the vertebrate nervous system: a promoter of plasticity in cell-cell interactions. *Trends Neurosci.* **19**:422-427.

Sakurai, T., M. Lustig, M. Nativ, J.J. Hemperly, J. Schlessinger, E. Peles, and M. Grumet. (1997). Induction of neurite outgrowth through contactin and Nr-CAM by extracellular regions of glial receptor tyrosine phosphatase beta. *J Cell Biol.* **136**:907-918.

Salmeen, A., J.N. Andersen, M.P. Myers, N.K. Tonks, and D. Barford. (2000). Molecular basis for the dephosphorylation of the activation segment of the insulin receptor by protein tyrosine phosphatase 1B. *Mol Cell.* **6**:1401-1412.

Sambrook, J., Fritsch, E.F. and Maniatis T. (1989). Molecular Cloning. A laboratory manual. Cold Spring Harbor Laboratory Press.

Sap, J., Y.P. Jiang, D. Friedlander, M. Grumet, and J. Schlessinger. (1994). Receptor tyrosine phosphatase R-PTP-kappa mediates homophilic binding. *Mol Cell Biol.* **14**:1-9.

Schaapveld, R.Q., J.T. Schepens, D. Bachner, J. Attema, B. Wieringa, P.H. Jap, and W.J. Hendriks. (1998). Developmental expression of the cell adhesion molecule-like protein tyrosine phosphatases LAR, RPTPdelta and RPTPsigma in the mouse. *Mech Dev.* **77**:59-62.

Schlessinger, J., A.N. Plotnikov, O.A. Ibrahimi, A.V. Eliseenkova, B.K. Yeh, A. Yayon, R.J. Linhardt, and M. Mohammadi. (2000). Crystal structure of a ternary

FGF-FGFR-heparin complex reveals a dual role for heparin in FGFR binding and dimerization. *Mol Cell.* **6**:743-750.

Seed, B. (1995). Developments in expression cloning. *Curr Opin Biotechnol.* **6**:567-573.

Selkoe, D.J. (1991). The molecular pathology of Alzheimer's disease. *Neuron.* **6**:487-498.

Serafini, T., S.A. Colamarino, E.D. Leonardo, H. Wang, R. Beddington, W.C. Skarnes, and M. Tessier-Lavigne. (1996). Netrin-1 is required for commissural axon guidance in the developing vertebrate nervous system. *Cell.* **87**:1001-1114.

Serra-Pages, C., N.L. Kedersha, L. Fazikas, Q. Medley, A. Debant, and M. Streuli. (1995). The LAR transmembrane protein tyrosine phosphatase and a coiled-coil LAR-interacting protein co-localize at focal adhesions. *Embo J.* **14**:2827-2838.

Serra-Pages, C., Q.G. Medley, M. Tang, A. Hart, and M. Streuli. (1998). Liprins, a family of LAR transmembrane protein-tyrosine phosphatase- interacting proteins. *J Biol Chem.* **273**:15611-15620.

Sertie, A.L., V. Sossi, A.A. Camargo, M. Zatz, C. Brahe, and M.R. Passos-Bueno. (2000). Collagen XVIII, containing an endogenous inhibitor of angiogenesis and tumor growth, plays a critical role in the maintenance of retinal structure and in neural tube closure (Knobloch syndrome). *Hum Mol Genet.* **9**:2051-2058.

Shamah, S.M., M.Z. Lin, J.L. Goldberg, S. Estrach, M. Sahin, L. Hu, M. Bazalakova, R.L. Neve, G. Corfas, A. Debant, and M.E. Greenberg. (2001). EphA receptors regulate growth cone dynamics through the novel guanine nucleotide exchange factor ephexin. *Cell.* **105**:233-44.

Shiroo, M., L. Goff, M. Biffen, E. Shivnan, and D. Alexander. (1992). CD45 tyrosine phosphatase-activated p59fyn couples the T cell antigen receptor to pathways of diacylglycerol production, protein kinase C activation and calcium influx. *Embo J.* **11**:4887-4897.

Sommer, L., M. Rao, and D.J. Anderson. (1997). RPTP delta and the novel protein tyrosine phosphatase RPTP psi are expressed in restricted regions of the developing central nervous system. *Dev Dyn.* **208**:48-61.

Song, H.J., G.L. Ming, and M.M. Poo. (1997). cAMP-induced switching in turning direction of nerve growth cones [published erratum appears in Nature 1997 Sep 25;389(6649):412]. *Nature.* **388**:275-9.

Song, H., G. Ming, Z. He, M. Lehmann, L. McKerracher, M. Tessier-Lavigne, and M. Poo. (1998). Conversion of neuronal growth cone responses from repulsion to

attraction by cyclic nucleotides. *Science.* **281**:1515-8.

Stamenkovic, I., D. Sgroi, A. Aruffo, M.S. Sy, and T. Anderson. (1991). The B lymphocyte adhesion molecule CD22 interacts with leukocyte common antigen CD45RO on T cells and alpha 2-6 sialyltransferase, CD75, on B cells. *Cell.* **66**:1133-1144.

Stein, E., and M. Tessier-Lavigne. (2001). Hierarchical organization of guidance receptors: silencing of netrin attraction by slit through a Robo/DCC receptor complex. *Science.* **291**:1928-1938.

Stier, H., and B. Schlosshauer. (1998). Different cell surface areas of polarized radial glia having opposite effects on axonal outgrowth. *Eur J Neurosci.* **10**:1000-10.

Stoker, A.W. (1994). Isoforms of a novel cell adhesion molecule-like protein tyrosine phosphatase are implicated in neural development. *Mech Dev.* **46**:201-217.

Stoker, A.W., B. Gehrig, F. Haj, and B.H. Bay. (1995). Axonal localisation of the CAM-like tyrosine phosphatase CRYP alpha: a signalling molecule of embryonic growth cones. *Development.* **121**:1833-44.

Stoker, A., and R. Dutta. (1998). Protein tyrosine phosphatases and neural development. *Bioessays.* **20**:463-472.

Stoker, A.W. (2001). Receptor tyrosine phosphatases in axon growth and guidance. *Curr Opin Neurobiol.* **11**:95-102.

Storms, S.D., A.C. Kim, B.H. Tran, G.J. Cole, and B.A. Murray. (1996). NCAM-mediated adhesion of transfected cells to agrin. *Cell Adhes Commun.* **3**:497-509.

Storms, S.D., V.M. Anvekar, L.D. Adams, and B.A. Murray. (1996). Heterophilic NCAM-mediated cell adhesion to proteoglycans from chick embryonic brain membranes. *Exp Cell Res.* **223**:385-94.

Streuli, M., N.X. Krueger, T. Thai, M. Tang, and H. Saito. (1990). Distinct functional roles of the two intracellular phosphatase like domains of the receptor-linked protein tyrosine phosphatases LCA and LAR. *Embo J.* **9**:2399-2407.

Streuli, M., N.X. Krueger, P.D. Ariniello, M. Tang, J.M. Munro, W.A. Blattler, D.A. Adler, C.M. Disteche, and H. Saito. (1992). Expression of the receptor-linked protein tyrosine phosphatase LAR: proteolytic cleavage and shedding of the CAM-like extracellular region. *Embo J.* **11**:897-907.

Sun, Q., S. Bahri, A. Schmid, W. Chia, and K. Zinn. (2000). Receptor tyrosine phosphatases regulate axon guidance across the midline of the Drosophila embryo. *Development.* **127**:801-12.

Sun, Q.L., J. Wang, R.J. Bookman, and J.L. Bixby. (2000). Growth cone steering by

receptor tyrosine phosphatase delta defines a distinct class of guidance Cue. *Mol Cell Neurosci.* **16**:686-95.

Sun, Q., B. Schindelholz, M. Knirr, A. Schmid, and K. Zinn. (2001). Complex genetic interactions among four receptor tyrosine phosphatases regulate axon guidance in Drosophila. *Mol Cell Neurosci.* **17**:274-91.

Swillens, S. (1995). Interpretation of binding curves obtained with high receptor concentrations: practical aid for computer analysis. *Mol Pharmacol.* **47**:1197-1203.

Szedlacsek, S.E., A.R. Aricescu, T.A. Fulga, L. Renault, and A.J. Scheidig. (2001). Crystal structure of PTP-SL/PTPBR7 catalytic domain: implications for MAP kinase regulation. *J Mol Biol.* **311**:557-568.

Taddei, M.L., P. Chiarugi, P. Cirri, D. Talini, G. Camici, G. Manao, G. Raugei, and G. Ramponi. (2000). LMW-PTP exerts a differential regulation on PDGF- and insulin-mediated signaling. *Biochem Biophys Res Commun.* **270**:564-569.

Takahashi, T., A. Fournier, F. Nakamura, L.H. Wang, Y. Murakami, R.G. Kalb, H. Fujisawa, and S.M. Strittmatter. (1999). Plexin-neuropilin-1 complexes form functional semaphorin-3A receptors. *Cell.* **99**:59-69.

Takahashi, T., and S.M. Strittmatter. (2001). Plexina1 autoinhibition by the plexin sema domain. *Neuron.* **29**:429-439.

Tamagnone, L., S. Artigiani, H. Chen, Z. He, G.I. Ming, H. Song, A. Chedotal, M.L. Winberg, C.S. Goodman, M. Poo, M. Tessier-Lavigne, and P.M. Comoglio. (1999). Plexins are a large family of receptors for transmembrane, secreted, and GPI-anchored semaphorins in vertebrates. *Cell.* **99**:71-80.

Tan, X., D.R. Stover, and K.A. Walsh. (1993). Demonstration of protein tyrosine phosphatase activity in the second of two homologous domains of CD45. *J Biol Chem.* **268**:6835-6838.

Tang, T.L., R.M. Freeman, Jr., A.M. O'Reilly, B.G. Neel, and S.Y. Sokol. (1995). The SH2-containing protein-tyrosine phosphatase SH-PTP2 is required upstream of MAP kinase for early Xenopus development. *Cell.* **80**:473-483.

Tao, J., C.C. Malbon, and H.Y. Wang. (2001). Insulin stimulates tyrosine phosphorylation and inactivation of protein- tyrosine phosphatase 1B in vivo. *J Biol Chem.* **276**:29520-29525.

Tartaglia, L.A., M. Dembski, X. Weng, N. Deng, J. Culpepper, R. Devos, G.J. Richards, L.A. Campfield, F.T. Clark, J. Deeds, and et al. (1995). Identification and expression cloning of a leptin receptor, OB-R. *Cell.* **83**:1263-1271.

Tear, G., R. Harris, S. Sutaria, K. Kilomanski, C.S. Goodman, and M.A. Seeger. (1996). *commissureless* controls growth cone guidance across the CNS midline in Drosophila and encodes a novel membrane protein. *Neuron*. **16**:501-514.

Tessier Lavigne, M., and C.S. Goodman. (1996). The molecular biology of axon guidance. *Science*. **274**:1123-33.

Tian, S.S., P. Tsoulfas, and K. Zinn. (1991). Three receptor-linked protein-tyrosine phosphatases are selectively expressed on central nervous system axons in the Drosophila embryo. *Cell*. **67**:675-80.

Tiganis, T., A.M. Bennett, K.S. Ravichandran, and N.K. Tonks. (1998). Epidermal growth factor receptor and the adaptor protein p52Shc are specific substrates of T-cell protein tyrosine phosphatase. *Mol Cell Biol*. **18**:1622-1634.

Tiganis, T., B.E. Kemp, and N.K. Tonks. (1999). The protein-tyrosine phosphatase TCPTP regulates epidermal growth factor receptor-mediated and phosphatidylinositol 3-kinase-dependent signaling. *J Biol Chem*. **274**:27768-27775.

Tigyi, G., D.J. Fischer, A. Sebok, C. Yang, D.L. Dyer, and R. Miledi. (1996). Lysophosphatidic acid-induced neurite retraction in PC12 cells: control by phosphoinositide-Ca2+ signaling and Rho. *J Neurochem*. **66**:537-48.

Tonks, N.K., C.D. Diltz, and E.H. Fischer. (1988). Purification of the major protein-tyrosine-phosphatases of human placenta. *J Biol Chem*. **263**:6722-6730.

Tonks, N.K., and B.G. Neel. (2001). Combinatorial control of the specificity of protein tyrosine phosphatases. *Curr Opin Cell Biol*. **13**:182-195.

Tracy, S., P. van der Geer, and T. Hunter. (1995). The receptor-like protein-tyrosine phosphatase, RPTP alpha, is phosphorylated by protein kinase C on two serines close to the inner face of the plasma membrane. *J Biol Chem*. **270**:10587-10594.

Tsen, G., W. Halfter, S. Kroger, and G.J. Cole. (1995). Agrin is a heparan sulfate proteoglycan. *J Biol Chem*. **270**:3392-3399.

Tsuda, M., K. Kamimura, H. Nakato, M. Archer, W. Staatz, B. Fox, M. Humphrey, S. Olson, T. Futch, V. Kaluza, E. Siegfried, L. Stam, and S.B. Selleck. (1999). The cell-surface proteoglycan Dally regulates Wingless signalling in Drosophila. *Nature*. **400**:276-280.

Turnbull, J., A. Powell, and S. Guimond. (2001). Heparan sulfate: decoding a dynamic multifunctional cell regulator. *Trends Cell Biol*. **11**:75-82.

Uetani, N., K. Kato, H. Ogura, K. Mizuno, K. Kawano, K. Mikoshiba, H. Yakura, M. Asano, and Y. Iwakura. (2000). Impaired learning with enhanced hippocampal long-term potentiation in PTPdelta-deficient mice. *Embo J*. **19**:2775-2785.

Van der Zee, C.E., ManT.Y., I. van der Heijden, E.M. Lieshout, and W.J. Hendriks. (2000). LAR protein tyrosine phosphatase deficient mice. *Eur. J. Neurosci.* **12 (suppl. 11)**:290.

Van Vactor, D. (1998). Adhesion and signaling in axonal fasciculation. *Curr Opin Neurobiol.* **8**:80-6.

Van Vactor, D. (1998). Protein tyrosine phosphatases in the developing nervous system. *Curr Opin Cell Biol.* **10**:174-81.

Van Vactor, D.V., and L.J. Lorenz. (1999). Neural development: The semantics of axon guidance. *Current Biology.* **9**:R201-4.

Venkataraman, G., Z. Shriver, R. Raman, and R. Sasisekharan. (1999). Sequencing complex polysaccharides. *Science.* **286**:537-542.

Vogel, W., R. Lammers, J. Huang, and A. Ullrich. (1993). Activation of a phosphotyrosine phosphatase by tyrosine phosphorylation. *Science.* **259**:1611-1614.

Wagner, J., D. Boerboom, and M.L. Tremblay. (1994). Molecular cloning and tissue-specific RNA processing of a murine receptor-type protein tyrosine phosphatase. *European Journal of Biochemistry.* **226**:773-782.

Wagner, J., L.A. Gordon, H.H. Heng, M.L. Tremblay, and A.S. Olsen. (1996). Physical mapping of receptor type protein tyrosine phosphatase sigma (PTPRS) to human chromosome 19p13.3. *Genomics.* **38**:76-78.

Wallace, M.J., C. Fladd, J. Batt, and D. Rotin. (1998). The second catalytic domain of protein tyrosine phosphatase delta (PTP delta) binds to and inhibits the first catalytic domain of PTP sigma. *Mol Cell Biol.* **18**:2608-2616.

Wallace, M.J., J. Batt, C.A. Fladd, J.T. Henderson, W. Skarnes, and D. Rotin. (1999). Neuronal defects and posterior pituitary hypoplasia in mice lacking the receptor tyrosine phosphatase PTPsigma. *Nat Genet.* **21**:334-338.

Walsh, F.S., and P. Doherty. (1997). Neural cell adhesion molecules of the immunoglobulin superfamily: role in axon growth and guidance. *Annu Rev Cell Dev Biol.* **13**:425-56.

Walton, K.M., K.J. Martell, S.P. Kwak, J.E. Dixon, and B.L. Largent. (1993). A novel receptor-type protein tyrosine phosphatase is expressed during neurogenesis in the olfactory neuroepithelium. *Neuron.* **11**:387-400.

Walz, A., S. McFarlane, Y.G. Brickman, V. Nurcombe, P.F. Bartlett, and C.E. Holt. (1997). Essential role of heparan sulfates in axon navigation and targeting in the developing visual system. *Development.* **124**:2421-2430.

Walzel, H., U. Schulz, P. Neels, and J. Brock. (1999). Galectin-1, a natural ligand for

the receptor-type protein tyrosine phosphatase CD45. *Immunol Lett.* **67**:193-202.

Wang, Y., and C.J. Pallen. (1991). The receptor-like protein tyrosine phosphatase HPTP alpha has two active catalytic domains with distinct substrate specificities. *Embo J.* **10**:3231-3237.

Wang, L., and J.L. Denburg. (1992). A role for proteoglycans in the guidance of a subset of pioneer axons in cultured embryos of the cockroach. *Neuron.* **8**:701-714.

Wang, J., and J.L. Bixby. (1999). Receptor tyrosine phosphatase-delta is a homophilic, neurite-promoting cell adhesion molecular for CNS neurons. *Mol Cell Neurosci.* **14**:370-384.

Weiss, A., and J. Schlessinger. (1998). Switching signals on or off by receptor dimerization. *Cell.* **94**:277-280.

Weng, L.P., X. Wang, and Q. Yu. (1999). Transmembrane tyrosine phosphatase LAR induces apoptosis by dephosphorylating and destabilizing p130Cas. *Genes Cells.* **4**:185-196.

Wilkinson, D.G. (2001). Multiple roles of EPH receptors and ephrins in neural development. *Nat Rev Neurosci.* **2**:155-164.

Williams, E.J., B. Mittal, F.S. Walsh, and P. Doherty. (1995). A Ca2+/calmodulin kinase inhibitor, KN-62, inhibits neurite outgrowth stimulated by CAMs and FGF. *Mol Cell Neurosci.* **6**:69-79.

Wills, Z., J. Bateman, C.A. Korey, A. Comer, and D. Van Vactor. (1999). The tyrosine kinase Abl and its substrate enabled collaborate with the receptor phosphatase Dlar to control motor axon guidance. *Neuron.* **22**:301-12.

Wishart, M.J., and J.E. Dixon. (1998). Gathering STYX: phosphatase-like form predicts functions for unique protein-interaction domains. *Trends Biochem Sci.* **23**:301-306.

Wu, D.-Y., and D.J. Goldberg. (1993). Regulated tyrosine phosphorylation at the tips of growth cone filopodia. *J. Cell Biol.* **123**:653-664.

Wu, L., A. Buist, J. den Hertog, and Z.Y. Zhang. (1997). Comparative kinetic analysis and substrate specificity of the tandem catalytic domains of the receptor-like protein-tyrosine phosphatase alpha. *J Biol Chem.* **272**:6994-7002.

Wu, X., and H.H. Gu. (2000). Dilution enhancement of COS cell expression cloning. *Anal Biochem.* **278**:74-80.

Xie, Y., T.T. Yeo, C. Zhang, T. Yang, M.A. Tisi, S.M. Massa, and F.M. Longo. (2001). The leukocyte common antigen-related protein tyrosine phosphatase receptor regulates regenerative neurite outgrowth in vivo. *J Neurosci.* **21**:5130-5138.

Yamaguchi, Y. (2001). Heparan sulfate proteoglycans in the nervous system: their diverse roles in neurogenesis, axon guidance, and synaptogenesis. *Semin Cell Dev Biol.* **12**:99-106.

Yan, H., A. Grossman, H. Wang, P. DEustachio, K. Mossie, J.M. Musacchio, O. Silvennoinen, and J. Schlessinger. (1993). A novel receptor tyrosine phosphatase-sigma that is highly expressed in the nervous system. *J Biol Chem.* **268**:24880-24886.

Yang, X.H., K.T. Seow, S.M. Bahri, S.H. Oon, and W. Chia. (1991). Two Drosophila receptor-like tyrosine phosphatase genes are expressed in a subset of developing axons and pioneer neurons in the embryonic CNS. *Cell.* **67**:661-73.

Zabolotny, J.M., Y.B. Kim, O.D. Peroni, J.K. Kim, M.A. Pani, O. Boss, L.D. Klaman, S. Kamatkar, G.I. Shulman, B.B. Kahn, and B.G. Neel. (2001). Overexpression of the LAR (leukocyte antigen-related) protein-tyrosine phosphatase in muscle causes insulin resistance. *Proc Natl Acad Sci U S A.* **98**:5187-5192.

Zhang, W.R., N. Hashimoto, F. Ahmad, W. Ding, and B.J. Goldstein. (1994). Molecular cloning and expression of a unique receptor-like protein-tyrosine-phosphatase in the leucocyte-common-antigen-related phosphatase family. *Biochemical Journal.* **302**:39-47.

Zhang, W.R., P.M. Li, M.A. Oswald, and B.J. Goldstein. (1996). Modulation of insulin signal transduction by eutopic overexpression of the receptor-type protein-tyrosine phosphatase LAR. *Mol Endocrinol.* **10**:575-584.

Zhang, S.H., J. Liu, R. Kobayashi, and N.K. Tonks. (1999). Identification of the cell cycle regulator VCP (p97/CDC48) as a substrate of the band 4.1-related protein-tyrosine phosphatase PTPH1. *J Biol Chem.* **274**:17806-17812.

Zheng, X.M., Y. Wang, and C.J. Pallen. (1992). Cell transformation and activation of pp60c-src by overexpression of a protein tyrosine phosphatase. *Nature.* **359**:336-339.

Zheng, X.M., R.J. Resnick, and D. Shalloway. (2000). A phosphotyrosine displacement mechanism for activation of Src by PTPalpha. *Embo J.* **19**:964-978.

Zondag, G.C., G.M. Koningstein, Y.P. Jiang, J. Sap, W.H. Moolenaar, and M.F. Gebbink. (1995). Homophilic interactions mediated by receptor tyrosine phosphatases mu and kappa. A critical role for the novel extracellular MAM domain. *J Biol Chem.* **270**:14247-50.

Zondag, G.C., A.B. Reynolds, and W.H. Moolenaar. (2000). Receptor protein-tyrosine phosphatase RPTPmu binds to and dephosphorylates the catenin p120(ctn). *J Biol Chem.* **275**:11264-11269.